CHARACTERIZATION OF VIRULENCE TRAITS AND THE UNDERLYING REGULATORY MECHANISMS OF *Xanthomonas citri* subsp. *citri*

By

YINPING GUO

A DISSERTATION PRESENTED TO THE GRADUATE SCHOOL
OF THE UNIVERSITY OF FLORIDA IN PARTIAL FULFILLMENT
OF THE REQUIREMENTS FOR THE DEGREE OF
DOCTOR OF PHILOSOPHY

UNIVERSITY OF FLORIDA

2011

To my parents, Zhi Zhang and Quanying Guo, and my husband, Sha Tao

ACKNOWLEDGMENTS

I would like to express the deepest gratitude to my academic advisor, Dr. Nian Wang, for the opportunity to pursue my research in his lab. His constant guidance and support helped me to survive many difficulties throughout the journey to achieve my PhD. I would also like to thank the members of my committee: Drs. Jeffrey Jones, James Preston, James Graham, and Zhonglin Mou for their advice, attention, and time. Special thanks go to Dr. Jeffrey Jones for the opportunity to learn mutagenesis technique in his lab.

I also wish to thank all the former and current members of Dr. Nian Wang's lab for creating a friendly and pleasant environment in which to work: Drs. Uma Shanker Sagaram, Jeong-Soon Kim, Pankaj Trivedi, Qing Yan, Jinyun Li, Aswathy Sreedharan, Nagaraju Akula, Valente Aritua, Sunitha Kogenaru, Ms. Neha Jalan, Ms. Lin Yang, and Mr. Vladimir Kolbasov. Drs. Uma Shanker Sagaram, and Jeong-Soon Kim assisted me with the characterization of the *galU* mutants. Ms. Lin Yang helped with the preparation of scanning electron microscope specimens. Mr. Vladimir Kolbasov helped with the growth curve assay of quorum sensing mutants in planta. Drs. Pankaj Trivedi, Qing Yan, Jinyun Li and Ms. Neha Jalan held valuable scientific (sometimes not scientific) discussions with me.

Special thanks are extended to friends and colleagues at the Citrus Research and Education Center, Department of Microbiology and Cell Science, and Department of Plant Pathology, ICBR at the University of Florida. I would like to acknowledge Ms. Diann Achor for teaching me how to operate the confocal scanning laser microscope and scanning electron microscope. I wish to thank Mr. Gerald Minsavage and Dr. José Francisco Lissoni Figueiredo in Dr. Jerry Jones' lab. Mr. Gerald Minsavage taught me

how to generate deletion mutants. Dr. José Francisco Lissoni Figueiredo generated the *hrpX* mutant. I am especially indebted to Drs. Yanping Zhang and Jason Li for the performance of microarray hybridization, microarray data normalization and statistical analysis. I also thank Drs. James Graham, William Dawson, Ron Brlansky, Larry Duncan and Micheal Davis and members of their labs for allowing me the use of their equipment.

Finally, I wish to acknowledge my family members including my brothers, Gaofeng and Chuangfeng Guo, my grandmother Lanying Gao and my aunt Xujun Zhang for all their encouragement in my pursuance of my Ph.D. Thanks go to the memory of my grandfather Shuanzhu Zhang for his example and integrity. I would especially like to thank my parents, Zhi Zhang and Quanying Guo. Without their support and love throughout my life, none of this would be possible. I most importantly thank my beloved husband and best friend, Sha Tao, for sticking with me through all the good and bad times, for having faith in me and for helping me to keep sane. His love, support and constant patience have taught me so much about sacrifice and compromise.

TABLE OF CONTENTS

page

LIST OF TABLES

LIST OF FIGURES

Abstract of Dissertation Presented to the Graduate School
of the University of Florida in Partial Fulfillment of the
Requirements for the Degree of Doctor of Philosophy

CHARACTERIZATION OF VIRULENCE TRAITS AND THE UNDERLYING REGULATORY MECHANISMS OF *Xanthomonas citri* subsp*. citri*

By

Yinping Guo

August 2011

Chair: Nian Wang
Major: Microbiology and Cell Science

Xanthomonas citri subsp. *citri* (XCC) is the causal agent of citrus canker which is one of the most serious diseases of citrus. Citrus canker has a significant impact on national and international citrus markets and trade. An understanding of virulence mechanism of XCC would assist the development of effective control measures against citrus canker. The goals of this study are to identify potential virulence traits of XCC and to characterize the underlying regulatory mechanisms coordinating gene expression in XCC during citrus canker infection. Transposon insertion mutagenesis showed that *galU* was required for biosynthesis of extracellular polysaccharides, capsular polysaccharide, biofilm formation, and virulence on host. Further study revealed that *galU* is critical for bacterial fitness in planta. To understand the regulatory mechanisms coordinating the expression of virulence traits in XCC, we designed and conducted genome-wide microarray analyses to identify genes under control of HrpG and HrpX, which are critical regulators for the pathogenicity of XCC. It showed that HrpG and HrpX not only control diverse virulence traits, but also regulate multiple cellular activities responding to the host environment, such as amino acid biosynthesis, oxidative phosphorylation, pentose-phosphate pathway, transport of sugar, iron and potassium, and the phenolic

catabolism. To study the regulatory mechanism of quorum sensing on virulence traits of XCC, the mutants of the core genes of quorum sensing, *rpfF*, *rpfC* and *rpfG* genes, were constructed. Comparison of the transcriptomes of QS mutants with that of wild type stain revealed that QS temporally regulates the expression of a large set of genes, including genes involved in chemotaxis and flagellar biosynthesis, genes related to metabolism, and genes encoding virulence traits such as type II secretion system substrates, type III secretion system and effectors. Cross talk between the QS regulon and HrpG regulon has also been identified, suggesting that the interplay of global signaling network by HrpG and QS assists XCC to coordinate the expression of multiple virulence traits for modification and adaptation to the host environment during infection. Altogether, this study demonstrated the complexity of signaling pathways underlying the regulation of XCC virulence traits and the interplay between the regulatory cascades.

CHAPTER 1
LITERATURE REVIEW

Citrus Canker

The genus *Xanthomonas* is an important group of Gram-negative plant pathogenic bacteria, which infect approximately 124 monocotyledonous and 268 dicotyledonous plants (Leyns et al. 1984; Chan and Goodwin 1999). Among the diseases caused by members of the genus *Xanthomonas*, citrus canker is one of the most serious diseases of most commercial citrus cultivars, resulting in significant losses worldwide. Citrus producing areas without citrus canker consider the pathogen a quarantine pest due to the potential threat to citrus production. Thus, citrus canker has a significant impact on national and international citrus markets and trade, particularly fresh fruit (Gottwald et al. 2002). Citrus canker is caused by *Xanthomonas citri* subsp. *citri* (XCC) (syn. *Xanthomonas citri*; *Xanthomonas campestris* pv. *citri* or *Xanthomonas axonopodis* pv. *citri*) (Cubero and Graham 2002; Schaad et al. 2006; Vauterin et al. 1995). The Asiatic form or A type of citrus canker is the most virulent and affects the widest range of hosts, including *Citrus* spp. and many closely related rutaceous plants. Citrus canker disease is characterized by formation of necrotic raised lesions on leaves, stems and fruits. The symptoms develop in the following steps (Graham et al. 2004): (1) circular, water soaked lesions form on leaf, fruit, and stem tissues at the beginning; (2) the lesions become raised and blister-like, and growing into white or yellow spongy pustules; and (3) the pustules darken and thicken into a corky canker. Under favorable conditions of high moisture and temperature, severe infection results in defoliation, dieback, badly blemished fruit, and premature fruit drop. The economic impact of citrus canker on citrus industry is not only from the yield and quality reduction of the crop, but also from the

loss of markets, since infected fruits become less valuable or unmarketable (Graham et al. 2004).

The measures used to prevent and control citrus canker depend on the situation of canker infection in different citrus growing areas: in regions where citrus canker does not occur or has been eradicated, quarantine measures have been used to prohibit the introduction and spread of citrus canker; in regions where citrus canker is endemic, integrated control measures have been applied, including eradication of trees, quarantine, production of pathogen-free nursery trees, use of windbreaks, decontamination and spray of antibiotics and copper-based products (Graham et al. 2004). The eradication by removal of infected and exposed trees is the most effective measure to eliminate citrus canker before its further spread. However, this practice has been suspended in Florida in 2006 because of the expansion of the epidemic statewide caused by hurricanes in 2004 and 2005 (Gottwald and Irey 2007). Therefore, new strategies are needed for the management of citrus canker in endemic areas of citrus canker.

Although the canker disease is hard to eradicate, the disease cycle of XCC is relatively simple. During wet weather, bacteria ooze from existing lesions to provide inoculum for dispersal. Wind-driven rain and contaminated equipment spread the inoculum over short distances to new growth and other plants. XCC enters the host through natural openings, like stomata, or wounds. After successful infection, it takes 7-60 days or more for highly visible symptoms to appear (Gottwald et al. 2002).

Virulence Traits Used by XCC

The complete genome of XCC has been determined (da Silva et al. 2002). XCC strain 306 has one circular chromosome consisting of 5,175,554 base pairs (bp), and

two plasmids: pXAC33 (33,699-bp) and pXAC64 (64,920-bp). There are 4,313 genes in the chromosome of XCC, including 2,710 genes with assigned functions, 1,603 hypothetical genes and 62 structural RNA genes. The pXAC33 has 21 genes with assigned functions and 21 hypothetical genes; the pXAC64 has 39 genes with assigned functions and 34 hypothetical. Approximately 6% of XCC genes are involved in pathogenicity, virulence and adaptation, including genes encoding type III secretion system (T3SS), T3SS effectors, cell-wall degrading enzymes (CWDEs), toxins, bacterial adhesins and surface structural elements, as well as *rpf* (regulation of pathogenicity factors) genes which are related to cell-cell signaling (da Silva et al. 2002). Those virulence traits play diverse roles in the different stages of XCC infection and can be defined into two categories: bacterial surface structures, and secretion systems and their substrates.

Bacterial Surface Structures Serve as a Dual-Edged Sword—Important Virulence Traits and Plant Immunity Inducers

A large set of genes encoding cell surface structures have been identified in XCC either by molecular or by *in silico* studies, including genes encoding extracellular polysaccharides (EPS), lipopolysaccharides (LPS), capsular polysaccharides (CPS), type IV pili, adhesins, and flagellum. These surface structures have been demonstrated to be involved in the infection process of XCC or other *Xanthomonas* spp., such as the attachment to the plant surface, protection of bacteria from environmental stresses and invasion of host intercellular space. However, some of those structures may also contribute to pathogen associate molecular patterns (PAMPs) which can be recognized by plant surface-arrayed pattern recognition receptor-like kinases and induce PAMP-triggered immunity (PTI), such as flagellin and LPS (Schneider and Collmer 2010).

Extracellular polysaccharides

EPS molecules appear to be released onto the cell surface with no visible means of attachment and form an amorphous layer on the outer surface (Roberts 1996). The EPS produced by xanthomonads, xanthan, consists of repeating pentasaccharide units with the mannose-(β1,4)-glucuronic acid-(β-1,2)-mannose-(α-1,3)-cellobiose structure (Jansson et al. 1975). The *gum* gene cluster, which consists of 12 genes (*gumB* to *gumM*), is responsible for EPS production in *Xanthomonas* spp. Due to its hydrated and anionic properties, EPS contributes to the bacterial survival against environmental stresses, particularly dehydration. Moreover, EPS is a major component of biofilm of *Xanthomonas* spp. Mutations in *gum* genes of *Xanthomonas* spp. cause the loss of EPS production, abnormal biofilm structure and impaired epiphytic survival on hosts (Chou et al. 1997; Dunger et al. 2007; Rigano et al. 2007; Kim et al. 2009b). Besides the contribution to bacterial survival against environmental stresses, EPS is also important as virulence factor in some systems. EPS was shown to suppress callose deposition in the plant cell wall (Yun et al. 2006).

Lipopolysaccharides

LPS is a unique and major outer membrane component of Gram-negative bacteria, which is a large molecule consisting of three domains: a membrane-associated lipid A, and a core oligosaccharide and polysaccharide side chains (O-antigen). The gene clusters of *Xanthomonas* spp. involved in LPS biosynthesis vary in numbers and sequence similarity (Lu et al. 2008). In XCC, those genes are located in two regions: genes encoding transferases, epimerases, translocases, and derived sugar transporters are located in the first region, whearas *xanAB* and *rmlDABC* genes

encoding nucleotide-sugar and dTDP-L rhamnose biosynthesis are located in the second region (da Silva et al. 2002).

LPS contributes to the structural integrity of the bacteria and also serves as protective barrier for bacteria against the attack of toxic chemicals in hostile environments. Mutations in LPS genes of XCC lead to impaired biofilm formation, increased sensitivity to environmental stresses and reduction of virulence (Li and Wang 2011). However, LPS is well-known as an endotoxin that elicits strong immune responses in animals. Furthermore, it has also been implicated as a major PAMP triggering basal defense responses in plant, which include oxidative burst, the production of reactive nitrogen species, the production of antimicrobial compounds (phytoalexins), thickening of the plant cell wall, and expression of pathogenesis-related genes (Newman et al. 2007).

Capsular polysaccharides

CPS is a highly hydrated molecule composed of repeating monosaccharides which are linked by glycosidic bond. It is bound to the cell surface via covalent link to either phospholipid or lipid A molecule and constitutes the outermost layer (capsule) of the bacterial cell. Capsules are found in a broad range of bacteria such as *Escherichia coli*, *Acinetobacter calcoaceticus*, *Erwinia stewartii*, *Klebsiella pneumonia* (Roberts 1996). The functions of capsule include prevention of desiccation, adherence to surface or other cells, and resistance to specific and nonspecific host immunity (Roberts 1996). The role of CPS in plant-pathogen interaction has not been fully elucidated. In XCC, mutation of *opsX* gene leads to decreased EPS production, the loss of capsule, abnormal LPS and the loss of virulence in citrus. Furthermore, capsule-like structures around XCC were observed in infected Mexican lime and Yuzu leaves by transmission

electron microscopy (Lee et al. 2009). These studies indicate that CPS is also important for XCC during infection.

Type IV pili

Type IV pili are filamentous appendages on cell surface and are responsible for bacterial twitching motility. They are also known as fimbrial adhesins for host colonization and adhesion in many animal and plant bacterial pathogens, such as *Pseudomonas aeruginosa* (Hahn 1997), and *P*. *syringae* (Hirano and Upper 2000). Comparative genomic analysis revealed that a large set of genes involved in type IV pilus biosynthesis exist in XCC genome (da Silva et al. 2002), including *fimA*, *fimT* and 26 *pil* genes (*pilA* to *pilY1* and *pilZ*).

Nonfimbrial adhesins

Besides the fimbrial adhesins, bacterial attachment also can be achieved by nonfimbrial adhesins, which are type V secretion system substrates such as the autotransporters of type V secretion system (e.g. YadA in *Yersinia* spp.) and two-partner secretion substrates (e.g. FhaA in *Bordetella pertussis*) (Gerlach and Hensel 2007). Comparative genomic analysis revealed that XCC contains multiple genes encoding nonfimbrial adhesins such as *xadA*, *xadB* and genes encoding filamentous hemagglutinins (e.g. *XACFhaB* and *XACFhaC*). Mutations in *XACFhaB* caused the lack of adhesion to abiotic and biotic surfaces, abortion of biofilm formation and reduced virulence in XCC, suggesting that hemagglutinin proteins are important for tissue colonization (Gottig et al. 2009b). Although other nonfimbrial adhesins have not been intensively studied in XCC, some of them have been reported to contribute to host attachment and are presumably involved in different infection stages in many plant pathogenic bacteria, such as XadA and XadB in *X. oryzae* pv. *oryzae* (Das et al. 2009),

HecA in *Erwinia chrysanthemi* (Rojas et al. 2002), HfxB and XadA in *Xylella fastidiosa* (Feil et al. 2007).

Flagellum

The flagellum is a tail-like projection which allows the flagellated bacterium to swim towards nutrients, or to move away from harmful chemicals. The flagellum is involved in surface attachment, biofilm formation, as well as in entering and exploiting hosts in many pathogenic bacteria such as *Helicobacter pylori*, *H. muslelae*, *Campylobacter jejuni*, and *Vibrio cholera* (Josenhans and Suerbaum 2002). Non-flagellated mutants showed significantly reduced ability to colonize the hosts.

XCC bears a single polar flagellum. Comparative genomic analysis revealed that XCC contains a full set of genes for flagellar biosynthesis and chemotaxis pathway (da Silva et al. 2002), suggesting that flagellum plays an important role in the XCC life cycle. Mutations in *fliC* and *flgE* in XCC , which encode flagellin and hook, respectively, resulted in decreased swimming motility, abnormal biofilm structure, and reduced virulence in host (Malamud et al. 2011).

The flagellum is also well known as PAMPs which induces defense response in plants or immunity in animals. Several studies showed that the flagellar motility is dispensable for the full virulence when bacteria live in hosts (Malamud et al. 2011; Schreiber and Desveaux 2011). Therefore, bacteria have to manipulate diverse virulence traits for better growth in host and also suppress flagellar functions for avoidance of host defense response.

Secretion Systems and Their Substrates

The transport of macromolecules across the bacterial cell membranes is an important function in bacteria, particularly in pathogenic bacteria. This critical function is

fulfilled by secretion systems. To date, secretion systems have been classified into seven types in bacteria, type I to type VII, according to their composition, function and substrates (Tseng et al. 2009). Except for type VII secretion system which is specific to Gram-positive bacteria, the other six secretion systems (type I to type VI) have been discovered in Gram-negative bacteria. Comparative genomic analyses revealed that all six secretion systems exist in XCC (da Silva et al. 2002; Van Sluys et al. 2002; Shrivastava and Mande 2008), although not all the secretion systems have been well studied in this bacterium.

Type I secretion system

Type I secretion system (T1SS), which is Sec-independent, exports substrates in a one-step process across both inner and outer membranes of bacteria. It consists of three major components: an ATP-binding cassette (ABC) transporter in the inner membrane, an outer membrane factor (OMF) serving as a protein channel in the outer membrane, and membrane fusion protein (MFP) connecting the inner and outer membrane components. The ABC-transporter specifically recognizes the C-terminal uncleaved secretion signal of T1SS substrates and provides the energy for the translocation by ATP hydrolysis. T1SS plays an important role in pathogenic bacteria by secreting toxins (e.g. hemolysins), lipases and proteases (Gerlach and Hensel 2007). T1SS has not been demonstrated to contribute to virulence of XCC yet. However, in a closely related species *X. oryzae* pv. *oryzae*,T1SS is required for transport of an avirulent factor AvrXa21, which can be recognized by its host receptor Xa21 resulting in a host resistance response (da Silva et al. 2004).

Type II secretion system

Type II secretion system (T2SS) was first identified in *K. oxytoca* (d'Enfert et al. 1987), and later was found as a common secretion system in many Gram-negative bacteria (Cianciotto 2005). A number of possible virulence factors are secreted via T2SS, including cell wall degrading enzymes (CWDEs), proteases, lipases and phosphatases. Unlike T1SS, it is a Sec-dependent system. T2SS mediated translocation occurs in two steps: the substrates with a signal peptide are translocated across the inner membrane via the Sec pathway; and then they are exported across the outer membrane via the T2SS translocation pore, which is formed by approximately 12-15 components in the outer membrane (Sandkvist 2001).

XCC has two independent T2SS, which are encoded by *xcs* and *xps* gene clusters (da Silva et al. 2002). Moreover, a large number of genes encoding T2SS substrates are present in XCC genome, particularly CWDEs (e.g. 6 copies of genes encoding pectinolytic enzymes and 12 copies of genes encoding cellulolitic and hemicellulolytic enzymes). Despite the progress in studying the T2SS, the precise contribution of T2SS substrates to the virulence of XCC remains largely unknown.

Type III secretion system

Type III secretion system (T3SS) is a key pathogenicity factor employed by most Gram-negative bacterial pathogens. T3SS is conserved in plant and animal pathogenic bacteria such as *Yersinia* spp., *Shigella flexneri*, *Salmonella typhimurium*, *E. coli*, *Ervinia amylovora*, *P. syringae*, *Xanthomonas* spp. and *Ralstonia solanacearum*. It consists of more than 20 proteins which form needle-like complex to deliver effector proteins directly from the bacterial cytoplasm into the host cells (Hueck 1998; Buttner and Bonas 2002). In plant pathogens, the T3SS genes are called *hrp* (hypersensitive

response and pathogenicity) genes and some are also refered to as *hrc* (hypersensitive response and conserved) genes. Those genes are required both for bacterial pathogenicity and induction of hypersensitive response on hosts and non-hosts, respectively (Lindgren et al. 1986; Alfano and Collmer 1997; Roine et al. 1997). The comparative genomic studies showed that the XCC genome has a *hrp* cluster which consists of 26 genes from *hpa2 to hrpF* (da Silva et al. 2002).

The substrates secreted into host cells by T3SS are called T3SS effectors, which are essential for the virulence of many plant pathogens. Many effectors have been identified as the products of avirulence genes that are recognized by corresponding plant disease resistance proteins, e.g., AvrBs1 in Xcv (Ronald and Staskawicz 1988). With the increase of sequenced bacterial genomes, candidate effectors were identified based on homology to known effectors from other pathogens by *in silico* prediction, e.g., *xopC* and *xopJ* (Noël et al. 2003). According to experimental and bioinformatic analyses, 24 T3SS effectors have been found in XCC genome (Moreira et al. 2010). Due to functional redundancies among T3SS effectors, mutation of individual effector genes usually does not affect bacterial virulence except PthA (Roden et al. 2004). PthA is a virulence determinant and can confer ability to cause canker-like symptom to strains that cannot cause canker (Swarup et al. 1991).

The major function of T3SS effector proteins is to optimize the host cell environment for bacterial growth either by interfering with host defense responses or by modifying the normal cellular function of host proteins (Nomura et al. 2005; Grant et al. 2006). This can be achieved by enzymatic activities of some T3SS effectors to modify host proteins and by transcription activator activities of effectors in AvrBs3/PthA family

to alter host transcriptome. Two families of T3SS effectors have shown cysteine protease activity such as YopJ/AvrRxv family and XopD. For instance, AvrXv4 from *X. campestris* pv. *vesicatoria* is a small ubiquitin-related modifier (SUMO) protease in YopJ/AvrRxv family. It blocks the SUMO-conjugation of plant proteins and subsequent proteolysis (Roden et al. 2004). The effectors in AvrBs3/PthA family are transcription activators which target host transcription. PthA is the first member of AvrBs3/PthA family which was experimentally identified for its virulence activity (Swarup et al. 1991). The amino acid sequences of effectors of AvrBs3/PthA family share striking features: a central repetitive region composed of nearly identical repeats of usually 34 amino acids, and a nuclear localization signal and an acidic activation domain (Gürlebeck et al. 2006). It has been demonstrated that AvrBs3 acts as a transcription activator and binds to the promoter of *upa20*, which encodes a transcription factor that induces plant cell hypertrophy (Kay et al. 2007).

Type IV secretion system

Type IV secretion system (T4SS) is a unique secretion system which can transport macromolecules (proteins or protein-DNA complexes) from bacterial cytoplasm into eukaryotic cells or other bacterial cells (Christie et al. 2005). As a one-step secretion system, the T4SS apparatus spans both inner and outer membranes of the Gram-negative bacterial cell and the cell envelope of Gram-positive bacterial cell. The well-studied T4SS is the *vir*-encoded system of *Agrobacterium tumefaciens*. It delivers T-DNA with protein from Ti plasmid of *A. tumefaciens* into the host to cause the formation of crown gall tumors. The homologous T4SS has been found in many bacteria, such as *H. pylori* (CAG; ComB), *P. aeruginosa* (TraS/TraB), *Bordetella pertussis* (Ptl), *E. coli* (Tra), *Legionella pneumophila* (Dot) (Christie et al. 2005). Moreover, it has been

demonstrated that T4SS also transports effector proteins into host cell to induce alteration of host cellular processes during infection. For instance, *H. pylori* translocates effector protein CagA into host cell and cause inflammatory responses and cystoskeletal alterations (Backert and Meyer 2006).

There are two T4SS gene clusters found in XCC, one in the chromosome and the other in the plasmid pXAC64. However, neither cluster allows a complete T4SS due to the lack of *virB5* and *virB7* in both clusters and the lack of *virD4* in the plasmid (da Silva et al. 2002). The products of those missing genes are important components for successful translocation of T4SS substrates or for the structural complex of the secretion system: VirD4 is a coupling protein which forms oligomers and binds to single-stranded DNA and double-stranded DNA for translocation; VirB5 is a minor component of T4SS pilus which may mediate pilus biosynthesis and is involved in adhesion; VirB7 is one component of the core complex and also links core complex and pilus constituents (Yeo and Waksman 2004). Therefore, it remains unclear if the two sets of T4SS are functional in XCC.

Type V secretion system

Type V secretion system (T5SS) is the simplest secretion system with respect to the number of protein components associated with the complex, and is also the largest family of protein-translocating outer membrane porins in Gram-negative bacteria (Yen et al. 2002). It is classified into three sub-groups based on the secretion mechanisms: T5aSS is the autotransporter system; T5bSS is the two-partner system and T5cSS is the oligomeric coiled-coil adhesin (Oca).T5aSS is a module of autotransporter protein containing three domains: a N-terminal signal peptide, a passenger domain and a translocation unit at C-terminal end. The autotranspoter protein with N-terminal signal

peptide is translocated from cytoplasm into periplasm via Sec-system. The C-terminal translocation unit inserts into the outer membrane and forms a beta-barrel secondary structure, which facilitates the translocation of the passenger domain into extracellular space. After translocation to the final destiny, the passenger domain either remains attached to the beta-barrel as an adhesin, or is cleaved from the beta-barrel and forms an active enzyme or toxin. In contrast to the single polypeptide of T5aSS, T5bSS consists of two separate proteins (one passenger and one transporter) whereas T5cSS contains trimeric proteins for the formation of beta-barrel secondary structure.

A large number of proteins, which are translocated via T5SS, contribute to bacterial virulence, including enzymes (proteases, peptidases, lipase, esterase), toxins, and adhesins (Gerlach and Hensel 2007). As mentioned above, a group of nonfimbrial adhesins are secreted via T5SS

Type VI secretion system

A novel secretion system, type VI secretion system (T6SS), was identified and characterized in *V. cholera* (Pukatzki et al. 2006) and *P. aeruginosa* (Mougous et al. 2006) in 2006. Comparative genomic analysis revealed the presence of T6SS in more than 25% of sequenced bacterial genomes, including many proteobacteria, planctomycetes, and acidobacteria (Shrivastava and Mande 2008). For example, XCC, *X. campestris*, and *X. oryzae* share 14 out of the total 18 genes belonging to T6SS of *V. cholera*. T6SS has been speculated to evolve from the bacteriophage base-plate, due to the homologies shared by several subunits of T6SS and subunits of the bacteriophage T4 tail spike (Cascales 2008). Although the detailed assembly mechanism is not clear, the T6SS forms a phage-tail-spike-like complex to inject effector proteins directly into host cytoplasm like T3SS and T4SS. It is required for virulence in animal and plant

pathogenic bacteria such as *V. cholera*, *Edwardsiella tarda*, *P. aeruginosa*, *Burkholderia mallei*, *A. tumefaciens*, *Pectobacterium atrosepticum* and *X. oryza* (Shrivastava and Mande 2008; Pukatzki et al. 2009).

Regulatory Mechanisms Coordinating the Expression of Virulence Traits

As we discussed above, a large number of virulence genes found in XCC genome are potential or known weapons employed by XCC for sucessful citrus canker infection. Bacteria have evolved global regulatory networks to coordinate the expression of these virulence traints which help them adapt to the environmental changes and evade the host defense. A few two-component signal transduction systems have been discovered to contribute to the global regulatory networks in *Xanthomonas* spp., including RavS/RavR, ColS/ColR, RpfC/RpfG (involved in quorum sensing (QS)), response regulator HrpG. Two-component systems usually consist of a membrane-bond histidine kinase sensor and a cytoplasmic response regulator. After perceiving a specific external signal, the histidine kinase sensor can be autophosphorylated and transfers a phosphoryl group to the receiver domain of cognate response regulator. Subsequently, the activated response regulator induces physiological changes by regulating the expression of target genes. A number of important physiological activities are under control of two-component systems in bacteria, including cell motility, biofilm formation, QS, and virulence, nutrition uptake. Since the first two-component system was discovered from *E. coli* (Ninfa and Magasanik 1986; Nixon et al. 1986), hundrends of two-component systems have been identified in bacteria, archaea and a few eukaryotic organisms, suggesting that two-componnet systems are one of the dominant mechanisms employed for detection and transduction of external signal (Stock et al. 2000).

Quorum Sensing Plays Critical Roles in Plant-Pathogenic Bacteria

QS is one of the sophisticated mechanisms of cell-to-cell communications in response to fluctuation in cell-population density. QS bacteria produce and release diffusible chemical signaling molecules into their environment. When the concentration of signaling molecules reaches a threshold, the bacteria detect and respond to this signal and alter their gene expression in order to regulate a diverse array of physiological activities. In the previous reports, there are various QS circuits identified from over 25 species of Gram-negative bacteria (Miller and Bassler 2001).

Among these QS systems, xanthomonads utilize novel signaling molecules rather than *N*-acyl derivatives of homoserine lactone (*N*-AHLs) which is used by most Gram-negative bacteria. Two different molecules for QS signaling were first discovered in *X. campestris* pv. *campestris*: (1) diffusible signaling factor (DSF), which has been characterized as the unsaturated fatty acid cis-11-methyl-dodecenoic acid (Wang et al. 2004); (2) diffusible factor (DF), which is an uncharacterized butyrolactone molecule. DF controls the production of the yellow pigment xanthomonadin and EPS (Poplawsky and Chun 1997), whereas DSF-mediated QS pathway regulates the production of extracellular enzymes (including proteases, pectinases and endoglucanase) and extracellular polysaccharides (EPS) as well as biofilm formation (Tang et al. 1991; Barber et al. 1997; Slater et al. 2000; Torres et al. 2007).The two molecules have overlapping functions and both are needed for the full virulence of *X. campestris* pv. *campestris*.

Compared to the DF-mediated QS, DSF-mediated QS has been studied extensively, To date, DSF has been found to be an important QS signal molecular in pathogens *Xylella*

fastidiosa (Newman et al. 2004), *Burkholderia cenocepacia* (Boon et al. 2008) and many *Xanthomonas* species (Chatterjee and Sonti 2002; Siciliano et al. 2006). The DSF-mediated QS pathway is conserved in those bacteria, in which *rpf* gene cluster is responsible for DSF production and signal transduction, including the core genes *rpfF*, *rpfC* and *rpfG* (Chatterjee and Sonti 2002; He et al. 2006; Siciliano et al. 2006). The *rpfF* gene encodes a putative enoyl-CoA hydratase that catalyzes the synthesis of signal molecule DSF. Extracellular DSF is sensed by a two-component signal transduction system consisting of the sensor protein RpfC and response regulator RpfG. Studies of DSF-mediated QS systems reveal that it has distinct regulatory functions among DSF-producing bacteria, although DSF-mediated QS pathway is conserved. For example, mutation in *rpfF* of *X. campestris* pv. *campestris* leads to defects in production of extracellular enzymes (e.g., proteases, pectinases and endoglucanase) and extracellular polysaccharides (EPS) as well as biofilm formation (Tang et al. 1991; Barber et al. 1997; Slater et al. 2000; Torres et al. 2007), whereas the *rpfF* mutants of *X. oryzae* pv*. oryzae* with reduced virulence are proficient for EPS and extracellular enzyme production (Chatterjee and Sonti 2002). In contrast to *Xanthomonas* spp., the *rpfF* mutants of *Xylella fastidiosa* are deficient in DSF production but are hypervirulent in host (Newman et al. 2004). It seems that the difference of DSF in regulation of diverse functions depends on plant pathogen species and their specific needs for infection.

However, the understanding of the downstream signaling pathway of QS in the bacterial cell is fragmentary. The demonstration that the HD-GYP domain of RpfG is a cyclic di-GMP phosphodiesterase indicates cyclic di-GMP is a second messenger in DSF signal transduction (Dow et al. 2006; Ryan et al. 2006). Cyclic di-GMP is

synthesized by proteins containing GGDEF domain which has diguanylate cyclase activity, whereas cyclic di-GMP is degraded by proteins containing EAL or HD-GYP domains which have phosphodiesterase. The high levels of cyclic-di-GMP promote biofilm formation, while low levels promote motility and transcription of virulence factors (Simm et al. 2004; Tischler and Camilli 2004; Römling et al. 2005). One important target of cyclic-di-GMP is Clp (cAMP receptor protein–like protein) which is a transcriptional activator. Microarray analyses reveal that Clp is involved in the DSF-mediated QS system in *X. campestris* pv. *campestris* (He et al. 2006; He et al. 2007). Cyclic-di-GMP binds to the Clp to prevent it from DNA binding and the induction of the expression of genes encoding extracellular enzymes, and genes involved in T3SS, and EPS biosynthesis (He et al. 2007). Two transcriptional factors, FhrR and Zur were identified in the transcriptomic analysis of Clp regulon of *X. campestris* pv. *campestris* (He et al. 2007). FhrR controls the expression of genes encoding flagellar, T3SS and ribosomal proteins, while Zur regulates genes involved in iron uptake, multidrug resistance and detoxification (Huang et al. 2009).

Transcriptome analysis of the RpfF regulon has significantly advanced understanding of the DSF-mediated QS regulons in bacteria. One pioneer work done by Zhang and colleagues compared the gene expression profile of the *rpfF* mutant with the wild-type strain of *X. campestris* pv. *campestris* using whole genome-wide microarray analysis. In that study, 165 genes were identified as belonging to the QS regulon, which were classified into 12 functional groups including genes encoding extracellular enzymes and genes involved in EPS production, flagellum synthesis, resistance to toxins and oxidative stress, and aerobic respiration and other processes (He et al.

2006). A later study utilizing proteomic analysis revealed that 48 proteins were differentially regulated by QS in *X. oryzae* pv. *orzicola*, 18 proteins of which were identified by mass spectrometry analysis to be involved in nitrogen transfer, protein folding, resistance to oxidative and flagellar synthesis (Zhao et al. 2011). However, considering the complicated QS signal transduction cascade, a comprehensive understanding of the RpfC and RpfG regulons is lacking.

Regulators HrpG and HrpX

In *Xanthomonas* spp., the expression of *hrp* gene cluster which encodes T3SS is positively controlled by regulators HrpG and HrpX (Wengelnik and Bonas 1996; Wengelnik et al. 1996b). HrpG is a response regulator of OmpR family and works with an unknown sensor kinase to detect environmental signals. Previous studies showed that the significant induction of *hrpG* expression was observed only in minimal media or in plant apoplast, rather than in rich media or on leaf surface (Wengelnik et al. 1996b).The activated HrpG positively controls the expression of *hrpX*, whose product is an AraC-type transcriptional activator. HrpX subsequently induces the expression of *hrp* gene cluster (Wengelnik and Bonas 1996). DNA affinity enrichment study revealed that HrpX binds to a conserved *cis*-regulatory element which is present in the promoter regions of *hrp* operons (Koebnik et al. 2006). This element with consensus sequence (TTCGC-N_{15}-TTCGC) was named the plant-inducible promoter (PIP). Besides the PIP box, another conserved sequence element (YANNRT) is present in the -10 promoter region of most *hrp* operons (Ciesiolka et al. 1999; Cunnac et al. 2004). However, a number of genes without a PIP box are also controlled by HrpX (Koebnik et al. 2006), indicating that PIP is not necessary for the expression of genes in HrpX regulon.

It seems that HrpX and HrpG not only regulate *hrp* genes, but also affect gene expression of other virulence factors, thus to coordinate the infection of the pathogen. The cDNA amplified fragment length polymorphism analysis in *X. campestris* pv. *vesicatoria* revealed that HrpG not only regulates the expression of *hrp* genes, but also positively controls T3SS effector and T2SS substrates. Recent studies showed that more type II secretion system (T2SS) substrate genes also belong to the HrpG and/or HrpX regulon (Furutani et al. 2004; Wang et al. 2008; Yamazaki et al. 2008). T2SS substrates including proteases, lipases and CWDEs might contribute to bacterial infection by degradation of the plant cell wall. Co-regulation of T3SS and T2SS may help bacteria overcome plant defenses and acquire nutrients for growth *in planta*. Despite the previous studies that have been performed to identify genes in the HrpG and/or HrpX regulon, no comprehensive study of the HrpG and HrpX regulons has been done in *Xanthomonas* spp.

RavS/RavR and ColS/ColR Two-Component Systems

Bioinformatic analysis of complete sequenced genomes of six *Xanthomonas* spp. revealed that each strain has a large number of genes encoding two-component systems, which account for approximately 3% of the genome sequence in these bacteria (Qian et al. 2008a).For instance, there are 114 genes in XCC genome encoding predicted sensor kinase and response regulators, 106 genes in *X. campestris* pv. *campestris* strains 8004 and ATCC33913, and 121 genes in *X. campestris* pv. *vesicatoria* 85-10 (Qian et al. 2008a). Besides RpfC/RpfG (in DSF-mediated QS) and response regulator HrpG that we discussed above, the well known two-component systems involved in virulence of *Xanthomonas* spp. also include RavS/RavR, ColS/ColR.

RavS/RavR two-component system was first determined to be involved in virulence of *X. campestris* pv. *campestris* strains ATCC33913 and XN1 (Qian et al. 2008b; He et al. 2009). The mutation of RavR orthologs resulted in decreased production of EPS and extracellular proteases as well as reduced bacterial virulence on hosts. However, mutation of the RavR homolog in *X. campestris* pv. *campestris* strain 8004 does not affect virulence (Osbourn et al. 1990). This difference in virulence suggests strain specific difference exist in the regulatory function of RavS/RavR (Qian et al. 2008b; He et al. 2009). RavS is a histidine kinase sensor containing two PAS domains in the N-terminal sensor region, while RavR is a response regulator containing both GGDEF and EAL domains. The presence of PAS domains in RavS suggests that RavS is involved in detection of signals from light, oxygen or redox potential (Hefti et al. 2004). Biochemical analysis showed that RavR acts as an EAL domain-associated cyclic di-GMP phosphodiesterase, suggesting that RavR controls virulence genes by regulating cyclic di-GMP level which works similarly to RpfC/RpfG system (He et al. 2009). Tanscriptomic analysis revealed that RavS/RavR controls more than 206 genes including *hrp* genes, genes involved in the productions of EPS, LPS and extracellular enzymes (He et al. 2009). Similar to the DSF-mediated QS system, RavS/RavR system also employs the global regulator Clp to regulate virulence gene expression, suggesting that bacteria coordinate the production of virulence traits by sensing population density and environmental stimuli (He et al. 2009).

ColS/ColR is another well-studied two-component system in *Xanthomonas* spp. It was first discovered in the biocontrol bacterium *P. fluorescens* as a regulatory system controlling the colonization of plant roots (Dekkers et al. 1998). Subsequently, this

system has been found in many bacteria, particularly in plant pathogens such as *P. syringae* (Buell et al. 2003), *R. solanacearum* (Salanoubat et al. 2002), *X. campestris* (Zhang et al. 2008), *X. oryzae* (Lee et al. 2005) and XCC (da Silva et al. 2002; Yan and Wang 2011). ColS is a histidine kinase sensor containing a HAMP domain, and ColR is an OmpR-type response regulator. Mutagenesis analysis conducted on XCC and *X. campestris* pv*. campestris* revealed that ColS/ColR system contributes to virulence by regulating the expression of genes involved in T3SS, LPS production, catalase activity and resistance to environmental stresses such as phenol, hydrogen peroxide and copper (Zhang et al. 2008; Yan and Wang 2011). Intriguingly, ColS/ColR system, which is not under control of key regulators HrpG and HrpX, regulates only *hrpC* and *hrpE* operons from *hrp* gene clusters in both xanthomonads. This indicates that besides HrpG/HrpX, other signaling systems like ColS/ColR also partially contribute to the regulation of key virulence trait T3SS.

Project Goals and Objectives

The goals of this study are to identify potential virulence factors of XCC and to characterize the regulatory mechanisms underlying the coordination of gene expression in XCC for citrus canker infection. The objectives are to (1) identify and characterize avirulent mutants from XCC Tn5 transposon library; (2) characterize the HrpG and HrpX regulons using whole-genome microarray; and (3) define the DSF-mediated QS regulon and the role of QS in citrus canker disease cycle.

CHAPTER 2
THE *galU* GENE IS ESSENTIAL FOR POLYSACCHARIDE PRODUCTION, PATHOGENICITY AND GROWTH IN PLANTA OF *Xanthomonas citri* subsp. *citri*

Introduction

Genome sequencing of XCC has greatly advanced our understanding of the interaction between XCC and citrus. XCC encodes 4,313 genes, including 2,710 genes with assigned functions, 1,603 without known functions and 62 structural RNA genes (da Silva et al. 2002). About 6% of XCC genes are involved in pathogenicity, virulence, and adaptation. Even though 62.83% of the predicted open reading frames have been assigned functions, functional studies are necessary to experimentally characterize the genes related to XCC pathogenesis and host adaptation. Transposon mutagenesis has been widely used for that purpose (Jacobs et al. 2003; Liberati et al. 2006; Salama and Manoil 2006; Laia et al. 2009).

GalU is a UTP-glucose-1-phosphate uridylyltransferase (synonym: UDP-glucose pyrophophorylase), catalyzes the formation of UDP-glucose from glucose 1-phosphate and UTP. UDP-glucose is involved in synthesis of glucosylated surface structures as a substrate for glucosyltransferase, and serves as a glycosyl donor in the enzymic biosynthesis of complex carbohydrates (Stimson et al. 1995). Mutations of the *galU* gene led to reduced virulence of a number of bacterial pathogens, including *E. coli* (Komeda et al. 1977; Ho and Waldor 2007), *K. pneumoniae* (Chang et al. 1996), *Shigella flexneri* (Sandlin et al. 1995), *Actinobacillus pleuropneumoniae* (Rioux et al. 1999), *V. cholerea* (Nesper et al. 2001), *P. aeruginosa* (Priebe et al. 2004), and Mesophilic *Aeromonas hydrophil*a (Vilches et al. 2007). The reduced virulence of those *galU* mutants was mainly associated with the changes in lipopolysaccharides, capsular polysaccharides (CPS), or exopolysaccharides (EPS). GalU was also reported to be

involved in adhesion of *E.coli* (Genevaux et al. 1999). However, the role of the *galU* gene in the virulence of XCC and other plant pathogenic bacteria has not been studied. In this study, we characterized the *galU* gene of XCC. This is part of our effort in characterizing critical genes involved in virulence of XCC. To our knowledge, it is the first report on *galU* for plant pathogenic bacteria.

Materials and Methods

Bacterial Strains and Growth Media

All the strains used in this study are listed in Table 2-1. XCC wild type 306 (rifamycin resistant) and mutant strains were grown in nutrient broth/agar (NB/NA) or NYG medium (Daniels et al. 1984) at 28ºC. *E*. *coli* strains were grown in Luria-Bertani (LB) medium at 37ºC. Antibiotics were used at the following concentrations (µg/mL): rifamycin (Rif), 50; kanamycin (Km), 50; ampicillin (Ap), 50; gentamicin (Gm), 5 and chloramphenicol (Cm), 35.

Construction of *Xanthomonas citri* subsp. *citri* Mutant Library

EZ-Tn5™ <R6Kγori/KAN-2>Tnp Transposome™ Kit (Epicentre, Madison, WI, U.S.A.) was used to make the mutant library of XCC following the manufacturer's instructions. The recovered cells were diluted 500-1000 times and spread on NA plates containing Rif + Km and incubated at 28ºC for 2-3 days. Mutants were kept at -80ºC in 20% glycerol for future use. The mutant library was screened by pathogenicity assays (described later) on susceptible host, Duncan grapefruit (*Citrus paradisi* Macf. cv. Duncan). The mutants that caused no or reduced symptoms were selected for further study.

Rescue Cloning of Two Non-Mucoid Mutants

Two non-mucoid mutants D12 and F6 (Table 2-1) were chosen from the mutant library for further analysis based on the non-pathogenic phenotype in pathogenicity assays. To identify the insertion site of the two mutants D12 and F6, the rescue cloning method was used following the manufacturer's instructions (Epicentre). Briefly, genomic DNA (1 µg) of D12 and F6 transformants were digested overnight with *Bam*H1 and *Sph*1 and end-repaired (made blunt-ended) using T4 DNA polymerase (New England Biolabs, Ipswich, MA, U.S.A) and 5'-phosphorylated in order to be self-ligated. The digested DNA was purified using Wizard® SV Gel and PCR Clean-Up System (Promega, Madison, WI, U.S.A.) and allowed to self ligate in the presence of T4 DNA ligase in 10 µL volume for 4 hours at 16ºC. The ligation mix was electroporated into TransforMax EC100D *pir*$^{+}$ electrocompetent *E. coli* (Epicentre). Cells were immediately transferred into a 17×100-mm round bottom polypropylene tube which has 1 mL Super optimal broth with catabolite repression (SOC) (Hanahan 1983) and gently mixed by pipetting. The cells were incubated for 1 h at 37ºC with gentle shaking and plated on LB agar containing Km Plasmid from Km resistant colonies was purified and sequenced with R6KAN-2 RP-1 and KAN-2 FP-1 primers (Table 2-2). Sequencing was performed at Interdisciplinary Center for Biotechnology Research sequencing facility at the University of Florida. Using the genome sequence of the XCC strain (da Silva et al. 2002), transposon insertion sites in F6 and D12 transformants were identified by alignment of the mutated loci and the corresponding sequence of XCC 306.

Nucleic Acid Isolation and PCR

Genomic DNA was extracted using the Wizard® Genomic DNA Purification Kit (Promega) following the protocol for isolating genomic DNA from bacteria. After DNA

precipitation, the pellet was dried in a Vacufuge (Eppendorf, Westbury, NY, U.S.A.) for 5 min and dissolved in DNA rehydration solution supplied with the kit. Bacterial plasmid DNA was isolated using Wizard® miniprep DNA purification system (Promega). The concentration and purity of DNA was determined using an Agilent 8453 UV-Visible spectrophotometer (Agilent Technologies, Santa Clara, CA, U.S.A.).

All conventional PCR reactions were performed in a Bio-Rad DNAEngine® Peltier thermal cycler (Bio-Rad, Hercules, CA, U.S.A.). Amplification of the DNA was performed in 50 µL total volumes with *Taq* DNA polymerase (Promega). The PCR conditions were 95°C for 5 min followed by 40 cycles of 30 s of denaturation at 95°C, 30 s of annealing at 52°C, and 1 to 3 min of extension depending on the length of the amplicons at 72°C.

Southern Blot Analysis

For Southern blot hybridization, genomic DNA samples were purified once again (after isolation using Wizard® Genomic DNA Purification Kit) using phenol:chloroform:isoamyl alcohol (25:24:1, v/v/v) and choloroform: isoamyl alcohol (24:1, v/v) following the standard molecular biology protocol (Sambrook and Russell, 2001). The DNA was precipitated, washed with 70% (v/v) ethanol and resuspended in RNase and DNase free water. Genomic DNA (3 µg per sample) was digested with *Bgl*II, subjected to electrophoresis on a 0.9% agarose gel and transferred to a positively charged nylon membrane (Roche, Indianapolis, IN, U.S.A.) according to standard procedures (Sambrook and Russell 2001). Probe generation, hybridization and chemiluminescent detection were performed using the DIG-High Prime DNA Labeling and Detection Starter Kit II as recommended by manufacturer (Roche).

Complementation of the *galU* Mutants

The entire *galU* gene with 624-bp upstream sequence and 388-bp downstream sequence was amplified from genomic DNA of XCC wild type strain 306 using PCR with primers CGU-F and CGU-R which contain a *Bam*H1 restriction site (Table 2-2). The resulting 1.9 kb fragment was ligated to pCR®2.1-TOPO® following the manufacturer's protocol (Invitrogen, Carlsbad, CA, U.S.A.), resulting in pCGU1.1. From pCGU1.1 a *Bam*HI fragment containing the *galU* gene was isolated and cloned into similarly digested pUFR053 which was treated with Alkaline Phosphatase, Calf Intestinal (New England Biolabs, Ipswich, MA, U.S.A.) (El Yacoubi et al. 2007), resulting in pCGU2.1 (Table 2-1). The plasmid pCGU2.1 was transferred into the *galU* mutants D12 and F6 (*galU*:Tn5) by triparental mating with helper *E. coli* strain containing pRK2013 (Swarup et al. 1991). The transconjugants were selected on NA with Rif and Gm. The presence of pCGU2.1 was verified using PCR. Complementation assays were conducted for EPS and CPS production, mucoid phenotype on NA medium, pathogenicity, and growth of the *galU* mutant in planta using plasmid pCGU2.1 containing an intact *galU* gene. Empty vector pUFR053 without the *galU* gene was used as control.

Quantitative Determination of EPS Production

For measurements of the quantity of EPS in culture supernatants, bacterial cells were grown in NB supplemented with 2% D-glucose at 28ºC for 24 h with shaking at 200 rpm. Then 10 mL of cultures were taken and cells were removed by centrifugation (5000×g for 20 min). Three volumes of 99% ethyl alcohol were added to the supernatants. The precipitated EPS was pelleted by centrifugation, dried and weighed (Vojnov et al. 1998). Three independent replicates were used for each strain. The test was performed three times independently and only results from one test were shown.

Capsule Assays

Bacteria were grown at 28°C on NA with appropriate antibiotics. Samples were prepared by mixing and spreading a loop of bacteria with one drop of distilled water on a precleaned slide, and air dried. The sample was stained with 1% crystal violet and washed with 20% copper sulfate supplied with the capsule stain kit (Eng Scientific Inc., Clifton, NJ, U.S.A.) following the manufacturer's instruction. The samples were photographed using a light microscope Leica DMLB2 (Leica Microsystems Wetzlar GmbH, Germany) under oil immersion lens at 1000 × magnification.

LPS Assays

Bacteria were grown overnight at 28°C in NB, M9 glucose medium (Clowes and Hayes 1968) or XVM2 medium (Wengelnik et al. 1996a). Ten mL cultures were harvested at the exponential phase of growth and pelleted. LPS was isolated and treated with proteinase K (Nesper et al. 2000), and then separated by sodium dodecyl sulfate-polyacrylamide gel electrophoresis (SDS-PAGE). Briefly, LPS samples were mixed with an equal volume of Laemmli sample buffer, pH 6.8, containing 62.5 mM Tris-HCl, pH 6.8, 2% SDS, 25% glycerol, and 0.01% bromophenol blue. The mixtures were boiled for 5 min, and 20 µL samples were loaded on precast Ready Gel Tris-HCl polyacrylamide gels (86 mm × 68 mm × 1.0 mm) containing 4 and 15% acrylamide in the stacking and separating gels, respectively (Bio-Rad Laboratories, Inc., Hercules, CA, U.S.A.). Electrophoresis was performed at 12 mA in the stacking gels and 25 mA in the separating gels until the bromophenol blue was 1 cm above the bottom of the gel. Immediately after electrophoresis the gel was stained using silver stain kit (Bio-Rad Laboratories).

Biofilm Assays

Biofilm formation was quantified in borosilicate glass tubes as described previously (Pratt and Kolter 1998). Bacteria were grown in NB under shaking to mid exponential growth and then diluted 1:10 in fresh NB containing appropriate antibiotics. One mL of diluted bacterial suspension was placed in each borosilicate glass tube (Fischer Scientific, Pittsburgh, PA, U.S.A.) and incubated without shaking for 48 h at 28°C. Culture media were poured out, and attached bacterial cells were gently washed three times with distilled water, incubated at 60°C for 20 min, and then stained with 1.5 mL 0.1% crystal violet for 45 min. The unbound crystal violet was decanted, and the wells were washed with water. The crystal violet stained cells were solubilized in 1.5 mL of ethanol-acetone (80:20, v/v). Biofilm formation was quantified by measuring absorbance at 590 nm using Agilent 8453 UV-Visible spectrophotometer. Ten replicates were used for quantitative measurement.

Pathogenicity Assays on Plants

Pathogenicity assays were conducted in a quarantine greenhouse facility at Citrus Research and Education Center, Lake Alfred, FL, U.S.A. Assays were performed using fully expanded, immature leaves of Duncan grapefruit. XCC wild type and mutant strains used in this assay were grown under shaking conditions at 28ºC for overnight in NB and were suspended in sterile tap water and the concentrations were adjusted to 10^8 CFU/mL. For the pathogenicity assays, bacterial suspensions of both 10^8 and 10^5 CFU/mL were injection infiltrated into leaves with a needleless syringe (Viloria et al. 2004; Rybak et al. 2009). The test was repeated three times with similar results. Disease symptoms were photographed 5, 10, and 12 days post inoculation (DPI).

Bacterial Growth Assays in Planta

For bacterial growth assays in the intercellular spaces of citrus leaves, the concentration of starting inoculum was 10^6 CFU/mL and whole leaves were inoculated by infiltration of the abaxial leaf surface with needleless syringe as described above. For co-inoculation, wild type 306 and D12 were mixed together (1:1) before inoculation. Briefly, bacterial cell counts were performed in four biological replications at each sampling time point (0, 1, 2, 3, 4, 6, 8, or 10 DPI). Leaf disks from inoculated leaves were excised with cork borer (1 cm^2 leaf area), which then were ground in 1 mL sterile tap water. The samples were serially diluted and plated on NA plates with appropriate antibiotics. The colonies were counted 48 hr after plating. The growth assays in planta were repeated three times independently with four replicates each time, but only one experiment was represented here.

RNA Extraction and Quantitative Reverse Transcription-PCR (QRT-PCR)

Bacteria were grown in XVM2 medium at 28°C with shaking at 200 rpm and 1 mL samples of culture were collected for XCC wild type and D12 at 13 hrs after inoculation. RNA was stabilized immediately by mixing with two volume of RNAprotect® bacterial reagent (Qiagen, Valencia, CA, U.S.A.) and incubated at room temperature for 5 min. Bacterial cells were centrifuged at 5000×g for 10 min and cell pellets were stored at -80°C prior to RNA extraction.

Cell pellets were treated with lysozyme and RNA extractions were performed using RNeasy® mini kit (Qiagen). Contaminated Genomic DNA was removed from RNA by treatment with a TURBO-DNA free™ kit (Ambion, Austin, TX, U.S.A.). The concentration of RNA was determined with NanoDrop ND-1000 spectrophotometer

(NanoDrop technologies, Wilmington, DE, U.S.A.) and adjusted to 50 ng/μL for QRT-PCR.

Fifteen target genes were chosen for expression study with 16S rRNA as the endogenous control and the primers listed in Table 2-3 were designed from sequences on XCC genome using DNASTAR software (DNASTAR, Inc., Madison, WI, U.S.A.). One step QRT-PCR was conducted on a 7500 Fast Real-Time PCR System (Applied Biosystems, Inc., Foster City, CA, U.S.A.) using Quantitect™ SYBR® Green RT-PCR kit (Qiagen). The total reaction volume of one step QRT-PCR was 25 μL and contained 2 × QuantiTect™ SYBR® Green RT-PCR Master Mix (12.5 μL), 10 μM gene-specific primers (1.25 μL), QuantiTect™ RT Mix (0.5 μL), and 50 ng of RNA template (1 μL). The reaction was incubated at 50°C for 30 min, and at 95°C for 15 min, cycled (40 times) at 94°C for 15 s, 53°C for 30 s, and 72°C for 30 s. The melting curve analysis was applied to verify the specificity and identity of QRT-PCR products. Three biological repeats were used for each strain. QRT-PCR was repeated once with another three independent biological repeats. Totally, six independent biological repeats were used for each strain.

The amount of fluorescence as a function of PCR cycle was plotted using 7500 Fast System SDS software and the threshold cycle (C_T) values for each gene were obtained. The ΔC_T values of each target gene were calculated by subtracting the C_T values of 16S rRNA (the endogenous control) from the C_T values of the target genes. The ΔC_T values of each gene for D12 and wild type were subjected to simple *t*-test using SAS and the $\Delta\Delta C_T$ values of target genes for D12 were yielded using wild type as calibrator as described previously (Yuan et al. 2006). The relative quantification of

target gene expression of D12 in XVM2 medium was generated using the formula $2^{-\Delta\Delta C_T}$, as relative-fold change in the transcript level with respect to the gene transcript level expression of wild type.

Results

Generation of the *galU* Mutants of XCC

Two non-mucoid XCC mutants, F6 and D12 were selected from the XCC EZ-Tn5 library. Compared to wild type 306 strain, the colonies of F6 and D12 on NA plates were smaller and less viscous. However, their growth rate was indistinguishable from wild type strain in NB broth (data not shown).

The sites of transposon insertion in F6 and D12 mutants were determined by rescue cloning. Sequencing results indicated that EZ-Tn5 was inserted between nucleotides 235-236 in D12 and between nucleotides 665-666 in F6 downstream of the translation start site (Figure 2-1A). The insertion of EZ-Tn5 in the *galU* gene was confirmed by PCR analysis. PCR with gene specific primers (*galU*-F1+*galU*-R1) targeted the amplification of interior region of *galU* (Table 2-2). This resulted in a 0.84 kb amplicon with XCC 306 genomic DNA as template but produced approximately 2.8 kb amplicons with F6 and D12 as templates due to the insertion of the 1.938 kb EZ-Tn5 transposon (Figure 2-1B). In addition, F6 and D12 transformants were confirmed to have a single copy of EZ-Tn5 using Southern blot analysis (Figure 2-1C). Southern blot analysis showed a DIG-labeled 675-bp Kan2 DNA fragment hybridizing to a 7.3 kb band of D12 and to a 2.8 kb band of F6. The size difference of bands hybridized for D12 and F6 resulted from difference in the relative distance and location of the transposon insertion sites from the restriction site of *Bgl*II, which was used for digestion of the genomic DNA, in the *galU* gene. For D12, EZ-TN5 (1.938 kb) was inserted into a *Bgl*II

fragment of 5.535 kb containing the 5' of the *galU* gene. For F6, EZ-TN5 (1.938 kb) was inserted into a *Bgl*II fragment of 0.9 kb containing the 3' of the *galU* gene. Consequently, a 7.3 kb band and a 2.8 kb band were hybridized for D12 and F6, respectively. This confirmed the insertion of a single copy of EZ-TN5 in the genomes of both F6 and D12 (Figure 2-1C). No hybridization was observed to the genomic DNA of XCC 306 wild type strain using the Kan2 probe.

The *galU* Gene Involvement with Polysaccharide Biosynthesis

In order to study the role of the galU gene in polysaccharide biosynthesis, the major polysaccharides of XCC, EPS, CPS, and LPS were investigated. Only one galU mutant, D12, was described here since no difference was observed between the two galU mutants D12 and F6. Significant difference in EPS production was observed between XCC wild type (1.325 mg/mL) and D12 (0.012 mg/mL). Complementation with the plasmid pCGU2.1 containing the entire galU gene restored EPS production of D12 (1.725 mg/mL). The empty vector pUFR053 did not affect EPS production (0.0175 mg/mL). D12 and wild type strains were stained using capsule stain kit and observed under microscope. XCC wild type strain was covered with capsule while capsule appeared to be absent in the galU mutant (Figure 2-2A). Complementation with plasmid pCGU2.1 restored the CPS phenotype of the D12 to wild type level. The empty vector pUFR053 did not complement the CPS production of D12 (Figure 2-2A). With proteinase K treatment, LPS pattern of the galU mutant strain was indistinguishable from that of wild type strain when they grew in NB, M9 glucose or XVM2 medium (data not shown). The mucoid phenotype of D12 strain was restored to that of the wild type colonies on NA by complementation with plasmid pCGU2.1 but not with the empty vector pUFR053 (data not shown).

The *galU* Gene Involvement with Biofilm Formation

Because of the significant effect of the *galU* gene on polysaccharide production, the *galU* gene was hypothesized to be involved in biofilm formation. As shown in Figure 2-2B, less biofilm was observed for the *galU* mutant compared to wild type strain. 10 replicates were used for quantitative measurement of biofilm. The absorbance of the crystal violet in biofilm staining assay of wild type strain (OD_{590} = 0.811 ± 0.083) was 12.5 times greater than that of the *galU* mutant strain D12 (OD_{590} = 0.065 ± 0.011). The biofilm formation of the D12 mutant strain was restored by complementation with plasmid pCGU2.1 containing the intact *galU* gene (OD_{590} = 1.753 ± 0.063) but not with the empty vector pUFR053 lacking the *galU* gene (OD_{590} = 0.040 ± 0.013).

Pathogenicity Assays

Pathogenicity assays indicated that neither F6 nor D12 elicited a reaction on grapefruit while wild type strain caused typical necrotic raised lesions typical of citrus canker on the leaves at a high bacterial inoculation concentration of 10^8 CFU/mL (Figure 2-3A). Similar results were observed for bacterial inoculation at a lower concentration of 10^5 CFU/mL (data not shown). Complementation with plasmid pCGU2.1 containing the entire *galU* gene restored the pathogenicity of D12 and F6 mutants and caused similar symptoms as wild type on grapefruit (Figure 2-3A). The empty vector pUFR053 without the *galU* gene did not complement the pathogenicity of both F6 and D12 and no symptoms were observed for both mutants on grapefruit leaves (Figure 2-3A).

Effects of Mutation of the *galU* Gene on Gene Expression of Key Virulence Genes

Loss of pathogenicity could result from down-regulation of key virulence genes. In order to test whether mutation of the *galU* gene affect gene expression of key virulence genes, QRT-PCR assays were conducted. XVM2 medium is reported to mimic the

environment of plant intercellular spaces and most virulence factors of *Xanthomonas* spp. can be induced in this medium (Wengelnik et al. 1996a; Astua-Monge et al. 2005). Therefore, D12 and wild type strains were grown in XVM2 medium, sampled at exponential phase and compared for the expression of 15 genes at transcription level using QRT-PCR. The 15 target genes included genes encoding enzymes involved in EPS and CPS biosynthesis, and virulence factors, such as type III secretion system (T3SS), effector proteins, and cell wall degrading enzymes (CWDE).

For QRT-PCR, the ΔC_T and $\Delta\Delta C_T$ values are more appropriate subjects for statistical analysis (Yuan et al. 2006). Student's t-test was performed for the ΔC_T of D12 and wild type strains, and $\Delta\Delta C_T$ values of target genes for D12 were yielded using wild type strain as calibrator. Table 2-4 shows that five genes were not differentially expressed in D12 and wild type strains when grown in XVM2, including three CWDE genes (XAC0160, *celD* and *pglA*), *kpsF* for CPS biosynthesis, and one T3SS effector *pthA*. However, the expression of seven genes was significantly up-regulated in D12 compared to the wild type strain, including two avirulence genes (*avr*XAC*E1*and *avrBs2*), one T3SS component *hrcV*, two T3SS regulator genes (*hrpG* and *hrpX*), one CWDE gene (*peh-1*) and *gumB* for EPS synthesis. Three genes encoding for CWDEs (XAC0028, *pelB* and XAC0165) were significantly down-regulated at transcription level in D12 compared to the wild type strain.

In Planta Growth of the *galU* Mutant

Since mutation of the *galU* gene did not impair most key virulence genes of XCC, loss of pathogenicity of the *galU* mutant was hypothesized to be due to the lack of growth in planta. To test this hypothesis, wild type and D12 mutant strains were tested for their growth in grapefruit leaves. Although no differences were observed between

wild type and the *galU* mutants in the ability to grow in NB medium (data not shown), growth of the *galU* mutant D12 was significantly reduced in planta compared to the wild type strain. The wild type strain population increased to 4×10^8 CFU/cm^2 at 10 DPI, compared to a population of 6×10^2 CFU/cm^2 for the *galU* mutant D12 in planta (Figure 2-3B). Strain D12 with complementation plasmid pCGU2.1 containing the entire *galU* gene grew to the same population level as the wild type in planta (Figure 2-3B). The empty vector pUFR053 without the *galU* gene did not restore the growth of D12 in planta.

To characterize whether wild type strain XCC affected the growth of the *galU* mutant in planta, wild type and D12 strains were co-inoculated into grapefruit leaves as described previously. Co-inoculation of wild type strain with D12 strain did not affect the growth of D12 in planta compared to D12 alone (Figure 2-3C).

Discussion

Multiple genes including *galETKM*, *galU* and *galR*, are involved in formation of the sugar nucleotide precursors, UDP-galactose and UDP-glucose, for polysaccharide synthesis. The *galETKM* genes normally form an operon while *galU* and *galR* genes are not clustered in the genome (Genevaux et al. 1999). The knockout of those genes affects the outer membrane properties of bacteria, and virulence to hosts in *K. pneumoniae* (Chang et al. 1996), *Streptococcus pneumoniae* (Mollerach et al. 1998), and *E. coli* O157:H7 (Ho and Waldor 2007). In this study, a *galU* mutant of XCC was characterized for effects on synthesis of major polysaccharides, pathogenicity, and growth in the intercellular spaces. Apparently, the *galU* gene in XCC is involved in EPS, and CPS production. This is consistent with the critical role of the UTP-glucose-1-phosphate uridylyltransferase, which is responsible for synthesis of UDP-glucose from

glucose 1-phosphate and UTP and galactose and glucose interconversion through the Leloir pathway and plays a pivotal role in carbohydrate metabolism in different organisms (Frey 1996). The phenotype apparently resulted from mutation of the *galU* gene rather than malfunction of downstream genes. The *galU* gene is the last gene of one operon containing XAC2295 encoding one hypothetical protein, XAC2294 encoding a lipopolysaccharide core biosynthesis protein, XAC2293 encoding a dehydratase, and the *galU* (da Silva et al. 2002). The intergenic space between the *galU* and the downstream gene *kefB* is 174-bp. The *galU* gene and the downstream *kefB* gene were predicted to belong to different operons based on operon prediction using SOFTBERRY (Softberry, Inc.). Thus, transposon mutation of the *galU* gene would not affect the function of the *kefB* gene. Plus, defects of EPS production, mucoid phenotype, pathogenicity, and growth in planta of the *galU* mutant were complemented to wild type level using plasmid pCGU2.1 containing an intact *galU* gene but not with the vector pUFR053 without the *galU* gene.

The mutation of the *galU* gene blocks the EPS and CPS polysaccharides biosynthesis in XCC. Both EPS and CPS polysaccharides are important components of bacterial outer surface. Capsular polysaccharides are linked to the cell surface while EPS molecules appear to be released onto the cell surface with no visible means of attachment and form an amorphous layer of outer surface (Roberts 1996). The EPS produced by xanthomonads, xanthan, consists of repeating pentasaccharide units with the mannose-(β1,4)-glucuronic acid-(β-1,2)-mannose-(α-1,3)-cellobiose structure (Jansson et al. 1975). Three sugar nucleotides, UDP-glucose, UDP-glucuronic acid and GDP-mannose, are required precursors for EPS synthesis. UDP-glucose is the

substrate for UDP-glucuronic acid synthesis and also affects the intercellular concentration of UDP-galatose (3). Mutation of the *galU* gene eliminated the synthesis of one of the major precursors, UDP-glucose, and may also affect UDP-glucuronic acid, for EPS synthesis in XCC. Therefore, EPS production is deficient in the *galU* mutant of XCC. Likewise, the deficiency of the major sugar nucleotide precursor, UDP-glucose, maybe UDP-galatose and UDP-glucuronic acid, resulting from mutation in GalU function, also accounts for the defect in CPS polysaccharide of the *galU* mutant. Previous study also indicates that GalU is involved in EPS and CPS polysaccharides synthesis (Mollerach et al. 1998; Mollerach and García 2000; Boels et al. 2001; Lai et al. 2001).

The lack of pathogenicity of the *galU* mutant results from its inability to grow in planta rather than from its effect on virulence genes. In order to understand why the *galU* mutant lost pathogenicity, we first investigated the effect of the *galU* gene on the expression of genes encoding EPS and CPS biosynthesis proteins, and key virulence factors, such as type III secretion system (T3SS), effector proteins, and cell wall degrading enzymes (CWDEs). Among them, the T3SS effector PthA is the pathogenicity determinant for XCC required to cause canker symptoms on hosts (Brunings and Gabriel 2003). The gene expression of *pthA* remained the same level in the *galU* mutant as in wild type strain. Overall, none of the virulence genes tested in this study showed reduced gene expression in the *galU* mutant except three CWDE genes whose involvement in virulence is still unknown in XCC. Growth assays indicate that the *galU* mutant grew poorly in the intercellular environment (Figure 2-3). This is probably due to deficiency in EPS and CPS polysaccharides synthesis which have been shown

to act as a barrier to stress conditions (Roberts 1996). Capsular polysaccharides have been reported to be essential for growth of the *Erwinia amylovora* in planta (Bugert and Geider 1995). Capsule-like structures around XCC were demonstrated in infected Mexican lime and Yuzu leaves by transmission electron microscopy (Lee et al. 2009). Interestingly, co-inoculation of wild type strain with D12 strain did not rescue the growth of D12 in planta*. Erwinia amylovora* exopolysaccharide amylovoran mutants can be rescued by wild type strains presumably by enveloping the mutant in a biofilm (Koczan et al. 2009). Apparently, the mechanism that the growth of the *galU* mutant was impaired in planta was different from that of the amylovoran mutants of *E. amylovora* and remains to be explored.

Interestingly, GalU represents a potential target for antimicrobial compounds screening to control citrus canker disease. Since GalU is required for XCC growth in planta, antimicrobial compounds inhibiting its activity should potentially render XCC virtually avirulent. In addition, prokaryotic UTP-glucose-1-phosphate uridylyltransferases appear to be completely unrelated to their eukaryotic counterparts and have totally different structures even though they have almost identical catalytic properties (Hossain et al. 1994). This interesting feature suggests that putative antimicrobial inhibitors of GalU might not be harmful for human and the citrus host.

In summary, our data provide insights of the roles of the *galU* gene in EPS, and CPS production as well as biofilm formation of XCC. Our study also suggests that the *galU* gene plays a pivotal role for XCC growth in the intercellular spaces of citrus leaves.

Table 2-1. Bacterial strains and plasmids used in this study

Strain or plasmid	Relevant characteristics	Reference or source
Strains		
E. coli		
Mach1™ T1R	F⁻ Φ80*lacZ*ΔM15 Δ*lacX*74 *hsdR*(r_K^-, m_K^+) Δ*recA*1398 *endA*1 *tonA*	Invitrogen
TransforMax	F⁻ *mcrA Δ(mrr-hsdRMS-mcrBC*) φ80d*lacZ*ΔM15 Δ*lacX*74 *recA*1 *endA*1	Epicentre
EC100D *pir*$^+$	*araD*139 Δ(*ara, leu*)7697 *galU galK* λ⁻ *rpsL nup*G *pir*$^+$ (DHFR)	
HB101	F⁻ *supE*44, *hsdS*20(r_B^- m_B^-), *recA*13, *ara*-14, *proA*2, *lacY*1, *galK*2, *rpsL*20, *xyl*-5, *mtl*-1, *leuB*6, *thi*	Boyer and Roulland-Dussoix 1969
X. citri subsp. *citr*i		
306	Rif^r, causes citrus canker on citrus	da Silva et al. 2002
D12	*galU*:Tn5 derivative of strain 306, Rif^r Km^r	This study
F6	*galU*:Tn5 derivative of strain 306, Rif^r Km^r	This study
CD	D12 containing pCGU2.1, Km^r, Cm^r, Gm^r	This study
CF	F6 containing pCGU2.1, Km^r, Cm^r, Gm^r	This study
Plasmids		
pCR®2.1-TOPO™	PUC ori f1 ori *lacZ*α$^+$ Km^r Ap^r	Invitrogen
pRk2013	ColE1 Km^r Tra$^+$, conjugation helper plasmid	Ditta et al. 1980
pUFR053	IncW Mob$^+$*mob*(P) *lacZ*α$^+$ Par$^+$ Cm^r Km^r, shuttle vector	El Yacoubi et al. 2007
pCGU1.1	*galU* gene from XCC 306 cloned in pCR®2.1-TOPO™	This study
pCGU2.1	*galU* gene on *Bam*HI fragment from pCGU1.1 cloned in pUFR053	This study

Table 2-2. Primers used in this study

Primer	Sequence (5’ → 3’)[a]
galU-F1	AGACAGTGCCGAAAGAAATGCTGC
galU-R1	AACAGCGATCAGGCAACAATCAGC
Kan2-F1	CGAGGCCGCGATTAAATTCCAACA
Kan2-R1	AGGCAGTTCCATAGGATGGCAAGA
KAN-2 FP-1	ACCTACAACAAAGCTCTCATCAACC
R6KAN-2 RP-1	CTACCCTGTGGAACACCTACATCT
CGU-F	AATGATggatccCTGCCAAAGCCTTGACGC
CGU-R	AACAGAggatccAACATCACCACGCCCAAC

[a] Lowercase nucleotides are not exact matches to the sequence and were introduced to add restriction enzyme site *Bam*H1.

Table 2-3. Genes and corresponding primers for QRT-PCR analysis

Gene	Product function[a]	Component or protein	Primer direction[b]	Sequence (5' → 3')[c]
16S rRNA		Ribosome component	F	CGCTTTCGTGCCTCAGTGTCAGTGTTGG
			R	GGCGTAAAGCGTGCGTAGGTGGTGGTT
hrpG	T3SS	T3SS regulator	F	GCCTTTCAATTCGCACGAGTTACACG
			R	CACACGCCGGGGCTGGAAAAGA
hrpX	T3SS	T3SS regulator	F	AGCGATCTCTGCGTTGTCCTAC
			R	ATACGCATCTTCGGCCTCTTCCTGA
hrcV	T3SS	T3SS component	F	GCGTTTGCGGCGTGCTTCATCT
			R	CAATCTGGTGGTAGGCCTGGTCGTTTTCTT
pthA	T3SS	T3SS effector	F	TGGCGTCGGCAAACAGTGGTC
			R	TGCTCCGGGGTCAGGTTCAGG
avrBs2	T3SS	Avirulence protein	F	CGCGCCAATCACGACAAGGACTACTAC
			R	CGGGCCAGCGTGCGGTTTTC
avrXacE1	T3SS	Avirulence protein	F	TCGCGCTGGGCCGGAACATACC
			R	GCGTCCGCGGCGATAACTCTTG
XAC0028	CWDE	Cellulase	F	CGCTCCACGCTGCTTTTCAT
			R	ATTCGGCACCGGACAGATTG
XAC0160	CWDE	Xylanase	F	CATGGCCTGGCGGTCCTTGTGCT
			R	GCGCGATCCGGCTGGCTTGTTC
XAC0165	CWDE	Xylosidase	F	AGGGCGGGGCGTTGCTGTTCTAC
			R	TCTTGCCGTCGGGACTGCTGTGA
peh-1	CWDE	Endopolygalacturonase	F	AGTGGCAACGCGTTTCTGACC
			R	CGCCTGCGTTGTTGCCCTTGAC
celD	CWDE	Glucan 1, 4-beta-glucosidase	F	GATTTCGGCCGAGCGTCTGGA
			R	GGATGCCGGCCTGGTTCTTCA
pglA	CWDE	Polygalacturonase	F	CAGCGCCGACGTCACCTTGTA
			R	GTAGCCGGGACGCGAATAGACC
pelB	CWDE	Pectate lyase II	F	GAACTTCGGCGTGCGTGTGGTG
			R	GTGAGCGAGGCGAAGATGGTGTTGTGGTC
gumB	EPS	Polysaccharide exporter	F	CTGACCGAAATCGAGAAGGGCACCAATC
			R	GCGCCACACCATCACAAGAGGAGTCAGTTC
kpsF	CPS	Arabinose 5-phosphate isomerase	F	GCTTCACCGCCGACGACTTC
			R	CGCTTGCGGCTCATTTCCATC

[a] T3SS: type III secretion system; CWDE: cell wall degrading enzymes; EPS: extracellular polysaccharides; CPS: capsular polysaccharide. [b] F: Forward; R: Reverse.
[c] The primers are derived from internal sequences of corresponding genes.

Table 2-4. Comparison of gene expression of key virulence genes in the wild type and the *galU* mutant culturing grown in XVM2 using QRT-PCR

Gene	Mean $\Delta\Delta C_T$[a]	SD	95% Confidence interval	P[b]	Fold change[c]
hrpG	-1.6804	0.5275	-2.3590, -1.0018	0.0003*	3.2052
hrpX	-2.1666	0.5206	-2.8363, -1.4968	<0.0001*	4.4896
hrcV	-2.0417	0.4961	-2.6799, -1.4035	<0.0001*	4.1173
pthA	-0.2077	0.3894	-0.7086, 0.2933	0.3774	1.1548
avrBs2	-2.1722	0.6046	-2.9499, -1.3944	<0.0001*	4.5071
*avr*Xac*E1*	-2.4682	1.0118	-3.7699, -1.1665	0.0018*	5.5335
XAC0028	2.2138	0.7257	1.2802, 3.1474	0.0004*	0.2156
XAC0160	0.5413	1.3596	-1.2078, 1.2903	0.5062	0.6872
XAC0165	1.2379	0.3362	0.8054, 1.6705	<0.0001*	0.4240
peh-1	-2.8464	0.9095	-4.0164, -1.6764	0.0003*	7.1920
celD	0.4748	1.0723	-0.9047, 1.8542	0.4609	0.7196
pglA	-0.5460	0.8444	-1.6322, 0.5402	0.2889	1.4600
pelB	1.2397	0.2500	0.9182, 1.5613	<0.0001*	0.4235
gumB	-0.9043	0.5975	-1.6730, -0.1356	0.0255*	1.8716
kpsF	-0.3704	0.9612	-1.6069, 0.8661	0.5196	1.2927

[a] The mean $\Delta\Delta C_T$ was determined using six biological replicates. [b] Values are significantly different when P is <0.05. [c] The fold change in expression in D12 was calculated using $2^{-\Delta\Delta C_T}$.

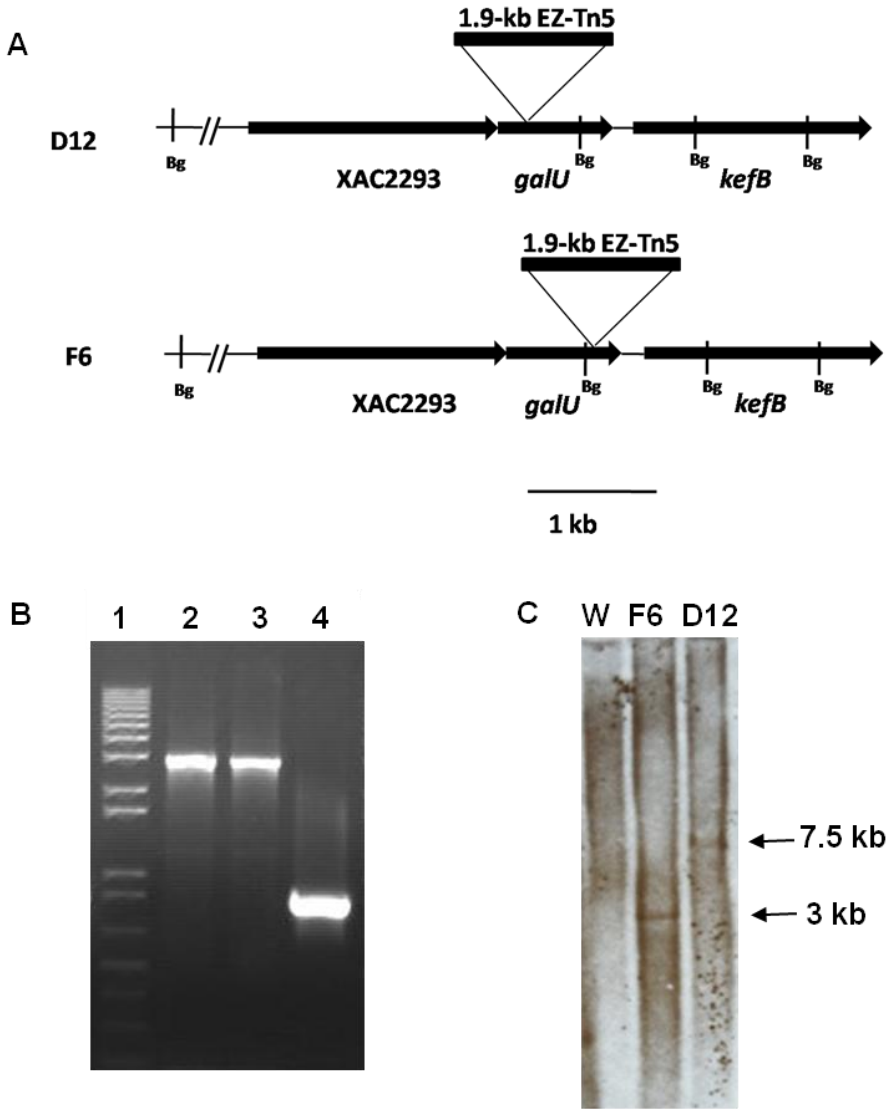

Figure 2-1. Sequence analysis of EZ-Tn5 insertion in the *galU* mutants. A) Genomic location of *galU* on the XCC chromosome and transposon insertion sites in the *galU* mutants. *kefB* encodes a transport protein, *galU* encodes a UTP-glucose-1-phosphate uridylyltransferase, and XCC2293 encodes a dehydratase protein. Bg, *Bgl*II restriction site. B) PCR analysis confirming insertion of EZ-Tn5 into the *galU* gene: agarose gel electrophoresis of DNA amplified using primers *galU*-F1 and *galU*-R1 targeting the interior region of the *galU* gene from XCC wild-type 306, D12, and F6 strains. Lane 1, Invitrogen 1 Kb Plus DNA size marker; lane 2, D12, lane 3, F6, lane 4, XCC strain 306. C) Southern blot of DNA of XCC wild-type strain 306 and *galU* mutants F6 and D12 digested with BglII. The membrane was probed with a 675-bp *kan-2* gene fragment that was amplified using PCR with primers Kan-F1 and Kan-R1. W, wild type.

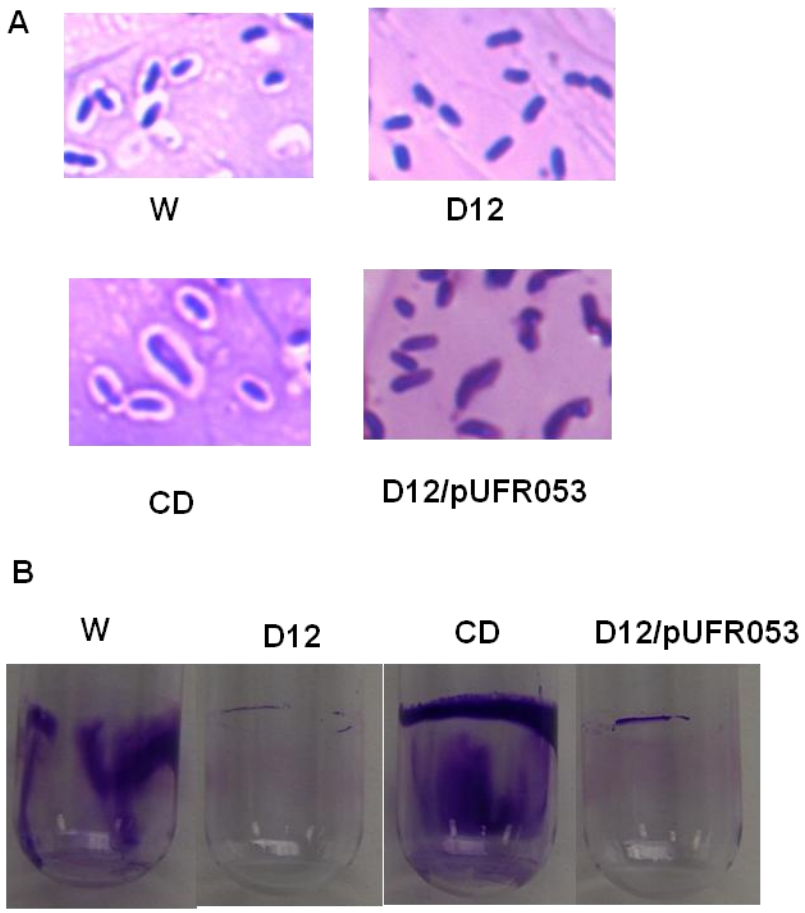

Figure 2-2. Effects of *galU* on the capsular polysaccharide and biofilm formation. A) Capsule-stained XCC strains observed with a light microscope (magnification, ×1,000). B) Biofilm formation by XCC strains as determined using crystal violet staining.

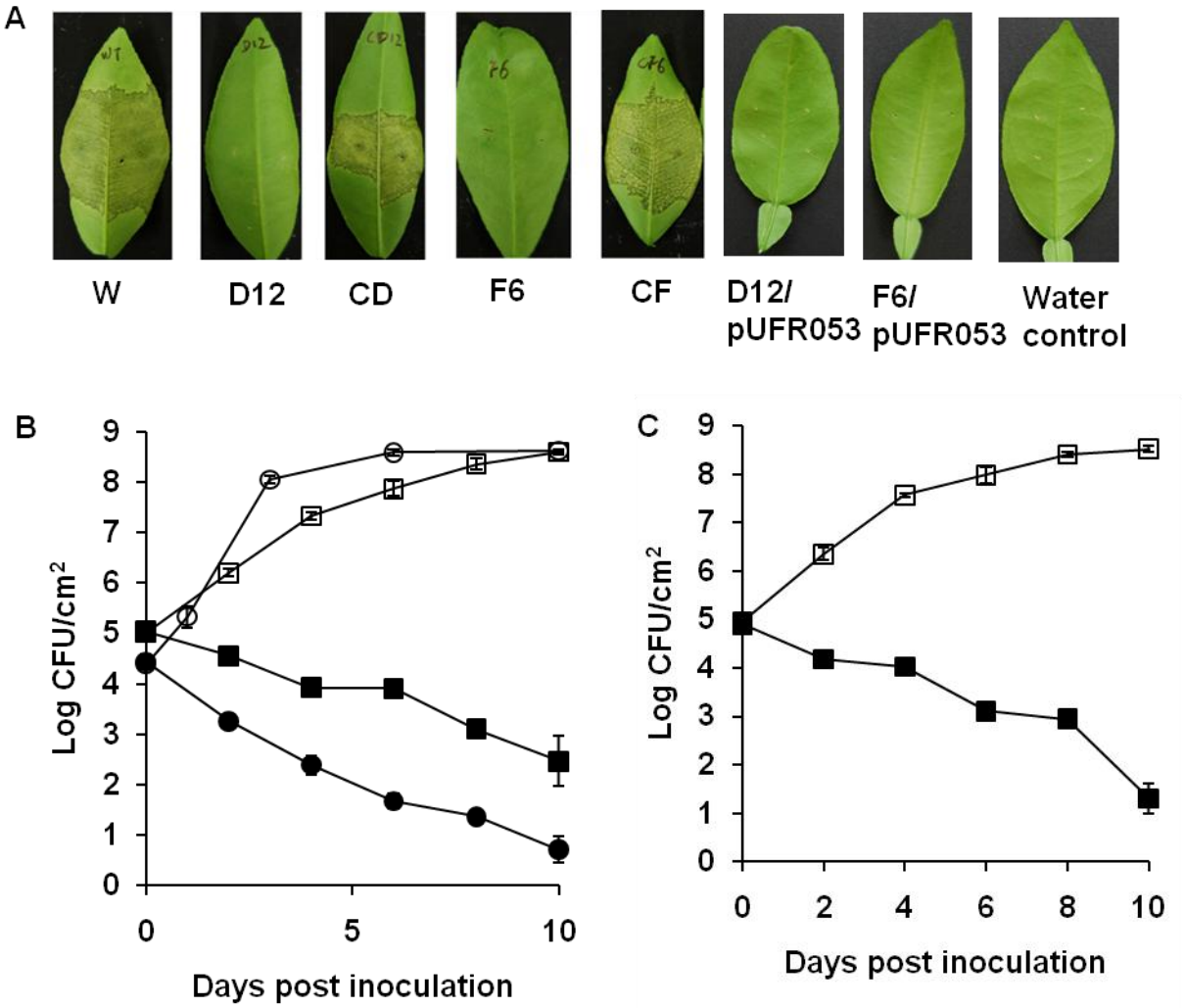

Figure 2-3. Pathogenicity assays and growth of XCC strains in planta. All strains were infiltrated into leaves with needleless syringes. A) Host responses of Duncan grapefruit inoculated with XCC strains. B) Growth of XCC wild-type strain 306, *galU* mutant D12, CD (complemented mutant D12), and D12/pUFR053 (D12 with empty vector pUFR053 in grapefruit leaves). C) Growth of coinoculated XCC wild-type strain 306 and *galU* mutant D12 in grapefruit leaves. □, wild-type strain 306; ■, D12; ○, CD; ●, D12/pUFR053. The in planta growth assays were repeated three times independently with four replicates each time, but the results of only one experiment are shown. The error bars indicate the standard errors of the means.

CHAPTER 3
HrpG AND HrpX PLAY GLOBAL ROLES IN COORDINATING DIFFERENT VIRULENCE TRAITS OF *Xanthomonas citri* subsp. *citri*

Introduction

The genus *Xanthomonas* is an important group of Gram-negative plant pathogenic bacteria, which infects approximately 124 monocotyledonous and 268 dicotyledonous plants (Leyns et al. 1984; Chan and Goodwin 1999). This genus has become an important model organism for studying plant-microbe interaction and for understanding bacterial pathogenicity and virulence mechanisms (Buttner and Bonas 2010). Among the diseases caused by members of the genus *Xanthomonas*, citrus canker is one of the most serious diseases of most commercial citrus cultivars resulting in significant losses worldwide. Citrus canker is caused by *Xanthomonas citri* subsp. *citri* (XCC) (Cubero and Graham 2002; Schaad et al. 2006; Vauterin et al. 1995). XCC infects citrus from rain splashed inoculums introduced directly through stomata or by wounds and grows in the intercellular spaces of the spongy mesophyll (Graham et al. 2004).

Tremendous progress has been made regarding pathogenicity and virulence mechanisms of *Xanthomonas*. The major genes involved in pathogenicity and virulence of *Xanthomonas* include type III secretion system (T3SS) genes, genes encoding cell-wall degrading enzymes (CWDEs), toxins, bacterial adhesins and surface structural elements, and *rpf* (regulation of pathogenicity factors) genes (da Silva et al. 2002).

Bacteria coordinate their virulence factors to overcome plant defenses, and manipulate the host for their survival in intercellular spaces. The *hrpX* gene, an AraC-type transcriptional activator, and *hrpG*, an OmpR family regulator, have been shown to be critical to the virulence of *Xanthomonas* and regulation of T3SS (Wengelnik and Bonas 1996; Wengelnik et al. 1996b). The T3SS and effectors secreted are critical for

pathogenicity and initiation of many diseases. *Xanthomonas hrp* cluster encodes more than 20 proteins which together function to inject effectors across the bacterial membrane and directly into host cells (Büttner and Bonas 2002; Brunings and Gabriel 2003). The expression of some structural genes of the T3SS and effector genes is regulated by HrpX (Wengelnik and Bonas 1996). Expression of *hrpX* is activated by HrpG as reported for *X. campestris* pv. *vesicatoria* (Wengelnik et al. 1996b).

It seems that HrpX and HrpG not only regulate T3SS and effector genes, but also affect gene expression of other virulence factors, thus to coordinate infection by the pathogen. Recent studies showed that some type II secretion system (T2SS) substrate genes also belong to the HrpG and/or HrpX regulon (Furutani et al. 2004; Wang et al. 2008; Yamazaki et al. 2008). T2SS substrates including proteases, lipases and CWDEs may contribute to bacterial infection by degradation of the plant cell wall. Co-regulation of T3SS and T2SS helps bacteria overcome plant defenses and acquire nutrients for growth *in planta*.

Although a few studies have been performed to identify genes in the HrpG and/or HrpX regulon, no comprehensive study has been done with *Xanthomonas* spp. In this study, we designed a genome-wide XCC oligonucleotide microarray for transcriptome analysis of the HrpX and HrpG regulons. Based on the microarray results, we expanded the knowledge of the HrpX and HrpG regulons with genes related to more functions such as chemotaxis and flagellar biosynthesis, transport, and a large set of unknown genes besides T3SS, effector, and T2SS substrate genes. We also found a cross-talk between HrpG regulatory cascade and quorum sensing.

Materials and Methods

Strains and Growth Conditions

All of the strains used in this study are listed in Table 3-1. XCC *hrpG* mutant was generated in this study as described below and the *hrpX* mutant was generated and confirmed as described in the previous study (Figueiredo et al. 2011). Wild type strain 306 (rifamycin resistant) (da Silva et al. 2002) and mutant strains were grown in nutrient broth (NB), on nutrient agar (NA), or in NYG medium (Daniels et al. 1984) at 28°C. *Escherichia coli* strains were grown in Luria-Bertani (LB) medium at 37°C. Antibiotics were used at the following concentrations: rifamycin (Rif), 50 µg/mL; kanamycin (Km), 50 µg/mL; ampicillin (Ap), 50 µg/mL; spectinomycin (Sp), 50 µg/mL; gentamicin (Gm), 5 µg/mL; and chloramphenicol (Cm), 35 µg/mL.

Generation of the *hrpG* Mutant

The 1,180-bp kanamycin resistance gene *kan*R was isolated from pBSL15 plasmid by *Eco*RI digestion, and ligated with similarly digested pGEM-T easy vector. The plasmid was named pUSS01-1 when the *kanR* and *lacZ* are in the same transcription direction, and the plasmid was named pUSS01-2 when they are not in the same transcription direction. The pUSS01-2 was chosen for further manipulation. The 693-bp upstream region of *hrpG* (86-bp at 5' of *hrpG*) was amplified using genomic DNA of XCC 306 as template and primers AChrpG-Nde1F3 and AChrpG-NSi1R2 (Table 3-2), and then cleaved with *Nde*I-*Nsi*I. The *Nde*I-*Nsil*I fragment was ligated into similarly digested pUSS01-2. The resulting construct was named as phrpGDV1-3' which contains the upstream sequence of *hrpG* at downstream of Km. The 834-bp fragment containing 436-bp region downstream of and 398-bp of coding region of *hrpG* was obtained by *Apa*I-*Sph*I digestion of the 1,200-bp fragment amplified using genomic DNA

of XCC 306 as template and primers AChrpG-Apa1F2 and AChrpG-R1 (Table 3-2). Then the 834-bp fragment was cloned into phrpGDV1-3'and located upstream of Km, which resulted in the construct phrpGDV1 carrying a mutated *hrpG* fragment consisting of Km cassette flanked by *hrpG* upstream and downstream fragments. The *hrpG* disruption fragment was cleaved out with *Bam*HI from phrpGDV1 and ligated with *Bam*HI-cut pOK1. The resulting recombinant construct, named as phrpGDV2, was transformed into *E. coli* DH5αλPIR (Huguet et al. 1998) and subsequently transformed into XCC 306. Transconjugants were selected on NYG medium supplemented with Rif and Sp. Positive colonies were replicated on both NA plates supplemented with 5% (w/v) sucrose, Sp and Rif, and NA with only Rif. The sucrose sensitive colonies were selected from NA Rif plate and dilution-plated on NA containing Rif, Km and 5% sucrose to select for resolution of the construct by a second cross-over event. The resulting *hrpG* mutant was confirmed by PCR analysis with three pairs of primers, AChrpG-Kpn1F4 and AChrpG-Kpn1R4, AChrpG-Apa1F2 and AChrpG-SphR3, AChrpG-F1 and AChrpG-Nsi1R2 (Table 3-2).

Complementation of the *hrpG* Mutant

The entire *hrpG* gene with 738-bp upstream sequence and 399-bp downstream sequence was amplified from genomic DNA of XCC wild type strain 306 using PCR with primers AChrpG-Kpn1F4 and AChrpG-Kpn1R4 which contain a *Kpn*I restriction site (Table 3-2). The resulting 1,929-bp fragment was ligated to PCR®2.1-TOPO® following the manufacturer's protocol (Invitrogen, Carlsbad, CA, U.S.A.), resulting in phrpG. From phrpG, a *Kpn*I fragment containing the *hrpG* gene was isolated and cloned into similarly digested pUFR053 which was treated with calf intestinal alkaline phosphatase (New England Biolabs, Ipswich, MA) (El Yacoubi et al. 2007), resulting in phrpGC. The

plasmid phrpGC was transferred into the *hrpG* mutant by triparental mating with a helper *E. coli* strain containing pRK2013 (Swarup et al. 1991). The transconjugants were selected on NA with Rif and Gm. The presence of phrpGC was verified using PCR.

Pathogenicity Assay

Pathogenicity assays were conducted in a quarantine greenhouse facility at Citrus Research and Education Center, Lake Alfred, FL. Assays were performed using fully expanded, immature leaves of Duncan grapefruit. XCC wild type and mutant strains used in this assay were grown with shaking overnight at 28ºC in NB, centrifuged down and suspended in sterile tap water and the concentrations were adjusted to 10^8 CFU/mL. For the pathogenicity assays, bacterial suspensions of both 10^8 and 10^5 CFU/mL were infiltrated into leaves with needleless syringes (Viloria et al. 2004; Rybak et al. 2009). The test was repeated three times with similar results. Disease symptoms were photographed at 5 days, 10 days and 12 days post inoculation (DPI).

RNA Extraction

Single bacterial colonies were picked and grown in 5 mL NB at 28°C for 24 h with shaking, and then transferred into 50 mL NB for overnight incubation. The bacterial cultures in middle exponential phase were centrifuged down, washed with XVM2 medium once, and inoculated in XVM2 medium with initial concentration OD_{600} = 0.03. Bacteria were grown in XVM2 medium with shaking at 200 rpm at 28°C and samples of culture were collected at three different time-points, OD_{600} 0.25, 0.4 and 0.5 (marked with A, B and C, correspondingly) according to the growth curve in XVM2 (Figure 3-1). Four biological replicates were used for each strain per time-point. RNA was stabilized immediately by mixing bacterial culture with two volumes of RNAprotect® bacterial

reagent (Qiagen) and incubated at room temperature for 5 min. Bacterial cells were centrifuged at 5000×g for 10 min and cell pellets were used for RNA extraction.

Cell pellets were treated with lysozyme and RNA extractions were performed using RiboPure^{TM} bacteria kit (Ambion). Contaminant genomic DNA was removed from RNA by treatment with TURBO DNA-free^{TM} kit (Ambion). RNA quantity was initially determined on a ND-8000 Nanodrop spectrophotometer (NanoDrop Technologies) and RNA quality was assessed using an Agilent 2100 bioanalyzer (Agilent Technologies).

XCC Oligonucleotide Microarray Design

Based on the annotated genome sequence of XCC strain 306 (da Silva et al. 2002), 8×15 K DNA microarray chips covering the whole genome of XCC 306 were designed using Agilent's eArray custom design tool and produced by Agilent Technologies (Agilent Technologies). Each of 4,427 protein coding genes has three unique optimized 60-mer oligonucleotide probes in microarray. Agilent's standard controls were printed on the array as well, allowing for measurement of proper hybridization conditions.

Microarray Hybridization

Microarray analysis using the Agilent microarray platform was performed at Interdisciplinary Center for Biotechnology Research (ICBR) Microarray Core Facility, the University of Florida. Labeled cDNA was generated using Fairplay III microarray labeling kit (Agilent Technologies). Five µg of total RNA input was used to generate labeled cDNA according to the manufacturer’s protocol. Briefly, cDNA was synthesized from 5 µg of the total RNA with AffinityScript HC and random primer and then modified cDNA was labeled with either cy3 or cy5; labeled cDNA was purified following the manufacturer's instructions. The microarray analysis was performed using the Agilent

8×15K XCC genome array. Four independent biological replicates were performed for three time-point comparisons with dye-swap design. A total of 300 ng of labeled cDNA per sample was used for the hybridization. A dye swap was performed to remove any bias from the labeling dyes. Hybridization was performed using Gene Expression Hybridization Kit (Agilent Technologies) according to user's manual in a hybridization oven for 17.5 h at 65°C. The arrays were washed according to the manufacturer's recommended protocols. Briefly, arrays were washed with Gene Expression Wash Buffer 1 containing 0.005% Triton-102 for 1 min at room temperature and then washed with 37°C warmed Gene Expression Wash Buffer 2 containing 0.005% Triton-102 for 1 min and dried with Agilent Stabilization and Drying Solution. The arrays were scanned using a dual-laser DNA microarray scanner (Model G2505C) (Agilent Technologies). The data were extracted from scanned image using Feature Extraction 10.1.1.1 software (Agilent Technologies).

Microarray Data Analysis and Statistical Methods

The raw data were imported into R environment and statistical tests were performed using BioConductor statistical software which is an open source and open development software project for analysis of microarray and other high-throughput data based primarily on the R programming language (Gentleman et al. 2004). Data preprocessing and normalization were performed using the Linear Models for Microarray Data (LIMMA) package (Smyth 2004). Raw mean signal intensities from all microarray spots were background corrected and normalized using within-array lowess approach. Log_2 transformed values were used for statistical analysis. Histograms, box plots and pair-wise scatter plots were generated to examine data quality and comparability. A linear modeling approach and the empirical Bayes statistics as

implemented in the LIMMA package (Smyth 2004) were then employed for differential expression analysis. The *p-values* were adjusted using the Benjamini and Hochberg method, designated as FDR (Benjamini and Hochberg 1995). Differentially expressed genes were ranked based on FDR, and genes with FDR less than 0.05 and a minimum absolute value of $\log_2$ fold-change greater than 0.585 (equivalent to 1.5 fold) were considered as significantly differentially expressed. If the gene has three probes and only one was filtered, the gene was removed from further analysis. The $\log_2$ fold change values of the differentially expressed genes were averaged from the values of the two or three probes of the corresponding genes, and shown in Table 3-3. Annotation for the differentially expressed genes were extracted from the Integrated Microbial Genome (IMG) database and the J. Craig Venter Institute (JCVI) database and manually verified. Hierarchical clustering analysis was performed with Cluster 3.0 using complete linking with un-centered correlation distance (de Hoon et al. 2004). The resulting dendograms were visualized using Java Treeview software (Saldanha 2004).

All primary data from transcriptome experiments as well as experimental protocols used are available from Gene Expression Omnibus datasets, the National Center of Biotechnology Information (accession number GSE24016).

Quantitative RT-PCR (QRT-PCR)

To verify the microarray result, QRT-PCR assays were conducted using the same set of RNA for microarray analysis. One µg of aliquot RNA samples used for microarray were reverse transcribed using RETROscript® kit with random hexamer primers (Ambion) for two-step QRT-PCR. Gene specific primers listed in Table 3-2 were designed to generate products 100 to 250-bp in length from sequences on XCC genome using DNASTAR software (DNASTAR). Real-time PCR was performed for all

four biological replicates obtained at time-point C on a 7500 Fast Real-Time PCR System (Applied Biosystems) using QuantiTect ™ SYBR® Green PCR kit (Qiagen) following the manufacturer's instructions. The 16S rRNA and gyrA were used as endogenous controls. The relative fold change of gene expression was calculated by using the formula $2^{-\Delta\Delta C}{}_T$ (Livak and Schmittgen 2001). The values of fold change were $\log_2$ transformed to compare with values generated from microarray analysis.

Motility Assays

The media for motility assays was XVM2 containing 0.3% agar for swimming and 0.7% agar for swarming. Bacteria were grown in NB overnight with shaking at 200 rpm, and then centrifuged down, washed and diluted to OD_{600} = 0.3 in sterile water. One µL suspension was spotted on the center of each swimming or swarming plate and incubated at room temperature. The assay was repeated three times independently in quadruplicate.

Results

Generation of the *hrpG* Mutant

The *hrpG* insertion mutant was generated by double cross-over homologous recombination in this study. The insertion of the Km cassette in *hrpG* was confirmed by PCR with three pairs of primers targeting different locations of inside and flanking regions of *hrpG*. The *hrpG* insertion mutant lost pathogenicity in grapefruit and showed no symptoms (Figure 3-2). The complementation plasmid containing the intact *hrpG* gene restored its pathogenicity *in planta*. The growth curves of both *hrpG* and *hrpX* mutants in XVM2 medium (Wengelnik et al. 1996a) were similar to that of the wild type strain (Figure 3-1).

Microarray Analyses and Validation of Microarray Data

In order to characterize the HrpG and HrpX regulons, microarray analyses were conducted to compare gene expression of the *hrpG* or *hrpX* mutants with that of the wild type strain 306 at different growth phases, respectively. The three time-points used in this time-course study, A (OD_{600} = 0.25), B (OD_{600} = 0.4), and C (OD_{600} = 0.5) (Figure 3-1), represent three growth phases (two in exponential phase and one in early stationary phase) of XCC in XVM2 medium. In this study, FDR=0.05 and absolute value of $\log_2$ fold change =0.585 (equivalent to fold change 1.5) were used as cut-off value. For the *hrpG* mutant, 99, 28 and 174 genes showed significant expression changes at time-point A, B and C, respectively (Figure 3-3). Similarly, 53, 63 and 159 genes were differentially expressed in the *hrpX* mutant at the three corresponding time-points (Figure 3-3). The greatest number of differentially expressed genes, and the greatest magnitude of changes, occurred at time-point C in both mutants (Figure 3-3). Overall, 232 genes belonged to the HrpG regulon while 181 genes belonged to the HrpX regulon (Table 3-3). HrpG and HrpX not only activated gene expression, but also repressed gene expression. For the *hrpG* mutant, 29, 9, and 95 genes were under-expressed and 70, 19, and 79 genes were over-expressed compared to the wild type strain at time points A, B, C, respectively. Similarly, 42, 58, and 104 genes were under-expressed and 11, 5, and 55 genes were over-expressed in the *hrpX* mutant at the three corresponding time-points (Figure 3-3).

Two-step quantitative RT-PCR (QRT-PCR) was used to validate the microarray data. Eight genes were chosen from Table 3-3 to compare data obtained from the two methods (Table 3-2), which showed under-expression at time-point C in both *hrpG* and *hrpX* mutant in microarray analysis. The resulting transcriptional ratio from QRT-PCR

analysis was $\log_2$ transformed and compared with the average $\log_2$ ratio values obtained by microarray analysis (Figure 3-4). Although the amplitude of fold changes between the two techniques is different for different genes, the general trend of gene expression is consistent.

Functional Classification of Differentially Regulated Genes

The 232 genes belonging to the HrpG regulon could be assigned to 18 functional categories according to the annotation from the JCVI role categories including amino acid biosynthesis; biosynthesis of cofactors, prosthetic groups, and carriers; cell envelope; cellular processes; central intermediary metabolism; DNA metabolism; energy metabolism; fatty acid and phospholipid metabolism; mobile and extrachromosomal element functions; protein fate; protein synthesis; regulatory functions; transcription; transport and binding proteins; hypothetical proteins; unknown function; unclassified, and not in JCVI (which means that the gene is not assigned to any JCVI categories) (Figure 3-5). The 181 genes of the HrpX regulon were assigned into 17 of the same functional categories as HrpG except mobile and extrachromosomal element functions. About 53.4% (124 of 232) of genes of the HrpG regulon and 49.7% (90 of 181) genes of the HrpX regulon were in the categories of hypothetical protein, unclassified, unknown function, and not in JCVI.

Clustering Analysis

Clustering analysis was performed to group genes with similar expression pattern. Genes with similar time-dependent regulation patterns were assigned to the specific clusters. This enables the characterization of clearer and more meaningful expression patterns from a large array of differentially regulated genes. Accordingly, five major clusters of genes were assigned (Figure 3-6).

Cluster I: It consists of 104 genes showing under-expression in the *hrpX* mutants at time-point C. Seventy three of them were also under-expressed in the *hrpG* mutant at time-point C. The genes in this cluster consist of genes encoding T3SS and T3SS effectors, T2SS substrates, and genes involved in amino acid biosynthesis, regulation pathway, and energy metabolism.

Cluster II: Up-regulated in both *hrpG* and *hrpX* mutants at time-point C. This cluster is composed of 31 genes, including those related to amino acid biosynthesis, DNA metabolism, and thiamine biosynthesis, and 23 hypothetical genes.

Cluster III: Up-regulated only in the *hrpG* mutant at time-point C but not in the *hrpX* mutant at any phase. It comprises of 44 genes encoding two-component regulation systems, chemotaxis and bacterial motility, amino acid biosynthesis, and sugar and starch metabolism.

Cluster IV: Down-regulated at any of the three time-points of the *hrpG* mutant but not in the *hrpX* mutant. It contains 44 genes, including those related to energy metabolism, cell envelope, substrate transport and binding, and regulation.

Cluster V: Up-regulated in the *hrpX* mutant only at time-point C but not in the *hrpG* mutant. It includes 19 genes, consisting of those responsible for histidine biosynthesis, energy metabolism, and ABC transporter.

Genes not in clusters included 48 genes showing altered expression at least at one time-point in either *hrpG* or *hrpX* mutant. They encode proteins responsible for energy metabolism, regulation, substrate transportation, and pathogenicity factors (PthA1-4).

T3SS and T3SS Effectors

The whole *hrp* gene cluster which contains 24 genes (XAC0393-XAC0417) were down-regulated in both *hrpG* and *hrpX* mutants. The magnitude of down-regulation of *hrp* genes in the *hrpX* mutant was greater than that in the *hrpG* mutant when compared at the same growth phase in XVM2. For instance, at time-point C, the expression of *hrp* genes was down-regulated 0.94 to 2.18 $\log_2$ fold (1.92 to 4.53 fold) in the *hrpG* mutant, while it was down-regulated 1.23 to 5.54 $\log_2$ fold (2.35 to 46.53 fold) in the *hrpX* mutant. The expression of most putative and known T3SS effector genes was under HrpG and HrpX regulation. Among 24 putative and known T3SS effectors found in XCC genome (Moreira et al. 2010), 23 effectors belong to the HrpG and/or HrpX regulon (Table 3-4). Except for the *pthA1-4* and *avrXACE2* genes, the remaining 18 effector genes were down-regulated in both mutants and grouped into Cluster I. The *pthA1-4* genes showed altered expression (over-expressed) at time-point A and B in the *hrpG* mutant, while the *avrXACE2* genes was over-expressed at time-point A in the *hrpG* mutant. HrpX did not regulate the expression of *pthA* and *avrXACE2* genes. In addition, one putative effector gene, XAC2990, was identified in this study. The protein sequence of this gene shares 45% identity to the putative T3SS effector RCFBP_mp20163 from *Ralstonia solanacearum* (Remenant et al. 2010). The products of both genes have a lipase domain which hydrolyzes ester linkages of triglycerides. It was reported that lipase acted as a virulence factor and played important roles in disease development caused by *Fusarium graminearum* (Feng et al. 2005) and *Pseudomonas aeruginosa* (Reimmann et al. 1997). Two genes, XAC3225 and XACb0007, sharing 99% identity with each other and encoding transglycosylase, belong to the HrpX regulon since their expression was down-regulated in the *hrpX* mutant at time-point C. It was reported that

XAC3225 shares high identity with *hopAJ1* of *P. syringae* pv. *tomato* strain DC3000, which is a T3SS helper protein contributing to effector translocation (Oh et al. 2007; Moreira et al. 2010). Mutation of XAC3225 reduced the disease symptoms on citrus (Moreira et al. 2010).

T2SS Substrates

Eight genes (Table 3-5) including *virK* (XAC0435), XAC0552, *phe*-1 (XAC0661), *xcp* (XAC0795), XAC0817, *pglA* (XAC2374), XAC2831 and XAC2835 which have been confirmed to encode T2SS substrate experimentally, showed under-expression in both mutants except for *pglA* (XAC2374) which was under-expressed only in the *hrpX* mutant at time-point C. Two of them, *pglA* (XAC2374) and *phe*-1 (XAC0661) encode CWDEs. In addition, 21 genes were predicted as putative T2SS substrates in this study based on the clustering with the known T2SS substrates, homology to known secreted proteins, as well as signal peptide prediction (Table 3-5). All these 21 genes encoding putative T2SS substrates were up-regulated by HrpX, and 12 of them were also up-regulated by HrpG (Table 3-5). In addition, XAC2654 encoding a plant natriuretic peptide-like protein in XCC (XACPNP) was under-expressed in both *hrpG* and *hrpX* mutants. Especially at time-point C in the *hrpX* mutant, its expression was more than five $\log_2$ fold lower than that in the wild type strain.

Signal Transduction and Regulation

Several genes belonging to the two-component system showed changed expression in this study (Table 3-6). Two genes encoding sensor kinases, XAC1488, and XAC2192, and two genes encoding response regulators, *rpfG* (XAC1877) and XAC2897, were up-regulated in the *hrpG* mutant at time-point C. Two genes (XAC1939 and XAC1940) encoding GGDEF family proteins showed similar expression pattern as

rpfG, which break down an important bacterial intracellular secondary messenger, 3, 5-cyclic diguanylic acid (cyclic-di-GMP). Gene *regS* (XAC1798) encoding a two-component system sensor protein showed over-expression in the *hrpG* mutant at time-point C. Gene *stkXAC1*(XAC1171) encoding a serine/threonine kinase showed under-expression in both mutants at time-point C. Gene *phoC* (XAC4369) encoding phosphatase precursor was under-expressed in the *hrpX* mutant at time-point C.

A few genes encoding transcriptional regulators were also differentially expressed in the study (Table 3-6). The expression of five genes (*rpoE* (XAC1682), XAC1555, XAC2166, XAC3445, and XAC4272) encoding one sigma factor RpoE and four transcriptional regulators were changed in the *hrpX* mutant. The expression of three transcriptional regulatory genes, XAC0917, *phoU* (XAC1573) and *flgM* (XAC1989) were changed only in the *hrpG* mutant. Two genes encoding transcription regulator, *pcaQ* (XAC0880) and XAC1455, showed altered expression in both *hrpX* and *hrpG* mutants.

Chemotaxis and Bacterial Motility

A number of genes involved in motility and chemotaxis were regulated at transcription level in the *hrpG* mutant. The *fliJ* gene (XAC1950), one of the flagellar genes whose product responds to chemotactic stimuli, was up-regulated in the *hrpG* mutant at time-point A. Two genes, *motB* (XAC1908), encoding flagellar motor protein D, and *fliO* (XAC1945), encoding flagellar protein for flagellum apparatus, were under-expressed in the *hrpG* mutant at time-point B. At time-point C, eight genes were over-expressed in the *hrpG* mutant, including chemotaxis genes, *cheA* (XAC2865), encoding chemotaxis histidine protein kinase, *cheW* (XAC1906), encoding a coupling protein, *cheY* (XAC1904), encoding chemotaxis response regulator, and genes in early flagellar biosynthesis which are responsible for flagellum basal body assembly, such as *flgF*

(XAC1982), encoding flagellar basal body rod protein, *fliF* (XAC1954), encoding flagellar M-ring protein, *fliI* (XAC1951), encoding flagellum-specific ATP synthase, and *fliG* (XAC1953) encoding flagellar motor switch protein. Gene *flgM* (XAC1989), encoding an anti-sigma-28 factor which is a negative regulator of flagellin synthesis, was over-expressed in the *hrpG* mutant at time-point C.

To test whether the expression changes of flagella genes we found from the microarray analysis led to motility changes in the *hrpG* mutant, both swarming and swimming assays were performed on XVM2 plates containing either 0.7% or 0.3% agar. The *hrpG* mutant did not show different swimming ability on XVM2 supplemented with 0.3% agar in the incubation period (data not shown). Greater swarming ability of the *hrpG* mutant was observed 13 days after plating on XVM2 containing 0.7% agar (Figure 3-7). This result is consistent with the microarray analysis of the *hrpG* mutant that most of the differentially expressed genes related to flagellar biosynthesis were changed at the early stationary phase.

Amino Acid Biosynthesis

Sixteen genes related to amino acid biosynthesis showed altered expression in this study (Table 3-3). Eight genes (XAC1828-XAC1835) involved in histidine biosynthesis were up regulated only in the *hrpX* mutant at time-point C. Two genes, *ilvC*(XAC3451) and *ilvG* (XAC3452), involved in valine, leucine and isoleucine biosynthesis, showed similar expression pattern to histidine biosynthesis genes. Three genes, *metE* (XAC0336) involved in cysteine and methionine metabolism, *dapA* (XAC1760) involved in lysine biosynthesis, and *asnB* (XAC1433) involved in alanine, aspartate and glutamate metabolism, showed expression changes in the *hrpG* mutant. Two genes involved in phenylalanine, tyrosine and tryptophan biosynthesis, *tyrA*

(XAC1525) and *pheA* (XAC3647) showed expression changes in both *hrpX* and *hrpG* mutants. PheA is a chorismate mutase which is a key enzyme in shikimate pathway related to aromatic amino acid synthesis. It was reported that chorismate mutase was either translocated to the periplasm or secreted in some pathogenic bacteria (Xia et al. 1993; Calhoun et al. 2001; Sasso et al. 2005). The chorismate mutase found in *X. oryzae* pv. *oryzae* XKK.12 is involved in virulence on its host rice (Degrassi et al. 2010).

General Metabolism and Transport

Many genes involved in general metabolism are regulated by HrpG and HrpX, including those involved in energy metabolism, fatty acid and phospholipid metabolism, and sugar transport (Table 3-3). Three genes *GNL* (XAC0548), *fruK* (XAC2502), *kdgK* (XAC0143) involved in pentose phosphate pathway were differentially expressed in the *hrpG* mutant. Three genes encoding cytochrome C oxidase, which is the complex IV in oxidative phosphorylation, were under-expressed in both mutants at time-point A. The *atpB* (XAC3655) gene in oxidative phosphorylation was over-expressed only in the *hrpX* mutant at time-point C. Three genes in fatty acid and phospholipid metabolism, *accD* (XAC0264), *fadE9* (XAC1313) and *paaF* (XAC1314) were over-expressed in the *hrpG* mutant at time-point C. Gene *paaF* also showed over-expression in the *hrpX* mutant at time-point A.

Thirteen genes encoding transport and binding proteins were differentially expressed in either *hrpG* or *hrpX* mutant (Table 3-3). Four genes encoding TonB-dependent receptors, XAC3050, XAC3489, XAC3444, and XAC1143, showed differential expression. These proteins are assembled in the outer membrane of Gram-negative bacteria and are mainly known in the transport of iron-siderophore complexes and vitamin B12 into the periplasm (Postle and Kadner 2003). In recent studies, novel

substrates of TonB-dependent receptors were revealed, such as nickel, zinc, maltodextrin, and sucrose (Neugebauer et al. 2005; Blanvillain et al. 2007; Schauer et al. 2007). XAC3489 shares 93% amino acid identity with XCC3358, which plays a major role in pathogenicity. The XCC3358 insertion mutant of *X. campestris* pv. *campestris* showed delayed symptom development compared to the wild type strain (Blanvillain et al. 2007). A few genes encoding transporters were differentially expressed in either *hrpG* or *hrpX* mutant, such as sugar transporters (e.g. *fucP* (XAC1556), *suc1* (XAC3488) and *fruA* (XAC2503)), K^+ transporter *kdpC* (XAC0758), ABC transporter components (XCC 0827-XAC0828), and MFS transporter (XAC1705).

Discussion

DNA microarray has been widely used to study the transcriptional responses of many organisms to genetic and environmental perturbations (Ye et al. 2001; Dharmadi and Gonzalez 2004). In this study, we developed the first whole-genome DNA microarray for XCC. In previous studies, two DNA microarray platforms have been designed and have played important roles in characterization the pathogenicity and virulence of XCC (Astua-Monge et al. 2005; Moreira et al. 2010). However, both previous microarrays represented part of the genome. The first XCC microarray only contains 279 XCC genes associated with pathogenicity and virulence (Astua-Monge et al. 2005), while the second XCC microarray only consists of 2,365 open reading frames (ORFs), which corresponds to 52.7% of the annotated ORFs of the XCC genome (Moreira et al. 2010). The microarray developed in our study represents all 4427 annotated protein coding ORFs. In addition, we used 8×15K format so that 8 microarrays could be printed on a single slide, which significantly reduces the variation when multiple slides are used (Tseng et al. 2001). The reliability of this array has been

proved with the following evidences: (1) gene expression of all randomly selected genes in the microarray result was validated in QRT-PCR (Figure 3-4); (2) T3SS and T3SS effector genes which have been shown to be regulated by HrpX and HrpG (Wengelnik and Bonas 1996; Wengelnik et al. 1996b; Wengelnik et al. 1999) were identified in our study (Tables 3-3 and 3-4); (3) T2SS substrate genes which have been shown to be controlled by HrpX and HrpG were confirmed using this microarray (Tables 3-3 and 3-5). Thus, our microarray provides a robust and comprehensive tool for transcriptome analysis of XCC.

HrpX and HrpG play important roles in coordinating different categories of genes. Firstly, they regulate pathogenicity and virulence genes to overcome the plant defense responses and survive in the intercellular spaces. The most well-known HrpG- and HrpX-dependent virulence factors were distributed in cluster I (Figure 3-6), including T3SS (*hrp* genes), T3SS effectors, T2SS substrates and XACPNP. The major roles of T2SS substrates include degradation of the plant cell wall, cytotoxicity, adherence, spread and transmission (Cianciotto 2005), which might facilitate the assembly of extracellular appendages of secretion systems such as T3SS and therefore promote pathogenesis. T3SS translocates the T3SS effector proteins into plant cells which either suppress the host defense or interfere with host cellular processes. For instance, some T3SS effectors act as cysteine proteases in plants such as XopD, a member of the YopJ/AvrRxv family (Noël et al. 2002; Grant et al. 2006). Members of the AvrBs3/PthA family of transcriptional factors directly interact with the host transcription to modulate the host gene expression (Schornack et al. 2006). Our microarray data showed that *pthA1-4* genes were not controlled by HrpX. However, the expression of *pthA1-4* genes

was induced in the *hrpG* mutant at time-point A and B. XCC employs XACPNP to mimic host PNP and to systemically regulate plant homeostasis, resulting in a suppressed host defense responses, and a better survival environment for bacteria (Gottig et al. 2009a). Importantly, a significant induction of *hrpG* expression was observed when *Xanthomonas* spp. entered the plant apoplast (Zhang et al. 2009). Thus, HrpG coordinates multiple virulence factors in the XCC infection process. Secondly, in addition to manipulation of plant defenses, XCC has to adapt its metabolism to the intercellular spaces, which are nutrient poor (Alfano and Collmer 1996) and laden with toxic substances (either preformed or induced) as part of the host defense responses (Osbourn 1996; Segura et al. 1999). Our data showed that XCC regulates multiple cellular activities responding to the host environment, such as amino acid biosynthesis, oxidative phosphorylation, pentose-phosphate pathway, transport of sugar, iron and potassium and the phenolic compounds catabolism pathway through HrpX and HrpG. XCC activates the gene expression of sugar transporters through HrpX and HrpG in order to take up more sugars as a carbon and energy source, particularly sucrose, glucose and fructose, which are the most common sugars in the plant apoplast (Joosten et al. 1990; Rico et al. 2009). The activation of a phenolic catabolism pathway could convert toxic plant chemicals to less toxic compounds or even carbon sources. Thirdly, we also identified a large set of unknown genes controlled by HrpG and HrpX. In all, 53.4% (124 out of 232 genes) of genes in the HrpG regulon and 49.7% (90 out of 181 genes) of genes in the HrpX regulon encode unknown proteins. Their roles are unknown in XCC infection. Nonetheless, the list might provide targets for further study. Among the unknown proteins, some seem to play important roles in XCC virulence. For

example, one putative effector gene, XAC2990, was predicted in this study. The protein sequence of this gene shares 45% identity to the putative T3SS effector RCFBP_mp20163 from *R. solanacearum* (Remenant et al. 2010).

The regulation of HrpX and HrpG on multiple cellular activities is through both direct and indirect controls (Figure 3-8). For the T3SS and T3SS effector genes, five T3SS genes and eight T3SS effector genes have been shown to contain PIP boxes in their promoter regions (da Silva et al. 2002). HrpX was shown to interact with the PIP box (Koebnik et al. 2006). For other genes controlled by HrpX and HrpG but without PIP box, one putative explanation is that HrpX/HrpG control multiple regulatory genes (Table 3-6 and Figure 3-8), which in turn regulate those genes. Totally, HrpX and HrpG manipulate the gene expression of 21 regulatory genes and one sigma factor gene (Table 3-6). Among the regulatory genes controlled by HrpG, *rpfG* encodes a response regulator (discussed below) in DSF-mediated QS system (Tang et al. 1991; Barber et al. 1997). RpfG was reported to regulate genes involved in synthesis of extracellular enzymes and EPS and biofilm formation (Slater et al. 2000). The regulation of flagellar genes might be related to the regulation of *flgM* and XAC0917 by HrpG. Gene *flgM* (XAC1989) over-expressed in the *hrpG* mutant at the early stationary phase, encodes an anti-sigma-28 factor which is involved in temporal regulation of flagellar biosynthesis (Yang et al. 2009). XAC0917 is a TetR family member. It was reported that FhrR, a TetR family member, positively regulates expression of the genes encoding flagellar and ribosomal protein genes, and negatively regulates expression of *hrp* genes, under the control of Clp in *X. campestris* pv. *campestris* (He et al. 2007). The *phoU* gene encodes a transcriptional regulator which participates in phosphate transport and also

negatively controls the expression of phosphate ABC transporter genes (Muda et al. 1992). The *stkXAC1*(XAC1171) gene encodes a serine/threonine kinase which plays important roles in a multitude of cellular processes, including cell division, proliferation, apoptosis, and differentiation (Manning et al. 2002). The HrpX and HrpG also manipulate the gene expression of multiple regulators including *pcaQ* (XAC0880), XAC1455, XAC1555, XAC4272, XAC3445, and XAC2166, which have not been studied extensively in XCC. However, their homologs have been studied in other bacteria. For example, the homolog of PcaQ (XAC0880), a LysR-family transcription regulator, activated the expression of the *pcaDCHGB* operon which encodes enzymes involved in phenolic compounds catabolism in *Agrobacterium tumefaciens* A348, (Parke 1996). In agreement with the regulation of PcaQ, two genes encoding subunits of protocatechuate 4, 5-dioxygenase, *pcaH* (XAC0878) and *ligA* (XAC0879), were under-expressed in both *hrpX* and *hrpG* mutants. Protocatechuate 4, 5-dioxygenase is the first enzyme in protocatechuate branch of β-ketoadipate pathway to use aromatic compounds as carbon sources (Parke 1996). XAC1455 shares 85% identity of amino acid sequence with XC_2827, which belongs to MarR family transcriptional regulator in *X. campestris* pv. *campestris* 8004. The product of XC_2827, designated as HpaR, is involved in hypersensitive response (HR), pathogenicity, and extracellular protease production in *X. campestris* pv. *campestris* and was positively regulated by HrpG and HrpX (Wei et al. 2007). Thus, it seems that HrpX and HrpG control multiple cellular activities through multiple regulatory genes.

Our data suggest that a cross-talk exists between HrpG and the QS system in XCC. The *rpfG* gene (XAC1877) was up-regulated at the early stationary phase in the

hrpG mutant. Two GGDEF genes showed similar expression pattern as *rpfG*, which break down an important bacterial intracellular secondary messenger, 3, 5-cyclic diguanylic acid (cyclic-di-GMP). RpfG is the response regulator in DSF-mediated QS system which mediates virulence, biofilm formation and many cellular activities in *Xanthomonas* spp. (Tang et al. 1991; Barber et al. 1997). RpfG contains an HY-GYP domain which interacts with GGDEF proteins to mediate signal transduction to cyclic-di-GMP. The cross-talk between DSF-mediated QS and HrpG regulon was also found in genome scale analysis of DSF regulon in *X. campestris* pv. *campestris* (He et al. 2006; He et al. 2007). In addition, for the *hrpG* mutant, 99, 28 and 174 genes showed significant expression changes at time-point A, B and C, respectively (Figure 3-5). Similarly, 53, 63 and 159 genes were differentially expressed in the *hrpX* mutant at the three corresponding time-points (Figure 3-5). The temporal changes of gene regulation might be related to QS. QS is likely to be involved in controlling the timing and level of gene expression in the HrpG regulon. Bacteria might balance DSF signal and host stimuli by timing the expression of virulence factors such as T3SS via subtle signal-sensing mechanisms. The messenger cyclic-di-GMP might be the molecule which links QS and HrpG regulatory cascade. RpfG and GGDEF proteins control the concentration of the central messenger cyclic-di-GMP. The high levels of cyclic-di-GMP promote biofilm formation, while low levels promote motility and transcription of virulence factors (Simm et al. 2004; Tischler and Camilli 2004; Römling et al. 2005). One important target of cyclic-di-GMP is Clp (cAMP receptor protein–like protein) which is a transcriptional activator. Cyclic-di-GMP binds to the Clp to prevent from DNA binding and the expression of genes encoding extracellular enzymes, and genes involved in T3SS, and

EPS biosynthesis (He et al. 2007). Two transcriptional factors, FhrR and Zur were identified in the transcriptomic analysis of Clp regulons of *X. campestris* pv. *campestris* (He et al. 2007). FhrR controls the expression of genes encoding flagellar, T3SS and ribosomal proteins, while Zur regulates genes involved in iron uptake, multidrug resistance and detoxification (Huang et al. 2009). Therefore, it is possible that bacteria temporally regulate the cellular functions to adapt to different phases of growth or infection through multiple signaling cascades including the QS system.

Comparison of the HrpX and HrpG regulons at different time-points gives us an insight of the dynamic expression of common genes shared by both regulons. Thirty-three genes were shared by the two regulons at time-point A, and 9 genes at time-point B, while 104 common genes were found at time-point C (Table 3-7). In general, 123 genes were overlapped in the two regulons at any of the three time-points, which corresponds to 68% of HrpX regulon (123 out of 181), and 53% of HrpG regulon (123 out of 232). The most common genes were grouped into cluster I which contains genes encoding T3SS, T3SS effectors and T2SS substrates. Interestingly, 58 genes in the HrpX regulon are HrpG-independent, while 109 genes in the HrpG regulon are HrpX-independent (Table 3-7). As to the HrpG-independent genes in HrpX regulon, further analysis reveals that 23 of them showed subtle expression changes (the absolute value of $\log_2$ fold change <0.585) with statistical significance FDR <0.05 in the *hrpG* mutant in at least one of the three time-points (particularly 17 of the 23 genes are in cluster I) (Table 3-3). As shown in Figure 3-6, the expression of genes in Cluster I responded to *hrpX* mutation more rapidly and dramatically than to HrpG mutation based the log2 fold value. Thus, those 23 genes might also belong to the HrpG regulon but have weaker

responses to HrpG. For the remaining 35 HrpG-independent genes in the HrpX regulon, one possibility is that the *hrpX* gene is regulated by other regulators besides HrpG. For instance, it was reported that Zur in *X. campestris* pv. *campestris* strain 8004 positively controls *hrp* gene expressions via HrpX (Huang et al. 2009). The HrpX-independent genes in HrpG regulon were as we expected since HrpG is upstream of HrpX in the regulatory cascade. These genes in the HrpG regulon include 10 regulatory genes and 11 genes related to chemotaxis and flagellar biosynthesis. Those regulatory genes contribute to controlling the large set of genes in the HrpG regulon and also indicate that HrpG is a master regulator in the pathogenesis process of XCC. In addition, we confirmed the repression effect of HrpG on bacterial motility due to the altered expression of genes involved in chemotaxis and flagellar biosynthesis by testing the motility of the *hrpG* mutant (Figure 3-7).

This study is the first exhaustive genome-wide analysis of HrpG and HrpX regulons in the *Xanthomonas* genus. We identified a large set of HrpX- and/or HrpG-dependent unknown or hypothetical proteins which might be candidate virulence genes, particularly the multiple ORFs in Cluster I. This study also provides us a global view of regulation cascades that control the expression of multiple virulence genes including T3SS, effector, and T2SS substrate genes during infection. Further microarray analysis of the mutants of the regulatory genes identified in this study will help us explore the regulation circuits of HrpG and HrpX regulons.

Table 3-1. Bacterial strains and plasmids used in this study

Strain or plasmid	Relevant characteristics[a]	Reference or source
Strains		
E. coli		
Mach1™ T1R	F$^-$ Φ80*lacZ*ΔM15 Δ*lacX*74 *hsdR*(r_K^-, m_K^+) Δ*recA*1398 *endA*1 *tonA*	Invitrogen
DH5α	F$^-$ Φ80*lacZ*ΔM15 Δ(*lacZYA-argF*) U169 *recA*1 *endA*1 *hsdR*17 (r_K^-, m_K^+) *phoA supE*44 λ$^-$ *thi*-1 *gyrA*96 *relA*1	Laboratory collection
DH5αλPIR	Host of pOK1; DH5α(λPIR)	Huguet et al. 1998
X. citri subsp. *citri*		
306	Rif^r, Causes citrus canker on citrus	da Silva et al. 2002
hrpG	*hrpG*::Km derivative of strain 306, Rif^r Km^r	This study
hrpX	*hrpX*: pCR®2.1-TOPO® derivative of strain 306, Rif^r Km^r AP^r	Figueiredo et al 2011
Plasmids		
pGEM-T easy	Ap^r, cloning vector,	Promega
pBSL15	Contains 1.2 kb Km cassette from pUC18, Ap^r Km^r	Alexeyev 1995
pCR®2.1-TOPO™	PUC ori f1 ori *lacZ*α$^+$ Km^r Ap^r, cloning vector	Invitrogen
pRK2013	ColE1 Kn^r Tra$^+$, conjugation helper plasmid	Ditta et al. 1980
pOK1	*sacB sacQ mobRK2 oriR6K*, Sp^r, Suicide vector,	Huguet et al. 1998
pUFR053	IncW Mob$^+$*mob*(P) *lacZ*α$^+$ Par$^+$ Cm^r Gm^r, shuttle vector	El Yacoubi et al. 2007
pUSS01-2	Km cassette from pBSL15 cloned in pGEM-T easy	This study
phrpGDV1-3’	The *NdeI-NsilI* fragment of upstream region of hrpG cloned to the downstream of Km cassette in pUSS01-2	This study
phrpGDV1	The *Apa*I-*Sph*I fragment containing 436-bp downstream region of *hrpG* cloned to the upstream of Km cassette in phrpGDV1-3’	This study
phrpGDV2	Km cassette flanked by the upstream and downstream region of *hrpG* from phrGDV1 cloned into pOK1	This study
phrpG	*hrpG* gene from XCC 306 cloned in pCR®2.1-TOPO™	This study
phrpGC	*hrpG* gene on *Kpn*I fragment from phrpG cloned in pUFR053	This study

[a] Rif^r, Km^r, Ap^r, Cm^r, Gm^r and Sp^r indicate resistance to rifampicin, kanamycin, ampicillin, chloramphenicol, gentamicin and spectinomycin, respectively.

Table 3-2. Primers used in this study

Primer	Sequence (5'→3')[a]
Primers used in mutagenesis and complementation	
AChrpG-Nde1F3	TTCAAAcatatgGATCGCTGCATCGTCGG
AChrpG-Nsi1R2	AACTCGatgcatCTGGCGCAAACGATTGTA
AChrpG-Apa1F2	TTGTCGgggcccTTTGTGAGTGCGCCAA
AChrpG-R1	TGTTCCTGTTGACGCAGGATGC
AChrpG-Kpn1F4	ATAGGCggtaccGGAACGTCACTGCT
AChrpG-Kpn1R4	GAATTTggtaccCTCTCTGAAAGCCATCG
AChrpG-F1	GCTTGCCGTCCAGATAAACGGTAT
AChrpG-Sph1R3	TGTTCCgcatgcTGTTGACGCAGGATGC
Primers used in QRT-PCR	
16s-F	CGCTTTCGTGCCTCAGTGTCAGTGTTGG
16s-R	GGCGTAAAGCGTGCGTAGGTGGTGGTT
avrBs2-F	CGCGCCAATCACGACAAGGACTACTAC
avrBs2-R	CGGGCCAGCGTGCGGTTTTC
hrcV-F	GCGTTTGCGGCGTGCTTCATCT
hrcV-R	CAATCTGGTGGTAGGCCTGGTCGTTTTCTT
avrXacE1-F	TCGCGCTGGGCCGGAACATACC
avrXacE1-R	GCGTCCGCGGCGATAACTCTTG
avrXacE3-F	ATGGAGGATGGCGGGCAGATGATGAATGTA
avrXacE3-R	CGATCTCGGCTCTGAATGCGTTTGTCCTG
XAC3090-F	ATCATCTCGGGCAGTTCGTTTATCA
XAC3090-R	AGGTGCCGGGCTTGTTTGCTGTTC
hpaF-F	ACGCGCCTGTCCAATCTCA
hpaF-R	CGGCATGCGCAACTCGGTCAATC
peh-1-F	AGTGGCAACGCGTTTCTGACC
peh-1-R	CGCCTGCGTTGTTGCCCTTGAC
xynB-F	CGCAATCGCCGCAAACCA
xynB-R	GCGCAGGCTTCACCAACTAC
gyrA-F	CGTCACGTTGATCCGTTTGT
gyrA-R	GCTTGCTTCGTCCACTCCCT

[a] Lowercase nucleotides are not exact matches to the sequence and were introduced to add restriction enzyme sites.

Table 3-3. Genes showing significant differential expression in *hrpG* and/or *hrpX* mutants compared with wild type strain at any of the three selected time points.

Locus tag	Gene symbol	hrpGA /WA[a]	hrpGB /WB[a]	hrpGC /WC[a]	hrpXA /WA[a]	hrpXB /WB[a]	hrpXC /WC[a]	Description	JCVI[b]	Cluster[c]
XAC3647	pheA	1.54	0.76	-1.22	-1.53	-2.15	-3.76	chorismate mutase	Amino acid biosynthesis	I
XAC1525	tyrA	NS	NS	0.86	NS	NS	0.76	prephenate dehydrogenase	Amino acid biosynthesis	II
XAC0802	-	NS	NS	-0.65	NS	-0.61	-1.79	sulfotransferase	Amino acid biosynthesis	I
XAC4213	-	NS	NS	-0.69	NS	NS	-1.12	hypothetical protein	Amino acid biosynthesis	I
XAC2947	apbE	NS	NS	0.93	NS	0.64	0.73	thiamine biosynthesis lipoprotein ApbE precursor	Biosynthesis of cofactors, prosthetic groups, and carriers	II
XAC2922	hrpW	1.77	NS	-1.42	-1.92	-2.77	-4.50	HrpW protein	Cell envelope	I
XAC0661	peh-1	1.50	0.68	-1.13	-1.38	-1.83	-2.65	endopolygalacturonase	Cell envelope	I
XAC2113	-	NS	NS	-0.91	NS	NS	-0.86	hypothetical protein	Cell envelope	I
XAC3878	-	1.06	NS	-0.97	-0.92	-1.61	-3.05	disulphide-isomerase	Cell envelope	I
XAC0076	avrBs2	NS	NS	-1.09	NS	NS	-1.98	avirulence protein	Cellular processes	I
XAC0782	ftsQ	-0.76	-0.76	NS	-0.74	NS	NS	cell division protein	Cellular processes	NOT
XAC0400	hpaA	NS	NS	-1.23	NS	-0.75	-2.01	HpaA protein	Cellular processes	I
XAC0403	hrcQ	NS	NS	-1.12	NS	-0.86	-2.06	HrcQ protein	Cellular processes	I
XAC0406	hrcU	NS	NS	-1.66	-0.65	-1.05	-2.53	type III secretion system protein HrcU	Cellular processes	I
XAC0397	hrpE	1.30	NS	-1.03	NS	-1.82	-2.91	HrpE protein	Cellular processes	I
XAC0394	hrpF	0.79	NS	-1.59	NS	-1.21	-2.64	HrpF protein	Cellular processes	I
XAC1265	hrpG	-1.52	-2.60	-4.19	1.57	0.91	NS	HrpG protein	Cellular processes	NOT
XAC4340	yrbE	-0.63	NS	NS	-0.64	NS	NS	toluene tolerance protein	Cellular processes	NOT
XAC0878	pcaH	0.76	NS	-1.10	-0.76	-1.00	-2.33	protocatechuate 4,5-dioxygenase subunit beta	Central intermediary metabolism	I
XAC0002	dnaN	0.59	NS	0.75	NS	NS	0.70	DNA polymerase III subunit beta	DNA metabolism	II
XAC3885	cox11	-0.62	NS	NS	-0.68	NS	NS	cytochrome C oxidase assembly protein	Energy metabolism	NOT

Table 3-3. Continued

Locus tag	Gene symbol	hrpGA /WA[a]	hrpGB /WB[a]	hrpGC /WC[a]	hrpXA /WA[a]	hrpXB /WB[a]	hrpXC /WC[a]	Description	JCVI[b]	Cluster[c]
XAC3887	ctaD	-0.60	NS	NS	-0.65	NS	NS	cytochrome C oxidase subunit I	Energy metabolism	NOT
XAC0879	ligA	0.86	NS	-1.14	NS	-1.02	-2.38	protocatechuate 4,5-dioxygenase subunit alpha	Energy metabolism	I
XAC1439	tpmT	NS	NS	1.54	NS	NS	1.33	thiopurine S-methyltransferase	Energy metabolism	II
XAC4327	uahA	NS	NS	-0.79	NS	NS	-1.43	allophanate hydrolase	Energy metabolism	I
XAC0363	vanA	NS	NS	-0.61	NS	NS	-1.04	vanillate O-demethylase oxygenase subunit	Energy metabolism	I
XAC4252	xynB	NS	NS	-0.68	NS	NS	-1.13	xylanase	Energy metabolism	I
XAC0562	mdcB	NS	NS	0.93	NS	NS	0.72	malonate decarboxylase subunit beta	Fatty acid and phospholipid metabolism	II
XAC1314	paaF	NS	NS	0.87	0.70	NS	NS	enoyl-CoA hydratase	Fatty acid and phospholipid metabolism	NOT
XAC2990	-	NS	NS	-0.61	NS	NS	-0.82	hypothetical protein	Fatty acid and phospholipid metabolism	I
XAC0501	-	1.37	NS	-1.35	-0.93	-1.95	-3.20	hypothetical protein	Hypothetical proteins	I
XAC0601	-	0.97	NS	-0.98	NS	-0.74	-1.91	hypothetical protein	Hypothetical proteins	I
XAC0829	-	NS	-0.74	NS	NS	NS	0.64	ABC transporter substrate binding protein	Hypothetical proteins	NOT
XAC0916	-	NS	NS	-0.90	NS	NS	-1.13	hydrolase	Hypothetical proteins	I
XAC1124	-	NS	NS	-0.62	NS	-0.67	-1.30	hypothetical protein	Hypothetical proteins	I
XAC1208	-	NS	NS	-0.99	NS	-0.76	-2.16	hypothetical protein	Hypothetical proteins	I
XAC1689	-	0.75	NS	0.86	NS	NS	0.89	hypothetical protein	Hypothetical proteins	II
XAC2782	-	-0.65	NS	NS	-0.67	NS	NS	hypothetical protein	Hypothetical proteins	NOT
XAC2827	-	0.83	NS	0.85	NS	NS	1.05	hypothetical protein	Hypothetical proteins	II
XAC3222	-	NS	NS	1.29	NS	NS	1.12	hypothetical protein	Hypothetical proteins	II
XAC4019	-	NS	NS	0.76	NS	NS	0.62	hypothetical protein	Hypothetical proteins	II
XACb0011	avrXacE3	0.98	NS	-1.25	-0.71	-1.64	-3.25	avirulence protein	Not in JCVI	I
XACb0007	mlt	1.33	0.85	NS	NS	NS	-0.86	COG2951M	Not in JCVI	I

Table 3-3. Continued

Locus tag	Gene symbol	hrpGA /WA[a]	hrpGB /WB[a]	hrpGC /WC[a]	hrpXA /WA[a]	hrpXB /WB[a]	hrpXC /WC[a]	Description	JCVI[b]	Cluster[c]
XACa0021	repA	NS	NS	0.82	NS	NS	0.75	replication protein A	Not in JCVI	II
XAC0099	-	1.09	NS	1.17	NS	NS	1.33	hypothetical protein	Not in JCVI	II
XAC0277	-	0.72	NS	-1.20	NS	-1.24	-2.67	hypothetical protein	Not in JCVI	I
XAC0315	-	0.80	NS	-0.86	NS	-0.71	-1.63	hypothetical protein	Not in JCVI	I
XAC0395	-	NS	NS	-1.22	NS	-0.86	-2.00	hypothetical protein	Not in JCVI	I
XAC0543	-	1.68	0.74	-1.42	-1.72	-3.44	-5.12	hypothetical protein	Not in JCVI	I
XAC0617	-	NS	NS	1.67	NS	NS	1.63	hypothetical protein	Not in JCVI	II
XAC0786	-	NS	NS	0.75	NS	NS	0.61	hypothetical protein	Not in JCVI	II
XAC0817	-	0.87	NS	-0.61	NS	-0.71	-1.49	hypothetical protein	Not in JCVI	I
XAC1172	-	0.73	NS	-1.31	-0.77	-1.17	-2.78	hypothetical protein	Not in JCVI	I
XAC1241	-	1.26	NS	-0.88	NS	-0.97	-1.89	hypothetical protein	Not in JCVI	I
XAC1412	-	NS	NS	1.08	NS	NS	0.95	hypothetical protein	Not in JCVI	II
XAC1563	-	NS	NS	1.51	NS	NS	1.29	hypothetical protein	Not in JCVI	II
XAC1572	-	NS	NS	2.40	NS	NS	1.62	hypothetical protein	Not in JCVI	II
XAC1683	-	NS	NS	-0.65	NS	NS	-1.03	hypothetical protein	Not in JCVI	I
XAC2357	-	NS	NS	1.94	NS	NS	1.95	hypothetical protein	Not in JCVI	II
XAC2370	-	0.79	NS	-0.87	NS	-0.77	-1.74	hypothetical protein	Not in JCVI	I
XAC2425	-	NS	NS	1.36	NS	NS	1.24	hypothetical protein	Not in JCVI	II
XAC2442	-	NS	NS	1.67	NS	NS	1.39	hypothetical protein	Not in JCVI	II
XAC2654	-	1.71	0.63	-1.20	-2.64	-3.82	-5.35	hypothetical protein	Not in JCVI	I
XAC2786	-	1.44	NS	-1.73	-1.15	-2.99	-4.83	hypothetical protein	Not in JCVI	I
XAC2787	-	NS	NS	-1.11	NS	-0.96	-2.46	hypothetical protein	Not in JCVI	I
XAC2876	-	0.71	NS	-0.81	NS	-0.68	-1.67	hypothetical protein	Not in JCVI	I
XAC3085	-	NS	NS	-1.56	NS	-1.72	-3.87	hypothetical protein	Not in JCVI	I
XAC3230	-	0.96	NS	-1.04	NS	-1.15	-2.33	hypothetical protein	Not in JCVI	I
XAC3291	-	NS	NS	0.75	NS	NS	0.87	hypothetical protein	Not in JCVI	II
XAC3337	-	NS	NS	0.70	NS	NS	0.67	hypothetical protein	Not in JCVI	II
XAC3646	-	1.30	0.74	-1.02	-0.91	-1.52	-2.59	hypothetical protein	Not in JCVI	I

Table 3-3. Continued

Locus tag	Gene symbol	hrpGA /WA[a]	hrpGB /WB[a]	hrpGC /WC[a]	hrpXA /WA[a]	hrpXB /WB[a]	hrpXC /WC[a]	Description	JCVI[b]	Cluster[c]
XAC3666	-	0.95	0.81	NS	NS	NS	-1.02	hypothetical protein	Not in JCVI	I
XAC3984	-	NS	NS	0.83	NS	NS	0.88	hypothetical protein	Not in JCVI	II
XAC4318	-	NS	NS	-0.59	NS	NS	-0.60	hypothetical protein	Not in JCVI	I
XACa0013	-	0.76	0.62	0.68	NS	NS	0.61	hypothetical protein	Not in JCVI	II
XACb0034	-	NS	NS	2.17	NS	NS	1.93	hypothetical protein	Not in JCVI	II
XACb0049	-	NS	NS	0.83	NS	NS	0.78	hypothetical protein	Not in JCVI	II
XACb0057	-	0.63	NS	0.79	NS	NS	0.83	hypothetical protein	Not in JCVI	II
XAC0286	avrXacE1	0.90	NS	-1.21	-0.91	-1.18	-2.56	avirulence protein	Protein fate	I
XAC0415	hrcC	NS	NS	-1.58	NS	NS	-1.60	HrcC protein	Protein fate	I
XAC0402	hrcR	NS	NS	-1.26	NS	-0.87	-2.03	type III secretion system protein	Protein fate	I
XAC0401	hrcS	NS	NS	-1.52	NS	-1.08	-2.57	HrcS protein	Protein fate	I
XAC0414	hrcT	NS	NS	-1.16	NS	-0.68	-1.95	HrcT protein	Protein fate	I
XAC0407	hrpB1	1.23	NS	-2.18	-1.78	-2.86	-4.57	HrpB1 protein	Protein fate	I
XAC0408	hrpB2	0.94	NS	-1.90	-1.11	-1.95	-3.72	HrpB2 protein	Protein fate	I
XAC0410	hrpB4	0.92	NS	-1.66	-0.75	-1.52	-2.95	HrpB4 protein	Protein fate	I
XAC0411	hrpB5	NS	NS	-1.34	NS	-0.85	-2.09	type III secretion system protein HrpB	Protein fate	I
XAC0413	hrpB7	NS	NS	-1.11	NS	-0.66	-1.90	HrpB7 protein	Protein fate	I
XAC1085	ppiD	NS	NS	0.85	NS	NS	0.64	peptidyl-prolyl cis-trans isomerase	Protein fate	II
XAC2831	-	NS	NS	-0.71	NS	NS	-0.97	extracellular serine protease	Protein fate	I
XAC0416	hpa1	1.93	NS	-1.42	-1.60	-4.29	-5.54	Hpa1 protein	Protein synthesis	I
XAC0404	hpaP	0.70	NS	-1.36	-0.63	-1.11	-2.51	HpaP protein	Protein synthesis	I
XAC3977	-	NS	NS	1.38	NS	NS	1.30	hypothetical protein	Protein synthesis	II
XAC0880	pcaQ	0.68	NS	-0.85	NS	-0.88	-2.00	transcriptional regulator	Regulatory functions	I
XAC1171	stkXac1	0.98	NS	-1.03	NS	-0.78	-2.03	serine/threonine kinase	Regulatory functions	I
XAC1455	-	0.64	NS	NS	NS	NS	-1.20	MarR family transcriptional regulator	Regulatory functions	I

Table 3-3. Continued

Locus tag	Gene symbol	hrpGA /WA[a]	hrpGB /WB[a]	hrpGC /WC[a]	hrpXA /WA[a]	hrpXB /WB[a]	hrpXC /WC[a]	Description	JCVI[b]	Cluster[c]
XAC3050	btuB	NS	NS	1.35	-1.13	NS	NS	TonB-dependent receptor	Transport and binding proteins	NOT
XAC3444	btuB	-0.94	NS	NS	5.13	4.13	3.42	TonB-dependent receptor	Transport and binding proteins	NOT
XAC1556	fucP	-0.71	NS	NS	-0.64	NS	NS	glucose-galactose transporter	Transport and binding proteins	NOT
XAC3489	fyuA	NS	NS	-0.61	-0.69	NS	NS	TonB-dependent receptor	Transport and binding proteins	NOT
XAC0412	hrcN	NS	NS	-1.22	NS	-0.82	-2.10	type III secretion system ATPase	Transport and binding proteins	I
XAC0827	nrtB	0.66	NS	NS	NS	NS	0.73	permease	Transport and binding proteins	NOT
XAC3170	bioI	NS	NS	-0.73	NS	NS	-1.40	cytochrome P-450 hydroxylase	Unclassified	I
XAC0417	hpa2	NS	NS	-0.94	NS	NS	-1.23	Hpa2 protein	Unclassified	I
XAC0396	hpaB	NS	NS	-1.67	NS	-1.25	-2.79	HpaB protein	Unclassified	I
XAC0393	hpaF	NS	NS	-1.32	NS	NS	-2.06	HpaF protein	Unclassified	I
XAC0409	hrcJ	1.03	NS	-1.90	-1.07	-2.18	-3.81	HrcJ protein	Unclassified	I
XAC0405	hrcV	NS	NS	-1.14	NS	-0.84	-1.85	HrcV protein	Unclassified	I
XAC0399	hrpD5	0.74	NS	-1.64	-0.73	-1.55	-3.08	HrpD5 protein	Unclassified	I
XAC0398	hrpD6	1.09	NS	-1.72	NS	-1.63	-3.21	HrpD6 protein	Unclassified	I
XAC1266	hrpXct	1.93	0.95	NS	1.60	1.97	1.58	HrpX protein	Unclassified	NOT
XAC3225	mltB	1.36	0.84	NS	NS	NS	-0.92	transglycosylase	Unclassified	I
XAC2653	S	NS	NS	0.81	NS	NS	0.73	phage-related tail protein	Unclassified	II
XAC4326	uahA	0.81	0.67	NS	NS	NS	-0.91	urea amidolyase	Unclassified	I
XAC0435	virK	1.49	0.67	-1.15	-1.54	-2.31	-3.55	VirK protein	Unclassified	I
XAC0552	-	0.99	NS	-1.24	-1.35	-1.79	-2.99	proteinase	Unclassified	I
XAC0754	-	NS	NS	-0.88	NS	-0.73	-1.85	hypothetical protein	Unclassified	I
XAC2123	-	NS	NS	0.71	NS	NS	0.65	hypothetical protein	Unclassified	II
XAC2178	-	NS	NS	0.71	NS	NS	0.62	hypothetical protein	Unclassified	II
XAC2853	-	2.03	0.97	-0.88	-2.40	-4.00	-5.08	cysteine protease	Unclassified	I
XAC3090	-	NS	NS	-0.93	NS	-0.64	-1.53	leucin rich protein	Unclassified	I

Table 3-3. Continued

Locus tag	Gene symbol	hrpGA /WA[a]	hrpGB /WB[a]	hrpGC /WC[a]	hrpXA /WA[a]	hrpXB /WB[a]	hrpXC /WC[a]	Description	JCVI[b]	Cluster[c]
XAC4333	-	0.78	NS	-1.30	NS	-1.12	-2.52	hypothetical protein	Unclassified	I
XAC0795	xcp	0.73	NS	-0.81	-0.62	-0.81	-1.83	protease	Unclassified	I
XAC1433	asnB	NS	NS	0.79	NS	NS	NS	asparagine synthetase B	Amino acid biosynthesis	III
XAC1760	dapA	NS	NS	-0.63	NS	NS	NS	dihydrodipicolinate synthase	Amino acid biosynthesis	IV
XAC0336	metE	NS	NS	0.91	NS	NS	NS	5-methyltetrahydropteroyltriglutamate--homocysteine methyltransferase	Amino acid biosynthesis	III
XAC0306	gatA	-0.66	NS	NS	NS	NS	NS	amidase	Biosynthesis of cofactors, prosthetic groups, and carriers	IV
XAC0429	glgY	NS	NS	-0.67	NS	NS	NS	maltooligosyltrehalose synthase	Cell envelope	IV
XAC0658	mreD	-0.61	NS	NS	NS	NS	NS	rod shape-determining protein	Cell envelope	IV
XAC3606	uptD	NS	NS	-0.59	NS	NS	NS	outer membran protein	Cell envelope	IV
XAC0267	-	-0.62	NS	NS	NS	NS	NS	hypothetical protein	Cell envelope	IV
XAC0677	-	NS	NS	-0.61	NS	NS	NS	hypothetical protein	Cell envelope	IV
XAC1749	-	-0.67	NS	NS	NS	NS	NS	hypothetical protein	Cell envelope	IV
XAC4042	-	NS	NS	-0.68	NS	NS	NS	hypothetical protein	Cell envelope	IV
XAC3224	avrXacE2	0.84	NS	NS	NS	NS	NS	avirulence protein	Cellular processes	NOT
XAC2865	cheA	NS	NS	0.70	NS	NS	NS	chemotaxis histidine protein kinase	Cellular processes	III
XAC1904	cheY	NS	NS	0.99	NS	NS	NS	chemotaxis response regulator	Cellular processes	III
XAC1982	flgF	NS	NS	1.34	NS	NS	NS	flagellar basal body rod protein FlgF	Cellular processes	III
XAC1954	fliF	NS	NS	1.05	NS	NS	NS	flagellar MS-ring protein	Cellular processes	III
XAC1953	fliG	NS	NS	1.09	NS	NS	NS	flagellar protein	Cellular processes	III
XAC1951	fliI	NS	NS	0.71	NS	NS	NS	flagellar protein	Cellular processes	III
XAC1950	fliJ	0.65	NS	NS	NS	NS	NS	flagellar FliJ protein	Cellular processes	NOT

Table 3-3. Continued

Locus tag	Gene symbol	hrpGA /WA[a]	hrpGB /WB[a]	hrpGC /WC[a]	hrpXA /WA[a]	hrpXB /WB[a]	hrpXC /WC[a]	Description	JCVI[b]	Cluster[c]
XAC1908	motB	NS	-0.98	NS	NS	NS	NS	flagellar motor protein MotD	Cellular processes	IV
XAC0604	treA	NS	NS	0.62	NS	NS	NS	trehalase	Cellular processes	III
XAC3053	-	-1.06	NS	NS	NS	NS	NS	hypothetical protein	Central intermediary metabolism	IV
XAC4223	rdgC	NS	-0.91	-0.60	NS	NS	NS	recombination associated protein	DNA metabolism	IV
XAC0265	acdA	-0.77	NS	NS	NS	NS	NS	acyl-CoA dehydrogenase	Energy metabolism	IV
XAC0652	adhC	NS	NS	0.62	NS	NS	NS	alcohol dehydrogenase class III	Energy metabolism	III
XAC2502	fruK	-0.71	NS	NS	NS	NS	NS	1-phosphofructokinase (fructose 1-phosphate kinase)	Energy metabolism	IV
XAC0548	GNL	NS	NS	-0.80	NS	NS	NS	gluconolactonase precursor	Energy metabolism	IV
XAC0143	kdgK	NS	NS	-0.60	NS	NS	NS	2-keto-3-deoxygluconate kinase	Energy metabolism	IV
XAC3114	pqqG	NS	NS	-0.70	NS	NS	NS	pyrroloquinoline quinone biosynthesis protein PqqB	Energy metabolism	IV
XAC1137	prpB	NS	-0.83	NS	NS	NS	NS	2-methylisocitrate lyase	Energy metabolism	IV
XAC3890	putA	NS	NS	0.94	NS	NS	NS	bifunctional proline dehydrogenase/pyrroline-5-carboxylate dehydrogenase	Energy metabolism	III
XAC0264	accD	NS	NS	0.89	NS	NS	NS	acyl-CoA carboxyltransferase beta chain	Fatty acid and phospholipid metabolism	III
XAC1313	fadE9	NS	NS	1.38	NS	NS	NS	acyl-CoA dehydrogenase	Fatty acid and phospholipid metabolism	III
XAC2215	ea59	NS	NS	0.68	NS	NS	NS	hypothetical protein	Hypothetical proteins	III
XAC1088	-	-0.61	NS	NS	NS	NS	NS	hypothetical protein	Hypothetical proteins	IV
XAC2828	-	-1.43	NS	NS	NS	NS	NS	hypothetical protein	Hypothetical proteins	IV
XAC2944	-	NS	NS	0.64	NS	NS	NS	hypothetical protein	Hypothetical proteins	III
XAC2946	-	NS	NS	0.65	NS	NS	NS	hypothetical protein	Hypothetical proteins	III
XAC3155	-	NS	NS	-0.72	NS	NS	NS	hypothetical protein	Hypothetical proteins	IV
XAC3763	-	NS	NS	0.71	NS	NS	NS	hypothetical protein	Hypothetical proteins	III

Table 3-3. Continued

Locus tag	Gene symbol	hrpGA /WA[a]	hrpGB /WB[a]	hrpGC /WC[a]	hrpXA /WA[a]	hrpXB /WB[a]	hrpXC /WC[a]	Description	JCVI[b]	Cluster[c]
XAC3783	-	0.88	NS	NS	NS	NS	NS	hypothetical protein	Hypothetical proteins	NOT
XAC1924	-	0.67	NS	NS	NS	NS	NS	transposase	Mobile and extrachromosomal element functions	NOT
XAC1945	fliO	NS	-1.38	NS	NS	NS	NS	flagellar protein	Not in JCVI	IV
XAC2422	kfrA	NS	NS	0.81	NS	NS	NS	plasmid-related protein	Not in JCVI	III
XAC2672	oar	NS	NS	1.13	NS	NS	NS	Oar protein	Not in JCVI	III
XACa0022	pthA1	0.82	0.81	NS	NS	NS	NS	avirulence protein	Not in JCVI	NOT
XACa0039	pthA2	0.77	0.81	NS	NS	NS	NS	avirulence protein	Not in JCVI	NOT
XACb0015	pthA3	0.80	0.82	NS	NS	NS	NS	avirulence protein	Not in JCVI	NOT
XACb0065	pthA4	0.80	0.76	NS	NS	NS	NS	avirulence protein	Not in JCVI	NOT
XAC0260	-	NS	NS	0.67	NS	NS	NS	hypothetical protein	Not in JCVI	III
XAC0549	-	NS	NS	-0.90	NS	NS	NS	hypothetical protein	Not in JCVI	IV
XAC0607	-	NS	NS	-0.63	NS	NS	NS	hypothetical protein	Not in JCVI	IV
XAC0747	-	0.77	NS	NS	NS	NS	NS	hypothetical protein	Not in JCVI	NOT
XAC1497	-	0.69	NS	NS	NS	NS	NS	hypothetical protein	Not in JCVI	NOT
XAC1971	-	NS	NS	0.97	NS	NS	NS	hypothetical protein	Not in JCVI	III
XAC1972	-	NS	NS	1.20	NS	NS	NS	hypothetical protein	Not in JCVI	III
XAC1990	-	NS	NS	1.04	NS	NS	NS	hypothetical protein	Not in JCVI	III
XAC2929	-	-0.82	NS	NS	NS	NS	NS	hypothetical protein	Not in JCVI	IV
XAC3131	-	NS	NS	0.63	NS	NS	NS	hypothetical protein	Not in JCVI	III
XAC3268	-	0.66	NS	NS	NS	NS	NS	hypothetical protein	Not in JCVI	NOT
XAC3497	-	1.04	NS	NS	NS	NS	NS	hypothetical protein	Not in JCVI	NOT
XAC3523	-	-0.67	NS	NS	NS	NS	NS	hypothetical protein	Not in JCVI	IV
XAC3636	-	NS	NS	0.87	NS	NS	NS	hypothetical protein	Not in JCVI	III
XAC3680	-	NS	NS	-0.68	NS	NS	NS	hypothetical protein	Not in JCVI	IV
XAC4026	-	NS	NS	0.70	NS	NS	NS	hypothetical protein	Not in JCVI	III
XAC4261	-	0.70	NS	NS	NS	NS	NS	hypothetical protein	Not in JCVI	NOT
XACa0002	-	0.68	NS	NS	NS	NS	NS	hypothetical protein	Not in JCVI	NOT

Table 3-3. Continued

Locus tag	Gene symbol	hrpGA /WA[a]	hrpGB /WB[a]	hrpGC /WC[a]	hrpXA /WA[a]	hrpXB /WB[a]	hrpXC /WC[a]	Description	JCVI[b]	Cluster[c]
XACa0030	-	NS	NS	0.69	NS	NS	NS	transposase	Not in JCVI	III
XACb0029	-	NS	NS	0.94	NS	NS	NS	hypothetical protein	Not in JCVI	III
XACb0073	-	0.80	NS	0.70	NS	NS	NS	hypothetical protein	Not in JCVI	NOT
XAC2566	alg2	NS	NS	0.93	NS	NS	NS	glycosyltransferase	Protein fate	III
XAC1521	grpE	NS	-0.63	NS	NS	NS	NS	heat shock protein GrpE	Protein fate	IV
XAC3782	map	0.73	NS	NS	NS	NS	NS	methionine aminopeptidase	Protein fate	NOT
XAC0104	-	NS	NS	-0.73	NS	NS	NS	metalloprotease	Protein fate	IV
XAC1425	fasD	NS	NS	0.95	NS	NS	NS	outer membrane usher protein FasD	Protein synthesis	III
XAC1633	gcd	-0.64	NS	NS	NS	NS	NS	glucose dehydrogenase	Protein synthesis	IV
XAC3089	-	NS	NS	0.61	NS	NS	NS	hypothetical protein	Protein synthesis	III
XAC1989	flgM	NS	NS	1.00	NS	NS	NS	flagellar protein	Regulatory functions	III
XAC1573	phoU	NS	NS	1.14	NS	NS	NS	phosphate regulon transcriptional regulator	Regulatory functions	III
XAC1798	regS	NS	0.60	NS	NS	NS	NS	two-component system sensor protein	Regulatory functions	NOT
XAC1877	rpfG	NS	NS	0.78	NS	NS	NS	response regulator	Regulatory functions	III
XAC0917	-	-0.73	NS	NS	NS	NS	NS	transcriptional regulator	Regulatory functions	IV
XAC1488	-	NS	NS	0.95	NS	NS	NS	sensor histidine kinase	Regulatory functions	III
XAC2192	-	NS	NS	0.76	NS	NS	NS	two-component system sensor protein	Regulatory functions	III
XAC2897	-	NS	NS	1.13	NS	NS	NS	response regulator	Regulatory functions	III
XAC3771	-	NS	NS	0.67	NS	NS	NS	hypothetical protein	Regulatory functions	III
XAC1320	-	NS	NS	-0.72	NS	NS	NS	regulatory protein	Transcription	IV
XAC2503	fruA	-0.81	NS	-0.63	NS	NS	NS	PTS system, fructose-specific IIBC component	Transport and binding proteins	IV
XAC1143	fyuA	NS	NS	0.93	NS	NS	NS	TonB-dependent receptor	Transport and binding proteins	III
XAC3856	-	NS	NS	-0.73	NS	NS	NS	hypothetical protein	Transport and binding proteins	IV
XAC1906	cheW	NS	NS	1.11	NS	NS	NS	chemotaxis protein	Unclassified	III

Table 3-3. Continued

Locus tag	Gene symbol	hrpGA /WA[a]	hrpGB /WB[a]	hrpGC /WC[a]	hrpXA /WA[a]	hrpXB /WB[a]	hrpXC /WC[a]	Description	JCVI[b]	Cluster[c]
XAC0159	estA1	NS	0.64	NS	NS	NS	NS	carboxylesterase type B	Unclassified	NOT
XAC1312	mmsA	NS	NS	1.69	NS	NS	NS	methylmalonate-semialdehyde dehydrogenase	Unclassified	III
XAC1507	mobL	NS	-0.72	NS	NS	NS	NS	plasmid mobilization protein	Unclassified	IV
XAC3228	orfS	-0.64	NS	NS	NS	NS	NS	cointegrate resolution protein S	Unclassified	IV
XAC3229	orfT	-0.69	NS	NS	NS	NS	NS	cointegrate resolution protein T	Unclassified	IV
XAC3605	uptE	NS	NS	-0.67	NS	NS	NS	outer membrane protein	Unclassified	IV
XAC1315	-	NS	NS	0.79	NS	NS	NS	enoyl-CoA hydratase	Unclassified	III
XAC1789	-	-0.78	NS	NS	NS	NS	NS	hypothetical protein	Unclassified	IV
XAC2117	-	-0.63	NS	NS	NS	NS	NS	hypothetical protein	Unclassified	IV
XAC2120	-	-0.73	NS	NS	NS	NS	NS	hypothetical protein	Unclassified	IV
XAC3073	-	0.63	NS	NS	NS	NS	NS	hypothetical protein	Unclassified	NOT
XAC3959	-	NS	NS	0.98	NS	NS	NS	hypothetical protein	Unclassified	NOT
XAC0209	yojM	NS	NS	-0.62	NS	NS	NS	superoxide dismutase like protein	Unclassified	IV
XAC1030	-	-0.66	NS	-0.76	NS	NS	NS	hypothetical protein	Unknown function	IV
XAC1939	-	NS	NS	0.65	NS	NS	NS	GGDEF family protein	Unknown function	III
XAC1940	-	NS	NS	0.82	NS	NS	NS	GGDEF family protein	Unknown function	III
XAC2483	-	-1.21	NS	NS	NS	NS	NS	hypothetical protein	Unknown function	IV
XAC3314	-	0.61	NS	NS	NS	NS	NS	hypothetical protein	Unknown function	NOT
XAC1833	hisA	NS	NS	NS	NS	NS	1.14	1-(5-phosphoribosyl)-5-[(5-phosphoribosylamino)methylideneamino] imidazole-4-carboxamide isomerase	Amino acid biosynthesis	V
XAC1831	hisB	NS	NS	NS	NS	NS	1.19	imidazole glycerol-phosphate dehydratase/histidinol phosphatase	Amino acid biosynthesis	V
XAC1830	hisC	NS	NS	NS	-0.80	NS	1.18	histidinol-phosphate aminotransferase	Amino acid biosynthesis	V

Table 3-3. Continued

Locus tag	Gene symbol	hrpGA /WA[a]	hrpGB /WB[a]	hrpGC /WC[a]	hrpXA /WA[a]	hrpXB /WB[a]	hrpXC /WC[a]	Description	JCVI[b]	Cluster[c]
XAC1829	hisD	NS	NS	NS	-0.72	NS	1.02	histidinol dehydrogenase	Amino acid biosynthesis	V
XAC1834	hisF	NS	NS	NS	NS	NS	1.07	imidazole glycerol phosphate synthase subunit HisF	Amino acid biosynthesis	V
XAC1828	hisG	NS	NS	NS	NS	NS	0.87	ATP phosphoribosyltransferase	Amino acid biosynthesis	V
XAC1832	hisH	NS	NS	NS	-0.66	NS	1.11	imidazole glycerol phosphate synthase subunit HisH	Amino acid biosynthesis	V
XAC3451	ilvC	NS	NS	NS	NS	NS	-0.71	ketol-acid reductoisomerase	Amino acid biosynthesis	I
XAC3452	ilvG	NS	NS	NS	NS	NS	-0.67	acetolactate synthase 2 catalytic subunit	Amino acid biosynthesis	I
XAC3340	cysG	NS	NS	NS	NS	NS	0.68	siroheme synthase	Biosynthesis of cofactors, prosthetic groups, and carriers	V
XAC4062	fhuA	NS	NS	NS	NS	NS	-0.68	TonB-dependent receptor	Cell envelope	I
XAC2374	**pglA**	**NS**	**NS**	**NS**	**NS**	**NS**	**-0.78**	**polygalacturonase**	**Cell envelope**	**I**
XAC1142	-	NS	NS	NS	0.76	NS	NS	hypothetical protein	Cell envelope	NOT
XAC0557	**appA**	**NS**	**NS**	**NS**	**NS**	**NS**	**0.80**	**6-phytase**	**Central intermediary metabolism**	**V**
XAC4369	**phoC**	**NS**	**NS**	**NS**	**NS**	**NS**	**-0.68**	**phosphatase precursor**	**Central intermediary metabolism**	**I**
XAC0803	-	NS	NS	NS	NS	NS	-0.66	methyltransferase	DNA metabolism	I
XAC3312	-	NS	NS	NS	0.81	NS	NS	glycosyl hydrolase	Energy metabolism	NOT
XAC3960	-	NS	NS	NS	NS	NS	0.90	oxidoreductase	Energy metabolism	V
XAC3655	atpB	NS	NS	NS	NS	NS	0.60	F0F1 ATP synthase subunit A	Energy metabolism	V
XAC3869	**bglX**	**NS**	**NS**	**NS**	**NS**	**NS**	**0.60**	**beta-glucosidase**	**Energy metabolism**	**V**
XAC3884	**cox3**	**NS**	**NS**	**NS**	**-0.67**	**NS**	**NS**	**cytochrome C oxidase subunit III**	**Energy metabolism**	**NOT**
XAC4251	**hrmI**	**NS**	**NS**	**NS**	**NS**	**NS**	**-0.61**	**glucuronate isomerase**	**Energy metabolism**	**I**

Table 3-3. Continued

Locus tag	Gene symbol	hrpGA /WA[a]	hrpGB /WB[a]	hrpGC /WC[a]	hrpXA /WA[a]	hrpXB /WB[a]	hrpXC /WC[a]	Description	JCVI[b]	Cluster[c]
XAC4221	-	**NS**	**NS**	**NS**	**NS**	**NS**	**0.63**	**hydrolase**	**Fatty acid and phospholipid metabolism**	**V**
XAC1013	-	NS	NS	NS	NS	NS	0.61	hypothetical protein	Hypothetical proteins	V
XAC4021	-	**NS**	**NS**	**NS**	**NS**	**NS**	**-0.65**	**hypothetical protein**	**Hypothetical proteins**	**I**
XAC1056	-	**NS**	**NS**	**NS**	**NS**	**NS**	**0.67**	**hypothetical protein**	**Not in JCVI**	**V**
XAC1681	-	**NS**	**NS**	**NS**	**NS**	**NS**	**-0.77**	**hypothetical protein**	**Not in JCVI**	**I**
XAC1715	-	NS	NS	NS	NS	NS	-0.66	hypothetical protein	Not in JCVI	I
XAC2009	-	**NS**	**NS**	**NS**	**NS**	**NS**	**-1.31**	**hypothetical protein**	**Not in JCVI**	**I**
XAC2517	-	**NS**	**NS**	**NS**	**NS**	**NS**	**-0.67**	**hypothetical protein**	**Not in JCVI**	**I**
XAC4063	-	**NS**	**NS**	**NS**	**NS**	**NS**	**-0.95**	**hypothetical protein**	**Not in JCVI**	**I**
XAC4321	-	**NS**	**NS**	**NS**	**NS**	**NS**	**-0.87**	**hypothetical protein**	**Not in JCVI**	**I**
XAC0108	atsE	NS	NS	NS	0.67	NS	NS	AtsE	Not in JCVI	NOT
XAC2300	rpmJ	NS	NS	NS	NS	NS	0.60	50S ribosomal protein L36	Not in JCVI	V
XAC1680	-	**NS**	**NS**	**NS**	**NS**	**NS**	**-0.72**	**serine protease**	**Protein fate**	**I**
XAC1014	-	NS	NS	NS	NS	NS	0.75	pseudouridylate synthase	Protein synthesis	V
XAC2164	-	NS	NS	NS	NS	NS	-0.61	hypothetical protein	Protein synthesis	I
XAC1555	-	NS	NS	NS	-0.65	NS	NS	transcriptional regulator	Regulatory functions	NOT
XAC2163	-	NS	NS	NS	NS	NS	-0.74	hypothetical protein	Regulatory functions	I
XAC2166	-	**NS**	**NS**	**NS**	**NS**	**NS**	**-1.02**	**transcriptional regulator**	**Regulatory functions**	**I**
XAC3445	-	NS	NS	NS	2.22	2.88	3.46	transcriptional regulator	Regulatory functions	NOT
XAC3446	-	NS	NS	NS	-0.71	NS	NS	hypothetical protein	Regulatory functions	NOT
XAC4272	-	NS	NS	NS	-0.62	NS	NS	LacI family transcription regulator	Regulatory functions	NOT
XAC1682	**rpoE**	**NS**	**NS**	**NS**	**NS**	**NS**	**-0.82**	**RNA polymerase sigma-E factor**	**Transcription**	**I**
XAC1705	-	**NS**	**NS**	**NS**	**NS**	**NS**	**-0.79**	**MFS transporter**	**Transport and binding proteins**	**I**

Table 3-3. Continued

Locus tag	Gene symbol	hrpGA /WA[a]	hrpGB /WB[a]	hrpGC /WC[a]	hrpXA /WA[a]	hrpXB /WB[a]	hrpXC /WC[a]	Description	JCVI[b]	Cluster[c]
XAC0758	kdpC	NS	NS	NS	0.93	NS	NS	potassium-transporting ATPase subunit C	Transport and binding proteins	NOT
XAC0828	nrtCD	NS	NS	NS	NS	NS	0.75	ABC transporter ATP-binding component	Transport and binding proteins	V
XAC3488	suc1	NS	NS	NS	-0.89	NS	NS	sugar transporter	Transport and binding proteins	NOT
XAC0340	**-**	**NS**	**NS**	**NS**	**NS**	**NS**	**-0.96**	**hypothetical protein**	**Unclassified**	**I**
XAC0418	**-**	**NS**	**NS**	**NS**	**NS**	**NS**	**-0.69**	**hypothetical protein**	**Unclassified**	**I**
XAC1651	-	NS	NS	NS	NS	NS	-0.76	TonB-like protein	Unclassified	I
XAC2788	-	**NS**	**NS**	**NS**	**NS**	**NS**	**-0.73**	**hypothetical protein**	**Unclassified**	**I**
XAC2832	-	**NS**	**NS**	**NS**	**NS**	**NS**	**-0.83**	**hypothetical protein**	**Unclassified**	**I**
XAC4184	-	**NS**	**NS**	**NS**	**-0.61**	**NS**	**NS**	**oxidoreductase**	**Unclassified**	**NOT**
XAC0263	accC	NS	NS	NS	0.61	NS	NS	biotin carboxylase	Unclassified	NOT
XAC1835	hisI	NS	NS	NS	NS	NS	1.06	bifunctional phosphoribosyl-AMP cyclohydrolase/phosphoribosyl-ATP pyrophosphatase protein	Unclassified	V
XAC0757	kdpB	NS	NS	NS	1.51	NS	NS	potassium-transporting ATPase subunit B	Unclassified	NOT
XAC2165	-	NS	NS	NS	NS	NS	-0.91	hydrolase	Unknown function	I

[a] Log_2-fold change was derived from mutant versus wild type at time points A, B, and C. NS = not significantly differentially expressed ($|log_2$-fold change$| < 0.585$ or false discovery rate > 0.05). [b] J. Craig Venter Institute (JCVI) functional categories. [c] Clusters were assigned based on clustering analysis. NOT = not assigned in any cluster. Genes highlighted in bold letter belong to HrpX regulon but showed subtle expression changes ($|log_2$-fold change$| < 0.585$ with false discovery rate < 0.05) in *hrpG* mutant in at least one of the three time points.

Table 3-4. Confirmed and putative type III secretion system effectors

Effector family	Locus tag	Domain[a]	Cluster	Homology	Reference
AvrBs2	XAC0076	pfam03009 - GDPD	I	AvrBs2 in *X. campestris* pv. *vesicatoria*	Kearney and Staskawicz 1990
AvrBs3(PthA1)	XACa0022	pfam03377 - Avirulence	NC		Al-Saadi et al. 2007
AvrBs3(PthA2)	XACa0039	pfam03377 - Avirulence	NC		Al-Saadi et al. 2007
AvrBs3(PthA3)	XACb0015	pfam03377 - Avirulence	NC		Al-Saadi et al. 2007
AvrBs3(PthA4)	XACb0065	pfam03377 - Avirulence	NC		Al-Saadi et al. 2007
HrpW (PopW)	XAC2922	pfam03211 - Pectate_lyase	I		Figueiredo et al. 2011
XopAD (Skwp,RSc3401)	XAC4213		I	Skwp from *R. solanacearum*	Guidot et al. 2007
XopAE (HpaF/G/PopC)	XAC0393	pfam00560 - LRR_1	I	Xcv8510 from *X. campestris* pv. *vesicatoria*	Noël et al. 2002
XopAI (HopO1 (HopPto, HopPtoS), HopAI1 (HolPtoAI))	XAC3230	pfam01129 - ART	I	XopE2 and XopE1 from *X. campestris* pv. *vesicatoria*	Thieme et al. 2007
XopAK (HopAK1 (HopPtoK, HolPtoAB) C terminal domain)	XAC3666		I	HopAK1 from *P. syringae pv. tomato*	Buell et al. 2003
XopE1 (AvrXacE1, HopX, AvrPphE)	XAC0286		I	AvrXacE1 and XopE1 from *X. campestris* pv. *vesicatoria*	Thieme et al. 2007
XopE2 (AvrXacE3, AvrXccE1)	XACb0011		I	XopE2 from *X. campestris* pv. *vesicatoria*	Thieme et al. 2007
XopE3 (AvrXacE2, HopX, AvrPphE)	XAC3224		NC	AvrXacE2	Hajri et al. 2009
XopF2	XAC2785		NS	XopF2 from *X. campestris* pv. *vesicatoria*	Roden et al. 2004
XopI	XAC0754	pfam00646 - F-box	I		Thieme et al. 2007
XopK	XAC3085		I	XOO1669 from *X. oryzae* pv. *oryzae*	Furutani et al. 2009
XopL	XAC3090	pfam00560 - LRR_1	I		Song and Yang 2010
XopN (HopAU1)	XAC2786		I	XopN from *X. campestris* pv. *vesicatoria*	Kim et al. 2009a
XopP	XAC1208		I	XopP from *X. campestris* pv. *vesicatoria*	Roden et al. 2004

Table 3-4. Continued

Effector family	Locus tag	Domain[a]	Cluster	Homology	Reference
XopQ (HopQ1)	XAC4333	pfam01156 - IU_nuc_hydro	I	XopQ from *X. campestris* pv. *vesicatoria*	Roden et al. 2004
XopR	XAC0277		I	XOO4134 from *X. oryzae* pv. *oryzae*	Furutani et al. 2009
XopV	XAC0601		I	XOO3803 from *X. oryzae* pv. *oryzae*	Furutani et al. 2009
XopX (HolPsyAE)	XAC0543		I	XopX from *X. campestris* pv. *vesicatoria*	Metz et al. 2005
XopZ (HopAS, AWR)	XAC2009		I	XOO2402 from *X. oryzae* pv. *oryzae*	Furutani et al. 2009
	XAC2990	pfam01764 - Lipase_3	I	RCFBP_mp20163 from *R. solanacearum*	Remenant et al. 2010

[a] domain analysis by Pfam. I, cluster I; NC, not in clusters; NS, no significant change on expression

Table 3-5. Confirmed and putative type II secretion system substrate proteins

Locus tag	Regulon	SP[a]	Domains[b]	Description	References
Experimentally validated T2SS substrates					
XAC0435	HrpG & HrpX	YES	pfam06903 - VirK	VirK protein	Yamazaki et al. 2008
XAC0552	HrpG & HrpX	YES	pfam00082 - Peptidase_S8 pfam09286 - Pro-kuma_activ	proteinase	Yamazaki et al. 2008
XAC0661	HrpG & HrpX	YES	pfam00295 - Glyco_hydro_28	endopolygalacturonase	Yamazaki et al. 2008
XAC0795	HrpG & HrpX	YES	pfam00082 - Peptidase_S8; pfam09286 - Pro-kuma_activ	protease	Yamazaki et al. 2008
XAC0817	HrpG & HrpX	YES	pfam03422 - CBM_6; pfam08306 - Glyco_hydro_98M; pfam08307 - Glyco_hydro_98C	hypothetical protein	Yamazaki et al. 2008
XAC2374	HrpX	YES	pfam00295 - Glyco_hydro_28	polygalacturonase	Yamazaki et al. 2008
XAC2831	HrpG & HrpX	YES	pfam00082 - Peptidase_S8; pfam01483 - P_proprotein	extracellular serine protease	Yamazaki et al. 2008
XAC2853	HrpG & HrpX	YES	pfam00112 - Peptidase_C1	cysteine protease	Yamazaki et al. 2008
Predicted T2S substrate					
XAC3451	HrpX	YES	pfam01450 – IlvC; pfam07991 - IlvN	ketol-acid reductoisomerase	
XAC3878	HrpG & HrpX	YES	pfam00085 - Thioredoxin	disulphide-isomerase	
XAC4252	HrpG & HrpX	YES	pfam00331 - Glyco_hydro_10	xylanase	
XAC4321	HrpX	YES		hypothetical protein;	XCV4423, putative secreted protein; Thieme et al. 2005
XAC4327	HrpG & HrpX	YES	pfam01425 - Amidase	allophanate hydrolase	
XAC4369	HrpX	YES	pfam01569 - PAP2	phosphatase precursor	
XAC0363	HrpG & HrpX	YES	pfam00355 - Rieske	vanillate O-demethylase oxygenase subunit	
XAC0501	HrpG & HrpX	YES	pfam03583 - LIP	hypothecital protein,	XAUB_33320, secreted lipase; Moreira et al. 2010
XAC0803	HrpX	YES	pfam08241 - Methyltransf_11	methyltransferase	
XAC1241	HrpG & HrpX	YES		hypothetical protein;	XALc_3071, hypothetical secreted protein; Pieretti et al. 2009
XAC2113	HrpG & HrpX	YES	pfam11737 - DUF3300	hypothetical protein;	XAUC_07560, secreted protein; Moreira et al. 2010

Table 3-5. Continued

Locus tag	Regulon	SP[a]	Domains[b]	Description	References
XAC2370	HrpG & HrpX	YES		hypothetical protein;	XCV2568, putative secredted protein; Thieme et al. 2005
XAC3647	HrpG & HrpX	YES	pfam01817 - CM_2	chorismate mutase	$AroQ_Y$; Degrassi et al. 2010
XAC0395	HrpG & HrpX	YES		hypothetical protein	
XAC0418	HrpX	YES		hypothetical protein	
XAC1124	HrpG & HrpX	YES	pfam08670 - MEKHLA	hypothetical protein	
XAC4021	HrpX	YES	pfam08811 - DUF1800	hypothetical protein	
XAC2832	HrpX	YES		hypothetical protein	
XAC4063	HrpX	YES	pfam11287 - DUF3088	hypothetical protein	
XAC4318	HrpG & HrpX	YES		hypothetical protein	

[a] SP, signal peptide prediction using Phobius. [b] domain analysis using Pfam database.

Table 3-6. Regulatory genes under control of HrpG and/or HrpX.

JCVI[a]	Locus tag	Gene symbol	hrpGA/ WA[b]	hrpGB/ WB[b]	hrpGC/ WC[b]	hrpXA/ WA[b]	hrpXB/ WB[b]	hrpXC/ WC[b]	Description
Both									
R	XAC1171	*stkXac1*	0.984	NS	-1.031	NS	-0.778	-2.025	serine/threonine kinase
R	XAC0880	*pcaQ*	0.675	NS	-0.854	NS	-0.883	-1.999	transcriptional regulator
R	XAC1455		0.638	NS	NS	NS	NS	-1.195	MarR family transcriptional regulator
HrpG regulon									
T	XAC1320		NS	NS	-0.716	NS	NS	NS	regulatory protein
U	XAC1939		NS	NS	0.652	NS	NS	NS	GGDEF family protein
R	XAC3771		NS	NS	0.675	NS	NS	NS	hypothetical protein; pfam03466 **-** LysR substrate binding domain[c]
R	XAC2192		NS	NS	0.759	NS	NS	NS	two-component system sensor protein
R	XAC1877	*rpfG*	NS	NS	0.780	NS	NS	NS	response regulator
U	XAC1940		NS	NS	0.817	NS	NS	NS	GGDEF family protein
R	XAC1488		NS	NS	0.951	NS	NS	NS	sensor histidine kinase
R	XAC1989	*flgM*	NS	NS	0.995	NS	NS	NS	flagellar protein
R	XAC2897		NS	NS	1.128	NS	NS	NS	response regulator
R	XAC1573	*phoU*	NS	NS	1.139	NS	NS	NS	phosphate regulon transcriptional regulator
R	XAC1798	*regS*	NS	0.601	NS	NS	NS	NS	two-component system sensor protein
R	XAC0917		-0.734	NS	NS	NS	NS	NS	transcriptional regulator
HrpX regulon									
R	XAC2166		NS	NS	NS	NS	NS	-1.021	transcriptional regulator
R	XAC2163		NS	NS	NS	NS	NS	-0.742	hypothetical protein; pfam07969 - Amidohydrolase family[c]

Table 3-6. Continued

JCVI[a]	Locus tag	Gene symbol	hrpGA/ WA[b]	hrpGB/ WB[b]	hrpGC/ WC[b]	hrpXA/ WA[b]	hrpXB/ WB[b]	hrpXC/ WC[b]	Description
R	XAC3445		NS	NS	NS	2.221	2.879	3.457	transcriptional regulator
R	XAC3446		NS	NS	NS	-0.708	NS	NS	hypothetical protein; pfam00486-Transcriptional regulatory protein, C terminal[c]
R	XAC4272		NS	NS	NS	-0.617	NS	NS	LacI family transcription regulator
R	XAC1555		NS	NS	NS	-0.653	NS	NS	transcriptional regulator
T	XAC1682	*rpoE*	NS	NS	NS	NS	NS	-0.822	RNA polymerase sigma-E factor

[a] JCVI functional categories. Categories: R = regulatory functions, T = transcription, U = unknown function. [b] Log_2 ratio of fold change was derived from mutants versus wild type at timepoints A, B, and C. NS: not significantly differentially expressed ($|log_2$ fold change$| < 0.585$ or FDR > 0.05). [c] Pfam analysis of the hypothetical proteins.

Table 3-7. Genes showing significant differential expression in both *hrpG* and *hrpX* mutants compared with wild type strain at selected time points.

JCVI[a]	Locus tag	Gene symbol	hrpGA /WA[b]	hrpGB /WB[b]	hrpGC /WC[b]	hrpXA /WA[b]	hrpXB /WB[b]	hrpXC /WC[b]	Description	Cluster[c]
Genes with significant differential expression in both hrpG and hrpX mutant at time point A										
Amino acid biosynthesis	XAC3647	pheA	1.54	0.76	-1.22	-1.53	-2.15	-3.76	chorismate mutase	I
Cell envelope	XAC0661	peh-1	1.50	0.68	-1.13	-1.38	-1.83	-2.65	endopolygalacturonase	I
Cell envelope	XAC2922	hrpW	1.77	NS	-1.42	-1.92	-2.77	-4.50	HrpW protein	I
Cell envelope	XAC3878	-	1.06	NS	-0.97	-0.92	-1.61	-3.05	disulphide-isomerase	I
Cellular processes	XAC0782	ftsQ	-0.76	-0.76	NS	-0.74	NS	NS	cell division protein	NOT
Cellular processes	XAC1265	hrpG	-1.52	-2.60	-4.19	1.57	0.91	NS	HrpG protein	NOT
Cellular processes	XAC4340	yrbE	-0.63	NS	NS	-0.64	NS	NS	toluene tolerance protein	NOT
Central intermediary metabolism	XAC0878	pcaH	0.76	NS	-1.10	-0.76	-1.00	-2.33	protocatechuate 4,5-dioxygenase subunit beta	I
Energy metabolism	XAC3885	cox11	-0.62	NS	NS	-0.68	NS	NS	cytochrome C oxidase assembly protein	NOT
Energy metabolism	XAC3887	ctaD	-0.60	NS	NS	-0.65	NS	NS	cytochrome C oxidase subunit I	NOT
Hypothetical proteins	XAC0501	-	1.37	NS	-1.35	-0.93	-1.95	-3.20	hypothetical protein	I
Hypothetical proteins	XAC2782	-	-0.65	NS	NS	-0.67	NS	NS	hypothetical protein	NOT
Not in JCVI	XAC0543	-	1.68	0.74	-1.42	-1.72	-3.44	-5.12	hypothetical protein	I
Not in JCVI	XAC1172	-	0.73	NS	-1.31	-0.77	-1.17	-2.78	hypothetical protein	I
Not in JCVI	XAC2654	-	1.71	0.63	-1.20	-2.64	-3.82	-5.35	hypothetical protein	I
Not in JCVI	XAC2786	-	1.44	NS	-1.73	-1.15	-2.99	-4.83	hypothetical protein	I
Not in JCVI	XAC3646	-	1.30	0.74	-1.02	-0.91	-1.52	-2.59	hypothetical protein	I
Not in JCVI	XACb0011	avrXacE3	0.98	NS	-1.25	-0.71	-1.64	-3.25	avirulence protein	I
Protein fate	XAC0286	avrXacE1	0.90	NS	-1.21	-0.91	-1.18	-2.56	avirulence protein	I
Protein fate	XAC0407	hrpB1	1.23	NS	-2.18	-1.78	-2.86	-4.57	HrpB1 protein	I
Protein fate	XAC0408	hrpB2	0.94	NS	-1.90	-1.11	-1.95	-3.72	HrpB2 protein	I
Protein fate	XAC0410	hrpB4	0.92	NS	-1.66	-0.75	-1.52	-2.95	HrpB4 protein	I
Protein synthesis	XAC0404	hpaP	0.70	NS	-1.36	-0.63	-1.11	-2.51	HpaP protein	I

Table 3-7. Continued

JCVI[a]	Locus tag	Gene symbol	hrpGA /WA[b]	hrpGB /WB[b]	hrpGC /WC[b]	hrpXA /WA[b]	hrpXB /WB[b]	hrpXC /WC[b]	Description	Cluster[c]
Protein synthesis	XAC0416	hpa1	1.93	NS	-1.42	-1.60	-4.29	-5.54	Hpa1 protein	I
Transport and binding proteins	XAC1556	fucP	-0.71	NS	NS	-0.64	NS	NS	glucose-galactose transporter	NOT
Transport and binding proteins	XAC3444	btuB	-0.94	NS	NS	5.13	4.13	3.42	TonB-dependent receptor	NOT
Unclassified	XAC0399	hrpD5	0.74	NS	-1.64	-0.73	-1.55	-3.08	HrpD5 protein	I
Unclassified	XAC0409	hrcJ	1.03	NS	-1.90	-1.07	-2.18	-3.81	HrcJ protein	I
Unclassified	XAC0435	virK	1.49	0.67	-1.15	-1.54	-2.31	-3.55	VirK protein	I
Unclassified	XAC0552	-	0.99	NS	-1.24	-1.35	-1.79	-2.99	proteinase	I
Unclassified	XAC0795	xcp	0.73	NS	-0.81	-0.62	-0.81	-1.83	protease	I
Unclassified	XAC1266	hrpXct	1.93	0.95	NS	1.60	1.97	1.58	HrpX protein	NOT
Unclassified	XAC2853	-	2.03	0.97	-0.88	-2.40	-4.00	-5.08	cysteine protease	I
Genes with significant differential expression in both hrpG and hrpX mutant at time point B										
Amino acid biosynthesis	XAC3647	pheA	1.54	0.76	-1.22	-1.53	-2.15	-3.76	chorismate mutase	I
Cell envelope	XAC0661	peh-1	1.50	0.68	-1.13	-1.38	-1.83	-2.65	endopolygalacturonase	I
Cellular processes	XAC1265	hrpG	-1.52	-2.60	-4.19	1.57	0.91	NS	HrpG protein	NOT
Not in JCVI	XAC2654	-	1.71	0.63	-1.20	-2.64	-3.82	-5.35	hypothetical protein	I
Not in JCVI	XAC0543	-	1.68	0.74	-1.42	-1.72	-3.44	-5.12	hypothetical protein	I
Not in JCVI	XAC3646	-	1.30	0.74	-1.02	-0.91	-1.52	-2.59	hypothetical protein	I
Unclassified	XAC2853	-	2.03	0.97	-0.88	-2.40	-4.00	-5.08	cysteine protease	I
Unclassified	XAC0435	virK	1.49	0.67	-1.15	-1.54	-2.31	-3.55	VirK protein	I
Unclassified	XAC1266	hrpXct	1.93	0.95	NS	1.60	1.97	1.58	HrpX protein	NOT
Genes with significant differential expression in both hrpG and hrpX mutant at time point C										
Amino acid biosynthesis	XAC3647	pheA	1.54	0.76	-1.22	-1.53	-2.15	-3.76	chorismate mutase	I
Amino acid biosynthesis	XAC0802	-	NS	NS	-0.65	NS	-0.61	-1.79	sulfotransferase	I
Amino acid biosynthesis	XAC4213	-	NS	NS	-0.69	NS	NS	-1.12	hypothetical protein	I

Table 3-7. Continued

JCVI[a]	Locus tag	Gene symbol	hrpGA /WA[b]	hrpGB /WB[b]	hrpGC /WC[b]	hrpXA /WA[b]	hrpXB /WB[b]	hrpXC /WC[b]	Description	Cluster[c]
Amino acid biosynthesis	XAC1525	tyrA	NS	NS	0.86	NS	NS	0.76	prephenate dehydrogenase	II
Biosynthesis of cofactors, prosthetic groups, and carriers	XAC2947	apbE	NS	NS	0.93	NS	0.64	0.73	thiamine biosynthesis lipoprotein ApbE precursor	II
Cell envelope	XAC2922	hrpW	1.77	NS	-1.42	-1.92	-2.77	-4.50	HrpW protein	I
Cell envelope	XAC3878	-	1.06	NS	-0.97	-0.92	-1.61	-3.05	disulphide-isomerase	I
Cell envelope	XAC0661	peh-1	1.50	0.68	-1.13	-1.38	-1.83	-2.65	endopolygalacturonase	I
Cell envelope	XAC2113	-	NS	NS	-0.91	NS	NS	-0.86	hypothetical protein	I
Cellular processes	XAC0397	hrpE	1.30	NS	-1.03	NS	-1.82	-2.91	HrpE protein	I
Cellular processes	XAC0394	hrpF	0.79	NS	-1.59	NS	-1.21	-2.64	HrpF protein	I
Cellular processes	XAC0406	hrcU	NS	NS	-1.66	-0.65	-1.05	-2.53	type III secretion system protein HrcU	I
Cellular processes	XAC0403	hrcQ	NS	NS	-1.12	NS	-0.86	-2.06	HrcQ protein	I
Cellular processes	XAC0400	hpaA	NS	NS	-1.23	NS	-0.75	-2.01	HpaA protein	I
Cellular processes	XAC0076	avrBs2	NS	NS	-1.09	NS	NS	-1.98	avirulence protein	I
Central intermediary metabolism	XAC0878	pcaH	0.76	NS	-1.10	-0.76	-1.00	-2.33	protocatechuate 4,5-dioxygenase subunit beta	I
DNA metabolism	XAC0002	dnaN	0.59	NS	0.75	NS	NS	0.70	DNA polymerase III subunit beta	II
Energy metabolism	XAC0879	ligA	0.86	NS	-1.14	NS	-1.02	-2.38	protocatechuate 4,5-dioxygenase subunit alpha	I
Energy metabolism	XAC4327	uahA	NS	NS	-0.79	NS	NS	-1.43	allophanate hydrolase	I
Energy metabolism	XAC4252	xynB	NS	NS	-0.68	NS	NS	-1.13	xylanase	I
Energy metabolism	XAC0363	vanA	NS	NS	-0.61	NS	NS	-1.04	vanillate O-demethylase oxygenase subunit	I
Energy metabolism	XAC1439	tpmT	NS	NS	1.54	NS	NS	1.33	thiopurine S-methyltransferase	II

Table 3-7. Continued

JCVI[a]	Locus tag	Gene symbol	hrpGA /WA[b]	hrpGB /WB[b]	hrpGC /WC[b]	hrpXA /WA[b]	hrpXB /WB[b]	hrpXC /WC[b]	Description	Cluster[c]
Fatty acid and phospholipid metabolism	XAC2990	-	NS	NS	-0.61	NS	NS	-0.82	hypothetical protein	I
Fatty acid and phospholipid metabolism	XAC0562	mdcB	NS	NS	0.93	NS	NS	0.72	malonate decarboxylase subunit beta	II
Hypothetical proteins	XAC0501	-	1.37	NS	-1.35	-0.93	-1.95	-3.20	hypothetical protein	I
Hypothetical proteins	XAC1208	-	NS	NS	-0.99	NS	-0.76	-2.16	hypothetical protein	I
Hypothetical proteins	XAC0601	-	0.97	NS	-0.98	NS	-0.74	-1.91	hypothetical protein	I
Hypothetical proteins	XAC1124	-	NS	NS	-0.62	NS	-0.67	-1.30	hypothetical protein	I
Hypothetical proteins	XAC0916	-	NS	NS	-0.90	NS	NS	-1.13	hydrolase	I
Hypothetical proteins	XAC4019	-	NS	NS	0.76	NS	NS	0.62	hypothetical protein	II
Hypothetical proteins	XAC1689	-	0.75	NS	0.86	NS	NS	0.89	hypothetical protein	II
Hypothetical proteins	XAC2827	-	0.83	NS	0.85	NS	NS	1.05	hypothetical protein	II
Hypothetical proteins	XAC3222	-	NS	NS	1.29	NS	NS	1.12	hypothetical protein	II
Not in JCVI	XAC2654	-	1.71	0.63	-1.20	-2.64	-3.82	-5.35	hypothetical protein	I
Not in JCVI	XAC0543	-	1.68	0.74	-1.42	-1.72	-3.44	-5.12	hypothetical protein	I
Not in JCVI	XAC2786	-	1.44	NS	-1.73	-1.15	-2.99	-4.83	hypothetical protein	I
Not in JCVI	XAC3085	-	NS	NS	-1.56	NS	-1.72	-3.87	hypothetical protein	I
Not in JCVI	XACb0011	-	0.98	NS	-1.25	-0.71	-1.64	-3.25	avirulence protein	I
Not in JCVI	XAC1172	-	0.73	NS	-1.31	-0.77	-1.17	-2.78	hypothetical protein	I
Not in JCVI	XAC0277	-	0.72	NS	-1.20	NS	-1.24	-2.67	hypothetical protein	I
Not in JCVI	XAC3646	-	1.30	0.74	-1.02	-0.91	-1.52	-2.59	hypothetical protein	I
Not in JCVI	XAC2787	-	NS	NS	-1.11	NS	-0.96	-2.46	hypothetical protein	I
Not in JCVI	XAC3230	-	0.96	NS	-1.04	NS	-1.15	-2.33	hypothetical protein	I
Not in JCVI	XAC0395	-	NS	NS	-1.22	NS	-0.86	-2.00	hypothetical protein	I
Not in JCVI	XAC1241	-	1.26	NS	-0.88	NS	-0.97	-1.89	hypothetical protein	I
Not in JCVI	XAC2370	-	0.79	NS	-0.87	NS	-0.77	-1.74	hypothetical protein	I

Table 3-7. Continued

JCVI[a]	Locus tag	Gene symbol	hrpGA /WA[b]	hrpGB /WB[b]	hrpGC /WC[b]	hrpXA /WA[b]	hrpXB /WB[b]	hrpXC /WC[b]	Description	Cluster[c]
Not in JCVI	XAC2876	-	0.71	NS	-0.81	NS	-0.68	-1.67	hypothetical protein	I
Not in JCVI	XAC0315	-	0.80	NS	-0.86	NS	-0.71	-1.63	hypothetical protein	I
Not in JCVI	XAC0817	-	0.87	NS	-0.61	NS	-0.71	-1.49	hypothetical protein	I
Not in JCVI	XAC1683	-	NS	NS	-0.65	NS	NS	-1.03	hypothetical protein	I
Not in JCVI	XAC4318	-	NS	NS	-0.59	NS	NS	-0.60	hypothetical protein	I
Not in JCVI	XACa0013	-	0.76	0.62	0.68	NS	NS	0.61	hypothetical protein	II
Not in JCVI	XAC0786	-	NS	NS	0.75	NS	NS	0.61	hypothetical protein	II
Not in JCVI	XAC3337	-	NS	NS	0.70	NS	NS	0.67	hypothetical protein	II
Not in JCVI	XACa0021	repA	NS	NS	0.82	NS	NS	0.75	replication protein A	II
Not in JCVI	XACb0049	-	NS	NS	0.83	NS	NS	0.78	hypothetical protein	II
Not in JCVI	XACb0057	-	0.63	NS	0.79	NS	NS	0.83	hypothetical protein	II
Not in JCVI	XAC3291	-	NS	NS	0.75	NS	NS	0.87	hypothetical protein	II
Not in JCVI	XAC3984	-	NS	NS	0.83	NS	NS	0.88	hypothetical protein	II
Not in JCVI	XAC1412	-	NS	NS	1.08	NS	NS	0.95	hypothetical protein	II
Not in JCVI	XAC2425	-	NS	NS	1.36	NS	NS	1.24	hypothetical protein	II
Not in JCVI	XAC1563	-	NS	NS	1.51	NS	NS	1.29	hypothetical protein	II
Not in JCVI	XAC0099	-	1.09	NS	1.17	NS	NS	1.33	hypothetical protein	II
Not in JCVI	XAC2442	-	NS	NS	1.67	NS	NS	1.39	hypothetical protein	II
Not in JCVI	XAC1572	-	NS	NS	2.40	NS	NS	1.62	hypothetical protein	II
Not in JCVI	XAC0617	-	NS	NS	1.67	NS	NS	1.63	hypothetical protein	II
Not in JCVI	XACb0034	-	NS	NS	2.17	NS	NS	1.93	hypothetical protein	II
Not in JCVI	XAC2357	-	NS	NS	1.94	NS	NS	1.95	hypothetical protein	II
Protein fate	XAC0407	hrpB1	1.23	NS	-2.18	-1.78	-2.86	-4.57	HrpB1 protein	I
Protein fate	XAC0408	hrpB2	0.94	NS	-1.90	-1.11	-1.95	-3.72	HrpB2 protein	I
Protein fate	XAC0410	hrpB4	0.92	NS	-1.66	-0.75	-1.52	-2.95	HrpB4 protein	I
Protein fate	XAC0401	hrcS	NS	NS	-1.52	NS	-1.08	-2.57	HrcS protein	I

Table 3-7. Continued

JCVI[a]	Locus tag	Gene symbol	hrpGA /WA[b]	hrpGB /WB[b]	hrpGC /WC[b]	hrpXA /WA[b]	hrpXB /WB[b]	hrpXC /WC[b]	Description	Cluster[c]
Protein fate	XAC0286	avrXacE1	0.90	NS	-1.21	-0.91	-1.18	-2.56	avirulence protein	I
Protein fate	XAC0411	hrpB5	NS	NS	-1.34	NS	-0.85	-2.09	type III secretion system protein HrpB	I
Protein fate	XAC0402	hrcR	NS	NS	-1.26	NS	-0.87	-2.03	type III secretion system protein	I
Protein fate	XAC0414	hrcT	NS	NS	-1.16	NS	-0.68	-1.95	HrcT protein	I
Protein fate	XAC0413	hrpB7	NS	NS	-1.11	NS	-0.66	-1.90	HrpB7 protein	I
Protein fate	XAC0415	hrcC	NS	NS	-1.58	NS	NS	-1.60	HrcC protein	I
Protein fate	XAC2831	-	NS	NS	-0.71	NS	NS	-0.97	extracellular serine protease	I
Protein fate	XAC1085	ppiD	NS	NS	0.85	NS	NS	0.64	peptidyl-prolyl cis-trans isomerase	II
Protein synthesis	XAC0416	hpa1	1.93	NS	-1.42	-1.60	-4.29	-5.54	Hpa1 protein	I
Protein synthesis	XAC0404	hpaP	0.70	NS	-1.36	-0.63	-1.11	-2.51	HpaP protein	I
Protein synthesis	XAC3977	-	NS	NS	1.38	NS	NS	1.30	hypothetical protein	II
Regulatory functions	XAC1171	stkXac1	0.98	NS	-1.03	NS	-0.78	-2.03	serine/threonine kinase	I
Regulatory functions	XAC0880	pcaQ	0.68	NS	-0.85	NS	-0.88	-2.00	transcriptional regulator	I
Transport and binding proteins	XAC0412	hrcN	NS	NS	-1.22	NS	-0.82	-2.10	type III secretion system ATPase	I
Unclassified	XAC2853	-	2.03	0.97	-0.88	-2.40	-4.00	-5.08	cysteine protease	I
Unclassified	XAC0409	hrcJ	1.03	NS	-1.90	-1.07	-2.18	-3.81	HrcJ protein	I
Unclassified	XAC0435	virK	1.49	0.67	-1.15	-1.54	-2.31	-3.55	VirK protein	I
Unclassified	XAC0398	hrpD6	1.09	NS	-1.72	NS	-1.63	-3.21	HrpD6 protein	I
Unclassified	XAC0399	hrpD5	0.74	NS	-1.64	-0.73	-1.55	-3.08	HrpD5 protein	I
Unclassified	XAC0552	-	0.99	NS	-1.24	-1.35	-1.79	-2.99	proteinase	I
Unclassified	XAC0396	hpaB	NS	NS	-1.67	NS	-1.25	-2.79	HpaB protein	I
Unclassified	XAC4333	-	0.78	NS	-1.30	NS	-1.12	-2.52	hypothetical protein	I
Unclassified	XAC0393	hpaF	NS	NS	-1.32	NS	NS	-2.06	HpaF protein	I

Table 3-7. Continued

JCVI[a]	Locus tag	Gene symbol	hrpGA /WA[b]	hrpGB /WB[b]	hrpGC /WC[b]	hrpXA /WA[b]	hrpXB /WB[b]	hrpXC /WC[b]	Description	Cluster[c]
Unclassified	XAC0754	-	NS	NS	-0.88	NS	-0.73	-1.85	hypothetical protein	I
Unclassified	XAC0405	hrcV	NS	NS	-1.14	NS	-0.84	-1.85	HrcV protein	I
Unclassified	XAC0795	xcp	0.73	NS	-0.81	-0.62	-0.81	-1.83	protease	I
Unclassified	XAC3090	-	NS	NS	-0.93	NS	-0.64	-1.53	leucin rich protein	I
Unclassified	XAC3170	bioI	NS	NS	-0.73	NS	NS	-1.40	cytochrome P-450 hydroxylase	I
Unclassified	XAC0417	hpa2	NS	NS	-0.94	NS	NS	-1.23	Hpa2 protein	I
Unclassified	XAC2178	-	NS	NS	0.71	NS	NS	0.62	hypothetical protein	II
Unclassified	XAC2123	-	NS	NS	0.71	NS	NS	0.65	hypothetical protein	II
Unclassified	XAC2653	S	NS	NS	0.81	NS	NS	0.73	phage-related tail protein	II

[a] J. Craig Venter Institute (JCVI) functional categories. [b] Log_2-fold change was derived from mutant versus wild type strain at time points A, B, and C. NS = not significantly differentially expressed ($|log_2$-fold change$| < 0.585$ or false discovery rate > 0.05). [c] Clusters were assigned based on clustering analysis. NOT = not assigned in any cluster.

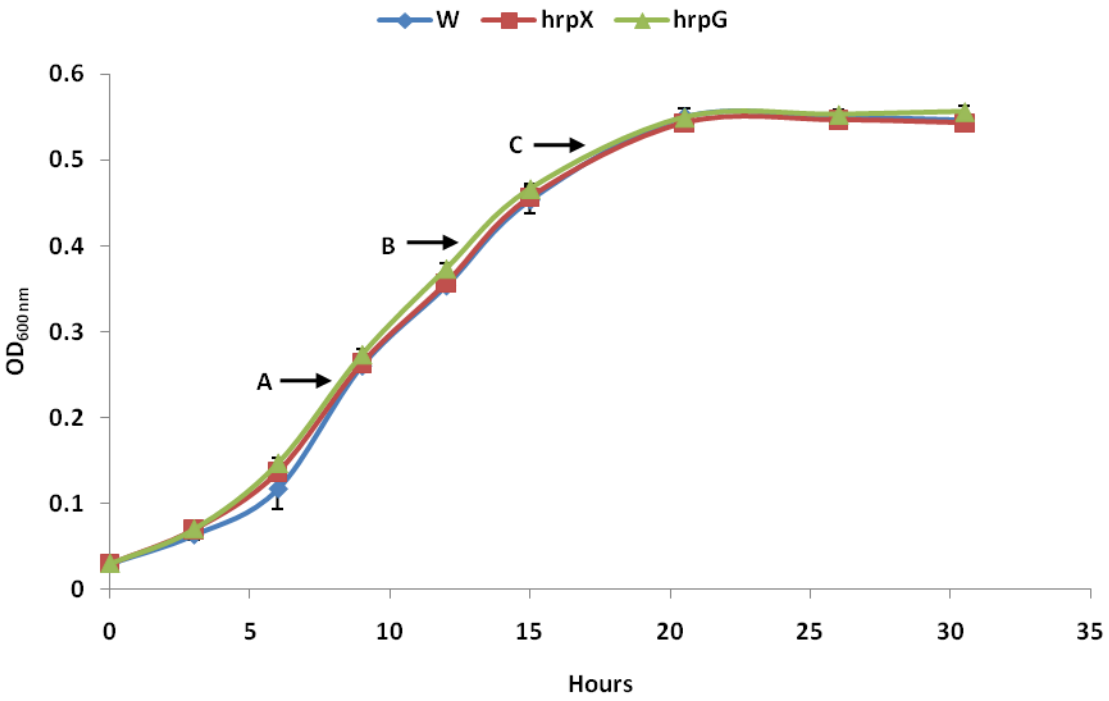

Figure 3-1. Growth curves of XCC strains in XVM2 medium. W: wild type XCC strain 306; hrpX: *hrpX* mutant; hrpG: *hrpG* mutant. The experiments were performed in triplicate and repeated three times with similar results and only one representative result was presented. The error bars represent the standard deviations of the means. Cell cultures were obtained at three different time-points. A, B and C represent the time-points of cell culture sampling, OD 0.25, 0.4 and 0.5, respectively.

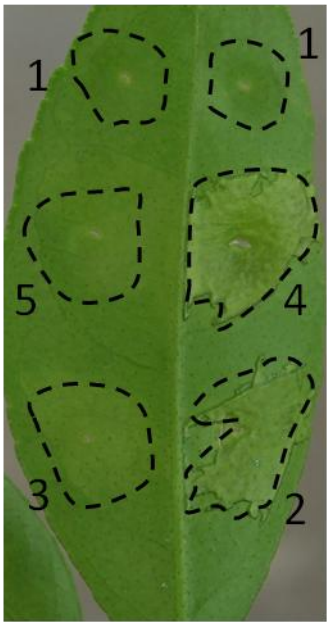

Figure 3-2. Pathogenicity assay of XCC strains by infiltration. 1: the mocked inoculation by sterile tap water; 2: wild type XCC strain 306; 3: *hrpG* mutant; 4: *hrpG* mutant carrying the complementation plasmid phrpGC. 5: *hrpG* mutant carrying the empty plasmid pUFR053. The assay was repeated three times independently using both 10^8 and 10^5 CFU/mL concentrations. The experiments were repeated three times with similar results and only one result was presented. The leaf shown was inoculated with 10^8 CFU/mL of strains and photographed on 5 DPI.

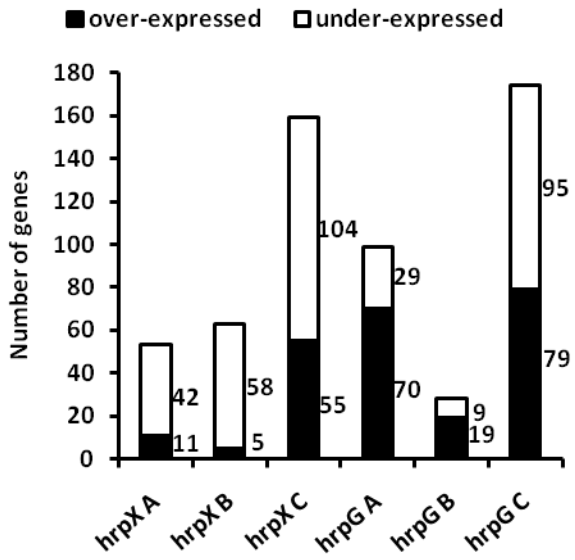

Figure 3-3. Diagram displaying the numbers of differentially expressed genes resulting from the comparison of the *hrpG* mutant versus the wild-type strain and the *hrpX* mutant versus wild-type strain at selected timepoints. Genes with the absolute value of log2-fold change >0.585 and false discovery rate <0.05 were selected as significantly differentially expressed genes. Black columns represent overexpressed genes in mutants and white columns represent underexpressed genes in either the hrpX or hrpG mutant. Numbers adjacent to the columns represent the numbers of genes in each condition.

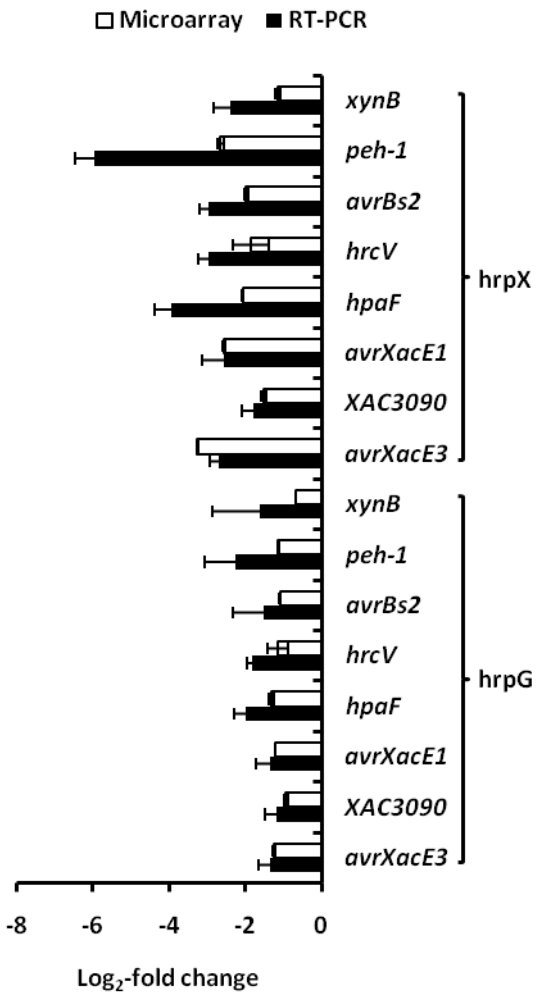

Figure 3-4. Comparison of gene expression by quantitative reverse-transcription polymerase chain reaction (QRT-PCR) and microarray. The log_2-fold change of each gene was derived from the comparison of either *hrpX* or *hrpG* mutant versus wild-type at timepoint C. Two genes, 16S rRNA and *gyrA*, were used as endogenous controls in QRT-PCR, both resulting in similar results. Only the QRT-PCR results with 16s rRNA as endogenous control are shown. Values of log2-fold change were means of four replicates. Experiments were repeated three times with similar results and only one result was presented. Error bars indicate standard deviation. White bars represent the values from microarray and black bars represent the values from QRT-PCR.

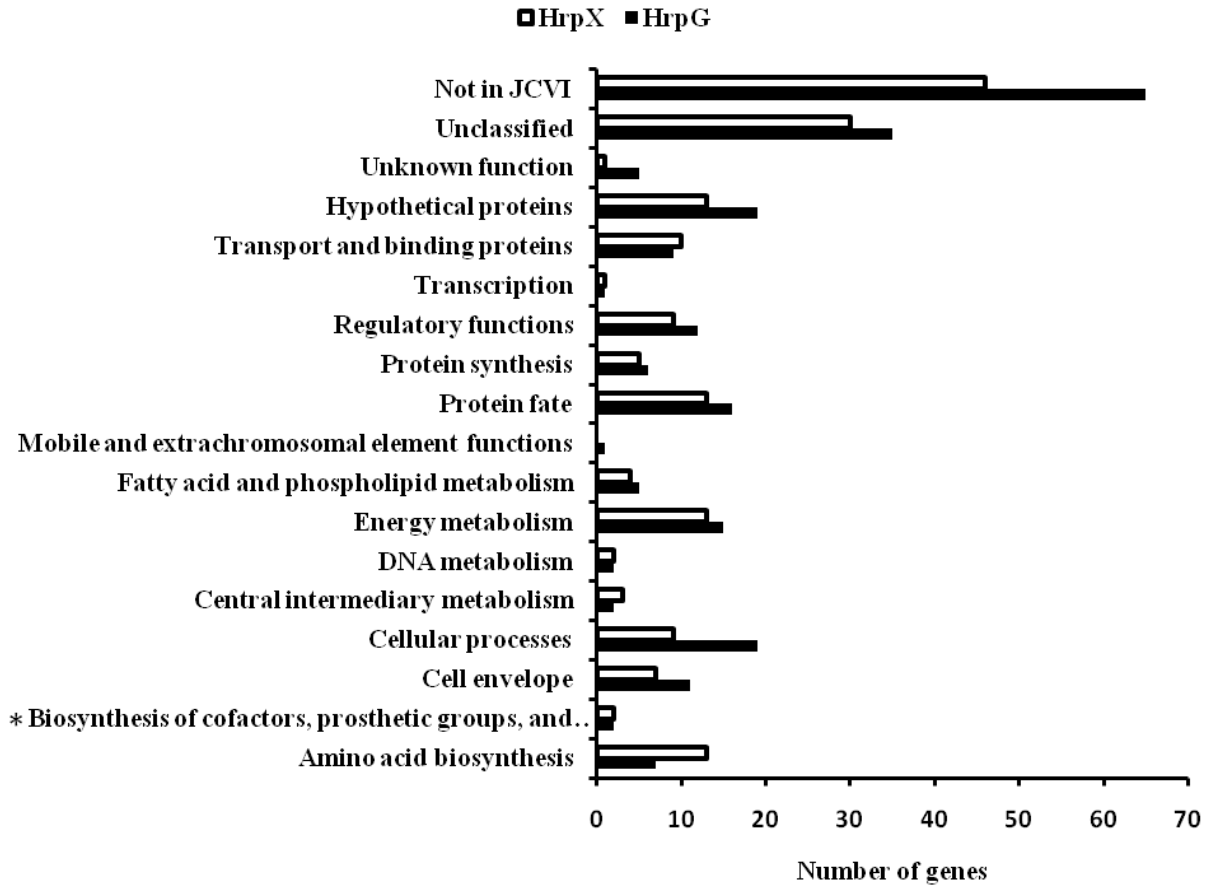

Figure 3-5. Distribution of genes of the HrpG and HrpX regulons that were assigned into various J. Craig Venter Institute functional categories. White and black bars represent genes in the HrpX and HrpG regulon, respectively. * indicates biosynthesis of cofactors, prosthetic groups, and carriers.

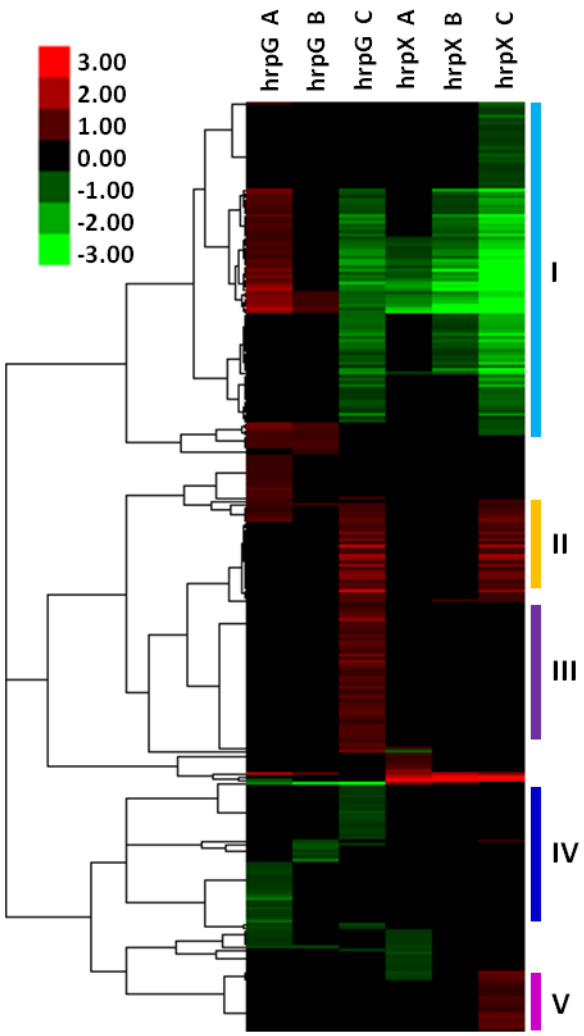

Figure 3-6. Hierarchical clustering of genes in the HrpG and HrpX regulons based on similar time-dependent expression patterns. Clustering analysis was performed with Cluster 3.0 using complete linking with uncentered correlation distance. Columns represent individual timepoints and rows represent individual genes. Red bars indicate overexpression in mutants and green bars indicate underexpression in mutants. The color scale portrays $\log_2$-fold change differences between the mutants and wild-type strains. Genes with the absolute values of log2-fold change < 0.585 (|fold change| < 1.5) were displayed in black. Five major clusters were assigned as I, II, III, IV, and V

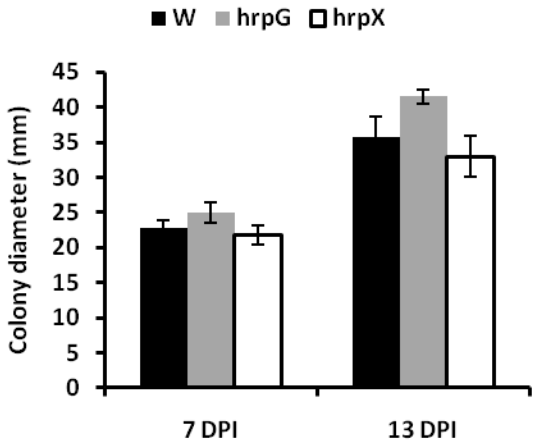

Figure 3-7. Swarming assay on XVM2 medium containing 0.7% agar. Black columns represent wild-type strain, gray columns represent the *hrpG* mutant, and white columns indicate the *hrpX* mutant. DPI = days post inoculation. Experiments were performed in quadruplicate and repeated three times with similar results; only one representative result was presented.

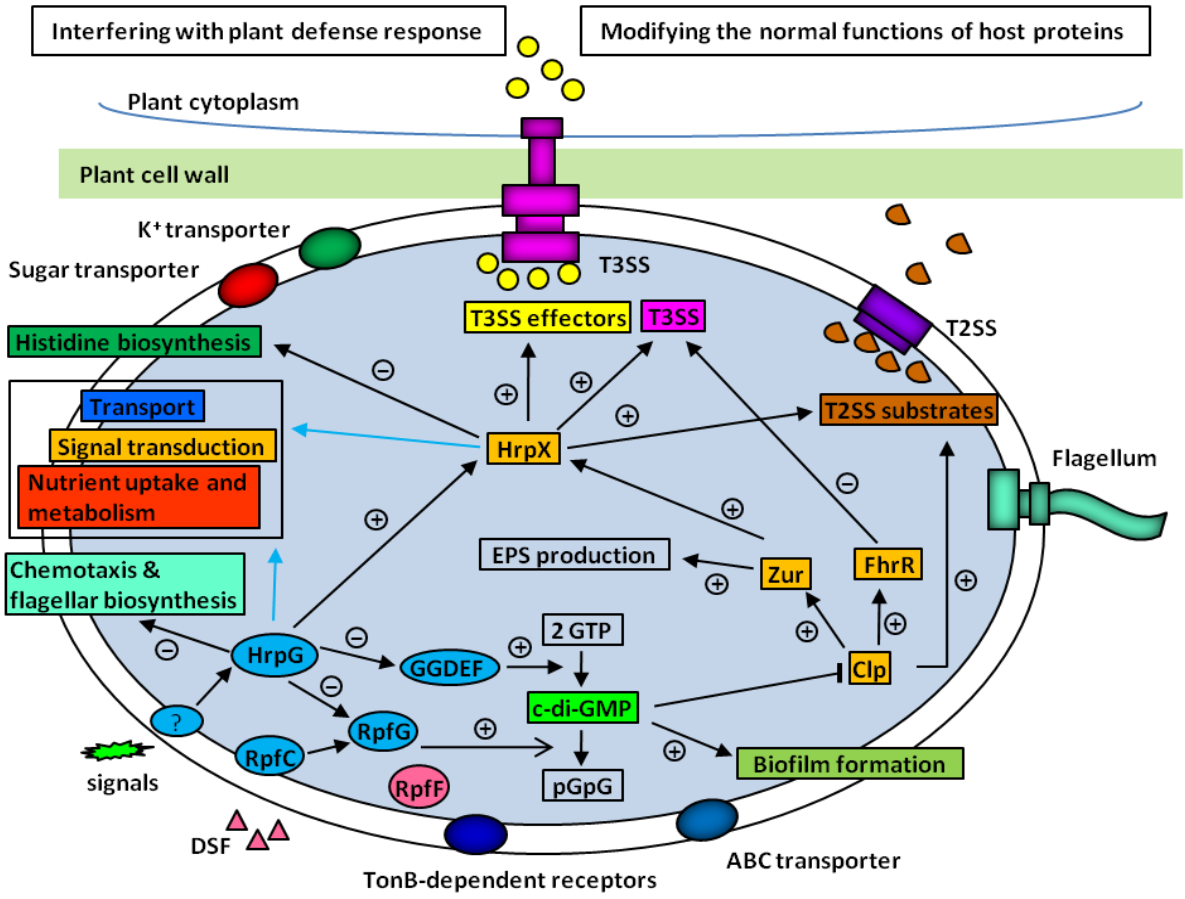

Figure 3-8. Schematic model of HrpG- and HrpX-related regulation cascades of *Xanthomonas* spp. HrpG is involved in four major aspects of regulatory cascades: 1) Inducing the transcription of HrpX, which in turn activates the expression of a large set of virulence genes. HrpX represses the transcription of genes involved in histidine biosynthesis at the same time, and also regulates the transcription of some genes involved in signal transduction and regulation, as well as transport which may result in change of nutrient uptake and energy metabolism. 2) HrpG represses the transcription of genes involved in chemotaxis and flagellar biosynthesis in order to repress bacterial motility at the early stationary phase of growth. 3) HrpG also controls the expression of genes related to signal transduction and regulation, transport and general metabolism. 4) HrpG cross-talks with DSF-mediated QS pathway via repressing the transcription of RpfG and two GGDEF proteins at the early stationary phase of growth. Those proteins contribute the concentration of the central messenger cyclic-di-GMP. One important target of cyclic-di-GMP is Clp which is a transcriptional activator. Cyclic-di-GMP binds to the Clp to prevent it from DNA binding and the expression of genes encoding extracellular enzymes, and genes involved in T3SS, and EPS biosynthesis. Blue lines indicate both positive and negative regulations occurring in different genes of the listed functional categories. + and – represent positive and negative transcriptional regulation, respectively.

CHAPTER 4
CHARACTERIZATION OF DSF-MEDIATED QUORUM SENSING REGULON AND ITS ROLE IN CITRUS CANKER INFECTION

Introduction

Quorum sensing (QS) is a sophisticated mechanism allowing bacteria to communicate via the exchange of chemical signals and to alter the behavior in population-wide scale. One unique type of QS signal molecule, a diffusible signal molecule (DSF) was identified in *Xanthomonas campestris* pv. *campestris* (Barber et al. 1997). It has been characterized as an unsaturated fatty acid, cis-11-methyl-dodecenoic acid (Wang et al. 2004), which is distinct from *N*-acyl derivatives of homoserine lactone (*N*-AHLs) used by most Gram-negative bacteria for cell-cell communication. DSF has been found to be an important QS signal molecular in pathogens *Xylella fastidiosa* (Newman et al. 2004), *Burkholderia cenocepacia* (Boon et al. 2008) and many *Xanthomonas* species (Chatterjee and Sonti 2002; Siciliano et al. 2006). The DSF-mediated QS pathway is conserved in those bacteria, in which the *rpf* gene cluster is responsible for the DSF production and signal transduction, including the core genes *rpfF*, *rpfC* and *rpfG* (Chatterjee and Sonti 2002; He et al. 2006; Siciliano et al. 2006). The *rpfF* gene encodes a putative enoyl-CoA hydratase that catalyzes the synthesis of signal molecule DSF. Extracellular DSF is sensed by a two-component signal transduction system consisting of the sensor protein RpfC and response regulator RpfG. Studies of DSF-mediated QS systems revealed that it has distinct regulatory actions on biological functions among DSF-producing bacteria, although DSF-mediated QS pathway is conserved. For example, mutation in *rpfF* of *X. campestris* pv. *campestris* leads to the defects in the production of extracellular enzymes (e.g., proteases, pectinases and endoglucanase) and extracellular polysaccharides (EPS) as

well as biofilm formation (Tang et al. 1991; Barber et al. 1997; Slater et al. 2000; Torres et al. 2007), while the *rpfF* mutants of *X. oryzae* pv. *oryzae* with reduced virulence are proficient for EPS and extracellular enzyme production (Chatterjee and Sonti 2002). In contrast to *Xanthomonas* spp., the *rpfF* mutants of *Xylella fastidiosa* are deficient in DSF production but are hypervirulent in the host (Newman et al. 2004). It seems that the difference of DSF in regulation of diverse functions depends on plant pathogen species and their specific needs for infection.

Transcriptome analysis of the RpfF regulon has significantly advanced understanding of the DSF-mediated QS regulons in bacteria. One pioneer study done by Zhang and his colleagues compared the gene expression profile of the *rpfF* mutant with the wild-type strain of *X. campestris* pv. *campestris* using whole genome-wide microarray analysis (He et al. 2006). In that study, 165 genes were identified as belonging to the QS regulon, which were classified into 12 functional groups including genes encoding extracellular enzymes and genes involved in EPS production, flagellum synthesis, resistance to toxins and oxidative, and aerobic respiration (He et al. 2006). A later study utilizing proteomic analysis revealed that 48 proteins were differentially regulated by QS in *X. oryzae* pv. *orzicola*, of which 18 proteins were identified by mass spectrometry analysis to be involved in nitrogen transfer, protein folding, resistance to oxidative and flagellar synthesis (Zhao et al. 2011). However, considering the complicated QS signal transduction cascade, a comprehensive understanding of the RpfC and RpfG regulons is lacking. In this study, we aimed to further advance our understanding of the QS regulatory network by characterizing the RpfF, RpfC, and RpfG regulons of one important model pathogen XCC through transcriptome analyses. We

also investigated the roles of DSF-mediated QS in the citrus canker disease cycle and its involvement in early attachment and in planta growth of XCC in citrus host.

Materials and Methods

Bacterial Strains and Growth Conditions

All of the strains used in this study are listed in Table 4-1. XCC mutant strains were generated in this study as described below. Wild type strain 306 (rifamycin resistant) (da Silva et al. 2002) and mutant strains were routinely grown in nutrient broth (NB), on nutrient agar (NA), or in nutrient yeast glycerol (NYG) medium (Daniels et al. 1984) at 28°C. The composition of XVM2 medium is described elsewhere (Wengelnik et al. 1996a). *Escherichia coli* strains were grown in Luria-Bertani (LB) medium at 37°C. Antibiotics were used at the following concentrations: rifamycin (Rif), 50 µg/mL; kanamycin (Km), 50 µg/mL; ampicillin (Ap), 50 µg/mL; spectinomycin (Sp), 50 µg/mL; gentamicin (Gm), 5 µg/mL; and chloramphenicol (Cm), 35 µg/mL.

Construction of Strains with Mutations in Genes Involved in DSF-Mediated QS Signaling

To construct the *rpfF* deletion mutant, the 1,610-bp fragment containing entire *rpfF* gene was amplified using genomic DNA of XCC 306 as template and primers rpfFF and rpfFR (Table 4-2). The fragment was cloned into pGEM-T easy vector, resulting in the construct named as pGEM-rpfF. After digesting with *Age*I and *Kpn*I, the construct pGEM-rpfF was blunt ended using T4 DNA polymerase and self ligated as pGEM-ΔrpfF. From pGEM- ΔrpfF, an *Apa*I-*Spe*I fragment containing *rpfF* gene with internal deletion was transferred into *Apa*I-*Xba*I digestd pOK1, resulting in pOK-ΔrpfF. The construct pOK-ΔrpfF was sequenced to confirm the deletion before conjugation. The pOK-ΔrpfF was transformed into *E. coli* DH5αλPIR (Huguet et al. 1998), and subsequently

transferred into XCC 306 by triparental mating with helper *E. coli* strain containing pRK2013 (Swarup et al. 1991). Transconjugants were selected on NYG medium supplemented with Rif and Sp. Positive colonies were replicated on both NA plates supplemented with 5% (w/v) sucrose, Sp and Rif, and NA with only Rif. The sucrose sensitive colonies were selected from NA plate containing Rif and dilution-plated on NA containing Rif, Km and 5% sucrose to select for resolution of the construct by a second cross-over event. The resulting markerless deletion mutant of *rpfF* was confirmed by PCR and sequencing.

To construct the *rpfC* deletion mutant of XCC, the 3,017-bp fragment containing the entire *rpfC* gene was amplified using genomic DNA of XCC 306 as template and primers rpfCF and rpfCR (Table 4-2), and then cloned into pGEM-T easy vector, resulting in pGEM-rpfC. The construct pGEM-rpfC was digested by *BstE*II to remove 1,116-bp from the interior of *rpfC*, and then self-ligated as pGEM-ΔrpfC. An *Apa*I-*Spe*I fragment containing *rpfC* with internal deletion was transferred from pGEM-ΔrpfC into *Apa*I-*Xba*I cutted pOK1, generating pOK-ΔrpfC. The deletion construct pOK-ΔrpfC was transferred into XCC 306 by triparental mating, and a deletion mutant of *rpfC* was selected using the method described above.

The in-frame deletion mutant of *rpfG* was constructed as follows. The 2,037-bp fragment containing the entire *rpfG* gene was amplified using genomic DNA of XCC 306 as template and primers rpfGF and rpfGR (Table 4-2), and then cloned into pGEM-T easy vector, resulting pGEM-rpfG. The pGEM-rpfG was digested by *BssH*II to remove 648-bp from the interior of *rpfG*, and then self-ligated as pGEM-ΔrpfG. An *Apa*I-*Spe*I fragment containing *rpfG* with in-frame deletion was transferred from pGEM-ΔrpfG into

with *Apa*I-*Xba*I cutted pOK1 to generate pOK-ΔrpfG. The deletion construct pOK-ΔrpfG was transferred into XCC 306 by triparental mating, and *rpfG* deletion mutant was selected using the method described above.

Complementation of the *rpfF*, *rpfC* and *rpfG* Mutants

To generate the complementation plasmid for *rpfF* mutant, the fragment containing the entire *rpfF* gene and its own promoter was amplified using genomic DNA of XCC 306 as template and primers rpfFF and rpfFR (Table 4-2). The fragment was cloned into pCR®2.1-TOPO® vector, resulting in the construct PCR-rpfF. The *Hind*III-*Xba*I fragment containing *rpfF* gene from PCR-rpfF was blunt ended by T4 DNA polymerase, and then cloned into pUFR053 which was digested by *Hind*III, and blunt ended and treated with calf intestinal alkaline phosphatase. The derivative construct, p53-rpfF, was transferred into rpfF mutant by triparental mating. The transconjugants were selected on NA with Rif and Gm.

To construct the complementation plasmid for rpfC mutant, the entire *rpfC* gene was amplified from genomic DNA of XCC 306 using PCR with primers rpfC-KpnF and rpfC-KpnR which contain a *Kpn*I restriction site (Table 4-2). The fragment was cloned into pCR®2.1-TOPO® vector, resulting in PCR-rpfC. The *Kpn*I-digested fragment containing rpfC gene was transferred from PCR-rpfC into *Kpn*I site of pUFR053. The derivative construct p53-rpfC was transferred into *rpfC* mutant by triparental mating and selected on NA with Rif and Gm.

To construct the complementation plasmid for rpfG mutant, an *EcoR*I fragment containing *rpfG* and its own promoter was transferred from pGEM-rpfG, and ligated to *EcoR*I site of pUFR034, resulting in p34-rpfG. The construct p34-rpfG was transferred into *rpfG* mutant by triparental mating, and selected on NA with Km.

RNA Extraction

Individual bacterial colonies were picked and grown in 5 mL NB at 28°C for 24 h with shaking, and then transferred into 50 mL NB for overnight incubation. The bacterial cultures in exponential phase were centrifuged, washed with XVM2 medium once, and inoculated in XVM2 medium with an initial concentration at OD_{600} = 0.03. Bacteria were grown in XVM2 medium with constant shaking at 200 rpm at 28°C and samples of culture were collected at 11 and 25 h, respectively according to the growth curve in XVM2 (Figure 4-1). Four biological replicates were used for each strain per time point. RNA was stabilized immediately by mixing bacterial culture with two volumes of RNAprotect® bacterial reagent (Qiagen) and incubated at room temperature for 5 min. Bacterial cells were centrifuged at 5000 × g for 10 min and cell pellets were used for RNA extraction.

Cell pellets were treated with lysozyme and proteinase K for 15 min, and RNA extractions were performed using RNeasy® Mini kit (Qiagen). Contaminated Genomic DNA was removed from RNA by treatment with TURBO DNA-free™ kit (Ambion). RNA quantity was initially determined on a ND-8000 Nanodrop spectrophotometer (NanoDrop Technologies) and RNA quality was assessed using the Agilent 2100 bioanalyzer (Agilent Technologies.).

Microarray Hybridization

Microarray analysis using the Agilent microarray platform was performed at Interdisciplinary Center for Biotechnology Research (ICBR) Microarray Core Facility, the University of Florida. Labeled cDNA was generated using Fairplay III microarray labeling kit (Agilent Technologies). Five µg of total RNA input was used to generate labeled cDNA according to the manufacturer's protocol. Briefly, cDNA was synthesized

from 5 µg of the total RNA with AffinityScript HC and random primer and then modified cDNA was labeled with either cy3 or cy5; labeled cDNA was purified following the manufacturer's instructions. The microarray analysis was performed using the Agilent 8×15K XCC genome array (Guo et al. 2011). Four independent biological replicates were performed for two time-point comparisons with dye-swap design. A total of 300 ng of labeled cDNA per sample was used for the hybridization. A dye swap was performed to remove any bias from the labeling dyes. Hybridization was performed using Gene Expression Hybridization Kit (Agilent Technologies) according to user's manual and was done in a hybridization oven for 17.5 h at 65°C. The arrays were washed according to the manufacturer's recommended protocols. Briefly, arrays were washed with Gene Expression Wash Buffer 1 containing 0.005% Triton X-102 for 1 min at room temperature and then washed with 37°C warmed Gene Expression Wash Buffer 2 containing 0.005% Triton X-102 for 1 min and dried by Agilent Stabilization and Drying Solution. The arrays were scanned using a dual-laser DNA microarray scanner (Model G2505C) (Agilent Technologies). The data were extracted from scanned image using Feature Extraction 10.1.1.1 software (Agilent Technologies).

Microarray Data Analysis and Statistical Methods

The raw data were imported into R environment and statistical tests were performed using BioConductor statistical software which is an open source and open development software project for analysis of microarray and other high-throughput data based primarily on the R programming language (Gentleman et al. 2004). Data preprocessing and normalization were performed using the Linear Models for Microarray Data (LIMMA) package (Smyth, 2004). Raw mean signal intensities from all microarray spots were background corrected and normalized using within-array lowess

approach. Log_2-transformed values were used for statistical analysis. Histograms, box plots and pair-wise scatter plots were generated to examine data quality and comparability. A linear modeling approach and the empirical Bayes statistics as implemented in the LIMMA package (Smyth 2004) were then employed for differential expression analysis. The *p-values* were adjusted using the Benjamini and Hochberg method, designated as false discovery rate (FDR) (Benjamini and Hochberg 1995). Differentially expressed genes were ranked based on FDR, and genes with FDR less than 0.01 and a minimum absolute value of log_2-fold change greater than 1 (equivalent to 2 fold) were considered as significantly differentially expressed. If the gene has three probes and only one was filtered, the gene was removed from further analysis. The log_2-fold change values of the differentially expressed genes were averaged from the values of the two or three probes of the corresponding genes, and shown in Table 4-3. Annotation for the differentially expressed genes was extracted from the Integrated Microbial Genome (IMG) database *and the* J. Craig Venter Institute (JCVI) database and manually verified.

All primary data from transcriptome experiments as well as experimental protocols used are available from Gene Expression Omnibus datasets, the National Center of Biotechnology Information (accession number GSE29877).

Quantitative Real-Time Two-Step RT-PCR (QRT-PCR)

To verify the microarray result, QRT-PCR assays were conducted using the same set of RNA for microarray analysis. One µg of aliquot RNA samples used for microarray were reverse transcribed using QuantiTect® Reverse Transcription kit with random hexamer primers (Qiagen) for two-step QRT-PCR. Gene specific primers listed in Table 4-2 were designed to generate products 100 to 250-bp in length from sequences on

XCC genome using DNASTAR software (DNASTAR). QRT-PCR was performed for all four biological replicates of rpfG mutant and wild type strain obtained at 11 h on a 7500 Fast Real-Time PCR System (Applied Biosystems) using QuantiTect™ SYBR® Green PCR kit (Qiagen) following the manufacturer's instructions. The 16S rRNA was used as endogenous controls. The relative fold change of gene expression was calculated by using the formula $2^{-\Delta\Delta C}{}_T$ (Livak and Schmittgen, 2001). The values of fold change were $\log_2$ transformed to compare with values generated from microarray analysis.

Motility Assays

The media for motility assays were NB or XVM2 containing 0.7% agar. Bacteria were grown in NB overnight with shaking at 200 rpm, and then centrifuged, washed and diluted to OD_{600} = 0.3 in sterile water. One µL suspension was spotted on the center of plate and incubated at room temperature. The assay was repeated three times independently in quadruplicate.

Protease Activity Test

To measure the activity of extracellular proteases produced by bacteria, bacterial cells were grown in NB at 28°C overnight with shaking at 200 rpm, then centrifuged down, washed and diluted to OD_{600} = 0.3 in sterile water. One µL suspension was spotted on 5% skim milk NA plate and incubated at room temperature. The protease activity was detected as zones of hydrolysis around the colonies. The assay was repeated three times independently in quadruplicate.

Pathogenicity Assay

Pathogenicity assays were conducted in a quarantine greenhouse facility at Citrus Research and Education Center, Lake Alfred, FL. Assays were performed using fully expanded, immature leaves of Duncan grapefruit (*Citrus paradisi* Macfadyen). XCC wild

type and mutant strains used in this assay were grown with shaking overnight at 28ºC in NB, centrifuged down and suspended in sterile tap water and the concentrations were adjusted to 10^8 CFU/mL. For the pathogenicity assays, bacterial solutions of 10^8, 10^5 or 10^4 CFU/mL were infiltrated into leaves with needleless syringes (Viloria et al. 2004; Rybak et al. 2009). The test was repeated three times with similar results. Disease symptoms were photographed at 6, 12 and 18 days post inoculation (DPI). For the lesion test, inoculated areas were marked on leaves and photographed on 18 DPI. Canker lesions from 10 inoculated leaves were quantified and the inoculated areas were calculated using the program ImageJ version 1.44p (Abramoff et al. 2004).

To mimic the natural infection process of XCC, bacterial suspensions of 10^8 CFU/mL were inoculated by spraying on the abaxial surface of Duncan grapefruit leaves. The inoculated plants were covered with plastic bags for 24 h to maintain 100% relative humidity, and then kept in greenhouse (approximately 50% relative humidity) for symptom development.

Attachment Assays

To measure the level of cells adhered to abiotic surface, bacteria grown overnight in NB or XVM2 medium were centrifuged, and the cell pellets were washed and resuspended in 10 mM phosphate buffer (pH 7.0) to OD_{600} = 1.0 (10^9 CFU/mL). Two hundred µL of each bacterial suspension were aliquoted into 1.5 mL plastic microcentrifuge tubes and incubated for 6 h at 28°C. The adherence was monitored by staining the attached bacteria with crystal violet (CV). Bacterial adhesion was measured after repetitive washing of the tubes to remove non-adherent cells and staining with 0.1% CV for 45 min at room temperature. Excess stain was removed by washing under running tap water, and the CV stain was solubilized by the addition of 250 µL volumes

of 99% ethanol added to each tube. CV was quantified with Agilent 8453 UV-visible spectrophotometer at 590 nm. The assay was repeated three times with 10 replicates each time.

To observe the bacterial adherence to biotic surface, bacterial suspension (OD_{600} = 1.0) was prepared as described above. Twenty µL of bacterial suspension was plated on the abaxial surface of detached Duncan grapefruit leaf and then incubated for 6 h in a moist chamber at 28°C. Inoculated leaves were washed twice with sterile tap water and stained with CV as for the abiotic surface (Gottig et al. 2009b).

To directly observe the bacterial adherence to leaf surface using confocal laser-scanning microscope (CLSM), constitutive GFP expression plasmid pUFZ75 (Zhang et al. 2009) was transformed into bacteria by electroporation. No difference in growth or adhesion to leaf and plastic surface could be detected between GFP-labeled bacteria and those lacking the GFP plasmid. The bacterial suspension was prepared and dropped on detached leave as described above. The inoculated leaves were incubated in a moist chamber at 28°C, and observed at 1 h and 6 h post inoculation, respectively. After washing twice with sterile tap water, inoculated areas were cut for microscopic observation. Bacterial adhesion was visualized using Leica TCS SL confocal laser-scanning microscope (Leica Microsystems Inc., Buffalo Grove, IL, U.S.A) with a 63× water objective in the microscope lab at Citrus Research and Education Center, Lake Alfred, FL, U.S.A. Three excitation/emission lines were used in observation as follows: green (excitation 488 nm, emission 500-545 nm) for detection of GFP-labeled strains, red (excitation 543 nm, emission 600-630 nm) for detection of cuticle, and blue

(excitation 633 nm, emission 680-750 nm) for detection of chlorophyll. The assay was performed three times independently in quadruplicate.

To further compare the location of bacterial cells relative to leaf tissue, we used a scanning electron microscope (SEM) in the microscope lab at Citrus Research and Education Center. The leaves inoculated with bacteria for 6 h were washed twice with sterile tap water, and inoculated areas were cut (about 0.5 cm^2) and fixed in 3% glutaraldehyde in 0.1 M phosphate buffer (pH 7.2) overnight. The fixed leaf discs were washed three times with 0.1 M phosphate buffer (pH 7.2), post-fixed in 2% OsO_4 in 0.1 M phosphate buffer (pH 7.2) for 4 h, and rinsed twice in 0.1 M phosphate buffer (pH 7.2). After rinsing, the leaf discs were subjected to dehydration in a sequence of ethanol solutions (10%, 20%, 30%, 40%, 50%, 60%, 70%, 80%, 90% and 100%) for 10 min each. The final wash in 100% ethanol was repeated three times. Leaf discs were critical-point dried in LADD critical point dryer (LADD Research, Williston, VT, U.S.A.), and then fixed on stubs and coated with gold-palladium using LADD sputter coater (LADD Research). SEM micrographs were taken in a Scanning Electron Microscope S-530 (Hitachi, Tokyo, Japan) at 20 kV. SEM analysis was performed twice, with six replicates for each sample.

Results

Generation of DSF-Mediated QS Mutants of XCC

To investigate the role of DSF-mediated QS in citrus canker infection, the deletion mutants of three critical genes *rpfF*, *rpfC* and *rpfG* in the DSF signal synthesis and transduction were generated by double cross-over recombination (Figure 4-2). The deletions were confirmed by sequence analysis of the corresponding PCR products. The QS mutants cannot form compact pellets as wild type strain when centrifuged down

from liquid media NB or XVM2 (Figure 4-3). To confirm the mutations in QS pathway, the three QS mutants were assayed for motility and extracellular protease production, which are well-known phenotypes controlled by DSF-mediated QS (Barber et al. 1997; Ryan et al. 2006). The QS mutants showed significant decrease in the production of proteases (Figure 4-4) and were defective in the motility (Figure 4-5). The phenotypes of all there mutants were restored to wild type level following complementation with corresponding genes *in trans* (Figure 4-3, 4-4 and 4-5).

QS is Required for the Full Virulence of XCC in Citrus Host

The role of QS in planta growth of XCC was evaluated by monitoring the population and symptoms of wild type and QS mutants on Duncan grapefruit, which is a susceptible host of XCC. Both wild type and QS mutants were infiltrated into young leaves of Duncan grapefruit with the initial concentration of 10^8 CFU/mL. No difference was observed with respect to time of appearance of lesions, and the magnitude of lesions (Figure 4-6A). When 10^5 CFU/mL was used as initial concentration, QS mutants produced fewer lesions formed than wild type (Figure 4-6B). However, the cell densities of QS mutants in planta were not significantly lower than wild type strain (about 50% less CFU/mL, data not shown). To quantify the difference in virulence between QS mutants and wild type, we used 10^4 CFU/mL to inoculate Duncan grapefruit leaves, photographed the inoculated leave at 18 DPI and then calculated lesion number per cm^2. The total amount of lesions caused by the *rpfF*, *rpfC*, and *rpf*G mutant were 50%, 32%, and 20%, respectively, of that caused by the wild-type strain in an area of 1 cm^2 (Figure 4-6C and D). Mutations of QS genes significantly reduced the lesions formed in Duncan grapefruit leaves ($P<0.001$, tested by one-way ANOVA).

The QS mutants also showed reduced virulence on spray-inoculated grapefruit compared with wild type strain.They still caused typical canker lesions but much fewer lesions compared with wild type strain (Figure 4-6E).

Overview of Microarray Analysis

To investigate the role of QS on global gene expression profile of XCC, XVM2 medium was used in this study to mimic the intercellular space of plant cells. The growth of QS mutants and wild type strain were monitored in XVM2 (Figure 4-1). Two time points, 11 h and 25 h, were chosen to represent exponential and stationary phases, respectively. In this study, false discovery rate (FDR) = 0.01 and absolute value of $\log_2$-fold change = 1.0 (equivalent to fold change of 2.0) were used as the cut-off value. At exponential phase, 119 (9 overexpressed and 150 underexpressed), 119 (4 overexpressed and 115 underexpressed), and 216 (63 overexpressed and 153 underexpressed) genes showed significant expression change in *rpfC*, *rpfF* and *rpfG* mutants relative to wild type strain, respectively (Table 4-3). The three QS mutants shared 101 (4 overexpressed and 97 underexpressed) differentially expressed genes at this phase. At stationary phase, 43 (4 overexpressed and 39 underexpressed), 104 (21 overexpressed and 83 underexpressed), and 214 (36 overexpressed and 178 underexpressed) genes were differentially expressed in *rpfC*, *rpfF* and *rpfG* mutants relative to wild type strain, respectively (Table 4-3). Similarly, 33 (3 overexpressed and 30 underexpressed) genes showed altered expression in all three mutants at this time. Upregulation by QS (showing underexpression in QS mutants) was obviously dominant over downregulation (showing overexpression in QS mutants) at both phases. Taking into account the different roles of the protein products of three *rpf* genes in QS pathway, the genes exhibited significantly differential expression in any of the three QS mutants

were considered as being QS regulated. Accordingly, 255 (63 overexpressed and 192 underexpressed) genes and 265 (47 overexpressed and 218 underexpressed) genes showed differential expression at exponential and stationary phases in any of the three QS mutants compared to the wild type, respectively. Thus, a total of 441 genes were considered as QS-regulated at one or more phases (Table 4-3), including 99 QS-downregulated genes (showing overexpression in any of the three gene mutants at any of the two phases), and 341 QS-upregulated genes (showing underexpression in any of the three gene mutants at any of the two phases), as well as 1 gene which was QS-upregulated at exponential phase but QS-downregulated at stationary phase. In other words, the expression of approximately 10% of all XCC genes is under the control of QS. The microarray data were validated using QRT-PCR on a subset of genes over- or underexpressed in the *rpfG* mutant relative to the wild type strain (Table 4-4).

Functional analysis showed that the 441 QS-regulated genes represented diverse aspects of bacterial physiology, classified into 19 functional categories according to the annotation from the J. Craig Venter Institute (JCVI) role categories (Table 4-3 and Figure 4-7). The largest percentage of QS-regulated transcripts (44.2%, 195 of 441) consists of unknown genes in the categories of hypothetical protein, unclassified, unknown function and not in JCVI. Sixty three genes representing 22.4% of the 281 known or predicted ORFs were involved in cellular processes, including 50 genes involved in chemotaxis and flagellar biosynthesis. Other functional categories with large numbers of QS-regulated genes included genes encoding transport and binding proteins (9.7%; 35/362), genes involved in energy metabolism (8.3%; 42/504), genes involved in protein fate (9.2%; 22/239), genes related to transcription (8.9%; 7/79),

genes involved in central intermediary metabolism (7.5%; 16/213), and genes encoding cell envelope (6.1%; 21/343).

The QS regulon differed in the two growth phases. Totally 255 genes were QS-regulated at the exponential phase, whereas 265 genes were identified as being QS-regulated at the stationary phase. Only 79 overlapped at both phases. The detailed information of the temporal regulation of diverse biological functions by QS was described below.

Chemotaxis and Flagellar Biosynthesis

One of the prominent transcriptional consequences of QS inactivation in XCC was the differential expression of a large number of genes involved in chemotaxis and flagellar biosynthesis. There are four clusters of genes related to chemotaxis and flagellar biogenesis in XCC genome (da Silva et al. 2002), which all exhibits QS-regulated pattern in this study (Table 4-3). At exponential phase, the “early” gene complex for flagellar basal-body-and-hook structure assembly (*flgACDEFGHIJKL*, *fliFGHIJKS*), and the late gene complex for flagellin and cap assembly (*fliC* and *fliD*) were significantly up-regulated by QS. Besides these, the up-regulated genes by QS at this phase included regulator genes *fliA*, *flgM*, *fleN* and 28 chemotaxis genes (10 copies of *ts*r, 3 copies of *cheA*, 2 *cheY*, 3 *cheW*, 2 cheR, 5 *mcp*, *che*Z, *cheV* and *parA*). At the stationary phase, only genes in the *fliGHIJK* cluster were up-regulated. The expression of the genes involved in motor and flagellar basal-body assembly (*fliELOQR*, *flhB*, *motB* and *flgB*) and the *flgA* gene involved in flagellar basal-body P-ring biogenesis were repressed by QS at this phase.

Cell Membrane Surface Structure and Transporters

Our microarray analysis revealed that QS is involved in the regulation of physiological adaption to the environmental changes by controlling the differential expression of a large set of genes encoding cell surface structure and transporters. At exponential phase, 15 genes involved in iron-uptake were down-regulated by QS, including *feoA*, *feoB*, *iroN*, *fecA*, *pfeA*, *fpvA*, *iucA*, 3 *fhuA* (XAC1435, XAC2185, XAC2941), XAC0492, XAC3178, *fhuE* (XAC3370 and XAC3498) and *phuR*. For instance, the *iucA* gene encoding an iron transporter was 3.37 $\log_2$-fold overexpressed in the *rpfG* mutant than in the wild-type strain (Table 4-3). The *fhuE* (XAC3498) gene, which encodes an outer membrane receptor for ferric iron uptake was 4.09 $\log_2$-fold overexpressed in the *rpfG* mutant than in the wild-type strain (Table 4-3). In contrast, the expression of 5 genes (*brf*, *cirA*, *btuB* (XAC2600), XAC2864, and *hppA*) involved in uptake of unknown substrates and *czcD* encoding a heavy metal transporter were up-regulated by QS at the exponential phase. Nine transporter genes (*nrtB* (XAC0827), *nrtCD* (CAC0828), *ssuA* (XAC0849 and XAC3198), *ssuB* (XAC0847 and XAC3196), *ssuC* (XAC0848 and XAC3197) and *fyuA*) were down-regulated, whereas 6 transporter genes (*betT*, *kdpA*, *kdpB*, *kdpC*, *bapA* and XAC3855) were up-regulated by QS. The genes *kdpA*, *kdpB* and *kdpC* encode subunits of potassium-transporting ATPase and *betT* encodes high-affinity choline transport.

Genes encoding outer membrane components were also regulated by QS at the two growth phases. At the exponential phase, a few genes encoding cell surface appendages were down-regulated, including two *xadA* genes (XAC3546 and XAC3548) which encode T5SS adhesin-like proteins, the *pilM* gene which is involved in type IV pilus assembly, as well as *hmsF*, *hmsR* and *hmsH* which are involved in PgaA adhesin

biosynthesis. However, three genes—*fimA* encoding type IV pilin, *pru* encoding secreted protein which may serve as fimbriae tip adhesion, and XAC0270 encoding unknown membrane protein—were up-regulated at the exponential phase. Nine genes encoding membrane surface components were up-regulated at the stationary phase, including 2 *mopB* genes (XAC1012 and XAC1021) encoding outer membrane proteins, 2 *blc* genes (XAC2561 and XAC4259) encoding outer membrane lipoproteins, the *ecnA* gene whose product directs the synthesis of a small cell envelop lippoprotein, and four hypothetical genes which are predicated as membrane proteins (XAC2139, XAC3844, XAC3845 and XAC3972). Only PgaA adhesion coding genes *hmsF* and *hmsH*, as well as *ompW* encoding outer membrane protein W, were down-regulated at the stationary phase

T2SS Substrates

T2SS substrates include the extracellular enzymes such as proteases, lipases, and cell-wall-degrading enzymes (e.g., cellulases, pectinases). They are important virulence traits for many plant pathogens, contributing to infection by degradation of the plant cell wall. Eight genes encoding extracellular enzymes—including 4 protease genes (XAC1034, XAC1512, XAC2853 and XAC2992), 3 cellulase genes (*egl* (XAC0029), *engXCA*, XAC0346), and *peh-1* encoding endopolygalacturonase—were up-regulated at both growth phases. Eleven T2SS substrate genes were differentially expressed at the exponential phase, including 10 genes up-regulated by QS (2 xylanase genes (XAC0933 and XAC0934), 3 cellulase genes (*egl* (XAC0028), *lamA* and *celS*), 2 pectate lyase genes (*pelB* and *pel*), 2 protease genes (XAC2763 and XAC2831) and 1 amylase gene *amy* (XAC0798), as well as 1 down-regulated protease gene XAC3545. At the stationary phase, besides the 8 genes encoding extracellular

enzymes as mentioned above, 3 more genes—including *xynB* encoding xylanase, *pglA* encoding pectate lyases and XAC351encoding protease—were up-regulated by QS.

One unique virulence factor XacPNP (XAC2654) was also positively controlled by QS at stationary phase. XacPNP is the homolog found only in XCC to plant natriuretic peptides (PNPs), which are extracellular molecules produced by plants to regulate plant responses in homeostasis and growth. It is secreted by XCC to suppressed host defense responses during infection via mimicking host PNP (Gottig et al. 2008).

T3SS and Effectors

T3SS is utilized by plant bacterial pathogens to secrete effector proteins directly into the host cell. T3SS translocon was encoded by a cluster of hypersensitive response and pathogenicity (*hrp*) genes. Genes encoding T3SS translocon and effectors were found in the QS regulon, including 8 structural genes and 9 effector genes. All those genes were up-regulated by QS at either the exponential or stationary phases. Three structural genes (*hrpB2*, *hrcJ* and *hpa1*) and 2 effector genes (XAC0543 and XAC2786) were up-regulated at both phases; another two structural genes (*hrcC* and *hpaB*) were up-regulated only at the exponential phase, whereas 3 structural genes (*hrpB1*, *hrpB4* and *hrpB5*) and 7 effector genes (*avrXacE1*, *avrXacE3*, *avrBs2*, *hrpW*, XAC1208, XAC4333 and XAC3085) were up-regulated only at the stationary phase.

Signal Transduction and Regulation

Several genes encoding transcriptional regulators and signal transduction system were differentially regulated by QS at both two growth phases. Three genes encoding two component systems (XAC1778, XAC1328 and XAC3273) and the *rpoN* gene (XAC1969) encoding RNA polymerase sigma-54 (σ^{54}) factor were up-regulated at both growth phases, whereas one transcription factor gene XAC3445 was down-regulated.

Two genes (*rrpX*, XAC1320) encoding transcription regulators, *algU* encoding sigma factor RpoE, *nucA* gene encoding endonuclease, and 7 regulatory genes (*vieA*, *entF*, XAC0424, XAC1993, *flgM*, *fliA* and *fleN*) were up-regulated at the exponential phase, while one regulatory gene (XAC2382) encoding GGDEF protein was down-regulated at the exponential phase. At the stationary phase, 3 transcription regulatory genes (*rbn*, *hrpX* and XAC0941) and four genes (*stkXac1*, tspO, XAC0644 and XAC1670) encoding the two component system were up-regulated by QS. Meanwhile, regulatory genes *flbD* and XAC1398 were down-regulated.

Stress Resistance

Genes encoding enzymes for bacterial resistance to environmental stress particularly peroxide were differentially regulate by QS. Multiple oxidative resistance genes were up-regulated by QS during growth in XVM2: 2 *catB* genes (XAC4029 and XAC4030) encoding catalases were up-regulated at exponential phase, while *srpA* encoding catalase, *cpo* encoding non-heme chloroperoxidase, and XAC1150 encoding peroxiredoxin were up-regulated at the stationary phase; *katE* encoding catalase were up-regulated at both growth phases. Three genes *algU*, XAC1320 and *mucD* which homologies are involved in the heat stress resistance and alginate production in *P. aeruginosa*, were up-regulated at the exponential phase. Besides the differential expression of those genes for specific stress resistances, the *cmfA* gene encoding conditioned medium factor was up-regulated at the exponential phase and XAC2369 encoding general stress protein was up-regulated at the stationary phase. Moreover, QS interacts with both genes at protein level: CmfA physically interacts with RpfC whereas XAC2360 physically interacts with RpfG (Andrade et al. 2006).

Metabolism

A large number of genes involved in metabolism, particularly in energy metabolism were differentially regulated by QS. A few genes related to energy metabolism were up-regulated by QS at both phases: *aceA* and *aslB* in TCA cycle; *ybdR* and *fdh* in fermentation; XAC2896 and XAC4182 in Electron transport; XAC1178 and XAC3738 encoding oxidoreductases. However, eight genes in energy metabolism were up-regulated only at the exponential phase—including genes in TCA cycle (*pdhA*, *pdhB* (XAC0443 and XAC0445) and *fumB*), genes in sugar metabolism (*galM*, *pqqG* and *ugt*) as well as *pcaD*, whereas four genes in energy metabolism including *qxtB* and XAC2983 in electron transport, *fucA1* and *ecaA* were down-regulated by QS only at this phase. Twelve genes in energy metabolism were up-regulated by QS at the stationary phase: XAC0154 and XAC0224 in sugar metabolism; XAC0794 in fermentation; XAC1174 in glycolysis; *cyoB*, XAC1476 and XAC4269 in electron transport; *rpfA* in TCA cycle; *gabD*, *gloA*, *glgX* and XAC2907 in other energy metabolism pathways. Gene *cydA* and *cydB* in electron transport were down-regulated at stationary phase. In addition, many genes encoding hydroxylase, oxidoreductase, and dehydrogenase, which are involved in energy metabolism and central intermediary metabolism were also up-regulated by QS at stationary phase: *bioI*, XAC1187 and XAC1188 encoding hydroxylases; XAC1189 encoding ferredoxin; XAC2051, *yagR* and *yagS* encoding oxidoreductases; *yagT*, *gcd*, *yahK*, XAC0158, XAC1180 and XAC2122 encoding dehydrogenases.

Besides the genes in energy metabolism, several genes related to sulfur metabolism, amino acid metabolism, fatty acid metabolism and protein fate were also temporally controlled by QS: the *gctA* gene in fatty acid metabolism was up-regulated at

the exponential phase; The genes *lig2*, *lig3* and XAC3037 in fatty acid metabolism were up-regulated at the stationary phase; XAC2948 and *piuB* genes in sulfur metabolism were down-regulated at the exponential phase; *metA*, *trpF* and XAC0802 in amino acid metabolism were up-regulated at the stationary phase; XAC2745, XAC3368 and *pfpI* encoding proteases involved in protein degradation were up-regulated at the stationary phase while XAC0787 in the same group were down-regulated at the stationary phase.

Regulation of *gum* genes

The gum gene cluster is responsible for EPS biosynthesis and is reported under the regulation of QS in previous studies (He et al. 2006). Surprisingly, no *gum* genes were identified as being QS regulated. To address if this is due to the growth media, we used QRT-PCR to compare the expression of *gum* genes in NB (rich medium) and XVM2 medium at the stationary phase. The *gumB* and *gumD* gene were selected for this test and showed lower transcript level in QS mutants than in wild type when bacteria were grown in NB. However, the transcript levels of those two genes in QS mutants were similar to those in wild type strain when bacteria were grown in XVM2 (Figure 4-10). This suggests that regulation of the expression of *gum* gene cluster by QS is medium-dependent, and an alternative parallel signaling system may exist to coordinate the expression of gum genes in XCC.

The Attachment of XCC Was Reduced by QS Mutations

Given the significant effect of QS on expression of chemotaxis and flagellar genes as well as genes encoding membrane surface components such as type IV pilus, we investigated if QS mediates the bacterial attachment event in pathogensis. First, the wild type strain and QS mutants were tested for their early attachment ability on abiotic surface (hydrophobic). The wild type strain attached to the hydrophobic surface much

better than these QS mutants, with more than 10 fold higher level of CV stain retained (Figure 4-8A and B). Most QS mutants cannot attach to the surface and their CV quantifications were similar to the negative buffer control (Figure 4-8A and B). In addition, wild type strain grown in XVM2 performed better in attachment assay than those grown in NB.

We also investigated the bacterial attachment on host leaf by placing the bacterial suspensions on the abaxial surface of Duncan grapefruit leaf. Similar to the results of attachment to abiotic surface, wild type strain grown in either XVM2 or NB attached to grapefruit leaf with CV stain remained, while the QS mutants were not able to attach to the leaf well showing basal level of CV stain as negative buffer control (Figure 4-8C).

To exam the difference in attachment to leaf by individual cells, we used CLSM to observe the GFP-labeled bacterial cells attached to leaf. The bacteria carrying the GFP plasmid did not affect the attachment to abiotic surface and biotic surface, or the virulence in planta (data not shown). Given the better performance of bacteria grown in XVM2, the GFP-labeled strains were grown in XVM2 prior to leaf attachment assay. After 1h of incubation, wild type cells started to aggregate to microcolonies (Figure 4-9A). In contrast, a few individual cells of the QS mutants could attach to leaf (Figure 4-9A). After 6 h of incubation, many more wild type cells attached to leaf and formed matrix on leaf (Figure 4-9B and C), while QS mutants formed microcolonies on leaf (Figure 4-9B). The leaf was scanned at different depths, which showed bacteria primarily located in the depression formed by the anticlinal wall of epidermal cells and around stomata, not on the top of periclinal wall of epidermal cells (Figure 4-9C). To confirm the observation, we used scanning electron microscope to exam the leaf

incubated with bacterial suspensions for 6 h. As shown in Figure 4-9D, many more wild type than QS mutants cells occupied in the depression between epidermal cells and around stomata.

Discussion

DNA microarray has been widely used to study the transcriptional responses of many organisms to genetic and environmental perturbations (Ye et al. 2001; Dharmadi and Gonzalez 2004). In the present study, we studied the QS regulon using one whole-genome DNA microarray for XCC 306. The reliability and robustness of this Agilent array have been confirmed in the transcriptome analyses of HrpG and HrpX regulons in our previous study (Guo et al. 2011). They were further validated in the present study. In this study, transcriptome analysis of the QS regulon identified genes involved in chemotaxis and flagellar biosynthesis, resistance to oxidative stress, T2SS substrates biosynthesis, biosynthesis of T3SS and effector proteins, type IV pili, T5SS adhesions, energy metabolism, fatty acid metabolism, signal transduction and regulation, as well as genes encoding transporters (Table 4-3). The regulation of those genes was consistent with the physiological assays, including motility assay (Figure 4-5), protease assay (Figure 4-4), attachment assays on abiotic and biotic surfaces (Figure 4-8).

Transcriptome analysis of the QS regulon by combining the RpfF, RpfC, and RpfG regulons has significantly advanced our understanding of the DSF-mediated QS regulons in bacteria. Compared to the pioneer work done by Zhang and colleagues on the QS regulon of *X. campestris* pv. *campestris* (He et al. 2006), we have further characterized the RpfC and RpfG regulons which have not been characterized in the past besides the RpfF regulon at the exponential and the stationary phases. To simplify our analysis, we have combined the RpfF, RpfC, and RpfC regulons as the QS regulon.

Thus, we were able to identify 441 genes which were regulated (up-regulated or down-regulated) by QS in XCC. Those genes were involved in a broad range of biological functions including genes encoding flagellar and chemotaxis biosynthesis, biosynthesis of T3SS and T3SS effectors, type IV pili, T5SS adhesins, iron uptake, T2SS substrates, metabolism (energy metabolism, amino acid metabolism, and fatty acid metabolism) and stress response. A large number of genes including genes encoding T3SS effectors, type IV pili, T5SS adhesions, stress response proteins and GGDEF proteins have not been reported previously to be regulated by QS and will further advance our understanding of the roles of QS.

Importantly, we have identified some interesting difference between the QS regulons in XCC and in *X. campestris* pv. *campestris*. (1) Most genes involved in iron uptake were down-regulated by QS in XCC whereas they were up-regulated in *X. campestris* pv. *campestris* (He et al. 2006). (2) Regulation of T3SS genes and T3SS effector genes were different between XCC and *X. campestris* pv. campestris: 8 T3SS genes (*hrp*) and 9 effector genes were up-regulated at the two growth phases in XCC, whereas 1 hrp gene was up-regulated and 9 hrp genes were down-regulated at both phases in *X. campestris* pv. *campestris* (He et al. 2006). (3) The regulation pattern of flagellar biosynthesis in XCC is different from *X. campestris* pv. *campestris* (He et al. 2006). Most genes involved in flagella biosynthesis were up-regulated at the exponential phase but nine were down-regulated at stationary phase in XCC. In contrast, the flagella biosynthesis genes were up-regulated at both phases in *X. campestris* pv. *campestris*. These discrepancies could be due to the differences in the two species. The *rpf* cluster of *X. campestris* pv. *campestris* contains 9 genes whereas

XCC contains only 7 genes and lacks *rpfI* and *rpfH* genes (da Silva et al. 2002). The *rpfH* gene encodes a protein structurally related to the sensory input domain of RpfC, indicating that it may also participate in the DSF signal transduction (Slater et al. 2000); RpfI is involved in regulation of the expression of proteases and endoglucanase (Dow et al. 2000). Furthermore, the difference in downstream regulators in the signaling cascades may also contribute to the discrepancies: Two known regulators FhrR and Zur in QS cascade of *X. campestris* pv. *campestris* are not found in XCC QS regulon, whereas the existence of HrpX is found in XCC QS regulon. In *X. campestris* pv. *campestris*, FhrR is responsible for the regulation of genes encoding flagella, T3SS and ribosome proteins, and Zur controls the iron uptake, multidrug resistance, and detoxification (He et al. 2007). Alternately, the discrepancies might be due to different growth media and culture conditions used in these studies: XVM2 was used in the present study which is a defined medium mimicking the apoplastic environment of plant leaf (Wengelnik et al. 1996a), while YEB rich medium (no iron supplemented) was used for the QS study in *X. campestris* pv. *campestris* (He et al. 2006). XVM2 is supplemented with Fe_2SO_4, which might explain the differential regulation of iron in the two systems. Likely, the differential regulation of T3SS genes in the two studies results from the two media used since the expression of T3SS genes was induced in planta or by XVM2 and repressed by rich medium in *X. campestris* pv. *vesicatoria* (Schulte and Bonas 1992; Wengelnik and Bonas 1996).

A dramatic difference was observed between the QS regulons in the exponential and the stationary stages. In total, 255 genes belonged to the QS regulon at the exponential phase, whereas 265 genes belonged to the QS regulon at the stationary

phase in this present study. Only 79 genes overlapped at the two phases. Similar situation was also observed in the studies of QS regulon in *Pseudomonas* spp. (Schuster et al. 2003; Wagner et al. 2003; Schreiber and Desveaux 2011). The expression of genes in flagellar biosynthesis and chemotaxis, type IV pili, T5SS adhesions, iron uptake were regulated at the exponential phase, whereas, genes encoding T3SS and effectors, fatty acid metabolism, amino acid metabolism were regulated at the stationary phase. Many functions such as energy metabolism, T2SS substrate biosynthesis, transporters, regulation are controlled in both phases. The differential regulation of biological functions during different growth phases suggest that bacteria adapt to environmental changes in different stages of infection. For example, flagellum is critical for bacterial motility and initial attachment to surfaces, as well as biofilm formation. However, it is also one of pathogen associate molecule patterns (PAMP) which strongly induces plant defense response. Therefore, XCC adapts to the environment by activating the flagella-mediated motility during early stage, which might mimic the invasion stage of infection, and repressing flagellar biosynthesis at the stationary state, which might mimic the late stage of infection, thus minimizing PAMP-induced host defense response. (Ellermeier and Slauch 2003; Wolfgang et al. 2004; Schreiber and Desveaux 2011).

A cross-talk between T3SS and QS in XCC was observed in this study. By comparing the QS and HrpG regulons (Guo et al. 2011), 62 genes were identified to be controlled by both systems (Table 4-5), including 11 genes involved in chemotaxis and flagellar biosynthesis, 8 genes encoding T2SS substrates, 8 genes encoding T3SS, 9 genes encoding T3SS effectors, 4 genes encoding transporters, 3 transcription

regulator genes and 6 genes related to energy metabolism, as well as 13 hypothetical genes. Both HrpG and QS positively regulated the expression of genes encoding T2SS substrates, T3SS and T3SS effectors at the early stationary and stationary phases. However, HrpG and QS showed opposite effect on the expression of genes involved in chemotaxis and flagellar biosynthesis: 8 of 11 chemotaxis and flagellar genes were repressed by HrpG at the early stationary phase while they were induced by QS at the exponential phase. Likely, this may be the strategy utilized by XCC to minimize PAMP (including flagella)-induced host defense by repressing flagellar biosynthesis and to suppress host defense by inducing T3SS effectors at the same time. XCC might coordinate its virulence traits through HrpX and QS and downstream regulators common to both systems such as *hrpX*, *stkXac1* and XAC1320 and *flgM*. Genes encoding T2SS substrates, T3SS and T3SS effectors are possibly controlled by both systems through HrpX at transcription level, since those functions are HrpX-dependent (Table 4-5) (Guo et al. 2011). Moreover, StkXac1 belonged to the HrpX regulon and may serve as a downstream regulator in controlling those biological functions. Both systems may regulate flagellar biosynthesis by controlling the anti-σ-28 factor FlgM, which is a negative regulator of flagellin synthesis. Gene flgM was positively regulated by QS at the exponential phase, whereas it was negatively regulated by HrpG at the early stationary phase. FlgM regulates flagellar assembly by binding to FliA, which results in inhibition of expression of genes for the late stage of flagellar assembly and also protects FliA from the proteolysis of Lon protease (Barembruch and Hengge 2007). Once the flagellar hook basal body forms a T3SS-like structure, it secretes FlgM into the extracellular space which results in the release of FliA and the activation of genes for

flagellin assembly. Our data suggests that the temporal regulation of FlgM by HrpG and QS may be important for the different stages of XCC infection. In addition, the crosstalk between the two systems might be underlined by intracellular level of the cyclic-di-GMP. The expression of *rpfG* and 2 genes encoding GGDEF proteins (XAC1939 and XAC1940) were repressed by HrpG at the early stationary phase (Guo et al. 2011). Totally, 6 genes (*vieA*, *rrpX*, XAC0424, XAC0644, XAC1993 and XAC2382) that encode products containing GGDEF or EAL or both domains were regulated by QS (Table 4-3). GGDEF domain is responsible for the messenger cyclic-di-GMP production while HD-GYP domain of RpfG (Ryan et al. 2006) and EAL domains are responsible for cyclic-di-GMP degradation. Moreover, the protein-protein interaction analysis showed that GGDEF domains of the products of two HrpG-repressed genes (XAC1939 and XAC1940) and three QS-regulated genes (XAC0424, XAC0644 and XAC2382) physically interact with HD-GYP domain of RpfG (Andrade et al. 2006), resulting in variation of the concentration of cyclic-di-GMP. The cyclic-di-GMP signaling pathway controls multiple biological functions via Clp and downstream regulators Zur and FhrR (He et al. 2007). Those regulators might link the QS and HrpG pathways as a regulatory network which integrates the information from diverse environmental cues and response by regulating the expression of genes for virulence and fitness.

QS seems to play critical roles in attachment, entering and colonization of XCC disease cycle by coordinating diverse virulence traits and cross-talking with other systems such as T3SS. Even though we have not been building up the relationship between different growth phases and different infection stages of XCC, it is very likely that the early infection stage in planta resembles the exponential phase of growth in

vitro since they both share low population of XCC and low DSF concentration. The differential regulation of diverse virulence traits by QS in the two different growth phases is supporting our notion that XCC is adapting to its environments through rapid changes in regulation. In first step of disease cycle, XCC attached to citrus leaf (abixial surface at most times), QS positively regulates genes encoding flagellar and chemotaxis which enable the bacteria sense and swim to the depression where the anticlinal walls of the epidermal cells join. Those depression areas are relatively more abundant in water and nutrients compared to the top area on leaf surface and protect XCC from sunlight damage and desiccation. XCC cells form microcolonies as early as 1 h after attachment (Figure 4-9A). Cells in the microcolonies are more capable of surviving environmental stresses than individual cells on leaf surface (Monier and Lindow 2003). Those microcolonies aggregate along the depression lines of the surface of epidermal cells (Figure 4-9B and C), which may rely on the cell surface appendages. In a previous study it was shown that the flagellar mutants of XCC cannot form mature biofilm on leaf surface and caused fewer lesions than wild type strain when spray inoculated them on citrus host (Malamud et al. 2011). The expression of genes encoding T2SS substrates was up-regulated and the expression of genes encoding transporter was differentially regulated (up- or down-regulated) during this process. T2SS substrates are degrading enzymes which promote the growth of bacteria in environmental niches and in hosts (Cianciotto 2005). Since leaf surface lacks nutrients and water, XCC also activates on its transporter to acquire critical elements from environment.

QS has been suggested to be important for *X. campestris pv. campestris* to enter the stomata by reverting stomatal closure, one innate immunity response of plant to

bacterial infection. Suppression of stomatal response by *X. campestris pv. campestris* requires an intact DSF/*rpf* system including functional RpfF and RpfC (Gudesblat et al. 2009). Likely, QS plays similar roles in XCC by facilitating the bacteria to move and enter the host through stomata. The low infection rates of the *rpfF*, *rpfC*, *rpfG* mutants compared to the wild-type strain XCC (Figure 4-6E) using spray inoculation might be partly due to its effect on stomatal opening. XacPNP has been reported to increase stomata opening (Gottig et al. 2008). Interestingly, the *xacPNP* gene was up-regulated by both HrpG and QS happened at the early stationary and stationary phases respectively even though not at the exponential phase (Table 4-5).

QS seems to play roles for XCC survival in the intercellular spaces and cause disease. Once XCC enters the plant apoplast, it has to modify the intercellular space for better growth and to suppress plant defense response caused by PAMPs. This is mainly achieved by HrpG and HrpX, which induce the expression of multiple virulence traits such as T3SS and T3SS effectors, and repress flagellar biosynthesis at the same time (Guo et al. 2011). However, our analysis showed that the regulator HrpX, several *hrp* genes, T3SS effector genes, and genes encoding T2SS substrates also belonged to QS regulon, suggesting that QS contributes to virulence via regulating those virulence traits. Milder symptoms were observed for the *rpfF*, *rpfC*, *rpfG* mutants compared to the wild-type strain XCC (Figure 4-6 A, B and C). This indicates that mutations of QS genes did not abolish the virulence of XCC, but reduced the virulence

In conclusion, we have significantly advanced our understanding of the QS regulation by characterization of the RpfC and RpfG regulons besides the RpfF regulon. RpfC and RpfG comprise the sensor kinase and the response regulator for detection of

the DSF signal and transduction to the downstream regulators. New functions of QS were revealed such as the control of type IV pili, T5SS adhesins, T3SS effectors, and the negative regulation on iron uptake. Importantly, a cross-talk between QS and HrpG was observed. We also provided evidence for the roles of QS in attachment of leaf surface and virulence of XCC.

Table 4-1. Bacterial strains and plasmids used in this study

Strain or plasmid	Relevant characteristics[a]	Reference or source
Strains		
E. coli		
Mach1™ T1R	F^- Φ80*lacZ*ΔM15 Δ*lacX*74 *hsdR*(r_K^-, m_K^+) Δ*recA*1398 *endA*1 *tonA*	Invitrogen
DH5α	F^- Φ80*lacZ*ΔM15 Δ(*lacZYA-argF*) U169 *recA*1 *endA*1 *hsdR*17 (r_K^-, m_K^+) *phoA supE*44 λ^- *thi*-1 *gyrA*96 *relA*1	Laboratory collection
DH5αλPIR	Host of pOK1; DH5α(λPIR)	Huguet et al. 1998
X. citri subsp. *citri*		
306	Rif^r, causes citrus canker on citrus	da Silva et al. 2002
rpfF	*rpfF* deletion mutant of strain 306, Rif^r	This study
rpfC	*rpfC* deletion mutant of strain 306, Rif^r	This study
rpfG	*rpfG* deletion mutant of strain 306, Rif^r	This study
Plasmids		
pGEM-T easy	Cloning vector; Ap^r	Promega
pCR®2.1-TOPO™	Cloning vector; PUC ori f1 ori *lacZ*α^+ Km^r Ap^r	Invitrogen
pRK2013	Conjugation helper plasmid; ColE1 Tra^+ Km^r	Ditta et al. 1980
pOK1	Suicide vector; *sacB sacQ mobRK2 oriR6K* Sp^r	Huguet et al. 1998
pUFR034	Shuttle vector; IncW Mob^+*mob*(P) *lacZ*α^+ Par^+ Km^r	DeFeyter et al. 1990
pUFR053	Shuttle vector; IncW Mob^+*mob*(P) *lacZ*α^+ Par^+ Cm^r Gm^r	El Yacoubi et al. 2007
pUFZ75	Constitutive GFP expression vector; *trp* promoter cloned upstream of the GFP cassette; Km^r	Zhang et al. 2009
pGEM-rpfF	1,610-bp fragment containing entire *rpfF* cloned in pGEM-T easy; Ap^r	This study
pGEM-ΔrpfF	pGEM-rpfF with deletion of 744-bp from the interior of *rpfF*; Ap^r	This study
pOK-ΔrpfF	*Apa*I-*Spe*I fragment containing ΔrpfF from pGEM-ΔrpfF cloned in pOK1; Sp^r	This study
PCR-rpfF	1,610-bp fragment containing entire *rpfF* cloned in pCR®2.1-TOPO™; Km^r Ap^r	This study
p53-rpfF	blunt ended *Hind*III-*Xba*I fragment containing *rpfF* from PCR-rpfF cloned in pUFR053; Cm^r Gm^r	This study

Table 4-1. Continued

Strain or plasmid	Relevant characteristics[a]	Reference or source
pGEM-rpfC	3,017-bp fragment containing entire *rpfC* cloned in pGEM-T easy; Ap^r	This study
pGEM-ΔrpfC	pGEM-rpfC with deletion of 1,116-bp from the interior of *rpfC*; Ap^r	This study
pOK-ΔrpfC	*Apa*I-*Spe*I fragment containing ΔrpfC from pGEM-ΔrpfC cloned in pOK1; Sp^r	This study
PCR-rpfC	2,590-bp fragment including entire *rpfC* cloned in pCR®2.1-TOPO™; Km^r Ap^r	This study
p53-rpfC	*Kpn*I fragment containing entire *rpfC* from PCR-rpfC cloned in pUFR053; Cm^r Gm^r	This study
pGEM-rpfG	2,037-bp fragment containing entire *rpfG* cloned in pGEM-T easy; Ap^r	This study
pGEM-ΔrpfG	pGEM-rpfG with deletion of 648-bp from the interior of *rpfG*; Ap^r	This study
pOK-ΔrpfG	*Apa*I-*Spe*I fragment containing ΔrpfG from pGEM-ΔrpfG cloned in pOK1; Sp^r	This study
p34-rpfG	*EcoR*I fragment containing entire *rpfG* from pGEM-rpfG cloned to pUFR034; Km^r	This study

[a] Rif^r, Km^r, Ap^r, Cm^r, Gm^r and Sp^r indicate resistance to rifampicin, kanamycin, ampicillin, chloramphenicol, gentamicin and spectinomycin, respectively.

Table 4-2. Primers used in this study

Primer	Sequence (5'→3')[a]
Primers used in mutagenesis and complementation	
rpfCF	CAGCAGAGCGAAAGCGTCAAGCA
rpfCR	CGGCCCTGGCGCTCAATGAAAA
rpfGF	GCTTCGAGCTGTTCATCAACGGTAAGG
rpfGR	GCGAGACCGATGCCAAGACTGAGATT
rpfFF	GGGCGAAATCGTCAAGGTGGTCAT
rpfFR	GCGAGTTCATCCAGCAATGCCTCAG
rpfC-kpnF	GGggtaccATCGGCTACGAACTGCT
rpfC-kpnR	TGggtaccATACGTCGCATCTTCAGG
Primers used in QRT-PCR	
16S-F	CGCTTTCGTGCCTCAGTGTCAGTGTTGG
16S-R	GGCGTAAAGCGTGCGTAGGTGGTGGTT
XAC1266-hrpX-F	AGCGATCTCTGCGTTGTCCTAC
XAC1266-hrpX-R	ATACGCATCTTCGGCCTCTTCCTGA
XAC0407-hrpB1-F	ACCCATGACAAGATTCAGGACGCT
XAC0407-hrpB1-R	CTTCCACGTAATTACCGCGCTTGA
XAC0415-hrcC-F	ATACGTCGCCGACAACAAGGATCT
XAC0415-hrcC-R	CGGAGATGTTTCGAATTTGCCGCT
XAC0416-hap1-F	ATTCTTTGAACACACAGCTCGGCG
XAC0416-hap1-R	TCGGCATTGTTGCTCTGCTGAA
XAC0798-amy-F	GCATCAGCAACTACAACGACGCTT
XAC0798-amy-F	TGAGATGGTCGAACGTCATGTGCT
XAC1854-feoA-F	ATCGTGGATTCCGTGGAGGAT
XAC1854-feoA-R	TGTAGCCCACCTGCACCAACAAT
XAC1904-cheY-F	ACGTGAACATGCCCAACATGGA
XAC1904-cheY-R	TGGCGATCAGCTGTTCTGGATTGA
XAC1954-fliF-F	AGAAGCCTGGCTATCAATCGCTGT
XAC1954-fliF-R	TGGTCGATCTTGTAGGGAATCTGC

Table 4-2. Continued

Primer	Sequence (5'→3')[a]
Xac1989-flgM-F	AAATCGAAGGCAATCTACCGACCG
Xac1989-flgM-R	TGCCGTTCTGCAATGCATCCTTCA
XAC2865-cheA-F	ACCATATCCATGCCCTGGTGGAAA
XAC2865-cheA-R	TGCGTTGCAGATACGTCTGCAGTT
XAC2922-hrpW-F	AGACGTCCGACCATTCCGACAAAT
XAC2922-hrpW-R	TGTGAACCACGATCGGACTGTTGA
XAC3176-fecA-F	ACCCTCAACGCCAGTTATGCCTAT
XAC3176-fecA-R	TGAAGTAATAGCCGGAAAGCGCGA
XAC3240-fimA-F	TGCTTCCATAGCGATCCCGCAATA
XAC3240-fimA-R	TGGTAGCAGTCGCAGTCAAACCAA
XAC3385-pilM-F	AGCCACCAATTACATTCCGTACCC
XAC3385-pilM-R	AAAGGCCTCCACGTCCATTACCTT
XAC3548-xacdA-F	TGAAGCAAGTGCGCGCGATTAT
XAC3548-xacdA-R	TTCGCTTCATTAACGCCTGACTCC
XAC3990-srpA-F	TCGCGATCTCAATTACGACCCGTT
XAC3990-srpA-R	GCGGCGATTGAACGATTGCGAATA
XAC2585-gumB-F	CTGACCGAAATCGAGAAGGGCACCAATC
XAC2585-gumB-R	GCGCCACACCATCACAAGAGGAGTCAGTTC
XAC2583-gumD-F	AAACCAGGTCGAACAGGTCTGGAT
XAC2583-gumD-R	AGCAGACCGAAATCGAACAGGTCA

[a] Lowercase nucleotides are not exact matches to the sequence and were introduced to add restriction enzyme sites.

Table 4-3. Genes showing significant differential expression in QS mutants compared with wild type strain at exponential and/or stationary phases.

Locus tag	Gene Symbol	rpfC/W Ex[a]	rpfF/W Ex[a]	rpfG/W Ex[a]	rpfC/W St[a]	rpfF/W St[a]	rpfG/W St[a]	Description	JCVI[b]
XAC0802	-	NS	NS	NS	NS	-1.21	NS	sulfotransferase	Amino acid biosynthesis
XAC3040	metA	NS	NS	NS	NS	-1.16	NS	homoserine O-acetyltransferase	Amino acid biosynthesis
XAC2719	trpF	NS	NS	NS	NS	NS	-1.03	N-(5'-phosphoribosyl)anthranilate isomerase	Amino acid biosynthesis
XAC2947	apbE	NS	NS	1.81	NS	NS	NS	thiamine biosynthesis lipoprotein ApbE precursor	Biosynthesis of cofactors, prosthetic groups, and carriers
XAC3340	cysG	NS	NS	NS	NS	NS	1.23	siroheme synthase	Biosynthesis of cofactors, prosthetic groups, and carriers
XAC1984	flgD	-1.99	NS	-1.76	NS	NS	NS	flagellar basal body rod modification protein	Cell envelope
XAC1427	pru	-1.57	-1.36	-1.36	NS	NS	NS	protein U	Cell envelope
XAC3921	ugt	-1.24	-1.01	-1.29	NS	NS	NS	glucosyltransferase	Cell envelope
XAC0661	peh-1	-1.05	-1.07	-1.99	-1.18	-1.38	NS	endopolygalacturonase	Cell envelope
XAC3524	-	2.77	2.54	2.49	1.24	2.01	1.14	hypothetical protein	Cell envelope
XAC3240	fimA	NS	-1.44	NS	NS	NS	NS	fimbrillin	Cell envelope
XAC3546	xadA	NS	NS	1.72	NS	NS	NS	outer membrane protein	Cell envelope
XAC3548	xadA	NS	NS	1.75	NS	NS	NS	outer membrane protein	Cell envelope
XAC1813	hmsH	NS	NS	2.57	NS	1.29	1.38	HmsH protein	Cell envelope
XAC3180	iucA	NS	NS	3.37	NS	NS	NS	iron transporter	Cell envelope
XAC3178	-	NS	NS	3.58	NS	NS	NS	hypothetical protein	Cell envelope
XAC2922	hrpW	NS	NS	NS	NS	-1.32	-1.53	HrpW protein	Cell envelope
XAC2374	pglA	NS	NS	NS	NS	-1.03	NS	polygalacturonase	Cell envelope
XAC3354	ompW	NS	NS	NS	NS	2.03	1.74	outer membrane protein W	Cell envelope
XAC3845	-	NS	NS	NS	NS	NS	-1.75	hypothetical protein	Cell envelope
XAC2139	-	NS	NS	NS	NS	NS	-1.61	hypothetical protein	Cell envelope
XAC3844	-	NS	NS	NS	NS	NS	-1.58	hypothetical protein	Cell envelope

Table 4-3. Continued

Locus tag	Gene Symbol	rpfC/W Ex[a]	rpfF/W Ex[a]	rpfG/W Ex[a]	rpfC/W St[a]	rpfF/W St[a]	rpfG/W St[a]	Description	JCVI[b]
XAC1012	mopB	NS	NS	NS	NS	NS	-1.53	outer membrane protein	Cell envelope
XAC2561	blc	NS	NS	NS	NS	NS	-1.30	outer membrane lipoprotein Blc	Cell envelope
XAC3972	-	NS	NS	NS	NS	NS	-1.21	hypothetical protein	Cell envelope
XAC4259	blc	NS	NS	NS	NS	NS	-1.16	lipocalin	Cell envelope
XAC1976	flgL	-2.50	-2.44	-1.15	NS	NS	NS	flagellar hook-associated protein FlgL	Cellular processes
XAC1931	cheZ	-2.25	-1.57	-1.29	NS	NS	NS	chemotaxis related protein	Cellular processes
XAC1932	cheY	-2.14	-1.55	-1.42	NS	NS	NS	chemotaxis protein	Cellular processes
XAC2448	mcp	-2.11	-2.09	-2.00	NS	NS	NS	chemotaxis protein	Cellular processes
XAC2866	mcp	-2.10	-2.10	-2.19	NS	NS	NS	chemotaxis protein	Cellular processes
XAC1977	flgK	-2.09	NS	NS	NS	NS	NS	flagellar hook-associated protein FlgK	Cellular processes
XAC1983	flgE	-2.04	-1.64	NS	NS	NS	NS	flagellar hook protein FlgE	Cellular processes
XAC1981	flgG	-1.91	NS	-1.94	NS	NS	NS	flagellar basal body rod protein FlgG	Cellular processes
XAC1973	fliS	-1.84	-1.81	-2.10	NS	NS	NS	flagellar protein	Cellular processes
XAC1979	flgI	-1.84	NS	-1.87	NS	NS	NS	flagellar basal body P-ring protein	Cellular processes
XAC1980	flgH	-1.84	NS	-1.83	NS	NS	NS	flagellar basal body L-ring protein	Cellular processes
XAC1978	flgJ	-1.81	NS	-1.55	NS	NS	NS	flagellar rod assembly protein/muramidase FlgJ	Cellular processes
XAC1985	flgC	-1.81	NS	-1.65	NS	NS	NS	flagellar basal body rod protein FlgC	Cellular processes
XAC2865	cheA	-1.77	-1.50	-1.87	NS	NS	NS	chemotaxis histidine protein kinase	Cellular processes
XAC1904	cheY	-1.77	-1.54	-1.90	NS	NS	NS	chemotaxis response regulator	Cellular processes
XAC2867	cheW	-1.75	-1.62	-1.80	NS	NS	NS	chemotaxis protein	Cellular processes
XAC1996	mcp	-1.73	-1.70	-1.98	NS	NS	NS	chemotaxis protein	Cellular processes

Table 4-3. Continued

Locus tag	Gene Symbol	rpfC/W Ex[a]	rpfF/W Ex[a]	rpfG/W Ex[a]	rpfC/W St[a]	rpfF/W St[a]	rpfG/W St[a]	Description	JCVI[b]
XAC1211	katE	-1.73	NS	NS	-1.44	-1.51	-2.20	catalase	Cellular processes
XAC1974	fliD	-1.73	-1.53	-1.92	NS	NS	NS	flagellar protein	Cellular processes
XAC3132	mcp	-1.71	-1.55	-2.01	NS	NS	NS	chemotaxis protein	Cellular processes
XAC1982	flgF	-1.68	-1.32	NS	NS	NS	NS	flagellar basal body rod protein FlgF	Cellular processes
XAC2447	cheW	-1.67	-1.30	-1.60	NS	NS	NS	chemotaxis protein	Cellular processes
XAC1930	cheA	-1.66	-1.30	-1.03	NS	NS	NS	chemotaxis related protein	Cellular processes
XAC1988	flgA	-1.65	NS	NS	NS	1.55	1.44	flagellar basal body P-ring biosynthesis protein FlgA	Cellular processes
XAC4029	catB	-1.65	-1.35	-1.78	NS	NS	NS	catalase precursor	Cellular processes
XAC1987	cheV	-1.64	-1.44	-1.85	NS	NS	NS	chemotaxis protein	Cellular processes
XAC1893	tsr	-1.64	-1.70	-1.70	NS	NS	NS	chemotaxis protein	Cellular processes
XAC1950	fliJ	-1.60	-1.58	-1.61	-1.34	-1.83	-1.35	flagellar FliJ protein	Cellular processes
XAC1895	tsr	-1.57	-1.56	-1.83	NS	NS	NS	chemotaxis protein	Cellular processes
XAC1951	fliI	-1.54	-1.30	-1.47	NS	-1.46	-1.11	flagellar protein	Cellular processes
XAC1897	tsr	-1.53	-1.59	-1.65	NS	NS	NS	chemotaxis protein	Cellular processes
XAC1899	tsr	-1.44	-1.52	-1.58	NS	NS	NS	chemotaxis protein	Cellular processes
XAC1903	cheA	-1.42	-1.33	-1.69	NS	NS	NS	chemotaxis protein	Cellular processes
XAC1894	tsr	-1.42	-1.37	-1.66	NS	NS	NS	chemotaxis protein	Cellular processes
XAC0064	-	-1.41	-1.39	-1.13	NS	NS	NS	acetyltransferase	Cellular processes
XAC1907	parA	-1.41	-1.11	-1.65	NS	NS	NS	chromosome partioning protein	Cellular processes
XAC1953	fliG	-1.41	-1.24	-1.81	-1.09	-1.45	NS	flagellar protein	Cellular processes
XAC1902	tsr	-1.40	-1.51	-1.36	NS	NS	NS	chemotaxis protein	Cellular processes
XAC1952	fliH	-1.38	-1.24	-1.42	NS	-1.36	NS	flagellar protein	Cellular processes
XAC3213	mcp1	-1.33	-1.39	-1.35	NS	NS	NS	chemotaxis protein	Cellular processes
XAC1949	fliK	-1.33	-1.49	-1.71	-1.24	-1.52	-1.29	flagellar protein	Cellular processes
XAC0611	tsr	-1.28	-1.04	NS	NS	NS	NS	chemotaxis protein	Cellular processes
XAC1896	tsr	-1.25	-1.12	-1.24	NS	NS	NS	chemotaxis protein	Cellular processes

Table 4-3. Continued

Locus tag	Gene Symbol	rpfC/W Ex[a]	rpfF/W Ex[a]	rpfG/W Ex[a]	rpfC/W St[a]	rpfF/W St[a]	rpfG/W St[a]	Description	JCVI[b]
XAC1954	fliF	-1.23	-1.05	-1.74	NS	NS	NS	flagellar MS-ring protein	Cellular processes
XAC1900	tsr	-1.22	-1.26	-1.32	NS	NS	NS	chemotaxis protein	Cellular processes
XAC0443	pdhB	-1.20	NS	-1.09	NS	NS	NS	branched-chain alpha-keto acid dehydrogenase subunit E2	Cellular processes
XAC1891	tsr	-1.19	-1.29	-1.27	NS	NS	NS	chemotaxis protein	Cellular processes
XAC1178	-	-1.13	NS	NS	-1.89	-1.95	-2.63	oxidoreductase	Cellular processes
XAC1909	motC	NS	NS	-1.10	NS	NS	NS	flagellar motor protein	Cellular processes
XAC3385	pilM	NS	NS	1.06	NS	NS	NS	fimbrial assembly membrane protein	Cellular processes
XAC0270	-	NS	NS	2.03	NS	NS	NS	hypothetical protein	Cellular processes
XAC0076	avrBs2	NS	NS	NS	NS	-1.07	NS	avirulence protein	Cellular processes
XAC1941	fliR	NS	NS	NS	NS	1.17	NS	flagellar biosynthetic protein	Cellular processes
XAC1937	flhB	NS	NS	NS	NS	1.32	NS	flagellar biosynthesis protein FlhB	Cellular processes
XAC1908	motB	NS	NS	NS	NS	1.54	NS	flagellar motor protein MotD	Cellular processes
XAC1955	fliE	NS	NS	NS	NS	1.94	1.78	flagellar protein	Cellular processes
XAC1986	flgB	NS	NS	NS	NS	2.03	NS	flagellar basal body rod protein FlgB	Cellular processes
XAC1942	fliQ	NS	NS	NS	NS	2.07	NS	flagellar biosynthesis	Cellular processes
XAC1948	fliL	NS	NS	NS	NS	2.16	1.81	flagellar protein	Cellular processes
XAC0719	betB	NS	NS	NS	NS	NS	-1.21	betaine aldehyde dehydrogenase	Cellular processes
XAC3990	srpA	NS	NS	NS	NS	NS	-1.15	catalase	Cellular processes
XAC0718	betA	NS	NS	NS	NS	NS	-1.02	choline dehydrogenase	Cellular processes
XAC0851	slfA	NS	NS	NS	NS	NS	1.51	NADH-dependent FMN reductase	Cellular processes
XAC0934	-	-1.67	-1.32	-1.36	NS	NS	NS	truncated xylanase	Central intermediary metabolism

Table 4-3. Continued

Locus tag	Gene Symbol	rpfC/W Ex[a]	rpfF/W Ex[a]	rpfG/W Ex[a]	rpfC/W St[a]	rpfF/W St[a]	rpfG/W St[a]	Description	JCVI[b]
XAC0933	-	-1.42	-1.14	-1.34	NS	NS	NS	truncated xylanase	Central intermediary metabolism
XAC3738	-	-1.28	NS	NS	-1.23	-1.16	-1.23	oxidoreductase	Central intermediary metabolism
XAC4036	piuB	NS	NS	1.77	NS	NS	NS	iron-uptake factor	Central intermediary metabolism
XAC2948	-	NS	NS	2.22	NS	NS	NS	sulfite reductase	Central intermediary metabolism
XAC2895	yagT	NS	NS	NS	NS	NS	-2.12	putative xanthine dehydrogenase iron-sulfur-binding subunit	Central intermediary metabolism
XAC2894	yagS	NS	NS	NS	NS	NS	-2.08	oxidoreductase	Central intermediary metabolism
XAC1180	-	NS	NS	NS	NS	NS	-1.68	short chain dehydrogenase	Central intermediary metabolism
XAC2893	yagR	NS	NS	NS	NS	NS	-1.62	oxidoreductase	Central intermediary metabolism
XAC1188	-	NS	NS	NS	NS	NS	-1.49	hydroxylase molybdopterin-containing subunit	Central intermediary metabolism
XAC2138	-	NS	NS	NS	NS	NS	-1.34	L-sorbosone dehydrogenase	Central intermediary metabolism
XAC2051	-	NS	NS	NS	NS	NS	-1.29	oxidoreductase	Central intermediary metabolism
XAC0585	-	NS	NS	NS	NS	NS	-1.23	hypothetical protein	Central intermediary metabolism
XAC2124	-	NS	NS	NS	NS	NS	-1.18	hypothetical protein	Central intermediary metabolism
XAC1189	-	NS	NS	NS	NS	NS	-1.16	ferredoxin	Central intermediary metabolism
XAC1187	-	NS	NS	NS	NS	NS	-1.10	hydroxylase large subunit	Central intermediary metabolism

Table 4-3. Continued

Locus tag	Gene Symbol	rpfC/W Ex[a]	rpfF/W Ex[a]	rpfG/W Ex[a]	rpfC/W St[a]	rpfF/W St[a]	rpfG/W St[a]	Description	JCVI[b]
XAC1890	cheR	-1.46	-1.43	-1.49	NS	NS	NS	chemotaxis protein methyltransferase	DNA metabolism
XAC2869	cheR	-1.27	NS	-1.34	NS	NS	NS	response regulator for chemotaxis	DNA metabolism
XAC4060	czcD	-1.25	NS	NS	NS	NS	NS	heavy metal transporter	DNA metabolism
XAC3915	radC	NS	NS	NS	NS	-1.06	NS	DNA repair protein RadC	DNA metabolism
XAC0035	-	NS	NS	NS	NS	NS	-1.53	hypothetical protein	DNA metabolism
XAC1186	uvrA2	NS	NS	NS	NS	NS	-1.24	excinuclease ABC subunit A	DNA metabolism
XAC2875	nfi	NS	NS	NS	NS	NS	-1.23	endonuclease V	DNA metabolism
XAC0612	engXCA	-4.38	-4.58	-4.29	-2.06	-3.09	-1.89	cellulase	Energy metabolism
XAC1285	lamA	-3.34	-3.31	-2.56	NS	NS	NS	endo-1,3-beta-glucanase	Energy metabolism
XAC0029	egl	-3.19	-3.32	-3.85	-3.96	-4.52	-3.80	cellulase	Energy metabolism
XAC0028	egl	-3.15	-2.51	-2.46	NS	NS	NS	cellulase	Energy metabolism
XAC1927	aslB	-2.35	-2.51	-2.73	-1.67	-2.65	-3.51	Fe-S oxidoreductase	Energy metabolism
XAC3507	celS	-1.68	-2.03	-1.69	NS	NS	NS	truncated cellulase S	Energy metabolism
XAC1975	fliC	-1.58	-1.79	-1.71	NS	NS	NS	flagellin	Energy metabolism
XAC3747	ybdR	-1.49	NS	NS	-1.27	-1.29	-1.85	Zn-dependent alcohol dehydrogenase	Energy metabolism
XAC1287	galM	-1.40	-1.42	NS	NS	NS	NS	aldose 1-epimerase	Energy metabolism
XAC2896	-	-1.40	NS	NS	NS	NS	-1.37	alcohol dehydrogenase	Energy metabolism
XAC3562	pel	-1.35	-1.22	NS	NS	NS	NS	pectate lyase	Energy metabolism
XAC0257	aceA	-1.29	NS	NS	-1.35	NS	NS	isocitrate lyase	Energy metabolism
XAC0445	pdhB	-1.27	NS	-1.21	NS	NS	NS	pyruvate dehydrogenase E1 beta subunit	Energy metabolism
XAC0446	pdhA	-1.26	-1.00	-1.19	NS	NS	NS	pyruvate dehydrogenase E1 alpha subunit	Energy metabolism
XAC0798	amy	-1.17	-1.21	NS	NS	NS	NS	alpha-amylase	Energy metabolism

Table 4-3. Continued

Locus tag	Gene Symbol	rpfC/W Ex[a]	rpfF/W Ex[a]	rpfG/W Ex[a]	rpfC/W St[a]	rpfF/W St[a]	rpfG/W St[a]	Description	JCVI[b]
XAC2028	fdh	-1.11	NS	NS	NS	-1.11	-1.68	glutathione-dependent formaldehyde dehydrogenase	Energy metabolism
XAC4079	ecaA	1.40	NS	1.06	NS	NS	NS	a-type carbonic anhydrase	Energy metabolism
XAC4327	uahA	NS	-2.41	NS	NS	-3.56	NS	allophanate hydrolase	Energy metabolism
XAC2986	pelB	NS	-1.19	NS	NS	NS	NS	pectate lyase II	Energy metabolism
XAC1886	pcaD	NS	NS	-1.98	NS	NS	NS	beta-ketoadipate enol-lactone hydrolase	Energy metabolism
XAC3114	pqqG	NS	NS	-1.13	NS	NS	NS	pyrroloquinoline quinone biosynthesis protein PqqB	Energy metabolism
XAC1460	fumB	NS	NS	-1.06	NS	NS	NS	fumarate hydratase	Energy metabolism
XAC3072	fucA1	NS	NS	1.06	NS	NS	NS	alpha-L-fucosidase	Energy metabolism
XAC2982	qxtB	NS	NS	1.09	NS	NS	NS	quinol oxidase subunit II	Energy metabolism
XAC2983	-	NS	NS	1.16	NS	NS	NS	quinol oxidase subunit I	Energy metabolism
XAC1811	hmsR	NS	NS	1.95	NS	NS	NS	N-glycosyltransferase PgaC	Energy metabolism
XAC1259	cyoB	NS	NS	NS	-1.07	NS	NS	cytochrome O ubiquinol oxidase subunit I	Energy metabolism
XAC4252	xynB	NS	NS	NS	NS	-1.12	NS	xylanase	Energy metabolism
XAC2336	cydA	NS	NS	NS	NS	1.72	1.57	cytochrome D ubiquinol oxidase subunit I	Energy metabolism
XAC3254	glgX	NS	NS	NS	NS	NS	-1.70	glycogen debranching enzyme	Energy metabolism
XAC0154	-	NS	NS	NS	NS	NS	-1.50	alpha-amylase	Energy metabolism
XAC0224	poxB	NS	NS	NS	NS	NS	-1.44	pyruvate dehydrogenase	Energy metabolism
XAC4269	-	NS	NS	NS	NS	NS	-1.29	nuclear receptor binding factor related protein	Energy metabolism
XAC0794	-	NS	NS	NS	NS	NS	-1.27	quinone reductase	Energy metabolism
XAC1476	-	NS	NS	NS	NS	NS	-1.27	hypothetical protein	Energy metabolism
XAC1174	-	NS	NS	NS	NS	NS	-1.24	hypothetical protein	Energy metabolism
XAC1882	rpfA	NS	NS	NS	NS	NS	-1.13	aconitate hydratase	Energy metabolism

Table 4-3. Continued

Locus tag	Gene Symbol	rpfC/W Ex[a]	rpfF/W Ex[a]	rpfG/W Ex[a]	rpfC/W St[a]	rpfF/W St[a]	rpfG/W St[a]	Description	JCVI[b]
XAC3632	gloA	NS	NS	NS	NS	NS	-1.10	lactoylglutathione lyase	Energy metabolism
XAC2907	-	NS	NS	NS	NS	NS	-1.09	hypothetical protein	Energy metabolism
XAC2469	gabD	NS	NS	NS	NS	NS	-1.03	succinate-semialdehyde dehydrogenase	Energy metabolism
XAC2337	cydB	NS	NS	NS	NS	NS	1.10	cytochrome D ubiquinol oxidase subunit II	Energy metabolism
XAC0830	tauD	NS	NS	NS	NS	NS	1.17	taurine dioxygenase	Energy metabolism
XAC0364	gctA	NS	NS	-1.14	NS	NS	NS	glutaconate CoA transferase subunit A	Fatty acid and phospholipid metabolism
XAC3037	-	NS	NS	NS	NS	NS	-1.38	hydrolase	Fatty acid and phospholipid metabolism
XAC2414	lig3	NS	NS	NS	NS	NS	-1.26	ATP-dependent DNA ligase	Fatty acid and phospholipid metabolism
XAC1341	lig2	NS	NS	NS	NS	NS	-1.03	ATP-dependent DNA ligase	Fatty acid and phospholipid metabolism
XAC0846	msuC	NS	NS	NS	NS	NS	1.04	FMNH2-dependent monooxygenase	Fatty acid and phospholipid metabolism
XAC1905	-	-1.59	-1.43	-1.77	NS	NS	NS	hypothetical protein	Hypothetical proteins
XAC3763	-	-1.47	-1.33	-1.45	NS	NS	NS	hypothetical protein	Hypothetical proteins
XAC1209	-	-1.33	NS	NS	NS	NS	NS	hypothetical protein	Hypothetical proteins
XAC0753	-	-1.31	NS	-1.63	NS	NS	NS	hypothetical protein	Hypothetical proteins
XAC1021	-	-1.11	-1.39	-1.59	-1.36	-1.59	-1.57	hypothetical protein	Hypothetical proteins
XAC1219	-	NS	NS	-1.69	NS	NS	NS	hypothetical protein	Hypothetical proteins
XAC0223	-	NS	NS	-1.04	NS	NS	NS	hypothetical protein	Hypothetical proteins
XAC0531	-	NS	NS	-1.03	NS	NS	NS	hypothetical protein	Hypothetical proteins
XAC2007	-	NS	NS	-1.01	NS	NS	NS	hypothetical protein	Hypothetical proteins

Table 4-3. Continued

Locus tag	Gene Symbol	rpfC/W Ex[a]	rpfF/W Ex[a]	rpfG/W Ex[a]	rpfC/W St[a]	rpfF/W St[a]	rpfG/W St[a]	Description	JCVI[b]
XAC1856	-	NS	NS	1.13	NS	NS	NS	hypothetical protein	Hypothetical proteins
XAC2878	-	NS	NS	1.21	NS	NS	NS	hypothetical protein	Hypothetical proteins
XAC2383	-	NS	NS	1.33	NS	NS	NS	phosphate-binding protein	Hypothetical proteins
XAC3619	-	NS	NS	1.91	NS	NS	NS	hypothetical protein	Hypothetical proteins
XAC0269	-	NS	NS	2.45	NS	NS	NS	hypothetical protein	Hypothetical proteins
XAC2944	-	NS	NS	2.59	NS	NS	NS	hypothetical protein	Hypothetical proteins
XAC2943	-	NS	NS	3.11	NS	NS	NS	hypothetical protein	Hypothetical proteins
XAC2945	-	NS	NS	3.42	NS	NS	NS	hypothetical protein	Hypothetical proteins
XAC1208	-	NS	NS	NS	NS	-1.12	NS	hypothetical protein	Hypothetical proteins
XAC3776	-	NS	NS	NS	NS	-1.10	-2.16	hypothetical protein	Hypothetical proteins
XAC2052	-	NS	NS	NS	NS	NS	-1.59	hypothetical protein	Hypothetical proteins
XAC2369	-	NS	NS	NS	NS	NS	-1.45	general stress protein	Hypothetical proteins
XAC2491	-	NS	NS	NS	NS	NS	-1.37	hypothetical protein	Hypothetical proteins
XAC1453	-	NS	NS	NS	NS	NS	-1.36	hypothetical protein	Hypothetical proteins
XAC3981	-	NS	NS	NS	NS	NS	-1.29	hypothetical protein	Hypothetical proteins
XAC3982	-	NS	NS	NS	NS	NS	-1.28	hypothetical protein	Hypothetical proteins
XAC3983	-	NS	NS	NS	NS	NS	-1.26	hypothetical protein	Hypothetical proteins
XAC1342	-	NS	NS	NS	NS	NS	-1.24	mRNA 3'-end processing factor	Hypothetical proteins
XAC2127	-	NS	NS	NS	NS	NS	-1.22	hypothetical protein	Hypothetical proteins
XAC0186	-	NS	NS	NS	NS	NS	-1.21	hypothetical protein	Hypothetical proteins
XAC2892	-	NS	NS	NS	NS	NS	-1.19	hypothetical protein	Hypothetical proteins
XAC0185	-	NS	NS	NS	NS	NS	-1.18	hypothetical protein	Hypothetical proteins
XAC1665	-	NS	NS	NS	NS	NS	-1.00	hypothetical protein	Hypothetical proteins
XAC3402	-	NS	NS	NS	NS	NS	1.12	hypothetical protein	Hypothetical proteins
XAC0829	-	NS	NS	NS	NS	NS	1.24	ABC transporter substrate binding protein	Hypothetical proteins

Table 4-3. Continued

Locus tag	Gene Symbol	rpfC/W Ex[a]	rpfF/W Ex[a]	rpfG/W Ex[a]	rpfC/W St[a]	rpfF/W St[a]	rpfG/W St[a]	Description	JCVI[b]
XAC3725	-	-2.18	NS	NS	-1.97	-1.22	NS	hypothetical protein	Mobile and extrachromosomal element functions
XAC1321	mucD	NS	NS	-1.45	NS	NS	NS	periplasmic protease	Mobile and extrachromosomal element functions
XAC2155	-	NS	NS	NS	NS	NS	-1.75	hypothetical protein	Mobile and extrachromosomal element functions
XAC1926	-	-2.28	-2.43	-2.56	-1.50	-2.55	-3.52	hypothetical protein	Not in JCVI
XAC1452	-	-2.15	-2.11	-2.51	NS	NS	NS	hypothetical protein	Not in JCVI
XAC3727	-	-2.09	NS	NS	-1.27	-1.24	NS	hypothetical protein	Not in JCVI
XAC4026	-	-1.91	-1.74	-2.29	NS	NS	NS	hypothetical protein	Not in JCVI
XAC4030	catB	-1.81	-1.68	-1.86	NS	NS	NS	catalase	Not in JCVI
XAC1034	-	-1.80	-2.06	-1.76	NS	-1.11	NS	peptidyl-Asp metalloendopeptidase	Not in JCVI
XAC1210	-	-1.78	NS	-1.12	-1.26	-1.25	-1.34	hypothetical protein	Not in JCVI
XAC3219	-	-1.56	-1.77	-2.06	-1.71	-2.18	-2.11	hypothetical protein	Not in JCVI
XAC0543	-	-1.51	-1.19	-1.95	-2.50	-2.80	-2.59	hypothetical protein	Not in JCVI
XAC1928	-	-1.49	-1.32	-1.66	NS	-1.49	-1.53	hypothetical protein	Not in JCVI
XAC3506	-	-1.49	-1.47	-1.41	NS	NS	NS	truncated cellulase S	Not in JCVI
XAC4091	-	-1.40	-1.66	-1.56	NS	-1.22	NS	hypothetical protein	Not in JCVI
XAC1990	-	-1.36	NS	-1.65	NS	NS	NS	hypothetical protein	Not in JCVI
XAC3787	-	-1.33	-1.56	-1.53	NS	-1.40	-1.16	hypothetical protein	Not in JCVI
XAC2786	-	-1.32	NS	-1.65	-1.75	-2.14	-1.97	hypothetical protein	Not in JCVI
XAC2268	-	-1.31	-1.23	-1.08	NS	NS	NS	hypothetical protein	Not in JCVI
XAC3533	-	-1.31	-1.63	-2.18	-1.88	-1.74	-2.11	hypothetical protein	Not in JCVI
XAC1634	-	-1.27	-1.08	-1.49	NS	NS	NS	hypothetical protein	Not in JCVI
XAC3018	-	-1.24	-1.17	-1.08	NS	-1.13	NS	hypothetical protein	Not in JCVI
XAC1972	-	-1.22	-1.21	-1.19	NS	NS	NS	hypothetical protein	Not in JCVI

Table 4-3. Continued

Locus tag	Gene Symbol	rpfC/W Ex[a]	rpfF/W Ex[a]	rpfG/W Ex[a]	rpfC/W St[a]	rpfF/W St[a]	rpfG/W St[a]	Description	JCVI[b]
XAC4321	-	-1.20	-1.08	NS	NS	NS	NS	hypothetical protein	Not in JCVI
XAC0817	-	-1.20	-1.23	-1.26	NS	-1.26	NS	hypothetical protein	Not in JCVI
XAC1971	-	-1.15	-1.21	-1.17	NS	NS	NS	hypothetical protein	Not in JCVI
XAC1778	-	-1.15	-1.18	-1.34	NS	-1.06	NS	sensor kinase	Not in JCVI
XAC1898	-	-1.12	NS	-1.36	NS	NS	NS	hypothetical protein	Not in JCVI
XAC3745	-	-1.12	NS	NS	-1.12	-1.08	-1.90	hypothetical protein	Not in JCVI
XAC3966	-	-1.09	NS	NS	-1.09	NS	-1.50	hypothetical protein	Not in JCVI
XAC3746	-	-1.08	NS	NS	-1.07	-1.05	-1.89	hypothetical protein	Not in JCVI
XAC2027	-	-1.06	NS	NS	NS	-1.12	-1.61	hypothetical protein	Not in JCVI
XAC3021	-	-1.05	NS	NS	NS	NS	NS	hypothetical protein	Not in JCVI
XAC1810	-	1.23	NS	2.35	NS	NS	1.07	hypothetical protein	Not in JCVI
XAC3926	-	1.24	NS	1.57	NS	NS	NS	hypothetical protein	Not in JCVI
XAC3523	-	2.06	2.00	2.33	NS	1.88	1.58	hypothetical protein	Not in JCVI
XAC3522	-	2.19	1.97	2.10	1.11	1.77	1.10	hypothetical protein	Not in JCVI
XAC3525	-	2.98	2.65	2.54	2.04	2.47	1.55	hypothetical protein	Not in JCVI
XAC1995	-	NS	-1.07	-1.20	NS	NS	NS	hypothetical protein	Not in JCVI
XAC0015	-	NS	NS	-1.31	NS	NS	NS	hypothetical protein	Not in JCVI
XAC1235	-	NS	NS	-1.26	NS	NS	NS	hypothetical protein	Not in JCVI
XAC1901	-	NS	NS	-1.08	NS	NS	NS	hypothetical protein	Not in JCVI
XAC2787	-	NS	NS	-1.07	NS	-1.60	-1.32	hypothetical protein	Not in JCVI
XACa0001	-	NS	NS	1.09	NS	NS	NS	hypothetical protein	Not in JCVI
XAC2887	-	NS	NS	1.61	NS	1.26	NS	hypothetical protein	Not in JCVI
XAC0272	-	NS	NS	2.43	NS	NS	NS	hypothetical protein	Not in JCVI
XAC0271	-	NS	NS	2.53	NS	NS	NS	hypothetical protein	Not in JCVI
XAC0822	-	NS	NS	3.27	NS	NS	NS	hypothetical protein	Not in JCVI
XAC0824	-	NS	NS	3.68	NS	NS	NS	hypothetical protein	Not in JCVI
XAC0825	-	NS	NS	4.10	NS	NS	NS	hypothetical protein	Not in JCVI

Table 4-3. Continued

Locus tag	Gene Symbol	rpfC/W Ex[a]	rpfF/W Ex[a]	rpfG/W Ex[a]	rpfC/W St[a]	rpfF/W St[a]	rpfG/W St[a]	Description	JCVI[b]
XAC3513	-	NS	NS	NS	-1.36	-1.20	-1.38	hypothetical protein	Not in JCVI
XAC2370	-	NS	NS	NS	NS	-1.42	-1.08	hypothetical protein	Not in JCVI
XACb0011	avrXacE3	NS	NS	NS	NS	-1.21	NS	-	Not in JCVI
XAC2026	-	NS	NS	NS	NS	-1.20	-1.67	hypothetical protein	Not in JCVI
XAC2250	-	NS	NS	NS	NS	-1.19	NS	hypothetical protein	Not in JCVI
XAC3715	-	NS	NS	NS	NS	-1.12	-1.53	hypothetical protein	Not in JCVI
XACb0028	-	NS	NS	NS	NS	-1.08	NS	-	Not in JCVI
XAC3085	-	NS	NS	NS	NS	-1.03	-1.23	hypothetical protein	Not in JCVI
XAC0086	-	NS	NS	NS	NS	1.06	NS	hypothetical protein	Not in JCVI
XAC0239	-	NS	NS	NS	NS	NS	-2.31	hypothetical protein	Not in JCVI
XAC3777	-	NS	NS	NS	NS	NS	-2.29	hypothetical protein	Not in JCVI
XAC1353	-	NS	NS	NS	NS	NS	-2.21	hypothetical protein	Not in JCVI
XAC3685	-	NS	NS	NS	NS	NS	-2.14	hypothetical protein	Not in JCVI
XAC3684	-	NS	NS	NS	NS	NS	-2.03	hypothetical protein	Not in JCVI
XAC0027	-	NS	NS	NS	NS	NS	-1.92	hypothetical protein	Not in JCVI
XAC0587	-	NS	NS	NS	NS	NS	-1.83	hypothetical protein	Not in JCVI
XAC3775	-	NS	NS	NS	NS	NS	-1.71	hypothetical protein	Not in JCVI
XAC3970	-	NS	NS	NS	NS	NS	-1.67	hypothetical protein	Not in JCVI
XAC1554	-	NS	NS	NS	NS	NS	-1.66	hypothetical protein	Not in JCVI
XAC2654	-	NS	NS	NS	NS	NS	-1.66	hypothetical protein	Not in JCVI
XAC1364	-	NS	NS	NS	NS	NS	-1.66	hypothetical protein	Not in JCVI
XAC2126	-	NS	NS	NS	NS	NS	-1.64	hypothetical protein	Not in JCVI
XAC2793	-	NS	NS	NS	NS	NS	-1.59	hypothetical protein	Not in JCVI
XAC2367	-	NS	NS	NS	NS	NS	-1.56	hypothetical protein	Not in JCVI
XAC3866	-	NS	NS	NS	NS	NS	-1.55	hypothetical protein	Not in JCVI
XAC2025	-	NS	NS	NS	NS	NS	-1.54	hypothetical protein	Not in JCVI
XAC3971	-	NS	NS	NS	NS	NS	-1.49	hypothetical protein	Not in JCVI

Table 4-3. Continued

Locus tag	Gene Symbol	rpfC/W Ex[a]	rpfF/W Ex[a]	rpfG/W Ex[a]	rpfC/W St[a]	rpfF/W St[a]	rpfG/W St[a]	Description	JCVI[b]
XAC3128	-	NS	NS	NS	NS	NS	-1.48	hypothetical protein	Not in JCVI
XAC4007	-	NS	NS	NS	NS	NS	-1.46	hypothetical protein	Not in JCVI
XAC2415	-	NS	NS	NS	NS	NS	-1.35	hypothetical protein	Not in JCVI
XAC2559	-	NS	NS	NS	NS	NS	-1.28	hypothetical protein	Not in JCVI
XAC0131	-	NS	NS	NS	NS	NS	-1.28	hypothetical protein	Not in JCVI
XAC3957	-	NS	NS	NS	NS	NS	-1.24	hypothetical protein	Not in JCVI
XAC3748	-	NS	NS	NS	NS	NS	-1.24	hypothetical protein	Not in JCVI
XAC2122	-	NS	NS	NS	NS	NS	-1.16	dehydrogenase	Not in JCVI
XAC3657	-	NS	NS	NS	NS	NS	-1.14	hypothetical protein	Not in JCVI
XAC0665	-	NS	NS	NS	NS	NS	-1.11	hypothetical protein	Not in JCVI
XAC2057	-	NS	NS	NS	NS	NS	-1.10	hypothetical protein	Not in JCVI
XAC0228	-	NS	NS	NS	NS	NS	-1.09	hypothetical protein	Not in JCVI
XAC1193	-	NS	NS	NS	NS	NS	-1.08	hypothetical protein	Not in JCVI
XAC2445	-	NS	NS	NS	NS	NS	-1.08	hypothetical protein	Not in JCVI
XAC3874	-	NS	NS	NS	NS	NS	-1.08	hypothetical protein	Not in JCVI
XAC3682	-	NS	NS	NS	NS	NS	-1.06	hypothetical protein	Not in JCVI
XAC1354	-	NS	NS	NS	NS	NS	-1.02	hypothetical protein	Not in JCVI
XAC0607	-	NS	NS	NS	NS	NS	1.42	hypothetical protein	Not in JCVI
XAC1945	fliO	NS	NS	NS	NS	NS	1.43	flagellar protein	Not in JCVI
XAC2151	yapH	-4.76	-4.60	-4.40	NS	-1.79	-1.08	YapH protein	Protein fate
XAC4182	-	-3.16	-2.88	-2.87	NS	-1.99	NS	cytochrome C biogenesis protein	Protein fate
XAC0465	-	-2.88	-3.00	-2.94	NS	-1.20	NS	metalloproteinase	Protein fate
XAC0540	-	-1.76	-1.90	-1.58	NS	-1.09	NS	ribonuclease	Protein fate
XAC2763	-	-1.75	-2.32	-2.39	NS	NS	NS	extracellular protease	Protein fate
XAC2831	-	-1.46	-1.62	-1.27	NS	NS	NS	extracellular serine protease	Protein fate
XAC2482	rrpX	NS	NS	-1.35	NS	NS	NS	transcriptional regulator	Protein fate

Table 4-3. Continued

Locus tag	Gene Symbol	rpfC/W Ex[a]	rpfF/W Ex[a]	rpfG/W Ex[a]	rpfC/W St[a]	rpfF/W St[a]	rpfG/W St[a]	Description	JCVI[b]
XAC0415	hrcC	NS	NS	-1.12	NS	NS	NS	HrcC protein	Protein fate
XAC0408	hrpB2	NS	NS	-1.08	NS	NS	-1.24	HrpB2 protein	Protein fate
XAC1512	-	NS	NS	-1.05	NS	-1.20	-1.41	serine peptidase	Protein fate
XAC0542	groEL	NS	NS	1.08	NS	NS	NS	chaperonin GroEL	Protein fate
XAC0541	groES	NS	NS	1.12	NS	NS	NS	co-chaperonin GroES	Protein fate
XAC3545	-	NS	NS	1.98	NS	NS	NS	protease	Protein fate
XAC2745	-	NS	NS	NS	-1.18	NS	NS	metallopeptidase	Protein fate
XAC1827	-	NS	NS	NS	1.34	NS	NS	hypothetical protein	Protein fate
XAC2932	pfpI	NS	NS	NS	NS	NS	-1.24	protease	Protein fate
XAC0407	hrpB1	NS	NS	NS	NS	NS	-1.19	HrpB1 protein	Protein fate
XAC0410	hrpB4	NS	NS	NS	NS	NS	-1.18	HrpB4 protein	Protein fate
XAC0286	avrXacE1	NS	NS	NS	NS	NS	-1.17	avirulence protein	Protein fate
XAC0411	hrpB5	NS	NS	NS	NS	NS	-1.17	type III secretion system protein HrpB	Protein fate
XAC3368	-	NS	NS	NS	NS	NS	-1.12	hypothetical protein	Protein fate
XAC0787	-	NS	NS	NS	NS	NS	1.47	peptidase	Protein fate
XAC2992	-	-2.36	-2.54	-2.69	-1.97	-2.58	-2.55	endoproteinase Arg-C	Protein synthesis
XAC0416	hpa1	NS	NS	-1.62	NS	NS	-1.03	Hpa1 protein	Protein synthesis
XAC0365	gctB	NS	NS	-1.18	NS	NS	NS	glutaconate CoA transferase subunit B	Protein synthesis
XAC1633	gcd	NS	NS	NS	NS	NS	-1.17	glucose dehydrogenase	Protein synthesis
XAC4006	trpS	NS	NS	NS	NS	NS	-1.08	tryptophanyl-tRNA synthetase	Protein synthesis
XAC3181	lysA	NS	NS	2.50	NS	NS	NS	diaminopimelate decarboxylase	Purines, pyrimidines, nucleosides, and nucleotides
XAC2868	vieA	-1.68	-1.44	-1.82	NS	NS	NS	response regulator	Regulatory functions
XAC3922	entF	-1.36	-1.15	-1.28	NS	NS	NS	ATP-dependent serine activating enzyme	Regulatory functions

Table 4-3. Continued

Locus tag	Gene Symbol	rpfC/W Ex[a]	rpfF/W Ex[a]	rpfG/W Ex[a]	rpfC/W St[a]	rpfF/W St[a]	rpfG/W St[a]	Description	JCVI[b]
XAC1989	flgM	-1.27	NS	-1.63	NS	NS	NS	flagellar protein	Regulatory functions
XAC3273	-	-1.14	-1.05	-1.35	-1.31	-1.38	-1.16	histidine kinase-response regulator hybrid protein	Regulatory functions
XAC1328	-	-1.09	NS	-1.29	NS	-1.17	-1.18	hypothetical protein	Regulatory functions
XAC1993	-	-1.08	NS	-1.34	NS	NS	NS	hypothetical protein	Regulatory functions
XAC2382	-	1.10	NS	1.34	NS	NS	NS	GGDEF family protein	Regulatory functions
XAC1812	hmsF	1.23	NS	2.53	NS	1.33	1.40	HmsF protein	Regulatory functions
XAC3445	-	NS	NS	3.20	NS	NS	3.01	transcriptional regulator	Regulatory functions
XAC1171	stkXac1	NS	NS	NS	NS	-1.13	NS	serine/threonine kinase	Regulatory functions
XAC1398	-	NS	NS	NS	NS	1.17	NS	hypothetical protein	Regulatory functions
XAC1670	-	NS	NS	NS	NS	NS	-1.51	response regulator	Regulatory functions
XAC1819	tspO	NS	NS	NS	NS	NS	-1.04	tryptophan-rich sensory protein	Regulatory functions
XAC0845	flbD	NS	NS	NS	NS	NS	1.03	transcriptional regulator	Regulatory functions
XAC3769	nucA	-2.37	-2.82	-2.59	NS	NS	NS	endonuclease precursor	Transcription
XAC1933	fliA	-1.95	NS	NS	NS	NS	NS	RNA polymerase sigma factor	Transcription
XAC1969	rpoN	-1.31	-1.21	-1.11	NS	-1.07	-1.11	RNA polymerase sigma-54 factor	Transcription
XAC1320	-	NS	NS	-1.50	NS	NS	NS	regulatory protein	Transcription
XAC1319	algU	NS	NS	-1.27	NS	NS	NS	RNA polymerase sigma factor RpoE	Transcription
XAC0941	-	NS	NS	NS	NS	NS	-1.28	transcriptional regulator	Transcription
XAC3875	rbn	NS	NS	NS	NS	NS	-1.23	ribonuclease BN	Transcription
XAC2864	-	-2.42	-2.16	-2.50	NS	NS	NS	hypothetical protein	Transport and binding proteins
XAC2600	btuB	-1.06	-1.09	NS	NS	NS	NS	TonB-dependent receptor	Transport and binding proteins
XAC2830	fhuA	-1.04	-1.15	NS	NS	NS	NS	TonB-dependent receptor	Transport and binding proteins

Table 4-3. Continued

Locus tag	Gene Symbol	rpfC/W Ex[a]	rpfF/W Ex[a]	rpfG/W Ex[a]	rpfC/W St[a]	rpfF/W St[a]	rpfG/W St[a]	Description	JCVI[b]
XAC1910	cirA	NS	-1.03	NS	NS	NS	NS	TonB-dependent receptor	Transport and binding proteins
XAC1149	-	NS	NS	-2.29	NS	NS	-1.22	bacterioferritin	Transport and binding proteins
XAC3856	-	NS	NS	-1.82	-1.53	-1.49	-1.84	hypothetical protein	Transport and binding proteins
XAC1438	brf	NS	NS	-1.65	NS	NS	NS	bacterioferritin	Transport and binding proteins
XAC3440	hppA	NS	NS	-1.09	NS	NS	NS	membrane-bound proton-translocating pyrophosphatase	Transport and binding proteins
XAC1854	feoA	NS	NS	1.16	NS	NS	NS	ferrous iron transport protein	Transport and binding proteins
XAC2185	fhuA	NS	NS	1.17	NS	NS	NS	ferrichrome-iron receptor	Transport and binding proteins
XAC1855	feoB	NS	NS	1.21	NS	NS	NS	ferrous iron transport protein B	Transport and binding proteins
XAC3071	iroN	NS	NS	1.31	NS	NS	NS	TonB-dependent receptor	Transport and binding proteins
XAC3179	yceE	NS	NS	1.55	NS	NS	NS	transport protein	Transport and binding proteins
XAC0492	-	NS	NS	1.64	NS	NS	NS	bacterioferritin-associated ferredoxin	Transport and binding proteins
XAC3620	pfeA	NS	NS	1.87	NS	NS	NS	outer membrane receptor FepA	Transport and binding proteins
XAC3176	fecA	NS	NS	2.40	NS	NS	NS	citrate-dependent iron transporter	Transport and binding proteins
XAC1435	fhuA	NS	NS	2.90	NS	NS	NS	iron receptor	Transport and binding proteins
XAC3370	fhuE	NS	NS	3.10	NS	NS	NS	outer membrane receptor for ferric iron uptake	Transport and binding proteins
XAC0176	fpvA	NS	NS	3.27	NS	NS	NS	ferripyoverdine receptor	Transport and binding proteins

Table 4-3. Continued

Locus tag	Gene Symbol	rpfC/W Ex[a]	rpfF/W Ex[a]	rpfG/W Ex[a]	rpfC/W St[a]	rpfF/W St[a]	rpfG/W St[a]	Description	JCVI[b]
XAC2941	fhuA	NS	NS	3.50	NS	NS	NS	TonB-dependent receptor	Transport and binding proteins
XAC3498	fhuE	NS	NS	4.09	NS	NS	NS	outer membrane receptor for ferric iron uptake	Transport and binding proteins
XAC0823	phuR	NS	NS	4.33	NS	NS	NS	outer membrane hemin receptor	Transport and binding proteins
XAC3444	btuB	NS	NS	6.41	NS	NS	3.44	TonB-dependent receptor	Transport and binding proteins
XAC3855	-	NS	NS	NS	NS	NS	-1.33	hypothetical protein	Transport and binding proteins
XAC0720	betT	NS	NS	NS	NS	NS	-1.16	high-affinity choline transport	Transport and binding proteins
XAC0756	kdpA	NS	NS	NS	NS	NS	-1.15	potassium-transporting ATPase subunit A	Transport and binding proteins
XAC2797	bapA	NS	NS	NS	NS	NS	-1.07	ABC transporter ATP-binding protein	Transport and binding proteins
XAC0758	kdpC	NS	NS	NS	NS	NS	-1.03	potassium-transporting ATPase subunit C	Transport and binding proteins
XAC3196	ssuB	NS	NS	NS	NS	NS	1.27	ABC transporter ATP-binding subunit	Transport and binding proteins
XAC0848	ssuC	NS	NS	NS	NS	NS	1.29	ABC transporter permease	Transport and binding proteins
XAC3197	ssuC	NS	NS	NS	NS	NS	1.35	ABC transporter permease	Transport and binding proteins
XAC0847	ssuB	NS	NS	NS	NS	NS	1.43	ABC transporter ATP-binding protein	Transport and binding proteins
XAC0828	nrtCD	NS	NS	NS	NS	NS	1.48	ABC transporter ATP-binding component	Transport and binding proteins
XAC0827	nrtB	NS	NS	NS	NS	NS	1.49	permease	Transport and binding proteins
XAC3201	fyuA	NS	NS	NS	NS	NS	1.74	TonB-dependent receptor	Transport and binding proteins
XAC2853	-	-2.98	-2.99	-3.80	-3.40	-4.20	-4.02	cysteine protease	Unclassified
XAC3868	yliI	-2.51	-2.47	-2.31	-1.86	-2.21	-2.05	dehydrogenase	Unclassified

Table 4-3. Continued

Locus tag	Gene Symbol	rpfC/W Ex[a]	rpfF/W Ex[a]	rpfG/W Ex[a]	rpfC/W St[a]	rpfF/W St[a]	rpfG/W St[a]	Description	JCVI[b]
XAC3726	-	-2.40	NS	NS	-2.20	-1.56	-1.03	hypothetical protein	Unclassified
XAC3014	rebB	-1.59	-1.62	-1.27	NS	-1.47	NS	RebB protein	Unclassified
XAC0066	-	-1.56	-1.76	-1.33	-1.27	-1.46	-1.18	microcystin dependent protein	Unclassified
XAC0067	mdpB	-1.46	-1.66	-1.27	-1.45	-1.47	-1.13	microcystin dependent protein	Unclassified
XAC0065	-	-1.39	-1.60	-1.33	NS	NS	NS	microcystin dependent protein	Unclassified
XAC0346	-	-1.31	-2.00	-1.88	-1.84	-2.42	-2.07	degenerated cellulase	Unclassified
XAC3016	rebA	-1.29	-1.36	-1.19	NS	-1.30	NS	RebA protein	Unclassified
XAC0435	virK	-1.28	NS	-1.61	-1.77	-2.14	-2.03	VirK protein	Unclassified
XAC1177	-	-1.25	NS	NS	-1.69	-1.79	-1.83	hypothetical protein	Unclassified
XAC3015	rebB	-1.24	-1.31	-1.27	NS	-1.22	NS	RebB protein	Unclassified
XAC1906	cheW	-1.21	-1.13	-1.40	NS	NS	NS	chemotaxis protein	Unclassified
XAC2832	-	-1.21	-1.44	-1.19	NS	NS	NS	hypothetical protein	Unclassified
XAC3019	-	-1.20	-1.10	NS	NS	NS	NS	hypothetical protein	Unclassified
XAC0444	-	-1.18	NS	NS	NS	NS	NS	hypothetical protein	Unclassified
XAC0330	cmfA	-1.15	-1.22	NS	NS	NS	NS	conditioned medium factor	Unclassified
XAC3017	rebB	-1.08	-1.21	-1.11	NS	-1.08	NS	RebB protein	Unclassified
XAC1879	rpfF	NS	-5.66	NS	NS	-5.56	NS	enoyl-CoA hydratase	Unclassified
XAC4326	uahA	NS	-2.52	NS	NS	-2.94	NS	urea amidolyase	Unclassified
XAC1234	-	NS	NS	-1.48	NS	NS	NS	hypothetical protein	Unclassified
XAC1236	-	NS	NS	-1.46	NS	NS	NS	hypothetical protein	Unclassified
XAC2536	-	NS	NS	-1.20	NS	-1.03	NS	hypothetical protein	Unclassified
XAC4199	-	NS	NS	-1.13	-1.47	-1.46	NS	polyvinylalcohol dehydrogenase	Unclassified
XAC0396	hpaB	NS	NS	-1.13	NS	NS	NS	HpaB protein	Unclassified
XAC0409	hrcJ	NS	NS	-1.08	NS	NS	-1.28	HrcJ protein	Unclassified
XAC3073	-	NS	NS	1.04	NS	NS	NS	hypothetical protein	Unclassified

Table 4-3. Continued

Locus tag	Gene Symbol	rpfC/W Ex[a]	rpfF/W Ex[a]	rpfG/W Ex[a]	rpfC/W St[a]	rpfF/W St[a]	rpfG/W St[a]	Description	JCVI[b]
XAC3175	mphE	NS	NS	1.93	NS	NS	NS	4-hydroxy-2-oxovalerate aldolase	Unclassified
XAC0590	-	NS	NS	1.93	NS	NS	NS	inner membrane protein	Unclassified
XAC2942	-	NS	NS	3.47	NS	NS	NS	putative hydroxylase	Unclassified
XAC3177	-	NS	NS	4.36	NS	NS	NS	hypothetical protein	Unclassified
XAC2788	-	NS	NS	NS	NS	-1.08	NS	hypothetical protein	Unclassified
XAC1266	hrpXct	NS	NS	NS	NS	-1.06	NS	HrpX protein	Unclassified
XAC3170	bioI	NS	NS	NS	NS	-1.05	NS	cytochrome P-450 hydroxylase	Unclassified
XAC4333	-	NS	NS	NS	NS	-1.02	NS	hypothetical protein	Unclassified
XAC0682	-	NS	NS	NS	NS	NS	-1.81	hypothetical protein	Unclassified
XAC0158	-	NS	NS	NS	NS	NS	-1.77	L-fucose dehydrogenase	Unclassified
XAC4008	ecnA	NS	NS	NS	NS	NS	-1.68	entericidin A	Unclassified
XAC0100	-	NS	NS	NS	NS	NS	-1.56	hypothetical protein	Unclassified
XAC3367	-	NS	NS	NS	NS	NS	-1.47	hypothetical protein	Unclassified
XAC0132	-	NS	NS	NS	NS	NS	-1.31	hypothetical protein	Unclassified
XAC2049	-	NS	NS	NS	NS	NS	-1.31	hypothetical protein	Unclassified
XAC0031	yahK	NS	NS	NS	NS	NS	-1.20	alcohol dehydrogenase	Unclassified
XAC0757	kdpB	NS	NS	NS	NS	NS	-1.11	potassium-transporting ATPase subunit B	Unclassified
XAC3514	-	NS	NS	NS	NS	NS	-1.11	serine protease	Unclassified
XAC3956	blc	NS	NS	NS	NS	NS	-1.10	outer membrane lipoprotein Blc	Unclassified
XAC3491	nonF	NS	NS	NS	NS	NS	-1.09	NonF-related protein	Unclassified
XAC1175	-	NS	NS	NS	NS	NS	-1.04	hypothetical protein	Unclassified
XAC4296	-	NS	NS	NS	NS	NS	-1.02	epimerase	Unclassified
XAC3198	ssuA	NS	NS	NS	NS	NS	1.12	alkanesulfonate transporter substrate-binding subunit	Unclassified
XAC0849	ssuA	NS	NS	NS	NS	NS	1.41	sulfonate binding protein	Unclassified

Table 4-3. Continued

Locus tag	Gene Symbol	rpfC/W Ex[a]	rpfF/W Ex[a]	rpfG/W Ex[a]	rpfC/W St[a]	rpfF/W St[a]	rpfG/W St[a]	Description	JCVI[b]
XAC3200	-	NS	NS	NS	NS	NS	1.56	nitrilotriacetate monooxygenase component A	Unclassified
XAC0850	ssuD	NS	NS	NS	NS	NS	1.57	alkanesulfonate monooxygenase	Unclassified
XAC3314	-	-1.84	-1.75	-1.32	NS	NS	NS	hypothetical protein	Unknown function
XAC1934	fleN	-1.70	NS	-1.78	NS	NS	NS	flagellar biosynthesis switch protein	Unknown function
XAC0350	-	-1.01	NS	-1.30	NS	NS	NS	hypothetical protein	Unknown function
XAC1218	yjdB	NS	NS	-1.69	NS	NS	NS	inner membrane protein	Unknown function
XAC1795	-	NS	NS	-1.25	NS	NS	NS	hypothetical protein	Unknown function
XAC0424	-	NS	NS	-1.17	NS	NS	NS	hypothetical protein	Unknown function
XAC2398	-	NS	NS	NS	NS	1.32	NS	hypothetical protein	Unknown function
XAC2483	-	NS	NS	NS	NS	1.42	NS	hypothetical protein	Unknown function
XAC4169	mltA	NS	NS	NS	NS	NS	-2.60	transglycosylase associated protein	Unknown function
XAC1150	-	NS	NS	NS	NS	NS	-1.35	peroxiredoxin	Unknown function
XAC2035	cpo	NS	NS	NS	NS	NS	-1.29	non-heme chloroperoxidase	Unknown function
XAC0422	-	NS	NS	NS	NS	NS	-1.28	ABC transporter substrate binding protein	Unknown function
XAC2446	-	NS	NS	NS	NS	NS	-1.23	hypothetical protein	Unknown function
XAC2165	-	NS	NS	NS	NS	NS	-1.13	hydrolase	Unknown function
XAC0644	-	NS	NS	NS	NS	NS	-1.03	response regulator	Unknown function

[a]. Log_2-fold change was derived from mutant versus wild type. Ex, exponential phase; St, stationary phase. NS = not significantly differentially expressed ($|log_2$-fold change$| < 1$ or false discovery rate > 0.01). [b] J. Craig Venter Institute (JCVI) functional categories.

Table 4-4. Microarray validation by QRT-PCR.

Locus tag	qRT-PCR log_2 fold change	Microarray log_2 fold change
XAC0403	-0.95	-0.79
XAC0407	-1.25	-0.94
XAC0415	-1.74	-1.12
XAC0416	-1.94	-1.62
XAC0798	-1.47	-0.88
XAC1265	-1.26	-0.83
XAC1854	1.37	1.16
XAC1904	-2.58	-1.90
XAC1954	-1.83	-1.74
XAC1989	-2.26	-1.63
XAC2865	-3.15	-1.87
XAC3176	2.74	2.40
XAC3385	0.75	1.06

[a] values represent transcript levels in *rpfG* mutant relative to those in wild type strain at exponential phase . Averages from three biological replicates are presented.

Table 4-5. Genes overlapped in QS and HrpG regulons.

Locus tag	HrpG Ex[a]	HrpG early St[a]	QS Ex[a]	QS St[a]	HrpX regulon[b]	Gene symbol	Description
Transporter and binding protein							
XAC3444	+	NS	-	-	Y	btuB	TonB-dependent receptor
XAC3856	NS	+	+	+	N	-	hypothetical protein
XAC0827	-	NS	NS	-	Y	nrtB	permease
XAC0829	+	NS	NS	-	Y	-	ABC transporter substrate binding protein
T3SS and effectors							
XAC0416	-	+	+	+	Y	hpa1	Hpa1 protein
XAC0410	-	+	NS	+	Y	hrpB4	HrpB4 protein
XAC0408	-	+	+	+	Y	hrpB2	HrpB2 protein
XAC0396	NS	+	+	NS	Y	hpaB	HpaB protein
XAC0415	NS	+	+	NS	Y	hrcC	HrcC protein
XAC0411	NS	+	NS	+	Y	hrpB5	type III secretion system protein HrpB
XAC0409	-	+	+	+	Y	hrcJ	HrcJ protein
XAC0407	-	+	NS	+	Y	hrpB1	HrpB1 protein
XAC0543	-	+	+	+	Y	-	hypothetical protein
XAC2786	-	+	+	+	Y	-	hypothetical protein
XAC1208	NS	+	NS	+	Y	-	hypothetical protein
XAC4333	-	+	NS	+	Y	-	hypothetical protein
XAC3085	NS	+	NS	+	Y	-	hypothetical protein
XAC2922	-	+	NS	+	Y	hrpW	HrpW protein
XAC0286	-	+	NS	+	Y	avrXacE1	avirulence protein
XACb0011	-	+	NS	+	Y	avrXacE3	avirulence protein
XAC0076	NS	+	NS	+	Y	avrBs2	avirulence protein

Table 4-5. Continued

Locus tag	HrpG Ex[a]	HrpG early St[a]	QS Ex[a]	QS St[a]	HrpX regulon[b]	Gene symbol	Description
Chemotaxis and flagellar biosynthesis							
XAC1945	+	NS	NS	-	N	fliO	flagellar protein
XAC1908	+	NS	NS	-	N	motB	flagellar motor protein MotD
XAC2865	NS	-	+	NS	N	cheA	chemotaxis histidine protein kinase
XAC1951	NS	-	+	+	N	fliI	flagellar protein
XAC1904	NS	-	+	NS	N	cheY	chemotaxis response regulator
XAC1954	NS	-	+	NS	N	fliF	flagellar MS-ring protein
XAC1953	NS	-	+	+	N	fliG	flagellar protein
XAC1982	NS	-	+	NS	N	flgF	flagellar basal body rod protein FlgF
XAC1950	-	NS	+	+	N	fliJ	flagellar FliJ protein
XAC1989	NS	-	+	NS	N	flgM	flagellar protein
XAC1906	NS	-	+	NS	N	cheW	chemotaxis protein
T2SS substrates							
XAC0661	-	+	+	+	Y	peh-1	endopolygalacturonase
XAC4252	NS	+	NS	+	Y	xynB	xylanase
XAC2831	NS	+	+	NS	Y	-	extracellular serine protease
XAC2853	-	+	+	+	Y	-	cysteine protease
XAC0817	-	+	+	+	Y	-	hypothetical protein
XAC4327	NS	+	+	+	Y	uahA	allophanate hydrolase
XAC2370	-	+	NS	+	Y	-	hypothetical protein
XAC0435	-	+	+	+	Y	virK	VirK protein
Regulators							
XAC1171	-	+	NS	+	Y	stkXac1	serine/threonine kinase
XAC1320	NS	+	+	NS	N	-	regulatory protein
XAC1266	+	+	NS	+	NA	HrpX protein	

Table 4-5. Continued

Locus tag	HrpG Ex[a]	HrpG early St[a]	QS Ex[a]	QS St[a]	HrpX regulon[b]	Gene symbol	Description
Metabolism and others							
XAC0802	NS	+	NS	+	Y	-	sulfotransferase
XAC2947	NS	-	-	NS	Y	apbE	thiamine biosynthesis lipoprotein ApbE precursor
XAC3114	NS	+	+	NS	N	pqqG	pyrroloquinoline quinone biosynthesis protein PqqB
XAC1633	+	NS	NS	+	N	gcd	glucose dehydrogenase
XAC3170	NS	+	NS	+	Y	bioI	cytochrome P-450 hydroxylase
XAC4326	-	NS	+	+	Y	uahA	urea amidolyase
Hypothetical protein							
XAC2944	NS	-	-	NS	N	-	hypothetical protein
XAC3763	NS	-	+	NS	N	-	hypothetical protein
XAC3523	+	NS	-	-	N	-	hypothetical protein
XAC2787	NS	+	+	+	Y	-	hypothetical protein
XAC0607	NS	+	NS	-	N	-	hypothetical protein
XAC4026	NS	-	+	NS	N	-	hypothetical protein
XAC1971	NS	-	+	NS	N	-	hypothetical protein
XAC1990	NS	-	+	NS	N	-	hypothetical protein
XAC1972	NS	-	+	NS	N	-	hypothetical protein
XAC2654	-	+	NS	+	Y	xacPNP	hypothetical protein
XAC3073	-	NS	-	NS	N	-	hypothetical protein
XAC2483	+	NS	NS	-	N	-	hypothetical protein
XAC3314	-	NS	+	NS	N	-	hypothetical protein

[a]. Differential expression of genes controlled by HrpG or QS. Ex, exponential phase; Early St, early stationary stationary phase; St, stationary phase. NS = not significantly differentially expressed ($|\log_2$-fold change$| < 1$ or false discovery rate > 0.01). +, up-regulation; -, down-regulation. [b] If the gene is in HrpX regulon. Y, yes; N, no; NA, not applicable.

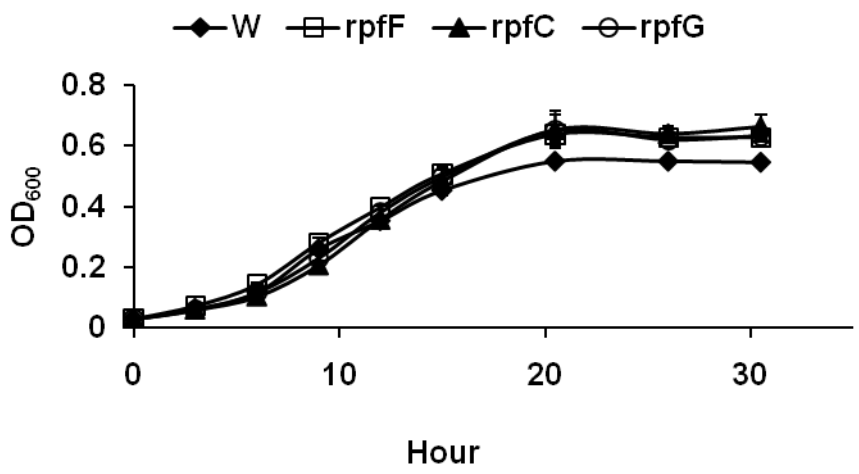

Figure 4-1. Growth curves of the QS mutants and wild type stain in XVM2. The assay was repeated three times independently in triplicate.

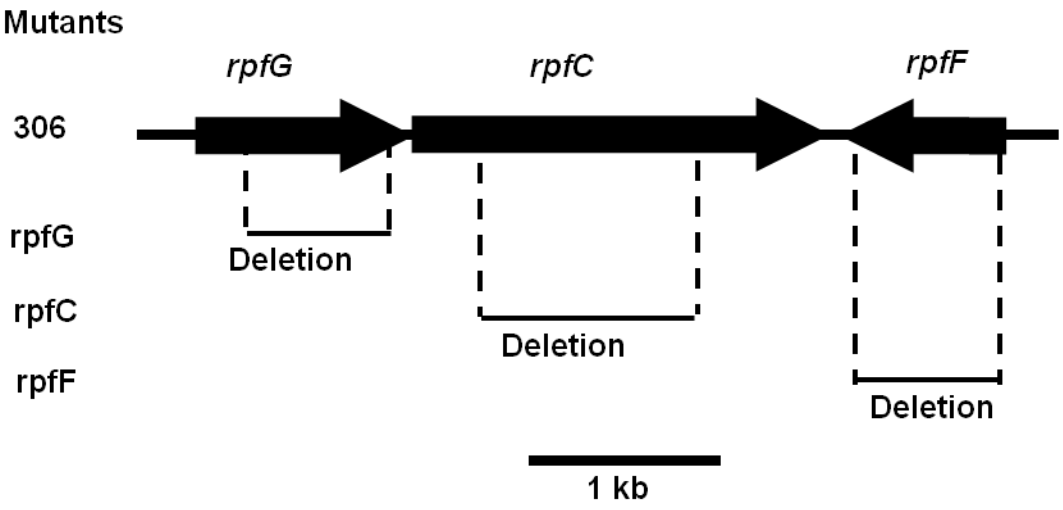

Figure 4-2. Schematic diagram of *rpfF*, *rpfC* and *rpfG* in the genome of XCC strain 306. The arrows represent the locations and orientations of the genes in the genome. The construction of *rpfF*, *rpfC* and *rpfG* deletion mutants is described in Materials and Methods.

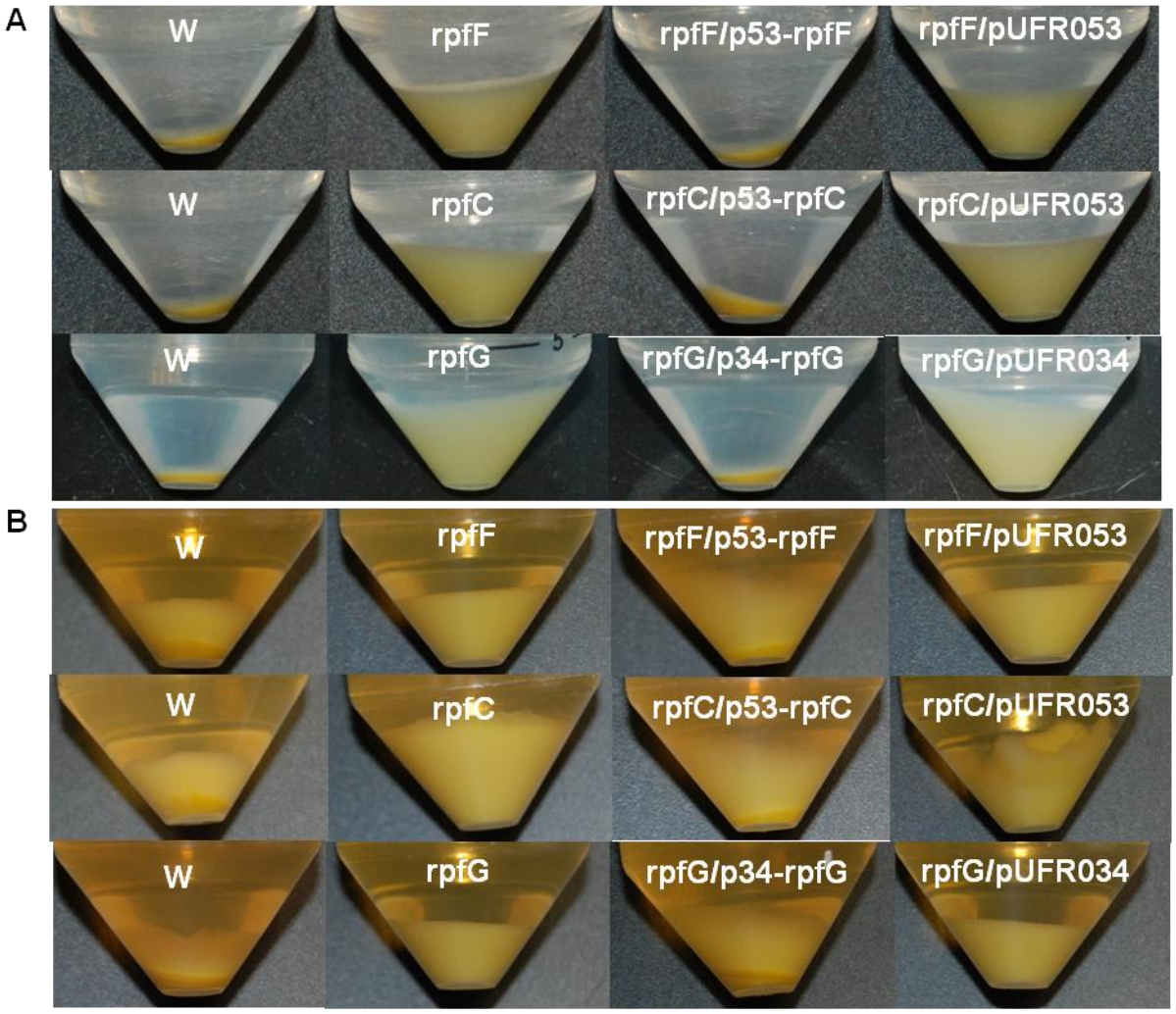

Figure 4-3. Phenotype difference between QS mutants and wild type strain after cultures were centrifuged down at 4,000 × g for 1 h. A) Bacteria were grown in XVM2 for 25 h before centrifuge; B) Bacteria were grown in NB for 25 h before centrifuge.

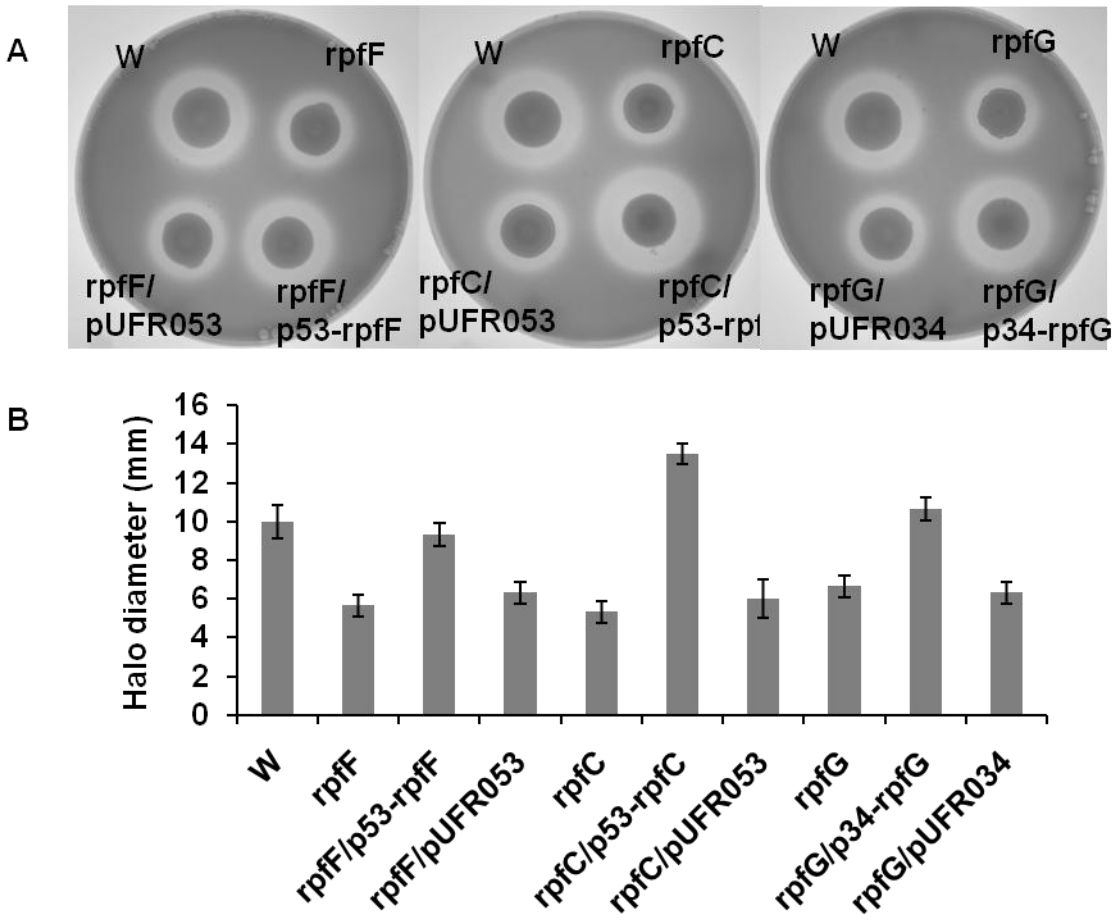

Figure 4-4. Mutants of rpfF, rpfC and rpfG reuced the production of extracellular proteases. A) Protease assay on skim milk plate for 6 DPI; B) Quantitative results of protease production by strain using halo diameter (outer layer of halo zone – colony diameter) as indicator. The assay was repeated three times independently in quadruplicate.

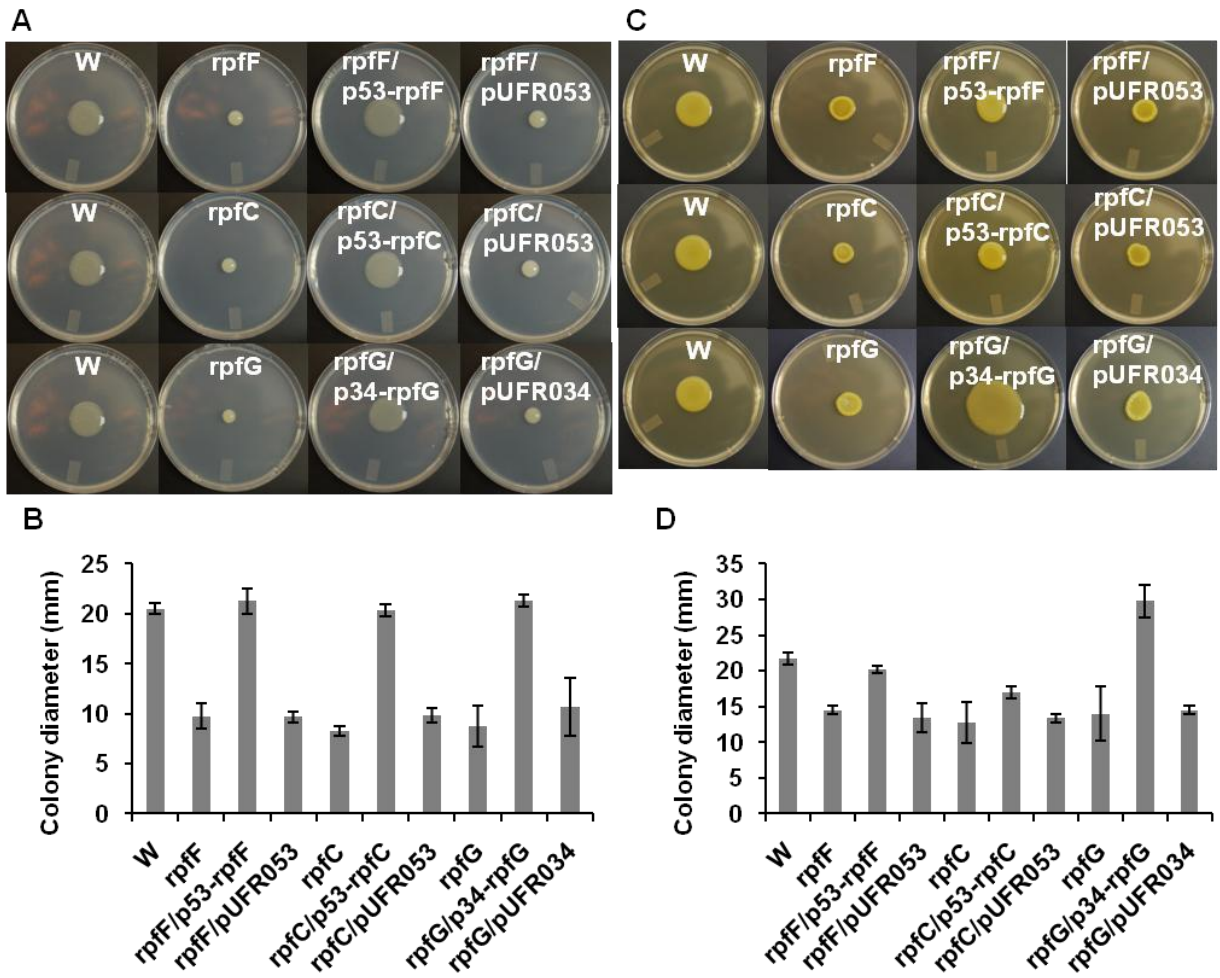

Figure 4-5. Mutants of *rpfF*, *rpfC* and *rpfG* reduced motility compared to wild type strain. A) Motility assay on XVM2 plate with 0.7% agar photographed at 6 DPI; B) Motility assay on NB plate with 0.7% agar photographed at 6 DPI; C) Quantification of motility result on XVM2 plate with 0.7% agar at 6 DPI; D) Quantification of motility result on NB plate with 0.7% agar at 6 DPI; The assay was repeated three times independently in quadruplicate.

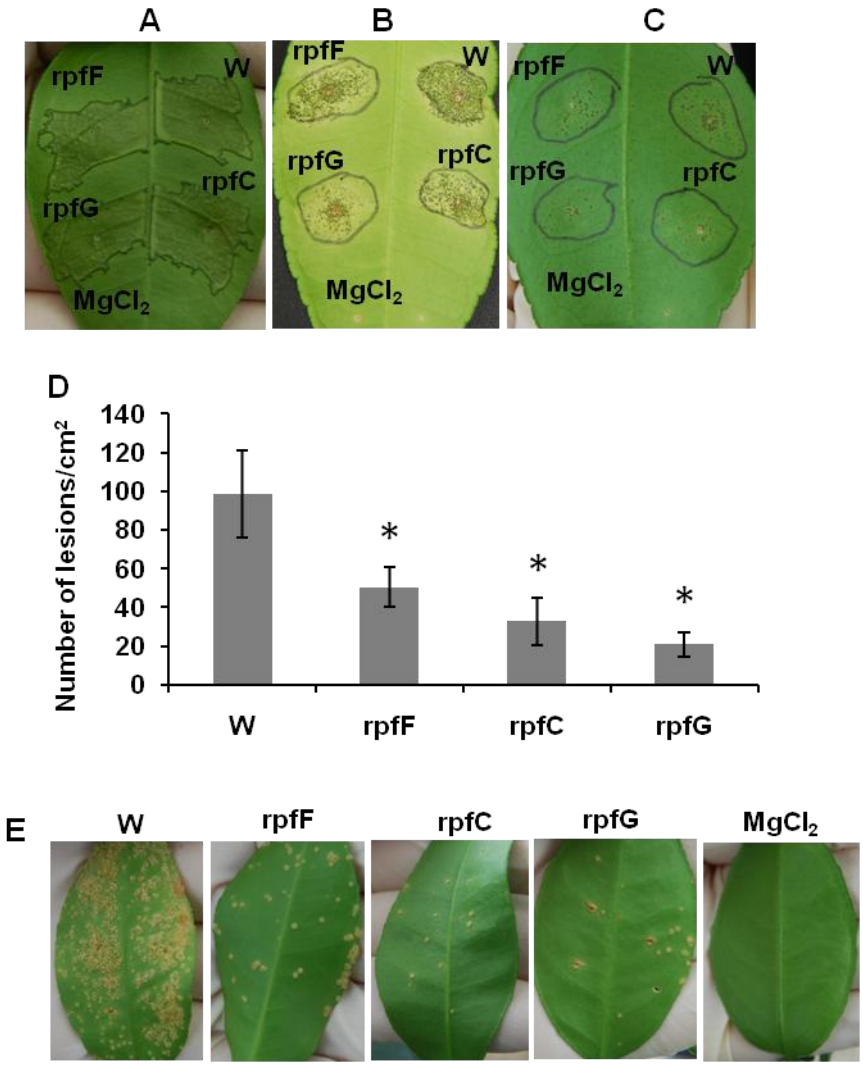

Figure 4-6. The virulence of XCC in planta is impaired by the mutations of *rpfF*, *rpfC* and *rpfG*. A) Duncan grapefruit leaves at 6 DPI with starting concentration of 10^8 CFU/ mL; B) Duncan grapefruit leaves at 18 DPI with starting concentration of 10^5 CFU/ mL; C) Duncan grapefruit leaves at 18 DPI with starting concentration of 10^4 CFU/ mL; D) Quantification of canker lesions in Duncan grapefruit leaves at 18 DPI with starting concentration of 10^4 CFU/ mL. Error bars represent standard deviation. *, statistically significant difference ((P < 0.001, tested by one-way ANOVA) between mutants and wild type strain. Three independent assays were performed with ten leaves each time. E) spray inoculation of XCC strains on abaxial side of Duncan grapefruit leaves. Inoculated leaves were photographed at 20 DPI. The 10 mM $MgCl_2$ solution was used as mocked control.

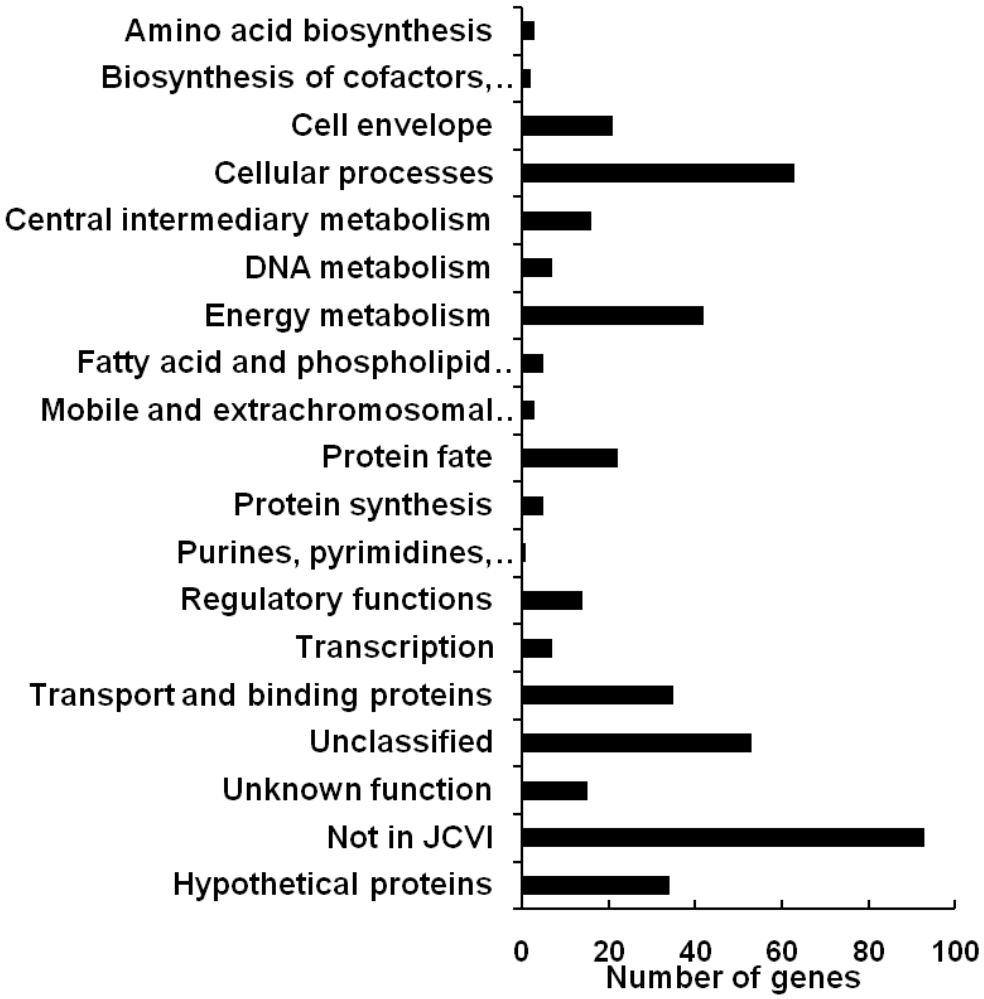

Figure 4-7. Genes in QS regulon distribute into various JCVI functional categories.

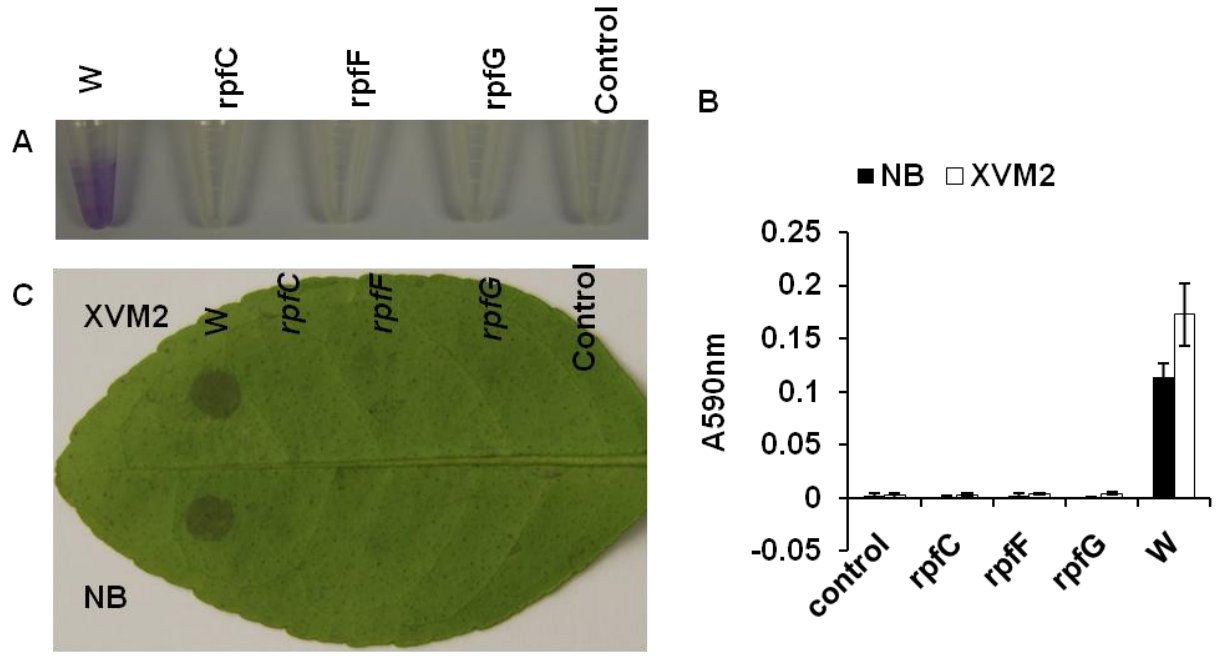

Figure 4-8. Mutants of *rpfF*, *rpfC* and *rpfG* reduced the attachment of XCC on abiotic and biotic surface. A) The attachment to abiotic surface of strains grown in NB or XVM2 media. A representative image of CV stain is shown. B) Quantification of bacterial attachment to abiotic surface. Columns represent the mean of CV stain measured spectrophotometrically (A590 nm) and error bars are standard deviations. The means were calculated using 10 tubes for each strain. The assay was performed three times independently and the representative results from one experiment were shown. C) The attachment to abaxial surface of Duncan grapefruit leaves of strains grown in NB or XVM2 media. The assay was performed three times with six leaves each time and similar results were obtained. Phosphate buffer (pH 7.2) was used as negative control in all assays.

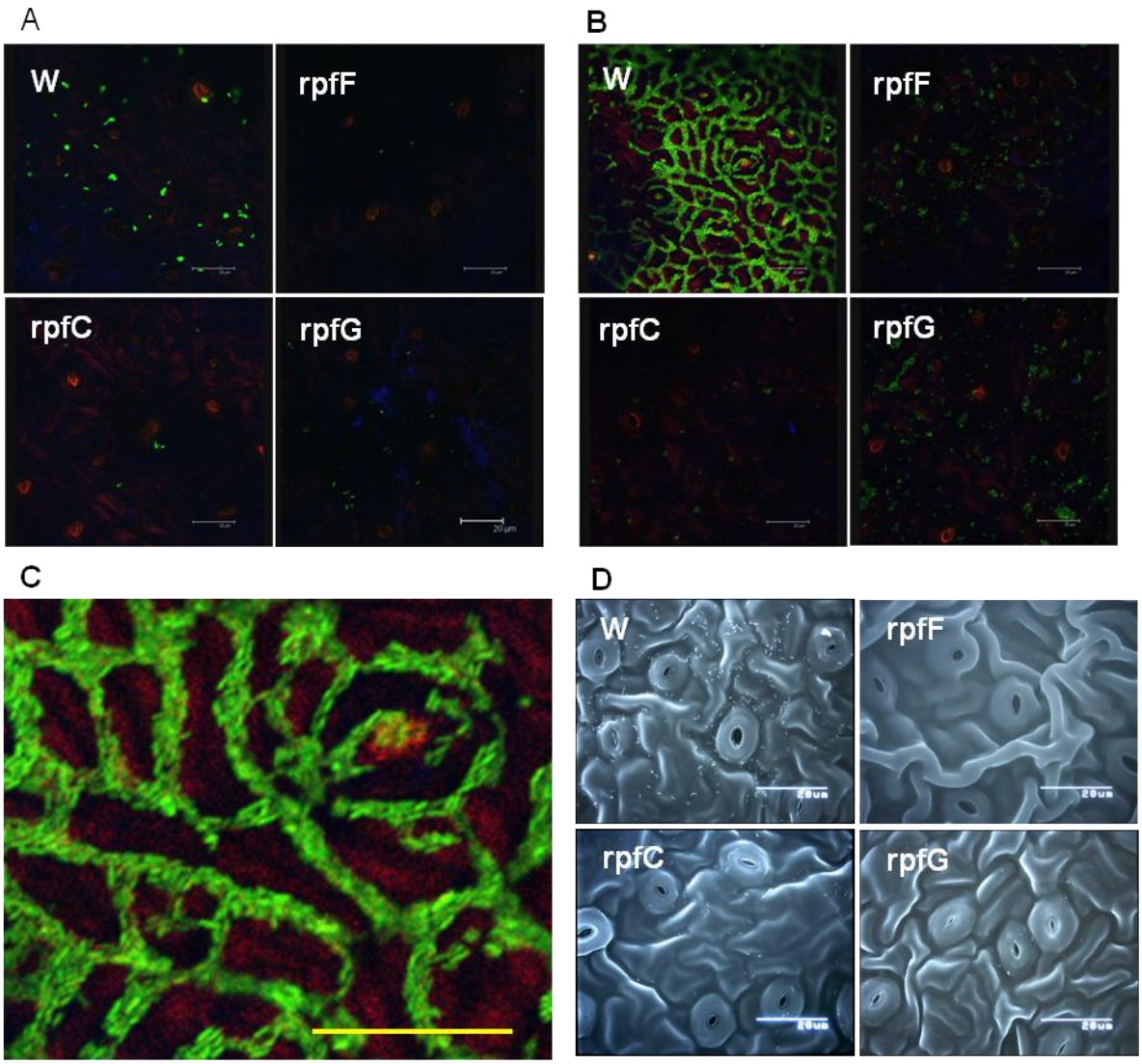

Figure 4-9. Microscopic analysis of bacterial attachment on abaxial surface of Duncan grapefruit leaves. GFP-labeled stains grown in XVM2 were used in confocal laser scanning microscopy analysis (A, B and C). A) The bacterial attachment to leaves at 1 h incubation. B) The bacterial attachment to leaves at 6 h incubation. C) A zoomed-in image of GFP-labeled wild type strain attached to leave at 6 h incubation. D) Scanning electron microscopy analysis of bacterial attachment on leaf surface at 6 h incubation. Three independent experiments were performed for each strain with similar results. Scale bars in all images represent 20 µm.

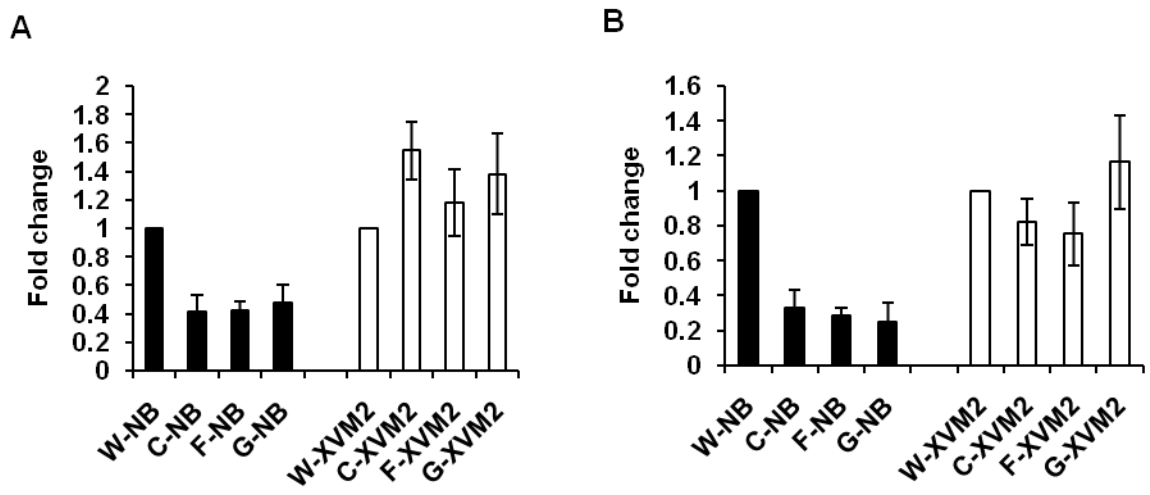

Figure 4-10. QRT-PCR results of the expression of *gumB* and gumD genes of QS mutants relative to wild type strain in NB and XVM2 medium. A) Fold changes of *gumB* genes in QS mutant compared to wild type in NB and XVM2. B) Fold changes of *gumD* genes in QS mutant compared to wild type in NB and XVM2.

CHAPTER 5
SUMMARY AND CONCLUSIONS

The goals of this study are to identify potential virulence traits of XCC and to characterize the underlying regulatory mechanisms coordinating gene expression in XCC during infection. XCC is the causal agent of citrus canker which is one of the most serious diseases of citrus. A large set of genes involved in virulence has been identified in XCC either by molecular or by *in silico* studies, including genes encoding EPS, LPS, CPS, type IV pili, adhesions, flagellum, and type I to VI secretion systems. However, the knowledge regarding the underlying regulatory mechanisms of XCC infection is still fragmentary. A better understanding of virulence and the underlying regulatory mechanism of XCC would assist the development of effective control measures against the citrus canker.

In order to identify potential virulence traits at large scale, we constructed an EZ-Tn5 transposon mutant library of XCC. The two *galU* mutants were first identified from this library for their nonpathogenic phenotype in planta. This present study indicated that the *galU* gene is required for biosynthesis of EPS, CPS, and biofilm formation. Further study showed that the loss of pathogenicity of the *galU* mutant results from its inability to grow in planta rather than from its effect on virulence genes. Co-inoculation of a *galU* mutant with wild type strain did not promote the growth of the *galU* mutant in planta. These data indicate that the *galU* gene contributes to XCC growth in the intercellular spaces and is involved in EPS and CPS synthesis and biofilm formation. Prokaryotic GalUs are completely unrelated to their eukaryotic counterparts and have totally different structures, suggesting that GalU is a potential target of antimicrobial compounds to control citrus canker disease.

To understand the underlying regulatory mechanisms coordinating virulence traits of XCC, we designed and conducted genome-wide microarray analyses to characterize the genes under control of HrpG and HrpX, which are regulators for the induction of T3SS in *Xanthomonas* spp. Our analyses revealed that 232 genes and 181 genes belong to the HrpG and HrpX regulons, respectively, suggesting that both regulators act as global regulators in XCC, directly and indirectly controlling multiple cellular activities responding to the host environment, such as amino acid biosynthesis, oxidative phosphorylation, pentose-phosphate pathway, transport of sugar, iron and potassium, and the phenolic catabolism. Our results suggest that HrpG and HrpX interplay with global signaling network and co-ordinate the expression of multiple virulence factors for modification and adaption of host environment during XCC infection.

To study the regulatory mechanism of QS on virulence and physiology of XCC, the mutants of the core genes of QS including *rpfF*, *rpfC* and *rpfG* genes were constructed. Pathogenicity assays showed that QS is required for the full virulence of XCC in planta. Mutations in *rpfF*, *rpfC* and *rpfG* decreased the production of extracellular proteases and bacterial motility. Comparison of the transcriptomes of QS mutants with that of wild type stain revealed that QS temporally regulates the expression of a large set of genes, including genes involved in chemotaxis and flagellar biosynthesis, genes related to energy metabolism, genes encoding T2SS substrates, T5SS adhesins, type IV pili, T3SS and T3SS effectors. The temporal regulation of QS regulon suggests the important role of QS in different stages of citrus canker infection, including attachment, invasion and growth in host apoplast.

A cross-talk between HrpG and DSF-mediated QS in XCC was observed in our study. Both regulatory systems control the expression of genes encoding T2SS substrates, T3SS structure, T3SS effector proteins, transporters, transcription regulator, genes related to energy metabolism, and genes involved in chemotaxis and flagellar biosynthesis. Due to the similar positive effect of HrpG and QS on the expression of genes encoding T2SS substrates, T3SS structure and effectors, it is speculated that QS assists HrpG to magnify the expression of the critical virulence traits. Moreover, their opposite effect on the expression of genes involved in chemotaxis and flagellar biosynthesis suggests that XCC minimizes PAMP-induced host defense by repressing flagellar biosynthesis and suppresses host defense by inducing T3SS effectors at the same time. We also proposed the possible intermediate junctions shared by two systems: shared regulatory genes such as *hrpX*, and cyclic-di-GMP level which controlled by RpfG and the proteins containing GGDEF and/or EAL domains.

All together, our study demonstrated that the complexity of signaling pathways underlying the regulation of XCC virulence and the interplay between the regulatory cascades. Further study of the identified potential virulence genes and the regulatory genes from the studies of HrpG regulon and QS regulon will give researcher greater insight into the virulence and underlying regulatory mechanisms of XCC, and will assist the development of effective control measures of citrus canker.

LIST OF REFERENCES

Abramoff, M.D., Magelhaes, P.J., and Ram, S.J. 2004. Image processing with ImageJ. Biophotonics Int.11:36-42.

Al-Saadi, A., Reddy, J.D., Duan, Y.P., Brunings, A.M., Yuan, Q., and Gabriel, D.W. 2007. All five host-range variants of *Xanthomonas citri* carry one *pthA* homolog with 17.5 repeats that determines pathogenicity on citrus, but none determine host-range variation. Mol. Plant-Microbe Interact. 20:934-943.

Alexeyev, M.F. 1995. Three kanamycin resistance gene cassettes with different polylinkers. Biotechniques 18:52, 54, 56.

Alfano, J.R., and Collmer, A. 1996. Bacterial pathogens in plants: life up against the wall. Plant Cell 8:1683-1698.

Alfano, J.R., and Collmer, A. 1997. The type III (Hrp) secretion pathway of plant pathogenic bacteria: trafficking harpins, Avr proteins, and death. J. Bacteriol. 179:5655-5662.

Andrade, M.O., Alegria, M.C., Guzzo, C.R., Docena, C., Rosa, M.C., Ramos, C.H., and Farah, C.S. 2006. The HD-GYP domain of RpfG mediates a direct linkage between the Rpf quorum-sensing pathway and a subset of diguanylate cyclase proteins in the phytopathogen *Xanthomonas axonopodis* pv *citri*. Mol. Microbiol. 62:537-551.

Astua-Monge, G., Freitas-Astua, J., Bacocina, G., Roncoletta, J., Carvalho, S.A., and Machado, M.A. 2005. Expression profiling of virulence and pathogenicity genes of *Xanthomonas axonopodis* pv. *citri*. J. Bacteriol. 187:1201-1205.

Backert, S., and Meyer, T.F. 2006. Type IV secretion systems and their effectors in bacterial pathogenesis. Curr. Opin. Microbiol. 9:207-217.

Barber, C.E., Tang, J.L., Feng, J.X., Pan, M.Q., Wilson, T.J., Slater, H., Dow, J.M., Williams, P., and Daniels, M.J. 1997. A novel regulatory system required for pathogenicity of *Xanthomonas campestris* is mediated by a small diffusible signal molecule. Mol. Microbiol. 24:555-566.

Barembruch, C., and Hengge, R. 2007. Cellular levels and activity of the flagellar sigma factor FliA of *Escherichia coli* are controlled by FlgM-modulated proteolysis. Mol. Microbiol. 65:76-89.

Benjamini, Y., and Hochberg, Y. 1995. Controlling the false discovery rate: a practical and powerful approach to multiple testing. J. Royal Stat. Soc. B 57:289-300.

Blanvillain, S., Meyer, D., Boulanger, A., Lautier, M., Guynet, C., Denancé, N., Vasse, J., Lauber, E., and Arlat, M. 2007. Plant carbohydrate scavenging through TonB-dependent receptors: a feature shared by phytopathogenic and aquatic bacteria. PLoS One 2:e224.

Boels, I., Ramos, A., Kleerebezem, M., and de Vos, W. 2001. Functional analysis of the Lactococcus lactis *galU* and *galE* genes and their impact on sugar nucleotide and exopolysaccharide biosynthesis. Appl. Environ. Microbiol. 67:3033-3040.

Boon, C., Deng, Y., Wang, L.H., He, Y., Xu, J.L., Fan, Y., Pan, S.Q., and Zhang, L.H. 2008. A novel DSF-like signal from *Burkholderia cenocepacia* interferes with *Candida albicans* morphological transition. ISME J. 2:27-36.

Boyer, H., and Roulland-Dussoix, D. 1969. A complementation analysis of the restriction and modification of DNA in *Escherichia coli*. J. Mol. Biol. 41:459-472.

Brunings, A.M., and Gabriel, D.W. 2003. *Xanthomonas citri*: breaking the surface. Mol. Plant Pathol. 4:141-157.

Buell, C., Joardar, V., Lindeberg, M., Selengut, J., Paulsen, I., Gwinn, M., Dodson, R., Deboy, R., Durkin, A., Kolonay, J., Madupu, R., Daugherty, S., Brinkac, L., Beanan, M., Haft, D., Nelson, W., Davidsen, T., Zafar, N., Zhou, L., Liu, J., Yuan, Q., Khouri, H., Fedorova, N., Tran, B., Russell, D., Berry, K., Utterback, T., Van Aken, S., Feldblyum, T., D'Ascenzo, M., Deng, W., Ramos, A., Alfano, J., Cartinhour, S., Chatterjee, A., Delaney, T., Lazarowitz, S., Martin, G., Schneider, D., Tang, X., Bender, C., White, O., Fraser, C., and Collmer, A. 2003. The complete genome sequence of the *Arabidopsis* and tomato pathogen *Pseudomonas syringae* pv. *tomato* DC3000. Proc. Natl. Acad. Sci. USA 100:10181-10186.

Bugert, P., and Geider, K. 1995. Molecular analysis of the ams operon required for exopolysaccharide synthesis of *Erwinia amylovora*. Mol. Microbiol. 15:917-933.

Buttner, D., and Bonas, U. 2002. Getting across--bacterial type III effector proteins on their way to the plant cell. EMBO (Eur. Mol. Biol. Organ.) J. 21:5313-5322.

Buttner, D., and Bonas, U. 2010. Regulation and secretion of *Xanthomonas* virulence factors. FEMS (Fed. Eur. Microbiol. Soc.) Microbiol. Rev. 34:107-133.

Calhoun, D.H., Bonner, C.A., Gu, W., Xie, G., and Jensen, R.A. 2001. The emerging periplasm-localized subclass of AroQ chorismate mutases, exemplified by those from *Salmonella typhimurium* and *Pseudomonas aeruginosa*. Genome Biol. 2: research0030.

Cascales, E. 2008. The type VI secretion toolkit. EMBO (Eur. Mol. Biol. Organ.) Rep. 9:735-741.

Chan, J.W., and Goodwin, P.H. 1999. The molecular genetics of virulence of *Xanthomonas campestris*. Biotechnol. Adv. 17:489-508.

Chang, H.Y., Lee, J.H., Deng, W.L., Fu, T.F., and Peng, H.L. 1996. Virulence and outer membrane properties of a *galU* mutant of *Klebsiella pneumoniae* CG43. Microb. Pathog. 20:255-261.

Chatterjee, S., and Sonti, R.V. 2002. *rpfF* mutants of *Xanthomonas oryzae* pv. *oryzae* are deficient for virulence and growth under low iron conditions. Mol. Plant-Microbe Interact. 15:463-471.

Chou, F.L., Chou, H.C., Lin, Y.S., Yang, B.Y., Lin, N.T., Weng, S.F., and Tseng, Y.H. 1997. The *Xanthomonas campestris gumD* gene required for synthesis of xanthan gum is involved in normal pigmentation and virulence in causing black rot. Biochem. Biophys. Res. Commun. 233:265-269.

Christie, P.J., Atmakuri, K., Krishnamoorthy, V., Jakubowski, S., and Cascales, E. 2005. Biogenesis, architecture, and function of bacterial type IV secretion systems. Annu. Rev. Microbiol. 59:451-485.

Cianciotto, N.P. 2005. Type II secretion: a protein secretion system for all seasons. Trends Microbiol. 13:581-588.

Ciesiolka, L.D., Hwin, T., Gearlds, J.D., Minsavage, G.V., Saenz, R., Bravo, M., Handley, V., Conover, S.M., Zhang, H., Caporgno, J., Phengrasamy, N.B., Toms, A.O., Stall, R.E., and Whalen, M.C. 1999. Regulation of expression of avirulence gene avrRxv and identification of a family of host interaction factors by sequence analysis of *avrBsT*. Mol. Plant-Microbe Interact. 12:35-44.

Clowes, R.C., and Hayes, W. 1968. Experiments in microbial genetics. Blackwell Scientific Publications, Oxford.

Cubero, J., and Graham, J.H. 2002. Genetic relationship among worldwide strains of *Xanthomonas* causing canker in citrus species and design of new primers for their identification by PCR. Appl. Environ. Microbiol. 68:1257-1264.

Cunnac, S., Boucher, C., and Genin, S. 2004. Characterization of the *cis*-acting regulatory element controlling HrpB-mediated activation of the type III secretion system and effector genes in Ralstonia solanacearum. J. Bacteriol. 186:2309-2318.

d'Enfert, C., Ryter, A., and Pugsley, A.P. 1987. Cloning and expression in *Escherichia coli* of the *Klebsiella pneumoniae* genes for production, surface localization and secretion of the lipoprotein pullulanase. EMBO (Eur. Mol. Biol. Organ.) J. 6:3531-3538.

da Silva, A.C., Ferro, J.A., Reinach, F.C., Farah, C.S., Furlan, L.R., Quaggio, R.B., Monteiro-Vitorello, C.B., Van Sluys, M.A., Almeida, N.F., Alves, L.M., do Amaral, A.M., Bertolini, M.C., Camargo, L.E., Camarotte, G., Cannavan, F., Cardozo, J., Chambergo, F., Ciapina, L.P., Cicarelli, R.M., Coutinho, L.L., Cursino-Santos, J.R., El-Dorry, H., Faria, J.B., Ferreira, A.J., Ferreira, R.C., Ferro, M.I., Formighieri, E.F., Franco, M.C., Greggio, C.C., Gruber, A., Katsuyama, A.M., Kishi, L.T., Leite, R.P., Lemos, E.G., Lemos, M.V., Locali, E.C., Machado, M.A., Madeira, A.M., Martinez-Rossi, N.M., Martins, E.C., Meidanis, J., Menck, C.F., Miyaki, C.Y., Moon, D.H., Moreira, L.M., Novo, M.T., Okura, V.K., Oliveira, M.C., Oliveira, V.R., Pereira, H.A., Rossi, A., Sena, J.A., Silva, C., de Souza, R.F., Spinola, L.A., Takita, M.A., Tamura, R.E., Teixeira, E.C., Tezza, R.I., Trindade dos Santos, M., Truffi, D., Tsai, S.M., White, F.F., Setubal, J.C., and Kitajima, J.P. 2002. Comparison of the genomes of two *Xanthomonas* pathogens with differing host specificities. Nature 417:459-463.

da Silva, F.G., Shen, Y., Dardick, C., Burdman, S., Yadav, R.C., de Leon, A.L., and Ronald, P.C. 2004. Bacterial genes involved in type I secretion and sulfation are required to elicit the rice Xa21-mediated innate immune response. Mol. Plant-Microbe Interact. 17:593-601.

Daniels, M., Barber, C., Turner, P., Sawczyc, M., Byrde, R., and Fielding, A. 1984. Cloning of genes involved in pathogenicity of *Xanthomonas campestris* pv. *campestris* using the broad host range cosmid pLAFR1. EMBO (Eur. Mol. Biol. Organ.) J. 3:3323-3328.

Das, A., Rangaraj, N., and Sonti, R.V. 2009. Multiple adhesin-like functions of *Xanthomonas oryzae* pv. *oryzae* are involved in promoting leaf attachment, entry, and virulence on rice. Mol. Plant-Microbe Interact. 22:73-85.

de Hoon, M.J., Imoto, S., Nolan, J., and Miyano, S. 2004. Open source clustering software. Bioinformatics 20:1453-1454.

DeFeyter, R., Kado, C.I., and Gabriel, D.W. 1990. Small, stable shuttle vectors for use in *Xanthomonas*. Gene 88:65-72.

Degrassi, G., Devescovi, G., Bigirimana, J., and Venturi, V. 2010. *Xanthomonas oryzae* pv. *oryzae* XKK.12 contains an AroQgamma chorismate mutase that is involved in rice virulence. Phytopathology 100:262-270.

Dekkers, L.C., Bloemendaal, C.J., de Weger, L.A., Wijffelman, C.A., Spaink, H.P., and Lugtenberg, B.J. 1998. A two-component system plays an important role in the root-colonizing ability of Pseudomonas fluorescens strain WCS365. Mol. Plant-Microbe Interact. 11:45-56.

Dharmadi, Y., and Gonzalez, R. 2004. DNA microarrays: experimental issues, data analysis, and application to bacterial systems. Biotechnol. Prog. 20:1309-1324.

Ditta, G., Stanfield, S., Corbin, D., and Helinski, D. 1980. Broad host range DNA cloning system for gram-negative bacteria: construction of a gene bank of *Rhizobium meliloti*. Proc. Natl. Acad. Sci. USA 77:7347-7351.

Dow, J., Fouhy, Y., Lucey, J., and Ryan, R. 2006. The HD-GYP domain, cyclic di-GMP signaling, and bacterial virulence to plants. Mol. Plant-Microbe Interact. 19:1378-1384.

Dow, J.M., Feng, J.X., Barber, C.E., Tang, J.L., and Daniels, M.J. 2000. Novel genes involved in the regulation of pathogenicity factor production within the *rpf* gene cluster of *Xanthomonas campestris.* Microbiology 146 (Pt 4):885-891.

Dunger, G., Relling, V., Tondo, M., Barreras, M., Ielpi, L., Orellano, E., and Ottado, J. 2007. Xanthan is not essential for pathogenicity in citrus canker but contributes to *Xanthomonas* epiphytic survival. Arch. Microbiol. 188:127-135.

El Yacoubi, B., Brunings, A., Yuan, Q., Shankar, S., and Gabriel, D. 2007. In planta horizontal transfer of a major pathogenicity effector gene. Appl. Environ. Microbiol. 73:1612-1621.

Ellermeier, C.D., and Slauch, J.M. 2003. RtsA and RtsB coordinately regulate expression of the invasion and flagellar genes in *Salmonella enterica* serovar Typhimurium. J. Bacteriol. 185:5096-5108.

Feil, H., Feil, W.S., and Lindow, S.E. 2007. Contribution of fimbrial and afimbrial adhesins of *Xylella fastidiosa* to attachment to surfaces and virulence to grape. Phytopathology 97:318-324.

Feng, J., Liu, G., Selvaraj, G., Hughes, G.R., and Wei, Y. 2005. A secreted lipase encoded by LIP1 is necessary for efficient use of saturated triglyceride lipids in *Fusarium graminearum*. Microbiology 151:3911-3921.

Figueiredo, J.F.L., Minsavage, G.V., Graham, J.H., White, F.F., and Jones, J.B. 2011. Mutational analysis of type III effector genes from *Xanthomonas citri* subsp. *citri*. Eur. J. Plant Pathol. doi: 10.1007/s10658-011-9757-7.

Frey, P.A. 1996. The Leloir pathway: a mechanistic imperative for three enzymes to change the stereochemical configuration of a single carbon in galactose. FASEB (Fed. Am. Soc. Exp. Biol.) J. 10:461-470.

Furutani, A., Takaoka, M., Sanada, H., Noguchi, Y., Oku, T., Tsuno, K., Ochiai, H., and Tsuge, S. 2009. Identification of novel type III secretion effectors in *Xanthomonas oryzae* pv. *oryzae*. Mol. Plant-Microbe Interact. 22:96-106.

Furutani, A., Tsuge, S., Ohnishi, K., Hikichi, Y., Oku, T., Tsuno, K., Inoue, Y., Ochiai, H., Kaku, H., and Kubo, Y. 2004. Evidence for HrpXo-dependent expression of type II secretory proteins in *Xanthomonas oryzae* pv. *oryzae*. J. Bacteriol. 186:1374-1380.

Genevaux, P., Bauda, P., DuBow, M., and Oudega, B. 1999. Identification of Tn10 insertions in the *rfaG*, *rfaP*, and *galU* genes involved in lipopolysaccharide core biosynthesis that affect *Escherichia coli* adhesion. Arch. Microbiol. 172:1-8.

Gentleman, R.C., Carey, V.J., Bates, D.M., Bolstad, B., Dettling, M., Dudoit, S., Ellis, B., Gautier, L., Ge, Y., Gentry, J., Hornik, K., Hothorn, T., Huber, W., Iacus, S., Irizarry, R., Leisch, F., Li, C., Maechler, M., Rossini, A.J., Sawitzki, G., Smith, C., Smyth, G., Tierney, L., Yang, J.Y., and Zhang, J. 2004. Bioconductor: open software development for computational biology and bioinformatics. Genome Biol. 5:R80.

Gerlach, R.G., and Hensel, M. 2007. Protein secretion systems and adhesins: the molecular armory of Gram-negative pathogens. Int. J. Med. Microbiol. 297:401-415.

Gottig, N., Garavaglia, B.S., Daurelio, L.D., Valentine, A., Gehring, C., Orellano, E.G., and Ottado, J. 2009a. Modulating host homeostasis as a strategy in the plant-pathogen arms race. Commun. Integr. Biol. 2:89-90.

Gottig, N., Garavaglia, B., Daurelio, L., Valentine, A., Gehring, C., Orellano, E., and Ottado, J. 2008. *Xanthomonas axonopodis* pv. *citri* uses a plant natriuretic peptide-like protein to modify host homeostasis. Proc. Natl. Acad. Sci. USA 105:18631-18636.

Gottig, N., Garavaglia, B.S., Garofalo, C.G., Orellano, E.G., and Ottado, J. 2009b. A filamentous hemagglutinin-like protein of *Xanthomonas axonopodis* pv. *citri*, the phytopathogen responsible for citrus canker, is involved in bacterial virulence. PLoS One 4:e4358.

Gottwald, T.R., and Irey, M.S. 2007. Post-hurricane analysis of citrus canker II: predictive model estimation of disease spread and area potentially impacted by various eradication protocols following catastrophic weather events. Plant Health Progress doi:10.1094/PHP-2007-0405-01-RS

Gottwald, T.R., Graham, J.H., and Schubert, T.S. 2002. Citrus canker: The pathogen and its impact. Plant Health Progress doi:10.1094/PHP-2002-0812-1001-RV.

Graham, J.H., Gottwald, T.R., Cubero, J., and Achor, D.S. 2004. X*anthomonas axonopodis* pv. *citri*: factors affecting successful eradication of citrus canker. Mol. Plant Pathol. 5:1-15.

Grant, S., Fisher, E., Chang, J., Mole, B., and Dangl, J. 2006. Subterfuge and manipulation: type III effector proteins of phytopathogenic bacteria. Annu. Rev. Microbiol. 60:425-449.

Gudesblat, G.E., Torres, P.S., and Vojnov, A.A. 2009. Xanthomonas campestris overcomes Arabidopsis stomatal innate immunity through a DSF cell-to-cell signal-regulated virulence factor. Plant Physiol. 149:1017-1027.

Guidot, A., Prior, P., Schoenfeld, J., CarrÃ¨re, S., Genin, S., and Boucher, C. 2007. Genomic structure and phylogeny of the plant pathogen *Ralstonia solanacearum* inferred from gene distribution analysis. J. Bacteriol. 189:377-387.

Guo, Y., Figueiredo, F., Jones, J., and Wang, N. 2011. HrpG and HrpX Play Global Roles in Coordinating Different Virulence Traits of *Xanthomonas axonopodis* pv. *citri*. Mol. Plant-Microbe Interact. 24:649-661.

Gürlebeck, D., Thieme, F., and Bonas, U. 2006. Type III effector proteins from the plant pathogen *Xanthomona*s and their role in the interaction with the host plant. J. Plant Physiol. 163:233-255.

Hahn, H.P. 1997. The type-4 pilus is the major virulence-associated adhesin of *Pseudomonas aeruginosa*--a review. Gene 192:99-108.

Hajri, A., Brin, C., Hunault, G., Lardeux, F., Lemaire, C., Manceau, C., Boureau, T., and Poussier, S. 2009. A "repertoire for repertoire" hypothesis: repertoires of type three effectors are candidate determinants of host specificity in *Xanthomonas*. PLoS One 4:e6632.

Hanahan, D. 1983. Studies on transformation of *Escherichia coli* with plasmids. J. Mol. Biol. 166:557-580.

He, Y.W., Boon, C., Zhou, L., and Zhang, L.H. 2009. Co-regulation of *Xanthomonas campestris* virulence by quorum sensing and a novel two-component regulatory system RavS/RavR. Mol. Microbiol. 71:1464-1476.

He, Y., Ng, A., Xu, M., Lin, K., Wang, L., Dong, Y., and Zhang, L. 2007. *Xanthomonas campestris* cell-cell communication involves a putative nucleotide receptor protein Clp and a hierarchical signalling network. Mol. Microbiol. 64:281-292.

He, Y., Xu, M., Lin, K., Ng, Y., Wen, C., Wang, L., Liu, Z., Zhang, H., Dong, Y., Dow, J., and Zhang, L. 2006. Genome scale analysis of diffusible signal factor regulon in *Xanthomonas campestris* pv. *campestris*: identification of novel cell-cell communication-dependent genes and functions. Mol. Microbiol. 59:610-622.

Hefti, M.H., Françoijs, K.J., de Vries, S.C., Dixon, R., and Vervoort, J. 2004. The PAS fold. A redefinition of the PAS domain based upon structural prediction. Eur. J. Biochem. 271:1198-1208.

Hirano, S.S., and Upper, C.D. 2000. Bacteria in the leaf ecosystem with emphasis on *Pseudomonas syringae*-a pathogen, ice nucleus, and epiphyte. Microbiol. Mol. Biol. Rev. 64:624-653.

Ho, T.D., and Waldor, M.K. 2007. Enterohemorrhagic *Escherichia coli* O157:H7 *gal* mutants are sensitive to bacteriophage P1 and defective in intestinal colonization. Infect. Immun. 75:1661-1666.

Hossain, S., Tanizawa, K., Kazuta, Y., and Fukui, T. 1994. Overproduction and characterization of recombinant UDP-glucose pyrophosphorylase from *Escherichia coli* K-12. J. Biochem. 115:965-972.

Huang, D.L., Tang, D.J., Liao, Q., Li, X.Q., He, Y.Q., Feng, J.X., Jiang, B.L., Lu, G.T., and Tang, J.L. 2009. The Zur of *Xanthomonas campestris* is involved in hypersensitive response and positively regulates the expression of the *hrp* cluster via *hrpX* but not *hrpG*. Mol. Plant-Microbe Interact. 22:321-329.

Hueck, C.J. 1998. Type III protein secretion systems in bacterial pathogens of animals and plants. Microbiol. Mol. Biol. Rev. 62:379-433.

Huguet, E., Hahn, K., Wengelnik, K., and Bonas, U. 1998. *hpaA* mutants of *Xanthomonas campestris* pv. *vesicatoria* are affected in pathogenicity but retain the ability to induce host-specific hypersensitive reaction. Mol. Microbiol. 29:1379-1390.

Jacobs, M., Alwood, A., Thaipisuttikul, I., Spencer, D., Haugen, E., Ernst, S., Will, O., Kaul, R., Raymond, C., Levy, R., Chun-Rong, L., Guenthner, D., Bovee, D., Olson, M., and Manoil, C. 2003. Comprehensive transposon mutant library of *Pseudomonas aeruginosa*. Proc. Natl. Acad. Sci. USA 100:14339-14344.

Jansson, P., Kenne, L., and Lindberg, B. 1975. Structure of extracellular polysaccharide from *Xanthomonas campestris*. Carbohydr. Res. 45:275-282.

Joosten, M.H.A.J., Hendrickx, L.J.M., and De Wit, P.J.G.M. 1990. Carbohydrate composition of apoplastic fluids isolated from tomato leaves inoculated with virulent or avirulent races of *Cladosporium fulvum* (syn. *Fulvia fulva*). Neth. J. Pl. Path. 96:103-112.

Josenhans, C., and Suerbaum, S. 2002. The role of motility as a virulence factor in bacteria. Int. J. Med. Microbiol. 291:605-614.

Kay, S., Hahn, S., Marois, E., Hause, G., and Bonas, U. 2007. A bacterial effector acts as a plant transcription factor and induces a cell size regulator. Science 318:648-651.

Kearney, B., and Staskawicz, B.J. 1990. Widespread distribution and fitness contribution of *Xanthomonas campestris* avirulence gene *avrBs2*. Nature 346:385-386.

Kim, J.G., Li, X., Roden, J.A., Taylor, K.W., Aakre, C.D., Su, B., Lalonde, S., Kirik, A., Chen, Y., Baranage, G., McLane, H., Martin, G.B., and Mudgett, M.B. 2009a. *Xanthomonas* T3S Effector XopN Suppresses PAMP-Triggered Immunity and Interacts with a Tomato Atypical Receptor-Like Kinase and TFT1. Plant Cell 21:1305-1323.

Kim, S.Y., Kim, J.G., Lee, B.M., and Cho, J.Y. 2009b. Mutational analysis of the *gum* gene cluster required for xanthan biosynthesis in *Xanthomonas oryzae* pv *oryzae*. Biotechnol. Lett. 31:265-270.

Koczan, J.M., McGrath, M.J., Zhao, Y., and Sundin, G.W. 2009. Contribution of *Erwinia amylovora* exopolysaccharides amylovoran and levan to biofilm formation: implications in pathogenicity. Phytopathology 99:1237-1244.

Koebnik, R., Kruger, A., Thieme, F., Urban, A., and Bonas, U. 2006. Specific binding of the *Xanthomonas campestris* pv. *vesicatoria* AraC-type transcriptional activator HrpX to plant-inducible promoter boxes. J. Bacteriol. 188:7652-7660.

Komeda, Y., Icho, T., and Iino, T. 1977. Effects of *galU* mutation on flagellar formation in *Escherichia coli*. J. Bacteriol. 129:908-915.

Lai, Y., Peng, H., and Chang, H. 2001. Identification of genes induced in vivo during *Klebsiella pneumoniae* CG43 infection. Infect. Immun. 69:7140-7145.

Laia, M., Moreira, L., Dezajacomo, J., Brigati, J., Ferreira, C., Ferro, M., Silva, A., Ferro, J., and Oliveira, J. 2009. New genes of *Xanthomonas citri* subsp. *citri* involved in pathogenesis and adaptation revealed by a transposon-based mutant library. BMC Microbiol. 9:12.

Lee, B.M., Park, Y.J., Park, D.S., Kang, H.W., Kim, J.G., Song, E.S., Park, I.C., Yoon, U.H., Hahn, J.H., Koo, B.S., Lee, G.B., Kim, H., Park, H.S., Yoon, K.O., Kim, J.H., Jung, C.H., Koh, N.H., Seo, J.S., and Go, S.J. 2005. The genome sequence of *Xanthomonas oryzae* pathovar *oryzae* KACC10331, the bacterial blight pathogen of rice. Nucleic Acids Res. 33:577-586.

Lee, I., Kim, K., Hyun, J., Lee, Y., and Park, E. 2009. Comparative ultrastructure of nonwounded Mexican lime and Yuzu leaves infected with the citrus canker bacterium *Xanthomonas citri* pv. *citri*. Microsc. Res. Tech. 72:507-516.

Leyns, F., De Cleene, M., Swings, J.G., and De Ley, J. 1984. The host range of the genus *Xanthomonas*. The Botanical Review 50:308-356.

Li, J., and Wang, N. 2011. The *wxacO* gene of *Xanthomonas citri* ssp. *citri* encodes a protein with a role in lipopolysaccharide biosynthesis, biofilm formation, stress tolerance and virulence. Mol. Plant-Pathol. 12:381-396.

Liberati, N., Urbach, J., Miyata, S., Lee, D., Drenkard, E., Wu, G., Villanueva, J., Wei, T., and Ausubel, F. 2006. An ordered, nonredundant library of *Pseudomonas aeruginosa strain* PA14 transposon insertion mutants. Proc. Natl. Acad. Sci. USA 103:2833-2838.

Lindgren, P.B., Peet, R.C., and Panopoulos, N.J. 1986. Gene cluster of *Pseudomonas syringae* pv. "*phaseolicola*" controls pathogenicity of bean plants and hypersensitivity of nonhost plants. J. Bacteriol. 168:512-522.

Livak, K.J., and Schmittgen, T.D. 2001. Analysis of relative gene expression data using real-time quantitative PCR and the $2^{-\Delta\Delta C_T}$ Method. Methods 25:402-408.

Lu, H., Patil, P., Van Sluys, M.A., White, F.F., Ryan, R.P., Dow, J.M., Rabinowicz, P., Salzberg, S.L., Leach, J.E., Sonti, R., Brendel, V., and Bogdanove, A.J. 2008. Acquisition and evolution of plant pathogenesis-associated gene clusters and candidate determinants of tissue-specificity in *Xanthomonas*. PLoS One 3:e3828.

Malamud, F., Torres, P.S., Roeschlin, R., Rigano, L.A., Enrique, R., Bonomi, H.R., Castagnaro, A.P., Marano, M.R., and Vojnov, A.A. 2011. The *Xanthomonas axonopodis* pv. *citri* flagellum is required for mature biofilm and canker development. Microbiology 157:819-829.

Manning, G., Plowman, G.D., Hunter, T., and Sudarsanam, S. 2002. Evolution of protein kinase signaling from yeast to man. Trends Biochem. Sci. 27:514-520.

Metz, M., Dahlbeck, D., Morales, C.Q., Al Sady, B., Clark, E.T., and Staskawicz, B.J. 2005. The conserved *Xanthomonas campestris* pv. *vesicatoria* effector protein XopX is a virulence factor and suppresses host defense in *Nicotiana benthamiana*. Plant J. 41:801-814.

Miller, M.B., and Bassler, B.L. 2001. Quorum sensing in bacteria. Annu. Rev. Microbiol. 55:165-199.

Mollerach, M., and García, E. 2000. The *galU* gene of *Streptococcus pneumoniae* that codes for a UDP-glucose pyrophosphorylase is highly polymorphic and suitable for molecular typing and phylogenetic studies. Gene 260:77-86.

Mollerach, M., Lopez, R., and Garcia, E. 1998. Characterization of the *galU* gene of *Streptococcus pneumoniae* encoding a uridine diphosphoglucose pyrophosphorylase: a gene essential for capsular polysaccharide biosynthesis. J. Exp. Med. 188:2047-2056.

Monier, J.M., and Lindow, S.E. 2003. Differential survival of solitary and aggregated bacterial cells promotes aggregate formation on leaf surfaces. Proc. Natl. Acad. Sci. USA 100:15977-15982.

Moreira, L., Almeida, N.J., Potnis, N., Digiampietri, L., Adi, S., Bortolossi, J., da Silva, A., da Silva, A., de Moraes, F., de Oliveira, J., de Souza, R., Facincani, A., Ferraz, A., Ferro, M., Furlan, L., Gimenez, D., Jones, J., Kitajima, E., Laia, M., Leite, R.J., Nishiyama, M., Rodrigues Neto, J., Nociti, L., Norman, D., Ostroski, E., Pereira, H.J., Staskawicz, B., Tezza, R., Ferro, J., Vinatzer, B., and Setubal, J. 2010. Novel insights into the genomic basis of citrus canker based on the genome sequences of two strains of *Xanthomonas fuscans* subsp. *aurantifolii*. BMC Genomics 11:238.

Mougous, J.D., Cuff, M.E., Raunser, S., Shen, A., Zhou, M., Gifford, C.A., Goodman, A.L., Joachimiak, G., Ordoñez, C.L., Lory, S., Walz, T., Joachimiak, A., and Mekalanos, J.J. 2006. A virulence locus of *Pseudomonas aeruginos*a encodes a protein secretion apparatus. Science 312:1526-1530.

Muda, M., Rao, N.N., and Torriani, A. 1992. Role of PhoU in phosphate transport and alkaline phosphatase regulation. J. Bacteriol. 174:8057-8064.

Nesper, J., Kapfhammer, D., Klose, K., Merkert, H., and Reidl, J. 2000. Characterization of *Vibrio cholerae* O1 antigen as the bacteriophage K139 receptor and identification of IS1004 insertions aborting O1 antigen biosynthesis. J. Bacteriol. 182:5097-5104.

Nesper, J., Lauriano, C., Klose, K., Kapfhammer, D., Kraiss, A., and Reidl, J. 2001. Characterization of *Vibrio cholerae* O1 El tor *galU* and *galE* mutants: influence on lipopolysaccharide structure, colonization, and biofilm formation. Infect. Immun. 69:435-445.

Neugebauer, H., Herrmann, C., Kammer, W., Schwarz, G., Nordheim, A., and Braun, V. 2005. ExbBD-dependent transport of maltodextrins through the novel MalA protein across the outer membrane of *Caulobacter crescentus*. J. Bacteriol. 187:8300-8311.

Newman, M.A., Dow, J.M., Molinaro, A., and Parrilli, M. 2007. Priming, induction and modulation of plant defence responses by bacterial lipopolysaccharides. J. Endotoxin Res. 13:69-84.

Newman, K.L., Almeida, R.P., Purcell, A.H., and Lindow, S.E. 2004. Cell-cell signaling controls *Xylella fastidiosa* interactions with both insects and plants. Proc. Natl. Acad. Sci. USA 101:1737-1742.

Ninfa, A.J., and Magasanik, B. 1986. Covalent modification of the *glnG* product, NRI, by the *glnL* product, NRII, regulates the transcription of the *glnALG* operon in *Escherichia coli*. Proc. Natl. Acad. Sci. USA 83:5909-5913.

Nixon, B.T., Ronson, C.W., and Ausubel, F.M. 1986. Two-component regulatory systems responsive to environmental stimuli share strongly conserved domains with the nitrogen assimilation regulatory genes *ntrB* and *ntrC*. Proc. Natl. Acad. Sci. USA 83:7850-7854.

Nomura, K., Melotto, M., and He, S. 2005. Suppression of host defense in compatible plant-*Pseudomonas syringae* interactions. Curr. Opin. Plant Biol. 8:361-368.

Noël, L., Thieme, F., Gäbler, J., Büttner, D., and Bonas, U. 2003. XopC and XopJ, two novel type III effector proteins from *Xanthomonas campestris* pv. *vesicatoria*. J. Bacteriol. 185:7092-7102.

Noël, L., Thieme, F., Nennstiel, D., and Bonas, U. 2002. Two novel type III-secreted proteins of *Xanthomonas campestris* pv. *vesicatoria* are encoded within the *hrp* pathogenicity island. J. Bacteriol. 184:1340-1348.

Oh, H.S., Kvitko, B.H., Morello, J.E., and Collmer, A. 2007. *Pseudomonas syringae* lytic transglycosylases coregulated with the type III secretion system contribute to the translocation of effector proteins into plant cells. J. Bacteriol. 189:8277-8289.

Osbourn, A.E. 1996. Preformed antimicrobial compounds and plant defense against fungal attack. Plant Cell 8:1821-1831.

Osbourn, A.E., Clarke, B.R., Stevens, B.J., and Daniels, M.J. 1990. Use of oligonucleotide probes to identify members of two-component regulatory systems in *Xanthomonas campestris* pathovar *campestris*. Mol. Gen. Genet. 222:145-151.

Parke, D. 1996. Characterization of PcaQ, a LysR-type transcriptional activator required for catabolism of phenolic compounds, from *Agrobacterium tumefaciens*. J. Bacteriol. 178:266-272.

Pieretti, I., Royer, M., Barbe, V., Carrere, S., Koebnik, R., Cociancich, S., Couloux, A., Darrasse, A., Gouzy, J., Jacques, M.A., Lauber, E., Manceau, C., Mangenot, S., Poussier, S., Segurens, B., Szurek, B., Verdier, V., Arlat, M., and Rott, P. 2009. The complete genome sequence of *Xanthomonas albilineans* provides new insights into the reductive genome evolution of the xylem-limited *Xanthomonadaceae*. BMC Genomics 10:616.

Poplawsky, A.R., and Chun, W. 1997. *pigB* determines a diffusible factor needed for extracellular polysaccharide slime and xanthomonadin production in Xanthomonas campestris pv. campestris. J. Bacteriol. 179:439-444.

Postle, K., and Kadner, R.J. 2003. Touch and go: tying TonB to transport. Mol. Microbiol. 49:869-882.

Pratt, L., and Kolter, R. 1998. Genetic analysis of *Escherichia coli* biofilm formation: roles of flagella, motility, chemotaxis and type I pili. Mol. Microbiol. 30:285-293.

Priebe, G., Dean, C., Zaidi, T., Meluleni, G., Coleman, F., Coutinho, Y., Noto, M., Urban, T., Pier, G., and Goldberg, J. 2004. The *galU* Gene of *Pseudomonas aeruginosa* is required for corneal infection and efficient systemic spread following pneumonia but not for infection confined to the lung. Infect. Immun. 72:4224-4232.

Pukatzki, S., McAuley, S.B., and Miyata, S.T. 2009. The type VI secretion system: translocation of effectors and effector-domains. Curr. Opin. Microbiol. 12:11-17.

Pukatzki, S., Ma, A.T., Sturtevant, D., Krastins, B., Sarracino, D., Nelson, W.C., Heidelberg, J.F., and Mekalanos, J.J. 2006. Identification of a conserved bacterial protein secretion system in *Vibrio cholerae* using the *Dictyostelium* host model system. Proc. Natl. Acad. Sci. USA 103:1528-1533.

Qian, W., Han, Z.J., and He, C. 2008a. Two-component signal transduction systems of *Xanthomonas* spp.: a lesson from genomics. Mol. Plant-Microbe Interact. 21:151-161.

Qian, W., Han, Z.J., Tao, J., and He, C. 2008b. Genome-scale mutagenesis and phenotypic characterization of two-component signal transduction systems in *Xanthomonas campestris* pv. *campestris* ATCC 33913. Mol. Plant Microbe Interact. 21:1128-1138.

Reimmann, C., Beyeler, M., Latifi, A., Winteler, H., Foglino, M., Lazdunski, A., and Haas, D. 1997. The global activator GacA of *Pseudomonas aeruginosa* PAO positively controls the production of the autoinducer N-butyryl-homoserine lactone and the formation of the virulence factors pyocyanin, cyanide, and lipase. Mol. Microbiol. 24:309-319.

Remenant, B., Coupat-Goutaland, B., Guidot, A., Cellier, G., Wicker, E., Allen, C., Fegan, M., Pruvost, O., Elbaz, M., Calteau, A., Salvignol, G., Mornico, D., Mangenot, S., Barbe, V., Médigue, C., and Prior, P. 2010. Genomes of three tomato pathogens within the *Ralstonia solanacearum* species complex reveal significant evolutionary divergence. BMC Genomics 11:379.

Rico, A., Jones, R., and Preston, G.M. 2009. Adaptation to the plant apoplast by plant pathogenic bacteria. Pages 63-89 in: Plant pathogenic bacteria: Genomic and molecular biology. N. S. Iacobellis, Collmer, A., Hutcheson, S.W., Mansfield, J. W., Morris, C. E., Murillo J., Schaad, N. W., Stead, D.E., Surico, G., and Ullrich, M, eds. Kluwer Academic Caister Academic Press, Dordrecht, The Netherlands.

Rigano, L.A., Siciliano, F., Enrique, R., Sendin, L., Filippone, P., Torres, P.S., Questa, J., Dow, J.M., Castagnaro, A.P., Vojnov, A.A., and Marano, M.R. 2007. Biofilm formation, epiphytic fitness, and canker development in *Xanthomonas axonopodis* pv. *citri*. Mol. Plant-Microbe Interact. 20:1222-1230.

Rioux, S., Galarneau, C., Harel, J., Frey, J., Nicolet, J., Kobisch, M., Dubreuil, J., and Jacques, M. 1999. Isolation and characterization of mini-Tn10 lipopolysaccharide mutants of *Actinobacillus pleuropneumoniae* serotype 1. Can. J. Microbiol. 45:1017-1026.

Roberts, I. 1996. The biochemistry and genetics of capsular polysaccharide production in bacteria. Annu. Rev. Microbiol. 50:285-315.

Roden, J.A., Belt, B., Ross, J.B., Tachibana, T., Vargas, J., and Mudgett, M.B. 2004. A genetic screen to isolate type III effectors translocated into pepper cells during *Xanthomonas* infection. Proc. Natl. Acad. Sci. USA 101:16624-16629.

Roine, E., Wei, W., Yuan, J., Nurmiaho-Lassila, E.L., Kalkkinen, N., Romantschuk, M., and He, S.Y. 1997. Hrp pilus: an hrp-dependent bacterial surface appendage produced by *Pseudomonas syringae* pv. *tomato* DC3000. Proc. Natl. Acad. Sci. USA 94:3459-3464.

Rojas, C.M., Ham, J.H., Deng, W.L., Doyle, J.J., and Collmer, A. 2002. HecA, a member of a class of adhesins produced by diverse pathogenic bacteria, contributes to the attachment, aggregation, epidermal cell killing, and virulence phenotypes of *Erwinia chrysanthemi* EC16 on *Nicotiana clevelandii* seedlings. Proc. Natl. Acad. Sci. USA 99:13142-13147.

Ronald, P., and Staskawicz, B. 1988. The avirulence gene *avrBs1* from *Xanthomonas campestris* pv. *vesicatoria* encodes a 50-kD protein. Mol. Plant-Microbe Interact. 1:191-198.

Ryan, R., Fouhy, Y., Lucey, J., Crossman, L., Spiro, S., He, Y., Zhang, L., Heeb, S., Cámara, M., Williams, P., and Dow, J. 2006. Cell-cell signaling in *Xanthomonas campestris* involves an HD-GYP domain protein that functions in cyclic di-GMP turnover. Proc. Natl. Acad. Sci. USA 103:6712-6717.

Rybak, M., Minsavage, G.V., Stall, R.E., and Jones, J.B. 2009. Identification of *Xanthomonas citri* ssp. *citri* host specificity genes in a heterologous expression host. Mol. Plant Pathol. 10:249-262.

Römling, U., Gomelsky, M., and Galperin, M.Y. 2005. C-di-GMP: the dawning of a novel bacterial signalling system. Mol. Microbiol. 57:629-639.

Salama, N.R., and Manoil, C. 2006. Seeking completeness in bacterial mutant hunts. Curr. Opin. Microbiol. 9:307-311.

Salanoubat, M., Genin, S., Artiguenave, F., Gouzy, J., Mangenot, S., Arlat, M., Billault, A., Brottier, P., Camus, J.C., Cattolico, L., Chandler, M., Choisne, N., Claudel-Renard, C., Cunnac, S., Demange, N., Gaspin, C., Lavie, M., Moisan, A., Robert, C., Saurin, W., Schiex, T., Siguier, P., Thébault, P., Whalen, M., Wincker, P., Levy, M., Weissenbach, J., and Boucher, C.A. 2002. Genome sequence of the plant pathogen *Ralstonia solanacearum*. Nature 415:497-502.

Saldanha, A.J. 2004. Java Treeview--extensible visualization of microarray data. Bioinformatics 20:3246-3248.

Sambrook, J., and Russell, D.W. 2001. Molecular cloning: a laboratory manual. Cold spring harbor laboratory press, Cold spring harbor.

Sandkvist, M. 2001. Biology of type II secretion. Mol. Microbiol. 40:271-283.

Sandlin, R., Lampel, K., Keasler, S., Goldberg, M., Stolzer, A., and Maurelli, A. 1995. Avirulence of rough mutants of *Shigella flexneri*: requirement of O antigen for correct unipolar localization of *IcsA* in the bacterial outer membrane. Infect. Immun. 63:229-237.

Sasso, S., Ramakrishnan, C., Gamper, M., Hilvert, D., and Kast, P. 2005. Characterization of the secreted chorismate mutase from the pathogen *Mycobacterium tuberculosis*. FEBS (Fed. Eur. Biochem. Soc.) J. 272:375-389.

Schaad, N., Postnikova, E., Lacy, G., Sechler, A., Agarkova, I., Stromberg, P., Stromberg, V., and Vidaver, A. 2006. Emended classification of *xanthomonad* pathogens on citrus. Syst. Appl. Microbiol. 29:690-695.

Schauer, K., Gouget, B., Carrière, M., Labigne, A., and de Reuse, H. 2007. Novel nickel transport mechanism across the bacterial outer membrane energized by the TonB/ExbB/ExbD machinery. Mol. Microbiol. 63:1054-1068.

Schneider, D.J., and Collmer, A. 2010. Studying plant-pathogen interactions in the genomics era: beyond molecular Koch's postulates to systems biology. Annu. Rev. Phytopathol. 48:457-479.

Schornack, S., Meyer, A., Römer, P., Jordan, T., and Lahaye, T. 2006. Gene-for-gene-mediated recognition of nuclear-targeted AvrBs3-like bacterial effector proteins. J. Plant Physiol. 163:256-272.

Schreiber, K.J., and Desveaux, D. 2011. AlgW regulates multiple *Pseudomonas syringae* virulence strategies. Mol. Microbiol. 80:364-377.

Schulte, R., and Bonas, U. 1992. Expression of the *Xanthomonas campestris* pv. *vesicatoria hrp* gene cluster, which determines pathogenicity and hypersensitivity on pepper and tomato, is plant inducible. J. Bacteriol. 174:815-823.

Schuster, M., Lostroh, C.P., Ogi, T., and Greenberg, E.P. 2003. Identification, timing, and signal specificity of *Pseudomonas aeruginosa* quorum-controlled genes: a transcriptome analysis. J. Bacteriol. 185:2066-2079.

Segura, A., Moreno, M., Madueno, F., Molina, A., and Garcia-Olmedo, F. 1999. Snakin-1, a peptide from potato that is active against plant pathogens. Mol. Plant-Microbe Interact. 12:16-23.

Shrivastava, S., and Mande, S.S. 2008. Identification and functional characterization of gene components of type VI secretion system in bacterial genomes. PLoS One 3:e2955.

Siciliano, F., Torres, P., Sendín, L., Bermejo, C., Filippone, P., Vellice, G., Ramallo, J., Castagnaro, A., Vojnov, A., and Marano, M.R. 2006. Analysis of the molecular basis of *Xanthomonas axonopodis* pv. *citri* pathogenesis in *Citrus lemon*. Electron. J. Biotechnol. 9:200-204.

Simm, R., Morr, M., Kader, A., Nimtz, M., and Römling, U. 2004. GGDEF and EAL domains inversely regulate cyclic di-GMP levels and transition from sessility to motility. Mol. Microbiol. 53:1123-1134.

Slater, H., Alvarez-Morales, A., Barber, C.E., Daniels, M.J., and Dow, J.M. 2000. A two-component system involving an HD-GYP domain protein links cell-cell signalling to pathogenicity gene expression in *Xanthomonas campestris*. Mol. Microbiol. 38:986-1003.

Smyth, G.K. 2004. Linear models and empirical bayes methods for assessing differential expression in microarray experiments. Stat. Appl. Genet. Mol. Biol. 3:Article 3.

Stimson, E., Virji, M., Makepeace, K., Dell, A., Morris, H., Payne, G., Saunders, J., Jennings, M., Barker, S., and Panico, M. 1995. Meningococcal pilin: a glycoprotein substituted with digalactosyl 2,4-diacetamido-2,4,6-trideoxyhexose. Mol. Microbiol. 17:1201-1214.

Stock, A.M., Robinson, V.L., and Goudreau, P.N. 2000. Two-component signal transduction. Annu. Rev. Biochem. 69:183-215.

Swarup, S., Feyter, D., R., Brlansky, R.H., Gabriel, and D.W. 1991. A pathogenicity locus from *Xanthomonas citri* enables strains from several pathovars of *Xanthomonas campestris* to elicit canker-like lesions on citrus. Phytopathology 81:802-809.

Tang, J.L., Liu, Y.N., Barber, C.E., Dow, J.M., Wootton, J.C., and Daniels, M.J. 1991. Genetic and molecular analysis of a cluster of *rpf* genes involved in positive regulation of synthesis of extracellular enzymes and polysaccharide in *Xanthomonas campestris* pathovar *campestris*. Mol. Gen. Genet. 226:409-417.

Thieme, F., Szczesny, R., Urban, A., Kirchner, O., Hause, G., and Bonas, U. 2007. New type III effectors from *Xanthomonas campestris* pv. *vesicatoria* trigger plant reactions dependent on a conserved N-myristoylation motif. Mol. Plant-Microbe Interact. 20:1250-1261.

Thieme, F., Koebnik, R., Bekel, T., Berger, C., Boch, J., Büttner, D., Caldana, C., Gaigalat, L., Goesmann, A., Kay, S., Kirchner, O., Lanz, C., Linke, B., McHardy, A., Meyer, F., Mittenhuber, G., Nies, D., Niesbach-Klösgen, U., Patschkowski, T., Rückert, C., Rupp, O., Schneiker, S., Schuster, S., Vorhölter, F., Weber, E., Pühler, A., Bonas, U., Bartels, D., and Kaiser, O. 2005. Insights into genome plasticity and pathogenicity of the plant pathogenic bacterium *Xanthomonas campestris* pv. *vesicatoria* revealed by the complete genome sequence. J. Bacteriol. 187:7254-7266.

Tischler, A.D., and Camilli, A. 2004. Cyclic diguanylate (c-di-GMP) regulates *Vibrio cholerae* biofilm formation. Mol. Microbiol. 53:857-869.

Torres, P.S., Malamud, F., Rigano, L.A., Russo, D.M., Marano, M.R., Castagnaro, A.P., Zorreguieta, A., Bouarab, K., Dow, J.M., and Vojnov, A.A. 2007. Controlled synthesis of the DSF cell-cell signal is required for biofilm formation and virulence in *Xanthomonas campestris*. Environ. Microbiol. 9:2101-2109.

Tseng, G., Oh, M., Rohlin, L., Liao, J., and Wong, W. 2001. Issues in cDNA microarray analysis: quality filtering, channel normalization, models of variations and assessment of gene effects. Nucleic Acids Res. 29:2549-2557.

Tseng, T.T., Tyler, B.M., and Setubal, J.C. 2009. Protein secretion systems in bacterial-host associations, and their description in the Gene Ontology. BMC Microbiol. 9 Suppl 1:S2.

Van Sluys, M.A., Monteiro-Vitorello, C.B., Camargo, L.E., Menck, C.F., Da Silva, A.C., Ferro, J.A., Oliveira, M.C., Setubal, J.C., Kitajima, J.P., and Simpson, A.J. 2002. Comparative genomic analysis of plant-associated bacteria. Annu. Rev. Phytopathol. 40:169-189.

Vauterin, L., Hoste, B., Kersters, K., and Swings, J. 1995. Reclassification of *Xanthomonas*. Int. J. Syst. Bacteriol. 45:472-489.

Vilches, S., Canals, R., Wilhelms, M., Salo, M.T., Knirel, Y.A., Vinogradov, E., Merino, S., and Tomas, J.M. 2007. Mesophilic *Aeromonas* UDP-glucose pyrophosphorylase (GalU) mutants show two types of lipopolysaccharide structures and reduced virulence. Microbiology 153:2393-2404.

Viloria, Z., Drouillard, D.L., Graham, J.H., and Grosser, J.W. 2004. Screening triploid hybrids of 'Lakeland' limequat for resistance to citrus canker. Plant Disease 88:1056-1060.

Vojnov, A., Zorreguieta, A., Dow, J., Daniels, M., and Dankert, M. 1998. Evidence for a role for the *gumB* and *gumC* gene products in the formation of xanthan from its pentasaccharide repeating unit by *Xanthomonas campestris*. Microbiology 144 (Pt 6):1487-1493.

Wagner, V.E., Bushnell, D., Passador, L., Brooks, A.I., and Iglewski, B.H. 2003. Microarray analysis of *Pseudomonas aeruginosa* quorum-sensing regulons: effects of growth phase and environment. J. Bacteriol. 185:2080-2095.

Wang, L., Rong, W., and He, C. 2008. Two *Xanthomonas* extracellular polygalacturonases, PghAxc and PghBxc, are regulated by type III secretion regulators HrpX and HrpG and are required for virulence. Mol. Plant. Microbe. Interact. 21:555-563.

Wang, L.H., He, Y., Gao, Y., Wu, J.E., Dong, Y.H., He, C., Wang, S.X., Weng, L.X., Xu, J.L., Tay, L., Fang, R.X., and Zhang, L.H. 2004. A bacterial cell-cell communication signal with cross-kingdom structural analogues. Mol. Microbiol. 51:903-912.

Wei, K., Tang, D.J., He, Y.Q., Feng, J.X., Jiang, B.L., Lu, G.T., Chen, B., and Tang, J.L. 2007. *hpaR*, a putative *marR* family transcriptional regulator, is positively controlled by HrpG and HrpX and involved in the pathogenesis, hypersensitive response, and extracellular protease production of *Xanthomonas campestris* pathovar *campestris*. J. Bacteriol. 189:2055-2062.

Wengelnik, K., and Bonas, U. 1996. HrpXv, an AraC-type regulator, activates expression of five of the six loci in the *hrp* cluster of *Xanthomonas campestris* pv. *vesicatoria*. J. Bacteriol. 178:3462-3469.

Wengelnik, K., Marie, C., Russel, M., and Bonas, U. 1996a. Expression and localization of HrpA1, a protein of *Xanthomonas campestris* pv. vesicatoria essential for pathogenicity and induction of the hypersensitive reaction. J. Bacteriol. 178:1061-1069.

Wengelnik, K., Rossier, O., and Bonas, U. 1999. Mutations in the regulatory gene *hrpG* of *Xanthomonas campestris* pv. *vesicatoria* result in constitutive expression of all *hrp* genes. J. Bacteriol. 181:6828-6831.

Wengelnik, K., Van den Ackerveken, G., and Bonas, U. 1996b. HrpG, a key *hrp* regulatory protein of *Xanthomonas campestris* pv. *vesicatoria* is homologous to two-component response regulators. Mol. Plant-Microbe Interact. 9:704-712.

Wolfgang, M.C., Jyot, J., Goodman, A.L., Ramphal, R., and Lory, S. 2004. *Pseudomonas aeruginosa* regulates flagellin expression as part of a global response to airway fluid from cystic fibrosis patients. Proc. Natl. Acad. Sci. USA 101:6664-6668.

Xia, T., Song, J., Zhao, G., Aldrich, H., and Jensen, R.A. 1993. The *aroQ*-encoded monofunctional chorismate mutase (CM-F) protein is a periplasmic enzyme in *Erwinia herbicola*. J. Bacteriol. 175:4729-4737.

Yamazaki, A., Hirata, A., and Tsuyumu, S. 2008. HrpG regulates type II secretory proteins in *Xanthomonas axonopodis* pv. *citri*. J. Gen. Plant Pathol. 74:138-150.

Yan, Q., and Wang, N. 2011. The ColR/ColS two-component system plays multiple roles in the pathogenicity of the citrus canker pathogen *Xanthomonas citri* subsp. *citri*. J. Bacteriol. 193:1590-1599.

Yang, T.C., Leu, Y.W., Chang-Chien, H.C., and Hu, R.M. 2009. Flagellar biogenesis of *Xanthomonas campestris* requires the alternative sigma factors RpoN2 and FliA and is temporally regulated by FlhA, FlhB, and FlgM. J. Bacteriol. 191:2266-2275.

Ye, R.W., Wang, T., Bedzyk, L., and Croker, K.M. 2001. Applications of DNA microarrays in microbial systems. J. Microbiol. Methods 47:257-272.

Yen, M.R., Peabody, C.R., Partovi, S.M., Zhai, Y., Tseng, Y.H., and Saier, M.H. 2002. Protein-translocating outer membrane porins of Gram-negative bacteria. Biochim. Biophys. Acta 1562:6-31.

Yeo, H.J., and Waksman, G. 2004. Unveiling molecular scaffolds of the type IV secretion system. J. Bacteriol. 186:1919-1926.

Yuan, J., Reed, A., Chen, F., and Stewart, C.J. 2006. Statistical analysis of real-time PCR data. BMC Bioinformatics 7:85.

Yun, M.H., Torres, P.S., El Oirdi, M., Rigano, L.A., Gonzalez-Lamothe, R., Marano, M.R., Castagnaro, A.P., Dankert, M.A., Bouarab, K., and Vojnov, A.A. 2006. Xanthan induces plant susceptibility by suppressing callose deposition. Plant Physiol. 141:178-187.

Zhang, S.S., He, Y.Q., Xu, L.M., Chen, B.W., Jiang, B.L., Liao, J., Cao, J.R., Liu, D., Huang, Y.Q., Liang, X.X., Tang, D.J., Lu, G.T., and Tang, J.L. 2008. A putative colR(XC1049)-colS(XC1050) two-component signal transduction system in *Xanthomonas campestris* positively regulates *hrpC* and *hrpE* operons and is involved in virulence, the hypersensitive response and tolerance to various stresses. Res. Microbiol. 159:569-578.

Zhang, Y., Callaway, E.M., Jones, J.B., and Wilson, M. 2009. Visualisation of *hrp* gene expression in *Xanthomonas euvesicatoria* in the tomato phyllosphere. Eur. J. Plant. Pathol. 124:379–390.

Zhao, Y., Qian, G., Yin, F., Fan, J., Zhai, Z., Liu, C., Hu, B., and Liuao, F. 2011. Proteomic analysis of the regulatory function of DSF-dependent quorum sensing in *Xanthomonas oryzae* pv. *oryzicola*. Microb, Pathog. 50:48-55.

BIOGRAPHICAL SKETCH

Yinping Guo was born in Handan, Hebei, China. From 2000 to 2004 she attended Henan University of Technology, Zhengzhou, Henan, China, where she received the Bachelor of Science in bioengineering. In 2004, she was admitted for the Master of Science program in the Graduate University of Chinese Academy Sciences, Beijing, China. During this time, she worked on the multilocus phylogeny of Streptomyces genus under the supervision of Dr. Ying Huang in Institute of Microbiology, Chinese Academy of Sciences, Beijing, China. Yinping married Sha Tao on May 8th, 2007 in Zhengzhou, Henan, China. She received her master's in June 2007. In August 2007, she joined the Ph.D program in the Department of Microbiology and Cell Science at the University of Florida. She began working with Dr. Nian Wang on virulence regulatory mechanisms of the citrus canker pathogen *Xanthomonas citri* subsp. *citri*. As a graduate student, Yinping has presented her work in numerous conferences and seminars including the 2009 and 2010 American Phytopathological Society Annual Meetings, 2010 Plant Production seminar at the Citrus Research and Education Center. She received 2009-2011 A.S. Herlong Endowed Scholarship, and 2009 T. A. Wheaton Graduate Student Travel Award. Yinping received her Ph.D. from the University of Florida in the summer of 2011.